2001

Functional Analysis of the Human Telomeric Protein TRF2

Agata Smogorzewska

Functional analysis of the human telomeric protein TRF2

A thesis presented to the faculty of The Rockefeller University in partial fulfillment of the requirements for the degree of Doctor of Philosophy

By

Agata Smogorzewska

Advisor

Titia de Lange

September 2001

The Rockefeller University

New York, New York

To all my teachers

Acknowledgments

It is impossible for me to say how grateful I am to Titia de Lange for her guidance, her encouragement, her scientific knowledge and her enthusiasm about science and my projects. If I had to create the perfect advisor, I would not be able to do any better. Titia, I thank you.

I would like to thank all of my collaborators: Jan Karlseder, with whom I set up the retroviral expression system, shared many reagents for the length regulation studies, and collected billions (no kidding) of cells for the t-loops experiments; Bas van Steensel, who made the HTC75 cell lines as presented in this thesis and who started many of the experiments using them; Jack Griffith, who patiently scored the t-loops; and Anna Jauch, who performed and interpreted the M-FISH experiments presented in Chapter 1.

Many thanks to all of the scientists who supplied reagents that were used in my research, especially Scott Lowe, who was generous with his knowledge and materials as used in the retroviral studies and Arnie Levine for sharing the antibodies against p53, HDM2, SV40 Tag, and pericentrin.

Thanks go to the current and past members of the de Lange lab: Jan Karlseder, for our many scientific interactions; Diego Loayza; Susan Smith; Giulia Celli; Alessandro Bianchi, for our discussions; Bas van Steensel; and Dominique (Kiki) Broccoli, for sharing the knowledge when I had just started in the lab. Thanks to all who have ensured that the lab functioned properly and have patiently handled my requests: Rita Rodney; Heidi Moss; Amy Himelblau; Laura Chang; Jason Lue; Heather Parsons; and Vanessa Marrero. Thanks to the sabbatical professors in

attendance in our lab for sharing their knowledge and for showing me different styles of working (hmmm, which one will I chose?): Carolyn Price; Daniela Rhodes; and Jim Haber.

Special thanks to Stewart (Stew) Barnes, whose help with the computers and administrative matters has been invaluable to me.

Great thanks to the MD/PhD program and its leaders, especially Olaf Andersen and Tom Sakmar, for placing such strong emphasis on science, and to the Rockefeller University for creating a magnificent environment for young scientists to flourish. The graduate student lunches with Friday speakers were one of the many highlights for me on and off campus.

I would like to thank my PhD advisory committee, Arnie Levine, Bob Roeder, and Titia de Lange, for their guidance, their insight, their enthusiasm and their willingness to dedicate their time so as to meet with me on a regular basis. Thanks go to my special committee member, Lea Harrington, for participating in the important final stages of my graduate career.

Thanks to all of my friends who have made these years wonderful and without whom it would be a very dull world: Jan, Titia, my softball teammates, my squash partners, Jon Weiner and my colleagues in his literature and science course. Great thanks to my husband, Dennis, who was with me from the time I applied to MD/PhD programs, who has cheered me on in times of success and distracted me in times of scientific draught. I believe we can make it a successful science-art union. Very special thanks to my family, who were my first teachers at the microscope and the distillation apparatus. Lastly, thanks to my parents for their constant encouragement and for always pushing me towards a happy ending.

Table of Content

List of Figures

List of Tables

List of Abbreviations

ATM-ataxia telangiectasia mutated

ATR- ATM and Rad-3 related

BrdU- bromo-deoxyuridine

bp- base pairs

CO-FISH- chromosome orientation FISH

DAPI- 4'6-diamidino-2-phenylindole

DNA-PK- DNA-dependent protein kinase

DNA-PKcs- DNA-PK catalytic subunit

DSB- double-strand break

EST- ever-shorter telomeres

FACS- fluorescence activated cell sorter

FISH- fluorescence in-situ hybridization

FITC- fluorescein isothiocyanate

HR - homologous recombination

hTERT- human telomerase reverse transcriptase

hTR- human telomerase RNA

IF- immunofluorescence

IR- ionizing radiation

kbp (kb)- kilo base pairs

KO- knockout

Lig4- DNA ligase IV

MEF- mouse embryonic fibroblast

M-FISH- multiplex fluorescence in-situ hybridization

mRNA- messenger RNA

NBS- Nijmegen breakage syndrome

NHEJ- non-homologous end joining

PCD- premature chromosome division

PD- population doubling

PNA- peptide nucleic acid

RNase- ribonuclease

SA β-gal- senescence associated β-galactosidase

SCID- severe combined immunodeficiency

SD- standard deviation

SPB- spindle pole body

TRAP- telomeric repeat amplification protocol

TRF- TTAGGG repeat binding factor

TRITC- tetramethyl rhodamine isothiocyanate

WCE- whole cell extract

Abstract

TTAGGG Repeat Binding Factor 2 (TRF2) is a ubiquitous human telomeric protein present at all telomeres throughout the cell cycle. TRF2 has been proposed to remodel telomeres into large lasso-like structures named t-loops. Removal of TRF2 from telomeres by expression of a dominant negative allele of TRF2 ($TRF2^{\Delta B\Delta M}$) led to dissolution of these structures and appearance of end-to-end fusions visible in metaphase and anaphase cells. Fusion formation was accompanied by the loss of G-overhang, but not by the loss of double stranded telomeric DNA, which can be documented to persist at the sites of fusions. Fusions were covalent and their formation was dependent on the nonhomologous end-joining (NHEJ) pathway as evidenced by the failure to form fusions in cells lacking Ligase IV. Furthermore, the fusions initiated genomic instability.

Expression of $TRF2^{\Delta B\Delta M}$ in primary human cells resulted in induction of senescence. The arrested cells exhibited elevated levels of p53, stabilization of which was accompanied by induction of its downstream effectors p21 and Bax. The Rb pathway was also affected, with pRb becoming hypophosphorylated. The importance of both the p53 and the Rb pathways was further evident from the fact that the expression of SV40 Tag alone bypassed the growth arrest. Separate elimination of p53 or Rb function could not do so, and the activity of the ATM PI3 kinase was not necessary for the arrest.

Expression of a different truncation allele of TRF2, $TRF2^{\Delta B}$ also resulted in senescence but the growth arrest was accompanied by rapid loss of telomeric DNA. In addition, this allele induced an unanticipated chromosome breakage phenotype.

Long-term overexpression of full length TRF2 resulted in the gradual shortening of telomeres, suggesting that TRF2 is a regulator of telomere maintenance. Although it is clear that TRF2 acts through positively regulating the shortening activities at telomeres, it is unknown at this time whether it influences the telomerase pathway.

Besides being present at telomeres, TRF2 also appears to be localized to centrosomes. The functional consequences of such localization are not known at this time; however, it is shown that telomere dysfunction can result in genome reduplication.

Introduction

The advent of linear chromosomes created an enormous problem for their bearers. Conventional polymerases that replicate circular genomes are unable to replicate the very ends of chromosomes. Each time the DNA is synthesized, a few base pairs are lost at one of the chromosome tips. This problem has been coined the "end-replication problem" (Watson 1972; Olovnikov 1973) and it stems from the enzymatic characteristics of DNA polymerases, which need a short RNA primer to initiate polymerization. Additionally, this primer can be extended only in the 5'-3' direction. These requirements give rise to different modes of replication of two DNA strands (Figure i-1). One of the strands, the leading strand, is made continuously by the extension of one primer and presumably results in the formation of a blunt-ended molecule. The other strand, the lagging strand, is formed through the synthesis of multiple RNA primers and their extension into Okazaki fragments. Eventually the primers are removed and the Okazaki fragments are joined together resulting in a continuous strand. Since the primer that is closest to the tip of the chromosome is also removed and the leftover gap cannot be filled in by any polymerase, the lagging strand synthesis cannot fully replicate the DNA end. Taking into consideration the length of the RNA primer, each division would result in disappearance of a minimum of 3 bp of DNA per end. The true losses are even greater in most organisms bearing linear chromosomes. This is evident from the presence of single-stranded 3' extensions of the G strand, which can be from 12-16 nucleotides long in ciliates (Klobutcher et al. 1981; Pluta et al. 1982; Henderson and Blackburn 1989), around 30 nucleotides long during S phase in *S. cerevisiae* (Wellinger et al. 1993; Wellinger et al. 1993), and as long as 300 nucleotides in human cells (Makarov et al. 1997). It also appears that the overhangs can be found on both chromosome ends. The most compelling evidence comes from

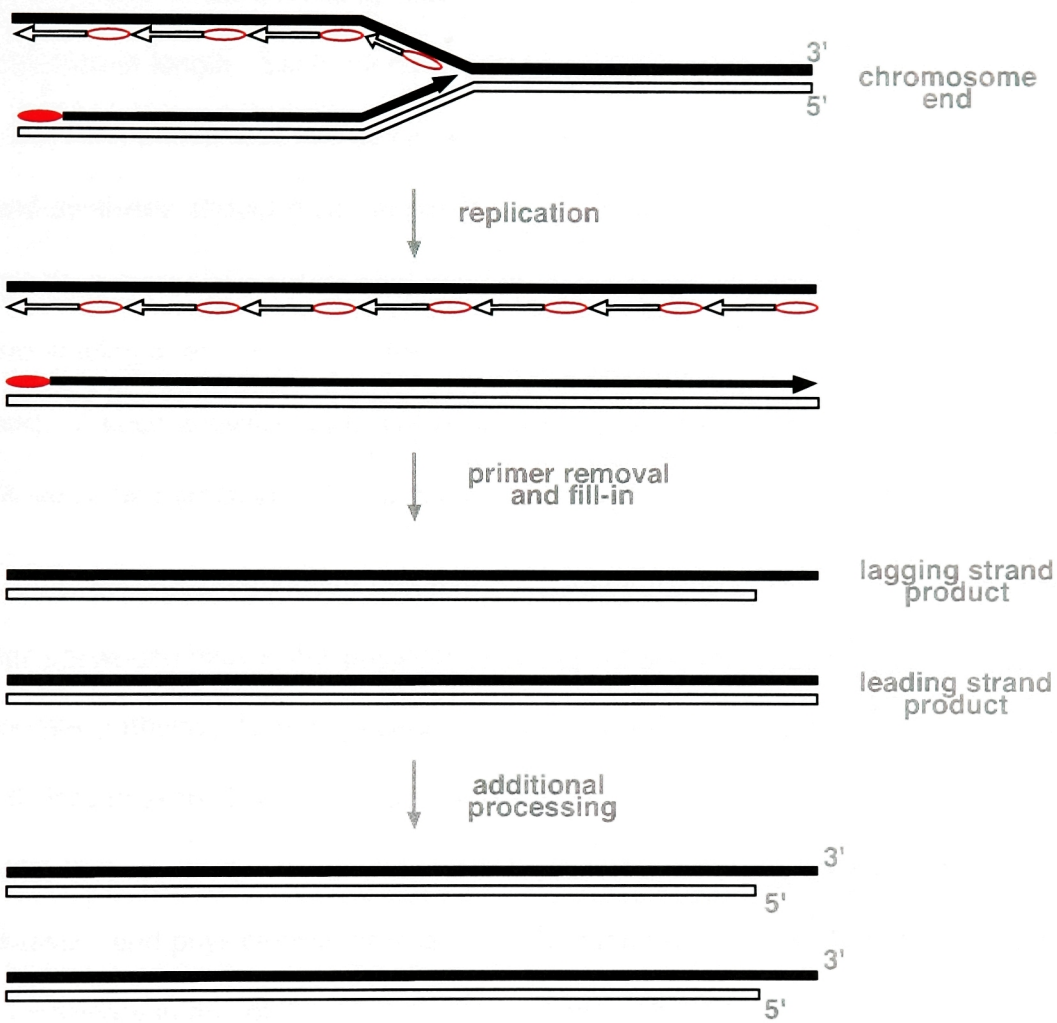

Figure i-1. **Schematic of replication at the very end of a chromosome**

The replication fork is moving from left to right.

RNA primer of leading strand

RNA primer of lagging strand

Okazaki fragment

the findings that both termini of human chromosomes (Makarov et al. 1997), as well as those of *Trypanosoma brucei* (Munoz-Jordan et al. 2001), and Tetrahymena (Jacob et al. 2001), end in an overhang that has been estimated to be up to a few hundred nucleotides in length. Such a long overhang on the lagging strand could be explained if the last RNA primer was laid down very far from the actual chromosome tip, but leading strand synthesis should theoretically result in a blunt end. The finding that it does not, suggests a nucleolytic activity that can create the single-stranded overhang, in the case of the leading strand, or extend the single stranded overhang, in the case of the lagging strand. If such activities were not counteracted, a substantial portion of chromosomal DNA would be permanently lost with each division.

A second pronounced problem that needs to be overcome by organisms with linear chromosomes is the physical presence of the DNA ends. Cells have evolved elaborate pathways to recognize and repair double-strand breaks (reviewed in Haber 2000; Hoeijmakers 2001). These pathways are necessary to eliminate chromosomal breaks that occur due to environmental stress, internal metabolism, including DNA replication, and physiological breaks acquired during development. Natural ends should not participate in any of these repair transactions. Therefore, the cellular machinery has to differentiate between telomeres and bona fide breaks within the genome.

These vital functions of compensating for DNA loss during replication as well as the protection of chromosomal ends from the repair activities are integrated in the telomere. First defined as a "free end" that has no ability to fuse with broken DNA (Muller 1938), the telomere is a sophisticated complex of repetitive DNA and associated proteins that can be found at all ends of linear chromosomes.

Telomeric DNA

Molecular studies of telomeres began with the finding that telomeric DNA was highly repetitive. The first telomeric DNA to be sequenced was from the ends of rDNA molecules of Tetrahymena and it was shown to consist of repeats of TTGGGG oriented 5' to 3' towards the chromosome terminus (the so called G strand), and of the complementary sequence of CCCCAA on the opposite strand (C strand) (Blackburn and Gall 1978). Soon, telomeric DNAs from other species were sequenced (Table i-1), and generally they were found to be built from similar simple repeats. There exist some exceptions, including the expanded telomeric repeat of *K.lactis* (McEachern and Blackburn 1994) and the irregular repeats of *S. cerevisiae* (Shampay et al. 1984) and *S.pombe* (Sugawara 1986). The greatest exception of all is the organism in which Muller first defined the telomeres. Telomeres of *Drosophila melanogaster* consist of repetitive sequences, but the repeats are retrotransposons of the non-LTR type (Biessmann et al. 1990; Levis et al. 1993; Sheen and Levis 1994). Although dipteran telomere structure and maintenance is unlike in any other organism, the telomeric functions are conserved (see below).

The telomeric repeat arrays can extend for a considerable length. In Tetrahymena, as in yeasts, telomeric tracts are approximately 300 bp in length (Blackburn and Gall 1978; Shampay et al. 1984), in human cells TTAGGG repeats range from 2 kbp to 25 kbp (Allshire et al. 1988; Moyzis et al. 1988; de Lange et al. 1990; Saltman et al. 1993) and in some mouse species including the laboratory *Mus musculus*, the telomeric DNA is as long as 50 kbp (Kipling and Cooke 1990). Taking into account the rate of replication-dependent telomere shortening, telomeric DNA can provide a substantial buffer against the loss of essential sequences found in the more centromere

Table i-1 Sequences of Telomeric DNA in Selected Species (adapted from (Henderson 1995))

Telomeric sequence	Species	Reference
TTGGGG	*Tetrahymena*	(Blackburn and Gall 1978)
TTTTGGGG	*Oxytricha, Euplotes*	(Klobutcher et al. 1981)
TTAGGG	*Trypanosoma brucei*	(Blackburn 1984; Van der Ploeg et al. 1984)
$T(G)_{2-3}(TG)_{1-6}$	*Saccharomyces cerevisiae*	(Shampay et al. 1984)
GGTTACA	*Schizosaccharomyces pombe*	(Sugawara 1986; Hiraoka et al. 1998)
ACGGATTTGATTAGGTATGTGGTGT	*Kluyveromyces lactis*	(McEachern and Blackburn 1994)
TTAGGC	*Caenorhabditis elegans*	(Cangiano 1993)
Het-A and TART retrotransposons*	*Drosophila melanogaster*	(Biessmann et al. 1990; Levis et al. 1993; Sheen and Levis 1994)
TTAGG	*Bombyx mori* (silkworm)	(Okazaki et al. 1993)
TTTAGGG	*Arabidopsis thaliana*	(Richards and Ausubel 1988)
TTAGGG	*Homo sapiens* and other vertebrates	(Moyzis et al. 1988)

*These are non-canonical since they are not maintained by telomerase.

proximal regions. However, in order for the single-celled organisms or species to be genetically immortal, telomeric DNA needs to be maintained at a stable length through the generations.

Core components of telomerase- RNA and the catalytic subunit

One of the most efficient and widely used ways of telomere maintenance is provided by telomerase, a ribonucleoprotein (Greider and Blackburn 1985; Greider and Blackburn 1987), which uses an RNA molecule as a template for addition of species specific telomeric repeats (Shippen-Lentz and Blackburn 1990; Yu et al. 1990). The RNA serves to align the telomeric 3' overhang with the template, and the catalytic subunit of telomerase, telomerase reverse transcriptase (TERT) (Lingner et al. 1997), reviewed in Nakamura and Cech 1998) synthesizes one repeat specified by the RNA. The enzyme can then relocate to the newly created end or to a different DNA substrate and continue synthesis. The synthesis of the G strand is closely followed by synthesis of the C strand (reviewed in Price 1997) to form the double stranded repeat array. The G-overhang found at chromosome ends could be made if the action of telomerase were not followed by the C strand synthesis. However, G-overhangs can be found in cells that lack telomerase (Dionne and Wellinger 1996; Makarov et al. 1997; Hemann and Greider 1999; Nikaido et al. 1999) suggesting that the nucleolytic activities mentioned earlier are responsible for their formation.

G-overhangs, as will be discussed later, have multiple functions. Chromosome tails can recruit single-stranded DNA binding proteins and can invade the double-stranded telomeric arrays. The overhangs are also necessary for telomerase-dependent

telomere maintenance since at least *in vitro*, telomerase is not capable of extending a blunt-ended DNA molecule (Greider and Blackburn 1987; Lingner and Cech 1996). Telomerase is less selective about the exact sequence of the overhang, and it elongates single-stranded non-telomeric sequences both *in vitro* (Greider and Blackburn 1987; Morin 1989; Harrington and Greider 1991; Morin 1991; Prowse et al. 1993), and *in vivo* (Shampay and Blackburn 1989; Wilkie et al. 1990; Lamb et al. 1993). This activity is thought to be important for the "healing" function of telomerase, through which broken ends can be capped by de novo addition of telomeric DNA (reviewed in Melek and Shippen 1996).

In unicellular organisms telomerase has a housekeeping function, and its two essential subunits are always expressed. However, It has been shown that the levels of telomerase RNA can increase at a specific developmental stage, for example during macronuclear development in Tetrahymena (Avilion et al. 1996). Mice express both telomerase subunits (Blasco et al. 1995; Greenberg et al. 1998; Martin-Rivera et al. 1998), as well as telomerase activity in most of their tissues (Prowse and Greider 1995). The catalytic subunit of the mouse telomerase, in contrast to the RNA subunit, is haplo-insufficient so that cells heterozygous for mTERT gradually shorten their telomeres (Liu et al. 2000).

Telomerase activity is repressed in most normal human tissues (Kim et al. 1994). Activity can be found only in ovaries and testis (Wright et al. 1996), and highly proliferative tissues including hematopoietic cells (Broccoli et al. 1995; Counter et al. 1995). Regulation of telomerase appears to be at the level of hTERT expression. hTR is present in many telomerase negative cells (Feng et al. 1995; Nakamura et al. 1997). hTERT message is only found in cells that express telomerase activity including most of

the primary tumors and tumor cell lines tested to date (Kilian et al. 1997; Meyerson et al. 1997; Nakamura et al. 1997). Additionally, expression of hTERT alone in human primary fibroblasts is sufficient to reconstitute functional telomerase activity (Bodnar et al. 1998; Vaziri and Benchimol 1998) suggesting that hTERT is the limiting component of telomerase in human cells. One of the outstanding questions in telomerase regulation is how hTERT gets repressed in most of human somatic tissues and how it gets activated in 90% of human tumors (reviewed in Shay and Bacchetti 1997).

Other telomerase components

Studies of telomerase components in many organisms have shown that many proteins associate with the RNA and the catalytic subunit *in vivo*. The best understood of those are the Est1 and Est3 proteins which are necessary for the *in vivo* telomerase function in *S. cerevisiae* but are dispensable for *in vitro* activity (Lingner et al. 1997). The Est proteins will be discussed later in the section on telomere length regulation.

Telomerase RNA from *S. cerevisiae* associates with Sm proteins *in vivo* (Seto et al. 1999). This association has been proposed to be important in the biogenesis of the RNA. In particular, the poly A tail is not removed efficiently from the RNA if the Sm proteins are precluded from binding to this RNA (Seto et al. 1999). Sm proteins were found not to interact with human RNA (hTR) (Le et al. 2000). Instead, two other proteins, hStau and L22 were found to interact with hTR in a three-hybrid screen as well as *in vivo*. Although their function is unknown, they are proposed to also play a role in hTR processing, assembly or localization (Le et al. 2000). Other components of the telomerase RNP might be heterogeneous nuclear ribonucleoprotein A1 (hnRNP A1) (LaBranche et al. 1998), and heterogeneous nuclear ribonucleoprotein C1 and C2

(hnRNP C1, hnRNP C2) (Ford et al. 2000). Immunoprecipitation of an amino-terminal part of hnRNP A1 (LaBranche et al. 1998), or of hnRNP C1 and C2 (Ford et al. 2000) brings down telomerase activity (LaBranche et al. 1998). In addition, all three hnRNPs are able to directly interact with hTR (Ford et al. 2000; Fiset and Chabot 2001) and hnRNP A1 can influence telomere length *in vivo* (Fiset and Chabot 2001). The latest addition to the proteins able to interact with telomerase RNA is La (Ford et al. 2001). Antibodies directed against this protein precipitate telomerase from a number of sources, and overexpression of La leads to telomere shortening.

Through extensive phylogenetic comparison, vertebrate telomerase RNA has been found to contain four very well conserved motifs (Chen et al. 2000). So far, only one of them, box H/ACA small nucleolar RNA–like domain (snoRNA), has been shown to be important for hTR accumulation, hTR 3' processing, and telomerase activity in human 293 cells transfection system (Mitchell et al. 1999). The H/ACA RNA motif seems to be able to associate with dyskerin (Mitchell et al. 1999), a putative pseudouridine synthase mutated in an X-linked form of the human disease dyskeratosis congenita (Heiss et al. 1998). Cells from patients with the disease show decreased levels of hTR, produce lower levels of telomerase activity, and, although further analysis of telomere length regulation is necessary, seem to have difficulty with telomere maintenance.

In Tetrahymena, two proteins, p80 and p95 copurify with telomerase activity and the telomerase RNA (Collins et al. 1995). In contrast to the predictions, the two proteins are not necessary for the telomerase accumulation or *in vitro* activity, but seem to play a role in telomere length regulation since removal of p80 or p95 lead to increased length of

micronuclear and macronuclear telomeres (Miller and Collins 2000). The mechanism of their function in telomere length regulation is unknown.

A human homologue of p80 has been identified (Harrington et al. 1997; Nakayama et al. 1997). Even though TEP1 interacts with the telomerase RNA and immunoprecipitation with a specific antibody against TEP1 brings down telomerase activity, complete removal of the protein in mice has no functional consequences on the *in vivo* telomerase activity or telomere maintenance (Liu et al. 2000), suggesting that TEP1 is not required or has a redundant function in the expression of telomerase function.

In general, telomerase associated proteins might be important in regulating biogenesis, stability, as well as the catalytic activity of telomerase. Further studies are needed to elucidate the exact requirements for all of the proteins. It will be interesting to see if there are multiple telomerase complexes in the cell and if so how they influence telomere function.

Alternative mechanism of telomere maintenance

In the absence of telomerase some cells are able to maintain their telomeres in alternative ways. In yeast, such an alternative mode relies on rearrangement and amplification of the telomeric regions and is dependent on the RAD52-mediated recombination (Lundblad and Blackburn 1993; Lendvay et al. 1996). The human and mouse alternative lengthening pathway (ALT) has also been proposed to involve recombination (Bryan et al. 1995; Bryan et al. 1997; Dunham et al. 2000; Niida et al. 2000). Finally, as mentioned above, *Drosophila melanogaster* and other Dipterans,

which lack telomerase altogether, counteract the shortening of their telomeres by stochastically placing retrotransposons at the end of their linear chromosomes (Biessmann et al. 1990).

Regulation of telomere maintenance

Alternative pathways of telomere maintenance are poorly understood and when cells use these pathways, length of their telomeres can become heterogenous and generally not very well regulated. When telomerase is available, on the other hand, telomeres stay stable through many divisions (Shampay and Blackburn 1988; Counter et al. 1992; van Steensel and de Lange 1997). To achieve such homeostasis, activities of replication, degradation, and DNA addition need to be tightly regulated. Understanding of this regulation has recently flourished, especially in *S. cerevisiae* where multiple factors are known to affect telomere length. Generally, factors that regulate length can be divided into those that affect activities at the very terminus of the DNA, and those that define the length setting of the double-stranded telomeric DNA array.

Regulation of telomere maintenance: the role of terminus factors

The best understood activity at the telomere terminus is the addition of telomeric DNA by telomerase. As mentioned before, telomerase is a reverse transcriptase with two essential subunits, an RNA component (TLC1 in budding yeast, hTR in humans, mTR in mouse), and the catalytic subunit (EST2 in budding yeast, hTERT in humans, mTERT in mouse). When one of these essential subunits is missing (Singer and Gottschling 1994; McEachern and Blackburn 1995; Lendvay et al. 1996),(Blasco et al.

1997; Lingner et al. 1997; Nakamura et al. 1998; Niida et al. 1998; Fitzgerald et al. 1999; Liu et al. 2000; Niida et al. 2000), or strongly inhibited (Hahn et al. 1999; Zhang et al. 1999; Miller and Collins 2000), the length homeostasis is perturbed and telomeres gradually and steadily shorten, giving rise to a phenotype which in yeast has been coined an Ever Shorter Telomeres (est) phenotype (Lundblad and Szostak 1989). Presence of the catalytically active telomerase is not sufficient for stable length maintenance, and the recruitment of telomerase to the telomere terminus engages both positive and negative regulators (reviewed in Evans and Lundblad 2000)

Cdc13p seems to orchestrate access of telomerase to the terminus. Based on *in vitro* binding data it is expected that Cdc13p resides on the single-stranded G-overhang (Lin and Zakian 1996; Nugent et al. 1996) and is able to interact with Est1p (Qi and Zakian 2000), which together with Est2p, TLC1 RNA, and Est3p forms the telomerase holoenzyme. The recruitment function of Cdc13p is further evidenced by experiments showing that the DNA binding domain of Cdc13p (DBD_{Cdc13}) fused to Est1p (Evans and Lundblad 1999) or Est3p (Hughes et al. 2000) rescues the est phenotype of cdc13-2^{est} allele, and that Cdc13-Est2p fusion bypasses the requirements for Est1p (Evans and Lundblad 1999).

A number of other proteins positively regulate telomerase function in yeast. Mutants in the Mre11p/Rad50p/Xrs2p complex have short telomeres (Kironmai and Muniyappa 1997; Boulton and Jackson 1998; Nugent et al. 1998) and are in the telomerase epistasis group since double mutants of telomerase and any of the components of the complex do not show a more severe phenotype than mutation in telomerase itself (Nugent et al. 1998). The complex has multiple biochemical and cellular functions (reviewed in Haber 1998) and it is still unclear how it participates in

telomere length regulation although it has been proposed that it might prepare the terminus for Cdc13p binding and/or telomerase action. The Mre11 complex appears to act synergistically with Ku, deletion of which also results in short telomeres (Porter et al. 1996; Boulton and Jackson 1998; Nugent et al. 1998; Polotnianka et al. 1998). As opposed to Mre11, Ku deletion also results in changes of the terminal structure of the telomere; the G-overhangs that normally are detectable only in S phase in yeast, now persist throughout the cell cycle (Gravel et al. 1998; Polotnianka et al. 1998). This suggests that Ku participates in telomere protection (discussed separately below) although it is not excluded that the two phenotypes of telomere shortening and presence of increased single-stranded DNA are related.

Interference with two other proteins leads to telomere shortening. Tel1 and Tel2 were identified in genetic screen for temperature sensitive mutants resulting in altered telomere length (Lustig and Petes 1986). Tel2p turned out to be an essential protein (Runge and Zakian 1996), which has characteristics of binding to both double-stranded and single-stranded telomeric DNA (Kota and Runge 1998; Kota and Runge 1999). Tel1p, is an ortholog of ATM (Ataxia Telangiectasia Mutated), a PI3 kinase mutated in patients with Ataxia Telangiectasia (Greenwell et al. 1995), and its kinase activity is necessary for telomere length regulation (Mallory and Petes 2000). Mec1p, another PI3 kinase from *S.cerevisiae,* that is more closely related to ATR, similarly influences telomere length (Ritchie et al. 1999). TEL1 or MEC1 deletion leads to telomeres of short but stable length. Removal of both of the proteins leads to progressive shortening characteristic of the est phenotype, suggesting that Tel1p and Mec1p act in separate pathways at telomeres. This is a similar situation to that found in *S. pombe* where simultaneous mutation of both the AT ortholog RAD3 and the ATM ortholog TEL1 lead to

a progressive telomere shortening (Naito et al. 1998). Epistasis analysis in *S. cerevisiae* showed that Tel1p is in the same pathway as the Mre11p complex described above, since the double mutants of tel1mre11, tel1rad50, and tel1xrs2 harbor telomeres that are of the same length as they were when only a single protein of the pair was mutated (Ritchie and Petes 2000). Moreover, Tel1p phosphorylates Xrs2p *in vitro* (Mallory and Petes 2000) and *in vivo* (Usui et al. 2001). This is analogous to the situation found in human cells where ATM is able to phosphorylate Nbs, an equivalent, although not obviously orthologous protein to Xrs2.

The proteins discussed above appear to positively regulate telomere length maintenance. Some of the same proteins apparently can also negatively regulate telomere length. In a recently identified mutant of Cdc13p (cdc13-5) (Chandra et al. 2001), telomerase elongates telomeres about 1000 bp beyond the usual setting. Additionally, the coordination between the G and C strand synthesis is lost with G-overhangs becoming unusually long in S phase. This aspect of Cdc13p function, as previously suggested (Grandin et al. 1997), is mediated by Stn1p, a Cdc13p interacting partner, since overexpression of Stn1p suppresses all phenotypes associated with cdc13-5. Overexpression of Stn1p also suppresses a telomere elongation defect in mutants of DNA polymerase alpha (pol1-12, pol1-16, and pol1-17) pointing to a pathway of coordination of G and C strand synthesis by telomeric proteins. A similar coordination appears to exist in other organisms. In *Euplotes*, inhibition of DNA polymerase alpha and delta results in increased length heterogeneity of the G strand and changes the length of the C strand (Fan and Price 1997). An additional telomeric protein in this pathway in yeast might be Ten1p, which interacts with both Cdc13p and Stn1p (Grandin et al.

2001). Some mutations in this protein lead to telomere elongation, although the nature of this elongation has not been yet compared with elongation of the cdc13-5 mutants.

The role of helicases at telomeres is just starting to be elucidated. Pif1p (Schulz and Zakian 1994), a 5'-3' helicase which by chromatin immunoprecipitation localizes to telomeres, when overexpressed causes telomere shortening (Zhou et al. 2000). Furthermore, Pif1p deletion or expression of catalytically dead helicase mutants leads to telomerase dependent telomere elongation. Based on the observation of telomere length changes and biochemical activity found in Pif1p, it has been suggested that Pif1p could dissociate the RNA template from the telomere thus negatively influencing telomerase function. Another helicase, Sgs1p has gained considerable attention due to its homology with helicases that are mutated in a number of human disorders that include Bloom syndrome and Werner syndrome. Mutant sgs1 has no effect on telomere homeostasis when telomerase is present (Watt et al. 1996). However, a double deletion of est2 and sgs1, leads to slightly faster telomere shortening than in est2 mutant alone. Biological meaning of this finding is unclear and currently the only telomere function of Sgs1p is in a choice of the type of alternative pathways used in cells when telomerase is not able to maintain telomeres (Cohen and Sinclair 2001; Huang et al. 2001; Johnson et al. 2001).

Regulation of telomere maintenance: the role of proteins bound to duplex telomeric DNA

All of the proteins discussed above, appear to function close to or at the terminus of the DNA. Work from *S.cerevisiae, S.pombe*, and humans, shows that proteins that bind along the telomere are also important for in-cis telomere length regulation. Rap1p

is an integral component of telomeric chromatin in *S. cerevisiae* (Conrad et al. 1990) and it directly interacts with telomeric DNA using its two Myb-like DNA binding domains (Konig et al. 1996). Rap1p has been established as a negative regulator of telomere length based on the facts that overexpression of the full-length protein leads to telomere elongation and increase in length heterogeneity (Conrad et al. 1990). Furthermore, growth of a strain with a temperature sensitive allele of Rap1p at semi-permissive temperature led to telomere shortening, which was rescued by expression of the wt allele (Conrad et al. 1990; Lustig et al. 1990). Further studies suggested that the number of Rap1p molecules bound to the chromosome end is counted and used as a gauge of the length of the telomeric repeat array (Marcand et al. 1997). In these studies, the C-terminal 174 amino acids of Rap1p were fused to a heterologous DNA binding domain of Gal4. By varying the number of Gal4 sites subtelomeric to an engineered telomere, the number of Rap1p molecules available for protein counting could be altered. A correlation was seen between the number of Rap1p C termini present on the telomere and the length of that telomere. The more Rap1p was tethered to the telomere, the shorter the final telomere length. The C terminus of Rap1p interacts with two proteins (Rap1 interacting factor 1 and 2, Rif1p and Rif2p) that are implicated in telomere length regulation. Overexpression of Rif1p and 2 leads to telomere shortening and their mutation or deletion lead to telomere elongation (Wotton and Shore 1997). Thus, like Rap1p they negatively regulate telomere elongation, although the mechanism of their function is completely unknown. The Rap1p C terminal domain also interacts with Sir3p and Sir4p proteins (Moretti et al. 1994), which participate in silencing at mating type loci as well as at telomeres in yeast. As opposed to deletion of Rif1p or 2, which leads to telomere elongation, removal of Sir proteins leads to moderate telomere shortening. It has been proposed that this shortening is very indirect and in the cells that

do not have Sir proteins, more Rap1p molecules are available to interact with Rif1 and Rif2, tilting the balance towards telomere shortening (Marcand et al. 1997).

Genetic screens have identified a number of double stranded telomere binding proteins that affect telomere length regulation in *S. pombe* (Cooper et al. 1997; Nimmo et al. 1998). A strain with a deleted Taz1 protein had very dramatically elongated telomeres. Taz1 is a ortholog of human TRF1 and TRF2 (see below) and like them uses Myb domains for DNA binding. The mechanism by which Taz1 regulates telomere length is not understood.

Telomere length regulation in mammals

Telomere length regulation in mammals will be described in detail in Chapter 3 of this thesis, but the rules observed in lower eukaryotes also apply to maintenance of telomere length in higher organisms. Although the details and molecular mechanisms might be vastly different, both the elongating and shortening activities have to be regulated and telomere associated proteins are best candidates for such forces.

As noted above, the overall telomerase activity in human cells is regulated at the level of expression of the catalytic subunit (hTERT) and generally, hTERT expressing cells have detectable telomerase activity (Kilian et al. 1997; Meyerson et al. 1997; Nakamura et al. 1997). However, there is ample experimental evidence that telomerase activity is very tightly regulated at each chromosome end. For example, tumor cells maintain their telomeres at a stable length, while they express high telomerase activity (Counter et al. 1992; Counter et al. 1994; van Steensel and de Lange 1997). Secondly, when new telomeres are formed by elongation of a transfected short telomeric "seed",

the final length of a new telomere matches that of the other telomeres in the cell. (Barnett et al. 1993; Hanish et al. 1994; Sprung et al. 1999). These findings suggest that the length of a single telomere can be monitored and adjusted.

In human cells, the double-stranded DNA binding telomere protein, TRF1 is at least in part responsible for telomere length monitoring. When TRF1 is overexpressed in a telomerase-positive cell line telomeres shorten (van Steensel and de Lange 1997). When TRF1 is removed from telomeres by overexpression of a dominant negative allele of TRF1, the telomeres elongate (van Steensel and de Lange 1997). In both cases the telomere length stabilizes at a new length setting, which can be maintained for many population doubling (Smogorzewska et al. 2000). The level of TRF1 present on the telomeres does not influence the telomerase activity detected in the extracts. Based on these findings it was proposed that TRF1 acts in cis and regulates length of an individual telomere (van Steensel and de Lange 1997). According to this model, long telomeres recruit a large amount of TRF1, which blocks telomere elongation. Due to the shortening activities, the telomeres then gradually decrease in length until they stop recruiting the inhibitory amount of TRF1. At that time, telomerase elongates the DNA ends, synthesizing more binding sites for TRF1, so that the cycle continues. This is a similar way of regulating telomere length to that of the counting mechanism that was discussed above for Rap1 (Marcand et al. 1997).

A number of other proteins clearly influence length regulation in human cells. Tankyrase (Smith et al. 1998) and TIN2 (Kim et al. 1999) both bind to TRF1 and most likely participate in length regulation through changing the binding of TRF1 to telomeric (Ye and de Lange; Smith et al. 1998; Smith and de Lange 2000). TRF2, a homologue of TRF1 regulates telomere length independently and through a different mechanism than

TRF1. Telomere length regulation by TRF2 and the associated factors will be discussed in Chapter 3 of this thesis.

As described earlier, telomerase associated proteins might play a role in telomere length regulation by affecting telomerase processing or stability. Telomeres of cells deficient in heterogeneous nuclear ribonucleoprotein A1 (hnRNP A1) are shorter than the telomeres in wt cells (LaBranche et al. 1998), and overexpression of UP1, an amino-terminal fragment of A1 leads to telomere elongation. Besides being associated with the telomerase RNA, hnRNP A1 has also been reported to interact with the single-stranded telomeric DNA *in vitro* (Ishikawa et al. 1993; LaBranche et al. 1998; Fiset and Chabot 2001), which led to a proposal that hnRNP might recruit telomerase to the telomere (Fiset and Chabot 2001). Mutation in another telomerase RNA binding protein, dyskerin, might result in increased shortening rates (Mitchell et al. 1999). Finally, overexpression of La, which binds telomerase RNA (Ford et al. 2001) leads to telomere shortening. These results suggest that proteins that interact with the telomerase RNA can positively and negatively regulate telomere length. Further biochemical and molecular studies will have to be done to decipher all of the interactions and the mechanism of telomere length regulation by these proteins.

As in yeast, human proteins involved in DNA damage signaling might also be involved in telomere length regulation. Although one study found no difference in telomere length homeostasis in cells that were deficient for Ataxia Telangiectasia Mutated (ATM), an ortholog of TEL1 (Sprung et al. 1997), primary fibroblasts from human patients affected with Ataxia Telangiectasia showed an increased rate of telomere shortening when cultured *ex vivo* (Vaziri et al. 1997). The issue of telomere shortening rates in these cells is confounded by the fact that these cells, due to genomic

instability, have very slow growth rates and they senesce prematurely, an event that might be influenced both by the telomere length as well as by accumulation of DNA damage. Peripheral T lymphocytes from patients with Ataxia telangiectasia were shown to have accelerated telomere shortening (Metcalfe et al. 1996), but again, AT patients are immunodefficient and the shorter telomere lengths might reflect increased turnover of stem cells supplying the peripheral leukocytes. In mice deficient for ATM, telomere length also appears to be decreased (Hande et al. 2001), suggesting that ATM might influence telomere length. Mutations in WRN protein in human cells, like mutations in ATM, lead to increased telomere shortening rates in human primary fibroblasts cultured *ex vivo* (Schulz et al. 1996), but again the same caveat about growth rates applies to these experiments.

The role of Ku70, Ku80 and DNA-PKcs in telomere length regulation in mammalian cells is controversial. SCID (severe combined immunodeficiency) mutation in mice removes part of the DNA-PKcs protein making it non-functional in V(D)J recombination. Comparison of telomere length in mice carrying SCID mutation with the telomere length in wt mice shows that SCID mice have longer telomeres (Hande et al. 1999; Goytisolo et al. 2001). When one of the groups compared telomere length of wt cells with those that had a complete null DNA-PKcs, the difference disappeared (Goytisolo et al. 2001). This could be explained if the SCID mutation created a gain of function mutation for telomere length maintenance. It is much harder to explain discrepancies in results of telomere length assessment in mice lacking Ku80. Even though the two groups worked with mice from the same source, one of the groups concluded that the KO cells had shorter telomeres than the wt cells (d'Adda di Fagagna et al. 2001), while the other group found no telomere changes between the two strains

(Samper et al. 2000). There is some data that suggest a slight shortening phenotype in the KO cells in the results of the second group ((Samper et al. 2000), Figure 5, left panel), although, the results would have to be very carefully quantified.

Similar discrepancy arose when these two groups looked at the role of poly(ADP-ribose) polymerase PARP in telomere length regulation. Again, one group has concluded that there was a telomere shortening phenotype (d'Adda di Fagagna et al. 1999), and the other, that there were none (Samper et al. 2001). This time, the mice both groups used were from different origin so there could be some strain differences giving rise to different results. It must be said, though, that the results of the group that claimed no difference in telomere length in mutant animals (Samper et al. 2001) were much more convincing and supplied a much more detailed analysis of the length phenotype in the KO animals. Also, this group has correctly concluded that there were no end-to-end chromosome fusions arising due to telomere deprotection, and all of the fusions that were seen in the mutant animals could be accounted for by the genomic instability observed in these animals rather then the telomere deprotection as suggested by d'Adda di Fagagna et al. (d'Adda di Fagagna et al. 1999).

Telomere protection and its regulation

The first cytological description of fusogenic potential of the broken ends came from Barbara McClintock, who observed dicentric chromosomes forming chromatin bridges in anaphase cells of *Zea mays* (McClintock 1938). While being pulled to the opposite poles of the dividing cell, dicentric chromosomes will break, resulting in newly formed ends moving to daughter cells. Two outcomes were observed. In the first one,

the broken end formed by rupture fused with its copy after the chromosome was replicated and because this created another dicentric chromosome the breakage-fusion-bridge cycle would continue through subsequent divisions. This occurred when the initial break arose in the endosperm and the breakage–fusion–bridge cycle continued through the development of that tissue. When the break occurred in the zygote, on the other hand, the cycle would cease and sporophytic tissue that developed behaved as if there were no free ends present. In the words of McClintock, the ends were healed. A healed chromosome stayed stable even when reintroduced into in the gametophytic or endosperm tissue. Two conclusions could be drawn from these observations. First, the broken ends were not stable and would fuse with another broken end to form a dicentric chromosome, which, in turn, would lead to the formation of a bridge in the next division. Second, some tissues were capable of healing broken ends. McClintock did not know it at the time, but the healing power in the zygote is most likely supplied by telomerase, whose activity is very high at that developmental stage, but very low in endosperm (Killan et al. 1998). Telomerase, when present, is able to add telomeric DNA to the broken end. The added DNA in turn recruits all the necessary components to create a non-fusogenic chromosome end, a telomere. This current interpretation of healing implies that to create a proper, protected end, there is a need for telomeric DNA serving as a binding site for proteins. If one of those components fails, a telomere will become nonfunctional and can become fusogenic.

There are many examples of failure of protection resulting from the lack of sufficient length of telomeric DNA to support proper telomere function. As noted in the section describing telomere length regulation, elimination of telomerase activity in all organisms studied to date leads to a gradual but constant loss of telomeric DNA (Singer

and Gottschling 1994; McEachern and Blackburn 1995; Lendvay et al. 1996),(Blasco et al. 1997; Lingner et al. 1997; Nakamura et al. 1998; Fitzgerald et al. 1999; Liu et al. 2000; Niida et al. 2000). Initially, this loss is associated with no abnormal phenotype showing that presence of telomerase per se is not necessary for end protection. Eventually telomeres become so short they are non-functional and become fusogenic.

End-to-end fusions are visible in cells derived from mice without functional telomerase due to deletion of the mTR gene (Blasco et al. 1997), but this phenotype only develops after the telomerase deficient mice have been bred for a number of generations allowing cell division during which the telomeres shorten. The number of generations to achieve telomere dysfunction varies from 3 to 6 (Blasco et al. 1997; Herrera et al. 1999) and is highly dependent on the initial length of telomeres in the KO strain. Similarly, removal of the telomerase catalytic subunit in *Arabidopsis thaliana* produces telomere dysfunction after a delay of 5 generations (Riha et al. 2001). Plant cells tolerate chromosomal abnormalities allowing for a spectacular display of fusions in very late generations of growth without telomerase. Nearly half of the of anaphases in terminal plants (those that do not give rise to offspring) carry at least one bridge.

A striking outcome of telomere dysfunction is found in *S. pombe* after loss of its telomeric DNA due to growth without the catalytic subunit of telomerase or in absence of both Rad3p and Tel1p. Molecular analysis of the genome of these cells revealed that all three chromosomes were circularized, thus circumventing the need for end protection (Naito et al. 1998; Nakamura et al. 1998). This is an example of healing of ends without formation of dicentric chromosomes, a pathway that apparently is available if an organism has a small number of chromosomes. As an aside, having circular

chromosomes is compatible with vegetative growth but meiosis is extremely inefficient in such cells (Naito et al. 1998; Nakamura et al. 1998).

All of the examples above deal with a gradual loss of telomeric DNA leading to chromosome fusions. In these cases, de-protection results from lack (or too little) of telomeric DNA. A number of recent experiments suggest that the proteins that bind to that DNA are ultimately the important players in protection. Based on the molecular outcome of their removal, protective proteins can be grouped in different categories. There are those that when removed lead to a very rapid destruction of only the C strand of the telomere, those that when removed lead to loss of both strands of the DNA and finally, there are those that cause deprotection but leave the telomeric DNA evidently intact.

The first category is represented by the Cdc13 complex. Cdc13p, and its associated factors Stn1p and Ten1p have been already discussed with regard to their function in telomere length regulation. Their essential function at the telomere stems from their ability to protect the end from nucleases. Mutations in all three proteins lead to rapid and specific degradation of the C strand (Garvik et al. 1995; Grandin et al. 1997; Grandin et al. 2001). The exact molecular nature of the protection is not yet understood, but it is known that all three proteins can interact with each other. Cdc13p binds to the single-stranded overhand and recruits the other two proteins, which in turn inhibit degradation. Cdc13p itself is dispensable for protection because anchoring of Stn1p to the overhang using the small DNA binding domain of Cdc13p is sufficient to inhibit the putative nucleases (Pennock et al. 2001). A less dramatic deprotection resulting in C strand degradation is seen in yeast lacking the Ku 70/80 heterodimer. In wild type cells long overhangs are present only in S phase, but in both Yku70 and Yku80 mutants, the

terminal structure of the DNA is altered and G-overhangs are present throughout the cell cycle (Gravel et al. 1998), suggesting that the Ku heterodimer is necessary for proper protection. Combining lack of Ku with lack of cdc13 exacerbates single mutant phenotypes (Nugent et al. 1998; Polotnianka et al. 1998), thus it seems that these proteins have distinct protective activities at the telomere.

Telomere end-binding protein (TEBP), the first telomeric protein to be isolated, binds to the very terminus of a single-stranded overhang found in *Oxytricha nova* macronuclear telomeric DNA (Gottschling and Zakian 1986). It is a heterodimer of α and β subunits and forms an extremely stable, non-covalent complex with the DNA. The DNA in this complex is completely resistant to Bal 31 exonuclease, establishing that the protein is able to protect the terminus *in vitro*. The crystal structure of the heterodimer complexed with its ss DNA substrate (Horvath et al. 1998) shows that the very terminus of the DNA is buried deeply in the cleft formed by the two proteins and thus, it is inaccessible to any activities that might degrade or extend the overhang.

Although the exact conserved orthologs of *Oxytricha*'s α and β subunits has been only found in *Stylonychia mytilis* (Fang and Cech 1991), many species, including humans, possess a protein that has sequence similarity to the DNA binding domain of the α subunit. Functional information on this protein comes from *S.pombe*, where deletion of Pot1, the ortholog of the α subunit from *Oxytricha* TEBP leads to a rapid degradation of both strands of telomeric DNA and results in circularization of all chromosomes (Baumann and Cech 2001). As opposed to the gradual telomere shortening that follows after removal of telomerase activity, these events are obvious within the first 5 to 10 generations of growth, showing that Pot1 is necessary for the protection of the DNA.

Removal of Taz 1 from the telomeres of S.pombe under certain circumstances (nitrogen starvation or rad22-/- background) also results in deprotection of telomeres (Godhino Ferreira and Promisel Cooper 2001). Unlike the examples so far, the telomeric DNA is not degraded but nevertheless the telomeres become fusogenic. Fusions are clearly created due to the non-homologous end joining since they require the Ku proteins, suggesting that Taz1 is necessary for protection from inappropriate repair activities at the telomere. Taz1 is itself a double-strand DNA binding protein that shares homology with the human TRF1 and TRF2 proteins (Cooper et al. 1997; Li et al. 2000). The mechanism of end-protection by these double-stranded telomeric DNA binding proteins will be explored further in Chapter 1 of this thesis.

It seems that even the non-canonical telomeres of D. melanogaster are protected with the help of a protein. Heterochromatin protein 1 (HP1) is a chromosomal protein that among other places is localized to telomeres (James et al. 1989). Although HP1 associates with transposable elements (van Steensel et al. 2001) it is interesting that its localization at telomeres is independent of presence of the retrotransposons since HP1 can also be found on terminally deleted chromosomes, which lack these elements (Fanti et al. 1998). Numerous mutants of HP1 give rise to end-to-end fusions of chromosomes (Fanti et al. 1998), showing its role in telomere protection. Currently it is a complete mystery how HP1 is able to protect the chromosome ends, especially if one notes that HP1 itself does not seem to have DNA binding ability (Singh et al. 1991; Powers and Eissenberg 1993). Mutation in another *Drosophila* protein, UbcD leads to formation of fusions. Although the nature of these fusions is unclear, it has been proposed that a ubiquitin-conjugating (E2) enzyme activity of UbcD might be necessary for proper behavior of telomeres in *D. melanogaster* (Cenci et al. 1997).

Currently, there is also little knowledge about how telomeres are protected in human cells. Observation of low level of telomere fusions, which retain telomeric DNA, occurring in mouse embryo fibroblasts that lack Ku70, Ku80 and DNA-PKcs (Bailey et al. 1999; Samper et al. 2000; Goytisolo et al. 2001), implicates this complex in end protection. Although Ku has been reported to interact with both of the double strand binding telomeric proteins TRF1 and TRF2 (Hsu et al. 2000),(Song et al. 2000), the data are insufficient for these conclusions and Ku may also simply localize to telomeres through its ability to interact with DNA ends (Walker et al. 2001) including DNA ends containing telomeric DNA (Bianchi and de Lange 1999).

How the protection of telomere ends might be achieved molecularly is suggested by the structure of *Oxytricha* TEBP, which shows how the very 3' end of chromosomes can be hidden in a deep hydrophobic protein pocket (Horvath et al. 1998). A tantalizing possibility of a second way of hiding the very end comes from a finding that telomeres in evolutionarily distant species end with a t-loop (Griffith et al. 1999; Murti and Prescott 1999; Munoz-Jordan et al. 2001)(Figure i-4). Observation of the chromosome termini from human and mouse cells using electron microscopy revealed that the telomere loops back forming a large duplex lariat called the t-loop (Griffith et al. 1999). The t-loop is stabilized by the strand-invasion of the 3' telomeric overhang into the double-stranded telomeric DNA. Such architectural remodeling of a telomere in effect masks the very end, thus eliminating the need for its direct protection by a TEBP-like protein. T-loops were also found at the chromosome ends in *T. brucei* (Munoz-Jordan et al. 2001), as well as at the ends of micronuclear polytene chromosomes of *O. fallax* (Murti and Prescott 1999). Thus *Oxytricha*, and possibly other organisms might use both the t-loop

directed protection, as well as the TEBP like protection of their termini, possibly at different times in the cell cycle (Baumann and Cech 2001; de Lange 2001).

No matter what the basis of telomere protection, there is ample evidence that lack of protection can have disastrous effects on the survival of the organism. Generally, when telomere function is compromised, cells grow very poorly and unless they find an alternative way of maintaining their telomeres, they undergo a terminal arrest or die. A few examples from recent literature illustrate this point.

A number of studies have explored what happens in the ciliate Tetrahymena when the RNA template is mutated resulting in incorporation of altered sequences into the telomere (Yu et al. 1990; Kirk et al. 1997). As discussed earlier, such changes may result in telomere length deregulation, presumably because changes in telomere sequence preclude or modify the binding of telomere protein necessary for length regulation. By the same token, some changes were severe enough to alter telomeric protection and lead to the appearance of large cells with abnormal nuclei and in many cases complete cessation of growth of certain strains (Yu et al. 1990). In particular, changing the telomeric sequence from GGGGTT to GGGGTTTT leads to a severe anaphase block with appearance of the telomere associations (Kirk et al. 1997). Although the cause of the growth arrest was misinterpreted at the time to mean that the telomere function was necessary for correct chromosome segregation, and not for protection of ends from fusions, the outcomes of telomere dysfunction were deadly for the organism.

Lack of telomere function in *S. cerevisiae* also has deleterious effects for cell survival. All of the Ever Shorter Telomeres (est) mutants (Lundblad and Szostak 1989; Lendvay et al. 1996) as well as the mutant lacking the RNA template (tlc1) (Singer and

Gottschling 1994) cease to grow and die when their telomeres become too short to support proper telomere function. Cultures only survive when telomeric DNA is restored through recombination dependent processes (Lundblad and Blackburn 1993). When this independent process is not available in rad52 mutants (Lundblad and Blackburn 1993), or double mutants of rad50 and rad51 (Le et al. 1999), lack of telomere maintenance is completely lethal.

The outcome of lack of telomere function in human cells will be explored in detail in Chapter 2 of this thesis but generally the result depends on the cell type. Some cells respond with permanent growth arrest, and others with apoptosis. When telomerase is inhibited in human tumor cell lines by expression of a dominant negative allele of telomerase (Hahn et al. 1999; Zhang et al. 1999) cells cease to grow and appear to undergo apoptosis. This phenotype is observed after an expected lag phase during which telomeres shorten. Since the replicative potential of cells expressing the dominant negative allele of hTERT is thwarted, such cells, as expected, do not give rise to tumors in nude mice (Hahn et al. 1999). A more recent study using a chemical inhibitor of telomerase led to a similar conclusion but instead of apoptosis, a cell cycle arrest with characteristics of senescence was seen (K. Damm, personal communication).

A mouse strain lacking the telomerase RNA gene is a good illustration of the consequences of telomere dysfunction at the organismal level. As discussed earlier, telomere dysfunction in mTERC -/- animals commences only after the mice have been bred for a number of generations. The development of chromosomal fusions, a marker of telomere deprotection, coincides with the appearance of adverse effects that include sterility due to abnormal spermatogenesis resulting in cell death in the testis (Hemann et al. 2001), decreased proliferative capacity of the hematopoietic tissues (Lee et al. 1998),

shortened life-span, and a reduced capacity to heal skin lesions or to respond to blood cell depletion (Rudolph et al. 1999). Additionally, the rate of spontaneous tumor formation rises in the late generations of mTERC -/- mice, suggesting that the instability that is triggered by telomere dysfunction might contribute to tumorigenesis (Rudolph et al. 1999).

Human telomeric proteins

In recent years we have seen an enormous surge in our knowledge of the protein components of mammalian telomeres. The first two human telomeric proteins, TRF1 and TRF2 and their interacting partners will be described in detail below. The presence of these proteins on telomeres is firmly established. Ku70, Ku80, and DNA-PKcs as noted above, have a protective function at telomeres. Recently chromatin IP analysis has revealed that all three proteins were somewhat enriched on the telomeric DNA as compared to bulk DNA as detected with an Alu repeat probe (d'Adda di Fagagna et al. 2001). It is unclear at this point, whether the association of Ku proteins with telomeres is constant or whether they bind at specific times. Human Pot1, an ortholog of Pot1p from *S.pombe* has been described (Baumann and Cech 2001) but there is no data yet on the localization or function of Pot1 in human cells. Finally, there is data to suggest that WRN and BLM proteins, both orthologs of Sgs1 RecQ helicase in *S. cerevisiae* can be present at telomeres. BLM has been reported to colocalize with a subfraction of the telomeres in human cells (Yankiwski et al. 2000), although the significance of such infrequent colocalization is unclear. WRN protein can be found mainly in the nucleoli of cells (Marciniak et al. 1998), but in cells that maintain their telomere length through an alternative mechanism described before (ALT), WRN can also reside in ALT associated

PML (AA-PML) bodies, where it colocalizes with PML, Rad52, TRF1, and TRF2 (Johnson et al. 2001). By analogy to Sgs1 in *S. cerevisiae*, WRN could play a role in telomere maintenance by the alternative pathways. The only indication that WRN protein might also play a role in regulating length in non-ALT cells comes from the finding that telomere shortening is accelerated in cells from Werner Syndrome patients (Schulz et al. 1996).

TRF1 and TRF2

TRF1 was identified in cell extracts as an activity that specifically bound to human TTAGGG repeats (Zhong et al. 1992; Chong et al. 1995). Biochemical characterization revealed a homodimeric protein (Bianchi et al. 1997) that uses two Myb-type helix turn helix motifs to bind to variably spaced sites of the sequence 5'-YTAGGGTTR-3' (Bianchi 1999). TRF1 is widely expressed and due to its binding activity, specifically localizes to telomeres at all stages of the cell cycle (Chong et al. 1995). Electron microscopy studies of TRF1 binding to arrays of TTAGGG repeats have shown that the protein is able to pair two duplex tracts of telomeric DNA (Griffith et al. 1998). Such architectural activity has been proposed to aid TRF1 in telomere length regulation. As will be discussed further in Chapter 3, TRF1 influences telomere length *in vivo* through regulating the elongation pathway of telomere length maintenance (Karlseder and de Lange; van Steensel and de Lange 1997)

Three proteins interact with TRF1 at telomeres. Tankyrase1 (Smith et al. 1998), Tankyrase2 (Kaminker et al. 2001), and TIN2 (Kim et al. 1999) were discovered in separate yeast-two-hybrid screens using TRF1 as bait. Tankyrase1, a poly (ADP-ribose) polymerase (PARP), binds to an acidic N-terminus of TRF1 and modifies it using

its catalytic activity. This modification alters TRF1's ability to bind to telomeric DNA *in vivo* and *in vitro* thus indirectly influencing telomere length (Smith et al. 1998; Smith and de Lange 2000). The biochemical role of TIN2 is less well defined but its influence on telomere length is also consistent with the regulation of TRF1's presence on the telomere (Ye and de Lange; Kim et al. 1999).

Early human cDNA sequencing efforts uncovered a cDNA fragment encoding a Myb domain that had striking similarities to that found in TRF1 (Bilaud et al. 1996). Cloning of the full-length cDNA revealed a protein, which due to its similarity to TRF1 and ability to bind TTAGGG repeats was named TTAGGG repeat binding factor 2 (TRF2) (Bilaud et al. 1997; Broccoli et al. 1997). As shown in Figure i-2, the highest conservation between TRF1 and TRF2 is found in the Myb domains (58%). This level of conservation is in agreement with the fact that both proteins recognize the same sequence *in vitro* (Bianchi et al.; Broccoli et al. 1997) as well as with the localization of TRF2 to telomeric DNA *in vivo* (Broccoli et al. 1997), and Figure i-3.

The second most conserved domain in TRF1 and TRF2 is the TRF homology domain (TRFH) (Broccoli et al. 1997; Li et al. 2000). This part of the protein is responsible for homotypic interactions (Bianchi et al. 1997) as well as interactions with other proteins (TIN2 (Kim et al. 1999) for TRF1, and hRap1 (Li et al. 2000) for TRF2). Although the sequence identity between TRF1 and 2 is only 29% within TRFH, crystal structures of these domains can be superimposed (Fairall et al. 2001). Despite this overall architectural conservation, the structure reveals slight differences between the dimer interfaces of TRF1 and 2 that include changes in the length of the interacting helices, differences in the side chain amino acids and in the hydrogen bonding pattern.

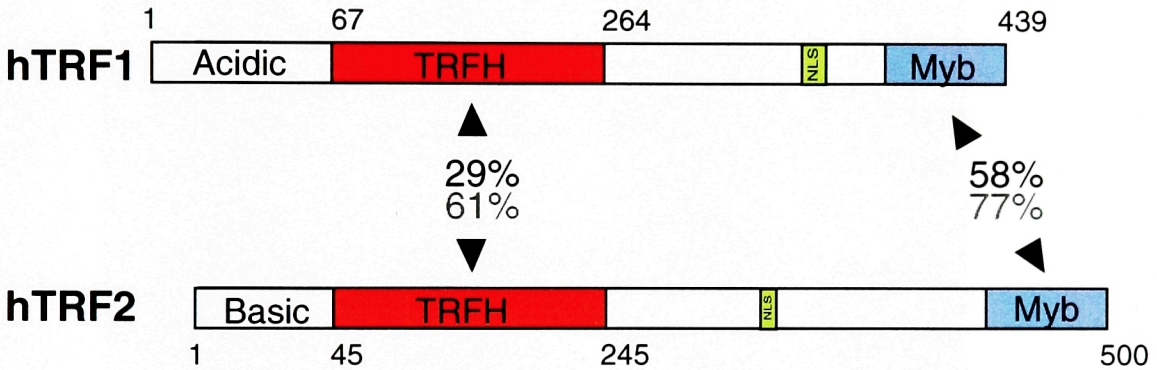

Figure i-2. **Schematic of domain structure of TRF1 and TRF2 (adapted from Broccoli et al., 1997; Griffith et al., 1999).** Not drawn to scale. Identities are shown in black, similarities in grey. TRF homology (TRFH) domain is used in homodimerization as well as in interactions with other factors specific for each protein. Myb domain is used in DNA binding.

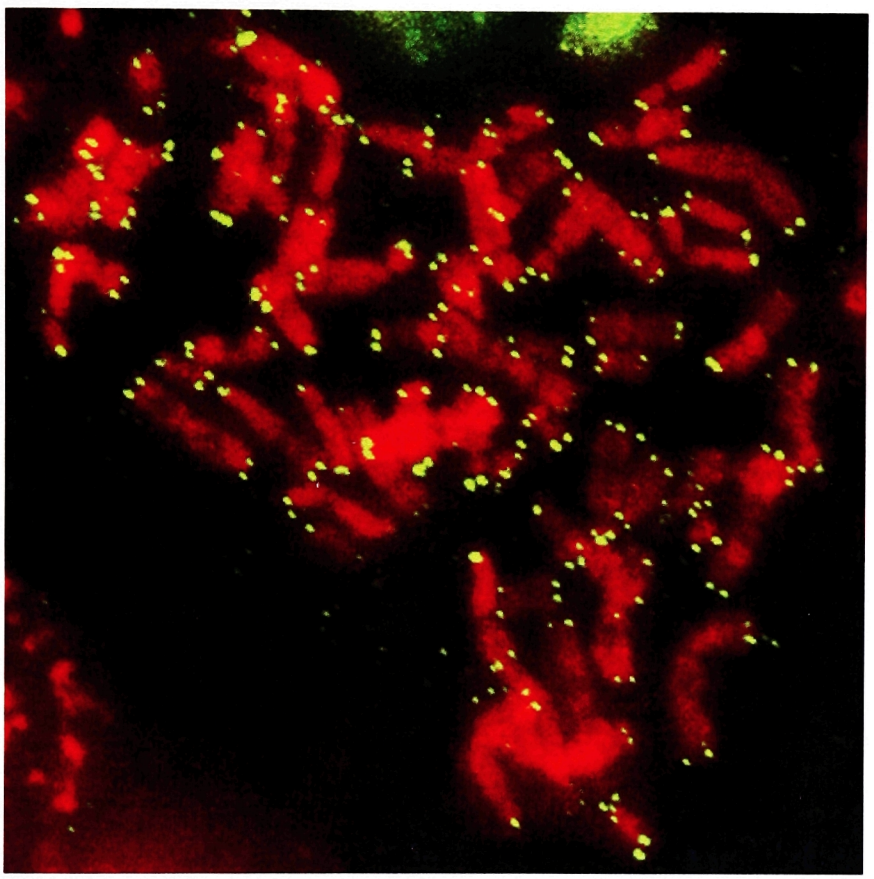

Figure i-3. **Localization of TRF2 to telomeres of human chromosomes.** Indirect immunofluorescence with 647 antibody (raised against full length TRF2 protein) on a metaphase spread of HeLaI.2.11 cells.

These findings explain why TRF1 and 2 fail to heterodimerize (Broccoli et al. 1997; Zhu et al. 2000).

Electron microscopic studies directly implicate TRF2 in t-loop formation. Baculovirus-derived TRF2 is able to induce invasion of the 3' single-stranded TTAGGG repeats into duplex telomeric DNA, forming t-loops *in vitro* (Griffith et al. 1999). A single-stranded overhang of six nucleotides of a G strand (TTAGGG) is sufficient for *in vitro* t-loop formation by TRF2 and it needs to be adjacent to the double-stranded telomeric DNA so that the double- to single-stranded transition is composed of TTAGGG sequence (Stansel et al. 2001). When the t-loop is formed, TRF2 can be visualized at its base where the invasion of the single-strand overhang is thought to occur (Griffith et al. 1999; Stansel et al. 2001). Based on these findings and the earlier studies of the biochemical activities of TRF1, a model for t-loop formation has been proposed (Griffith et al. 1999; Stansel et al. 2001) and Figure i-4. In this model, TRF1 pairs the telomeric sequences and TRF2 aids in the invasion by the single-stranded overhang into the telomeric repeats. Besides creating the t-loops, telomeric proteins might also stabilize these structures.

TRF2, like TRF1 has multiple binding partners. Rap1, an ortholog of *S. cerevisiae's* Rap1 (discussed earlier) has been identified in a yeast-two-hybrid screen with TRF2 as bait. Like the yeast Rap1p, hRap1 is implicated in telomere length regulation although its mode of action is not yet understood (Li et al. 2000). However, unlike the yeast protein, hRap1 does not bind to DNA directly and uses TRF2 as an anchor. Further analysis of known telomeric proteins in *S. pombe* revealed that Taz1 is an ortholog of the human TRF proteins (Li et al. 2000). This suggests that the telomeric complex in *S. pombe* resembles the human complex more than it does the *S.*

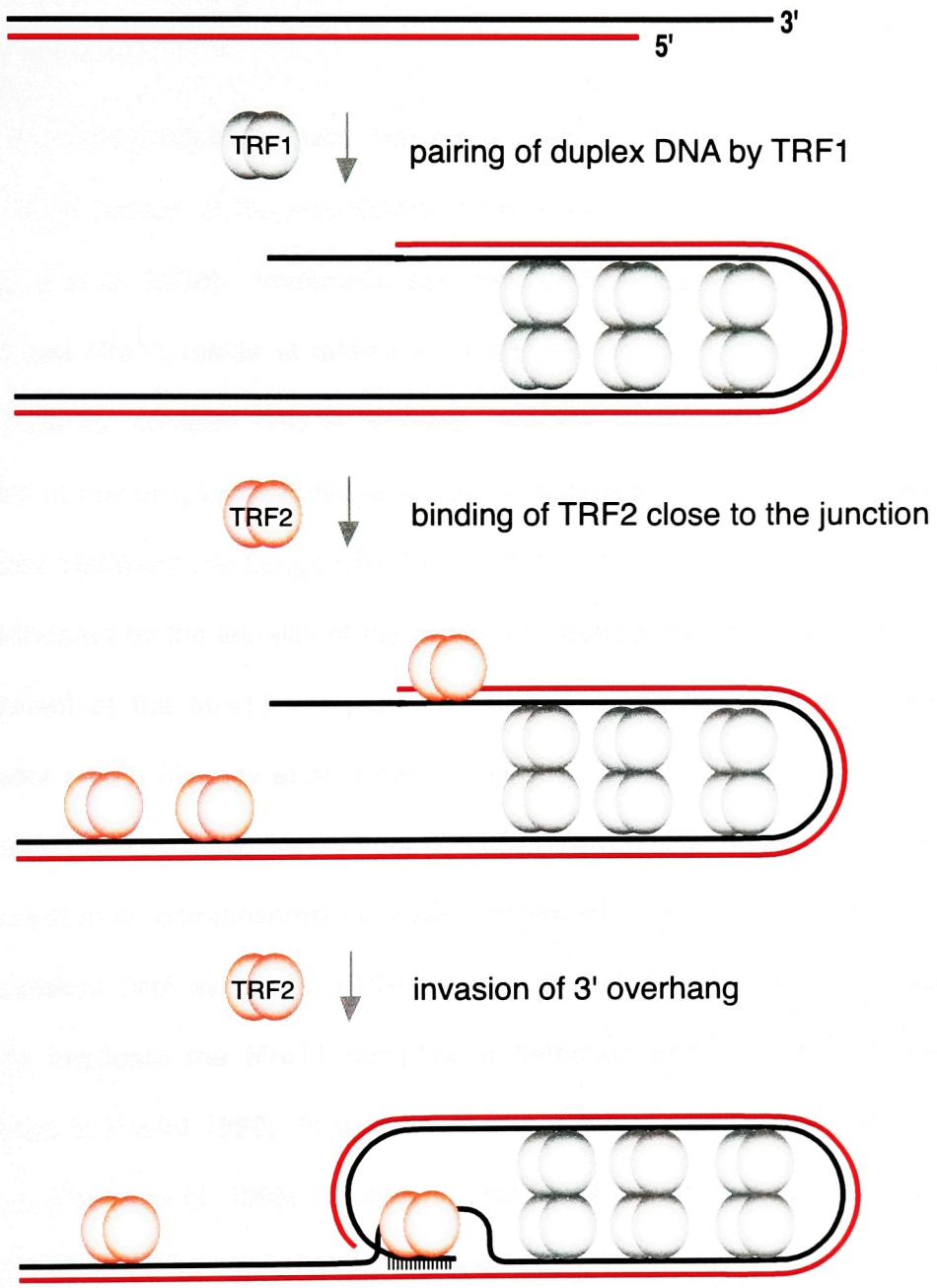

Figure i-4. **Schematic of t-loop formation.** Adapted from (Griffith et al.,1999; Steensel et al., 2001).

cerevisiae's telomeric complex. It also suggests that the ancestral telomeres had both Rap1 like molecules and a TRF-like molecules, and the budding yeast lost the TRF like component.

Immunoprecipitation with antibodies against TRF2 from human cells revealed that a small portion of the Rad50/Mre11/Nbs repair complex associates with TRF2 *in vivo* (Zhu et al. 2000). Immunofluorescence and cell cycle experiments showed that Rad50 and Mre11 reside at telomeres during all stages of the cell cycle, whether as Nbs1 joins the complex only in S-phase. Genetic studies have implicated the Mre11 complex in homologous recombination and in telomere maintenance in yeast (reviewed in (Haber 1998)and (de Lange and Petrini 2001)). Studies in mammalian systems have been hindered by the lethality of the organisms lacking the complex. However, NBS1, a component of the Mre11 complex, is mutated in patients with Nijmegen breakage syndrome (NBS) (Carney et al. 1998; Varon et al. 1998) and Mre11 itself is mutated in an Ataxia-Telangiectasia-like disorder (A-TLD) (Stewart et al. 1999). NBS and ATLD are characterized by chromosomal instability, increased sensitivity to ionizing radiation, and radioresistant DNA synthesis (RDS) (Carney et al. 1998; Stewart et al. 1999). These findings implicate the Mre11 complex in detection and signaling of DNA damage (reviewed in Petrini 1999). In agreement, the complex rapidly localizes to the sites of damage (Nelms et al. 1998). Moreover, Nbs is a substrate for phosphorylation by ATM (Gatei et al. 2000; Lim et al. 2000; Wu et al. 2000; Zhao et al. 2000) and it is necessary for the ATM dependent S phase checkpoint (Lim et al. 2000). Currently the functional consequences of the telomeric localization of the Mre11 complex are unknown although it has been suggested that the complex could generate the 3' G-overhangs or could

participate in formation, stabilization and/or resolution of t-loops (Zhu et al. 2000; de Lange and Petrini 2001)

The experimental part of this thesis concentrates on TRF2. Its function has been explored using an *ex vivo* primary cell culture system, in which a number of different cell types were used in order to gain a better understanding of the protein. First, I describe in detail the role of TRF2 in protection of chromosome ends. Then, I show that the removal of TRF2 from the telomeres leads to the rapid induction of senescence in primary cells. This will be followed by description of TRF2 as an essential regulator of telomere length, mainly, if not exclusively involved in determining the shortening rate of telomeres. Chapter 4 describes telomere loss and growth arrest phenotypes associated with a truncation allele of TRF2 that lacks its N-terminal basic domain, and suggests that this domain is important for the proper function of TRF2. In Chapter 5 an additional phenotype of loss of TRF2 function, whole genome reduplication and aberrant centrosome duplication, as well as the finding of TRF2 at centrosomes will be discussed.

Chapter 1

The role of TRF2 in telomere end protection

Introduction

Telomeres confer protection onto chromosome ends. Early cytological studies revealed that ends devoid of telomeres are spontaneously repaired by fusion with other broken ends (McClintock 1938). Telomeric DNA seems to be a necessary component of the protected terminus. In human somatic cells, which naturally lack, or have a very low level of telomerase, telomeres shorten by 50-200 bp per division (Cooke and Smith 1986; Harley et al. 1990; Hastie et al. 1990). Once a certain, still ill-defined- length setting is reached, telomeres lose their ability to protect and become fusogenic, resulting in the formation of dicentric chromosomes (Wolman 1964; Thompson and Holliday 1975; Benn 1976).

End-to-end fusions also arise in tumors where in many cases their appearance has been correlated with short telomere length ((Counter et al. 1992; Saltman et al. 1993), reviewed in de Lange 1995). As pointed out previously (de Lange 1995), resolution of dicentric chromosomes can lead to loss of heterozygosity (LOH), gene amplification and chromosomal rearrangements, events that are hallmarks of many cancer cells. However, most human cancer cells are characterized by high level of telomerase activity (reviewed in Shay and Bacchetti 1997), hence telomere-directed chromosomal abnormalities might be important at the early stages of the tumor development.

In the past four years, the mouse strain lacking the telomerase RNA (mTERC KO) became a very fruitful model system for studying telomere dysfunction and its consequences for tumorigenesis. Cells derived from mice null for telomerase exhibit end-to-end fusions (Blasco et al. 1997). In mice, as in humans, telomeres become fusogenic only after they become short, which in a mouse can take 4 to 6 generations of

growth without telomerase (Blasco et al. 1997; Herrera et al. 1999). It has been proposed that lack of telomeres in the aging mice of the late generation mTERC KO could be responsible for the increased rate of spontaneous cancers seen in these animals (Rudolph et al. 1999). The majority of tumors in such mice originated from highly proliferative cells that were expected to divide extensively during the animal's life, leading to increased attrition of their telomeres. In agreement, the tumor cells were found to display a 3-18 fold increase in chromosome fusions (Rudolph et al. 1999). Recent studies (Artandi et al. 2000) further substantiate the notion that lack of telomeres leads to increased genomic instability and enhanced tumorigenesis (reviewed in DePinho 2000).

A number of different repair pathways participate in the maintenance of general stability of the genome (reviewed in Hoeijmakers 2001). Two of these pathways, homologous recombination (HR) and non-homologous end joining (NHEJ) are pertinent to the repair of double-stranded DNA breaks. Engagement of both of the pathways at telomeres should be avoided. HR involving telomeric repeats might lead to poorly-regulated telomere lengthening (Dunham et al. 2000). NHEJ activity at telomeres could lead to formation of end-to-end fusions.

The core of NHEJ pathway consists of five proteins (Ku80, Ku70, DNA-PKcs, DNA Ligase IV [Lig4], and XRCC4) that work in concert to repair site specific breaks, which occur during a physiological event of V(D)J recombination in the immune system, as well as random breaks occurring in the genome (reviewed in Critchlow and Jackson 1998). Surprisingly, lack of Ku70, Ku80 or DNA-PKcs in mouse cells leads to a mild telomere deprotection phenotype (Bailey et al. 1999; Samper et al. 2000; Goytisolo et al. 2001). The function of the DNA-PK complex in telomere protection seems to be

independent of its function in NHEJ, since deletion of the other two components of the pathway- Lig4 or XRCC4, which together are thought to act in the ligation step of the repair reaction (Lieber 1999), do not show telomere end-to-end fusions ((Ferguson et al. 2000; Gao et al. 2000), this chapter).

The molecular mechanism of protection by telomeric DNA has been proposed to involve formation of the t-loop (Griffith et al. 1999), a large, lasso-like structure in which the telomeric G-overhang is tucked into the double-stranded telomeric DNA. Although repetitive arrays like the telomeric DNA might be imagined to spontaneously form t-loops, it has been shown that the telomeric proteins aid in t-loop formation and/or stabilization. In particular, TTAGGG repeat binding factor 2 (TRF2) is capable of generating t-loops *in vitro* when supplied with a substrate with duplex TTAGGG repeats ending with the telomeric 3' single-stranded overhang (Griffith et al. 1999; Stansel et al. 2001). Electron microscopic analysis of *in vitro* formed t-loops revealed that TRF2 can be visualized at the base of the t-loop where the invasion of the single strand is thought to occur Griffith et al. 1999; Stansel et al. 2001).

TRF2 is one of two proteins that directly bind to the mammalian telomeric DNA (Bilaud et al. 1997; Broccoli et al. 1997). It binds DNA as a homodimer using two Myb related helix-turn-helix domains brought together by the dimerization of the TRF2 polypeptide through a TRF homology (TRFH) domain (Broccoli et al. 1997; Fairall et al. 2001). Another distinct domain of TRF2 is its N-terminus, which is highly basic (pI of 9) (Broccoli et al. 1997). TRF2 resides at all telomeres throughout the cell cycle (Broccoli et al. 1997).

This chapter focuses on the role of TRF2 in telomere protection. Experiments described in this section show that loss of TRF2 from telomeres leads to telomere

deprotection, which manifests itself in formation of end-to-end fusions, visible as dicentric chromosomes in metaphase cells and chromosome bridges in anaphase cells. The fusions are covalent and are formed through Ligase 4 action on chromosome ends that most likely have lost the single-stranded G-overhangs. Breakage of end-to-end fusions in subsequent divisions can lead to translocations, which are markers of genomic instability. The mechanism of protection by TRF2 is suggested by the decrease in the frequency of t-loops in cells without functional TRF2. Unregulated dissolution of the t-loops is proposed to constitute a necessary event leading to fusion formation after TRF2 inhibition. Furthermore, these findings suggest that short telomeres in senescent or tumor cells become deprotected because they fail to recruit sufficient amount of TRF2 to support t-loop formation.

Results

To study the function of TRF2 at human telomeres, a dominant negative allele of TRF2 was expressed in a number of different cell types. The design of the dominant negative allele was guided by the knowledge that TRF2, like TRF1 is a dimeric protein (Bianchi et al. 1997; Broccoli et al. 1997), which preferably uses two Myb domains to efficiently bind the telomeric DNA (Bianchi et al. 1999). A protein containing the dimerization domain but lacking the Myb domain should be able to interact with the endogenous protein and preclude it from binding to telomeres. Additionally, a highly basic N-terminal domain of TRF2 was removed and replaced with a myc tag to facilitate discrimination between the dominant negative allele and the endogenous protein. Thus, the dominant negative allele of TRF2 used in these studies lacks the Myb domain and the basic domain of the protein and is designated TRF2$^{\Delta B \Delta M}$ (Figure 1-1). The full length TRF2 (FLTRF2) was used as a control for many of the studies and sometimes included

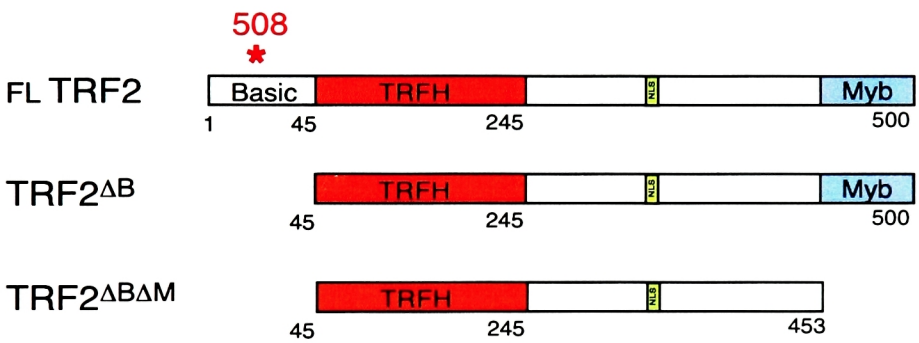

Figure 1-1. **Schematic of TRF2 alleles used in these studies.** In some experiments, constructs with a N-terminal FLAG or MYC tag were used. Untagged FL TRF2 included the endogenous methionine as the first amino acid. Untagged deletion alleles included a methionine in front of amino acid 45 and ended with amino acid 453 or 500, as indicated. In N-terminally tagged FL TRF2, the tag was fused in-frame with the 2nd amino acid of the protein, and in tagged $TRF2^{\Delta B}$ and $TRF2^{\Delta B\Delta M}$ alleles, the tag was fused to amino acid 45. Asterisk indicates a segment of TRF2 that is recognized by antibody 508. Antibody 647, raised against a full length protein, recognizes all of the alleles used in this study.

an N-terminal tag, as indicated in the text. The protein lacking only the basic domain ($TRF2^{\Delta B}$) will be discussed separately (Chapter 4) since this allele is able to localize to telomeres and phenotypes associated with its expression are different from an inhibition of telomeric TRF2 by dominant negative TRF2.

Two different systems were employed to overexpress TRF2 alleles (Figure 1-2). One of them made use of retroviral vectors, which when transfected into a packaging cell line produced replication-deficient retroviral particles that were subsequently used for infection of human and mouse primary fibroblasts. A timeline of experiments following retroviral infection is shown in Figure 1-2 (top). Cells were infected three times in 5-hour intervals and the selection was started on the following day. Puromycin or hygromycin were the most commonly used markers for infection of the TRF2 alleles. Selection produced a pure population of expressing cells within 3 and 5 days for puromycin and hygromycin, respectively. Expression of the alleles was confirmed by immunofluorescence with appropriate antibodies and by western analysis.

A second system used in these studies is an inducible expression system in the HTC75 cell line, a Tetracyclin-inducible derivative of HT1080 human fibrosarcoma cell line previously used to study the function of TRF1 in telomere length regulation (van Steensel and de Lange 1997). An untagged full length TRF2 or a FLAG-tagged $TRF2^{\Delta B\Delta M}$ were placed under control of a Tetracyclin-controlled promoter and were stably transfected into the HTC75 cells. Subsequently, single cell clones were isolated and named P clones (FLTRF2) or T clones ($TRF2^{\Delta B\Delta M}$). A control cell line expressing no exogenous protein was also created and named B27. As opposed to the retroviral system described above, selection of stable clones gave rise to clonal populations of cells, requiring analysis of a number of clones of each type. The

Retroviral delivery system (primary fibroblasts)

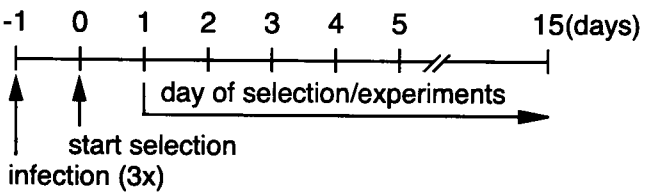

Tetracyclin-inducible system (HTC75 cells)

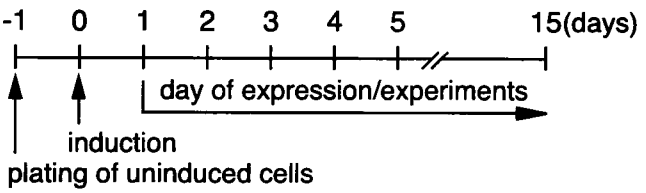

Figure 1-2. **Timeline of experiments using the retroviral delivery system and the Tetracyclin-inducible system.** Alleles of TRF2 shown in Figure 1-1 were delivered using retroviral vectors or were stably transfected and induced by removal of doxycyclin (Tetracyclin derivative) from the media. Expression of all alleles was confirmed using immunofluorescence and western blotting.

Tetracyclin-inducible system was set up such that removal of doxycyclin from the medium resulted in a relief of repression and appearance of expression of the alleles. For clarity, "induced" will mean that the indicated allele was expressed and "non-induced" that it was not expressed. Expression of the alleles reached its highest levels within one day after induction (van Steensel et al. 1998) and this was the day that was designated to be the first day of expression (Figure 1-1, bottom).

In order to test the effects of expression of a FLTRF2 and TRF2$^{\Delta B\Delta M}$ allele on endogenous TRF1 and TRF2, a subclone of human HeLa1 cells (Saltman et al. 1993), HeLa1.2.11 with particularly long telomeres of 15-40 kbp (Griffith et al. 1999), were infected with a myc-tagged FLTRF2 and myc-tagged TRF2$^{\Delta B\Delta M}$ (Figure 1-3). One day after infection the cells were fixed and immunostained with an antibody recognizing the myc tag (9E10), an endogenous and transduced FLTRF2 (508), and TRF1 (371). Antibody 508 was raised against a peptide present in the basic domain and it recognizes the full-length TRF2 but not TRF2$^{\Delta B\Delta M}$ or TRF2$^{\Delta B}$ (van Steensel et al. 1998). FLTRF2, when overexpressed, gave high nucleoplasmic staining with overlaid punctate staining that co-localized with TRF1 (Figure 1-3, B, top panel), suggesting that some of the expressed TRF2 localizes to telomeres. Moreover, the TRF1 staining pattern did not change with FLTRF2 expression, indicating that presence of TRF1 on telomeres was largely unperturbed. A diminished level of TRF1 on telomeres has been noticed in cells that expressed the FLTRF2 at a very high level (van Steensel et al. 1998), suggesting that a very high load of telomeric TRF2, as sometimes achieved in transient transfection experiments, might be able to displace some of the TRF1 from telomeres. TRF2$^{\Delta B\Delta M}$, when overexpressed, gave a diffuse nucleoplasmic staining and efficiently removed the endogenous TRF2 from the telomeres, visualized as loss of punctate staining of

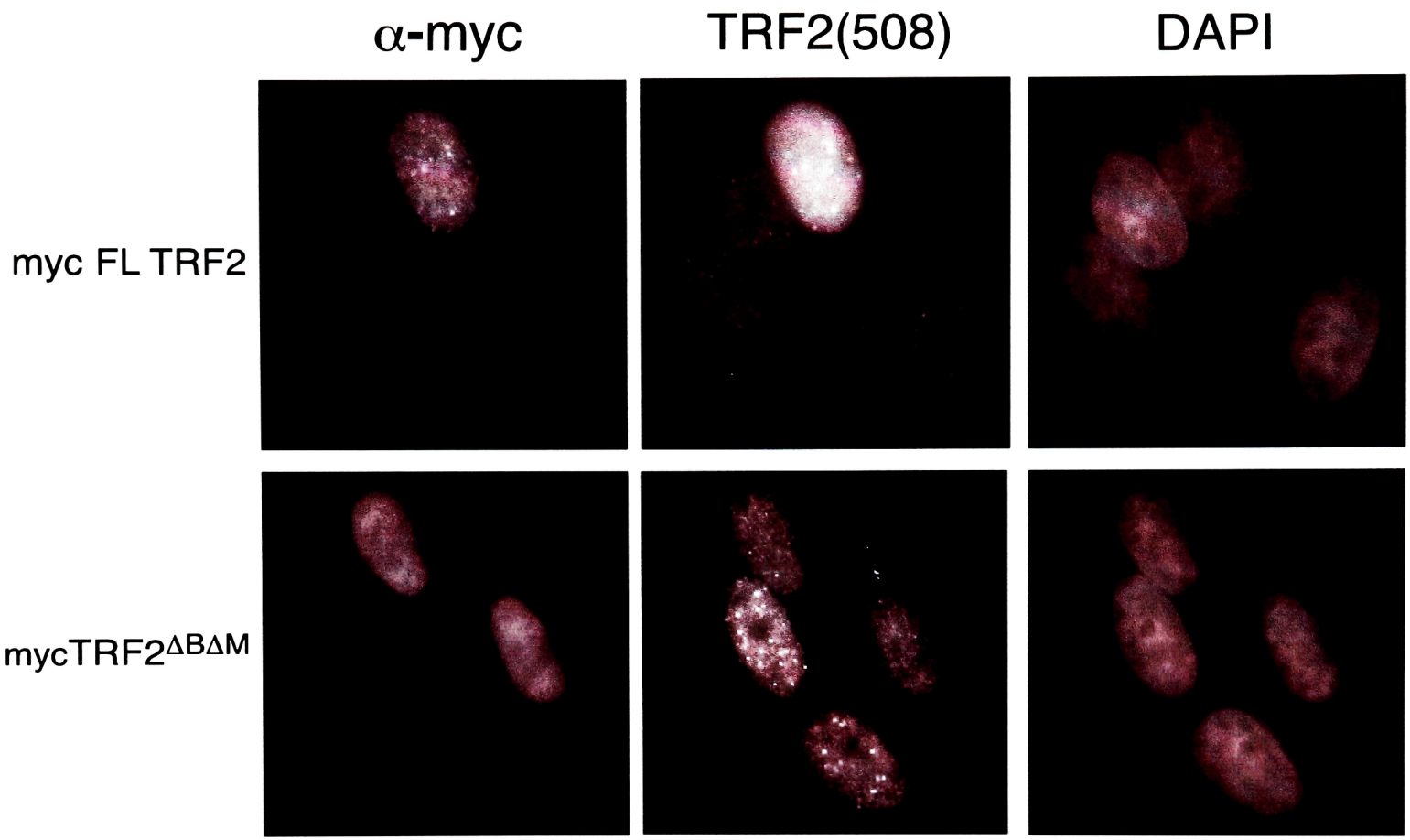

Figure 1-3. **Effects of expression of myc-tagged full length TRF2 and TRF2$^{\Delta B\Delta M}$ on endogenous TRF1 and TRF2.** Indirect immunofluorescence of HeLaI.2.11 cells infected with myc-tagged FLTRF2 or TRF2$^{\Delta B\Delta M}$. Analysis was performed one day after infection on non-selected cells. Staining with an antibody against a myc tag (9E10) reveals infected cells. Endogenous TRF2 and FLTRF2 is visualized with antibody 508 **(A)**, and TRF1 with antibody 371 **(B)**. Legend continues on the next page

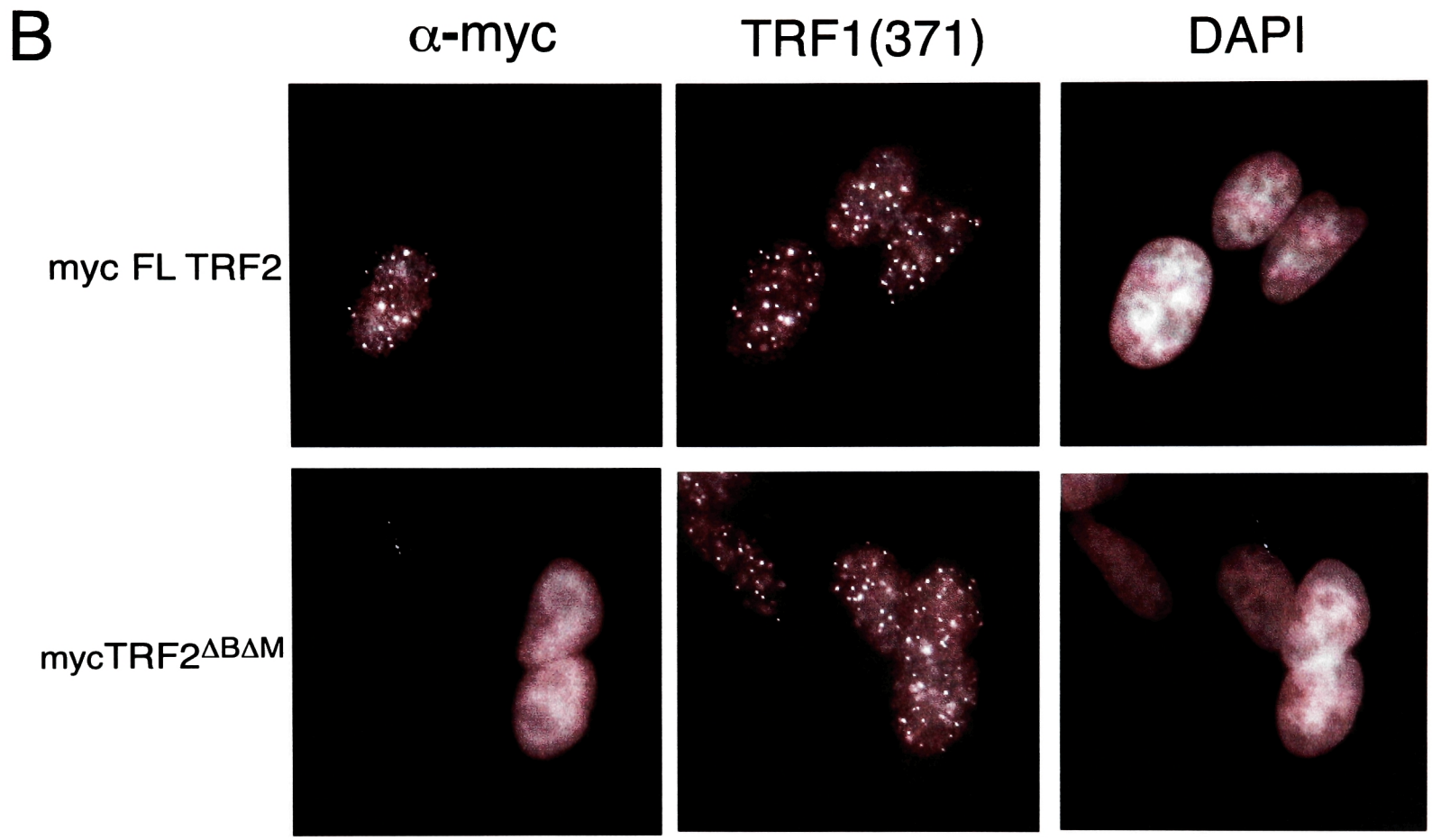

Figure 1-3 cont. Legend continued from the previous page: Antibody 508 was raised against a peptide (GRRASRSSGRARRGRHEPGLGGP AEAG) present in the basic domain of TRF2 and it recognizes FLTRF2, and the endogenous TRF2 but does not recognize $TRF2^{\Delta B \Delta M}$. DNA was counterstained with DAPI.

endogenous TRF2 when the myc-tagged TRF2$^{\Delta B\Delta M}$ was expressed (Figure 1-3, A, bottom panel). Telomeric TRF1 did not seem to be affected by TRF2$^{\Delta B\Delta M}$ expression (Figure 1-3, B, bottom panel).

Expression of TRF2 $^{\Delta B\Delta M}$ in the HTC75 cells and in human primary fibroblasts led to appearance of frequent anaphase bridges and lagging chromosomes (Figure 1-4). Such anaphase abnormalities were very rare in any other cell line analyzed, including non-induced HTC75 T cell lines (van Steensel et al. 1998), IMR90 cells that did not express any exogenous proteins (vector in Figure 1-4, A, Table 1-1), or FLTRF2 expressing cells (Table 1-1). Quantification of the frequency of anaphase bridges in the HTC75 T4 cell line on the 4th day of induction revealed a very low frequency of anaphase bridges and lagging chromosomes (less than 0.1 events per anaphase) when expression of TRF2$^{\Delta B\Delta M}$ was not induced. The frequency of bridges and lagging chromosomes increased to 0.7 abnormalities per anaphase with induction of TRF2$^{\Delta B\Delta M}$ (van Steensel et al. 1998). Similarly, IMR90 cells infected with a control virus or FLTRF2, showed only 0.2 fusions per anaphase (Table 1-2) and the expression of the TRF2$^{\Delta B\Delta M}$ allele induced frequent anaphase bridges (1.5 chromosome fusions per anaphase) when scored on day 7 of selection.

Anaphase bridges can arise from abnormal chromosomes with more than one centromere being pulled in opposite directions by the mitotic spindle. If this is the origin of anaphase bridges when TRF2 is inhibited, chromosome fusions in TRF2$^{\Delta B\Delta M}$-expressing cells should be also visible as dicentric chromosomes in metaphase spreads. Indeed, when TRF2$^{\Delta B\Delta M}$ was expressed in IMR90 cells (Figure 1-5) or in HTC75 T cell lines (Figure 1-6 and (van Steensel et al. 1998)) multiple end-to-end fusions are visible. They include both single chromatid arm fusions and double chromatid fusions

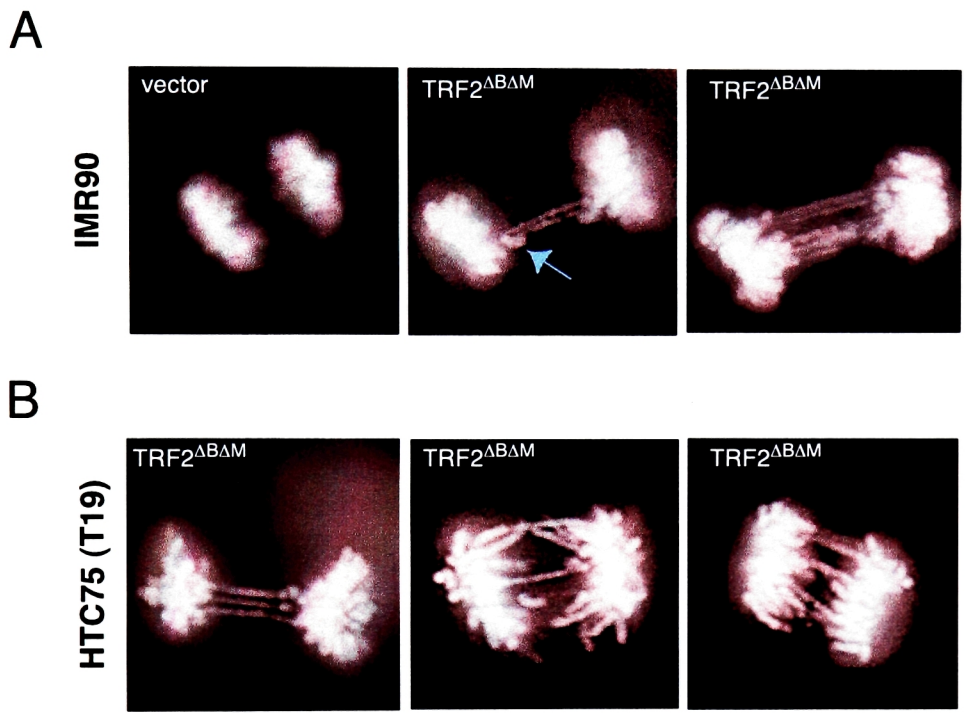

Figure 1-4. **Anaphase bridges in TRF2$^{\Delta B\Delta M}$-expressing IMR90 human primary fibroblasts and HTC75 fibrosarcoma cells**. **A.** Anaphases of IMR90 cells infected with a vector control virus carrying no exogenous TRF2 (vector) or TRF2$^{\Delta B\Delta M}$ (TRF2$^{\Delta B\Delta M}$) on day 7 of selection. **B.** Anaphases of HTC75-T19 cell line expressing TRF2$^{\Delta B\Delta M}$ (TRF2$^{\Delta B\Delta M}$). Expression of TRF2$^{\Delta B\Delta M}$ was induced for 6 days. DNA was stained with DAPI. The arrow points to a lagging chromosome.

Table 1-1. Induction of fusions in anaphase and metaphase IMR90 primary fibroblasts infected with control vector, full length TRF2, and TRF2$^{\Delta B \Delta M}$. All alleles had a N-terminal myc tag. 50 anaphase cells were analyzed for all infections. Scoring of events was done on day 7 of selection and was done on coded samples. Pieces and breaks were also scored in this experiment (see Table 4-2).

Viral vector	Fusions[a] per anaphase	Fraction of anaphases with fusions	Number of metaphases scored	Fusions per metaphase	Fraction of metaphases with fusions
pLPC	0.2	8%	98	0.06	6%
PLPC TRF2	0.3	20%	115	0.2	17%
pLPCTRF2$^{\Delta B \Delta M}$	1.5[b]	78%	57	2.2	55%

[a] including bridges and lagging chromosomes

[b] 0.4 lagging chromosomes per anaphase, 1.1 bridges per anaphase

Table 1-2. Induction of fusions in metaphase cells expressing no exogenous protein or TRF2$^{\Delta B \Delta M}$. The HTC75 T4 and T19 cells were grown under conditions resulting in repression or induction of the dominant negative allele of TRF2, TRF2$^{\Delta B \Delta M}$. The HTC75 B27 cell line which does not express any exogenous protein was used as a control. Metaphase spreads were prepared on day 4 of induction and number of fusions was assessed in 50 metaphase spreads.

Cell line	TRF2 allele	Induction	Fraction of metaphases with fusions	Fusions per metaphase
HTC75 **B27**	none	-	22%	0.2
HTC75 **T4**	TRF2$^{\Delta B \Delta M}$	-	38%	0.4
HTC75 **T4**	TRF2$^{\Delta B \Delta M}$	+	77%	2.4
HTC75 **T19**	TRF2$^{\Delta B \Delta M}$	-	52%	0.6
HTC75 **T19**	TRF2$^{\Delta B \Delta M}$	+	78%	3.5

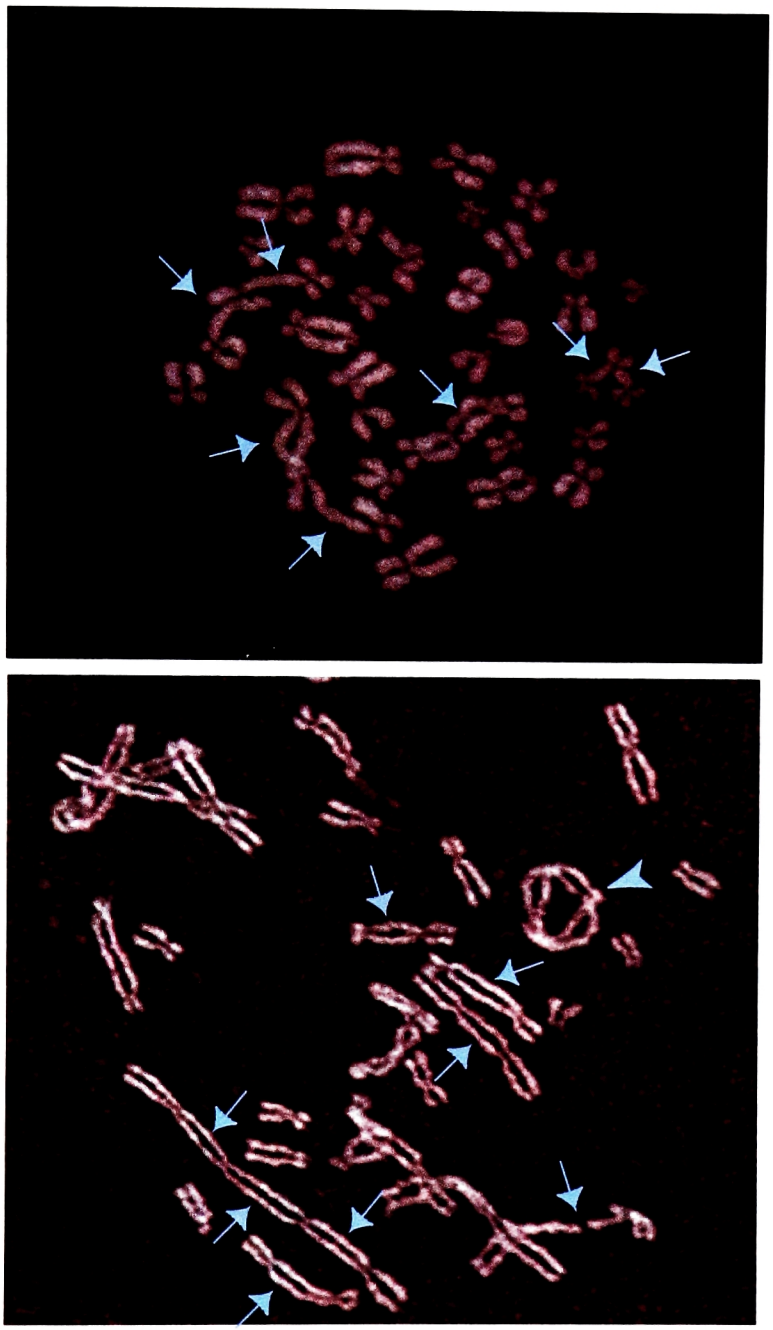

Figure 1-5. **Telomere fusions in metaphases of TRF2$^{\Delta B \Delta M}$-expressing IMR90 human primary fibroblasts.** Metaphase spreads of IMR90 cells expressing TRF2$^{\Delta B \Delta M}$ prepared on day 7 of selection. Chromosomes were stained with DAPI. Many likely chromatid and chromosome end-to-end fusions are seen (arrows). The arrowhead is pointing to a likely ring chromosome.

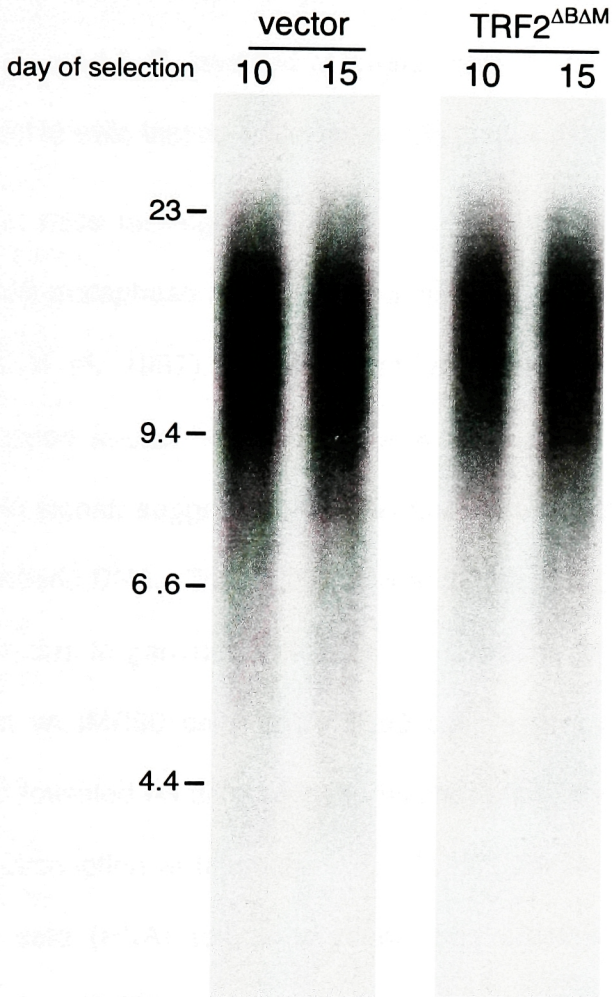

Figure 1-6. **Telomere length analysis in IMR90 primary fibroblasts expressing TRF2$^{\Delta B\Delta M}$.** Southern blot of telomeric restriction fragments from cells carrying no exogenous TRF2 (vector) or TRF2$^{\Delta B\Delta M}$ (TRF2$^{\Delta B\Delta M}$). Genomic DNA was isolated from cells on the indicated days of selection, digested with HinfI and RsaI, fractionated on a 0.7% agarose gel, and hybridized with a TTAGGG repeat probe. The molecular weights of marker DNAs are indicated in kb.

(chromosome fusions). However, sister chromatids were never observed to form fusions. Quantification of the fusions in 50 metaphases of HTC75 T4 and T19 cell lines induced to express TRF2$^{\Delta B\Delta M}$ for 4 days, and IMR90 TRF2$^{\Delta B\Delta M}$ cells on the 7th day of selection (Table 1-1 and 1-2) revealed a greater than 6 fold increase in fusion frequency when compared to cells that do not express exogenous TRF2 or express the FLTRF2 allele.

In mice lacking a telomerase RNA subunit, telomeres gradually shorten and eventually metaphase spreads reveal the presence of chromosome end-to-end fusions (Blasco et al. 1997). When such spreads are further analyzed by performing fluorescence in-situ hybridization with a telomeric probe, sites of fusions show no telomeric signal, suggesting that the fusions formed between chromosomes that have lost telomeric DNA. To ask if end-to-end fusions induced by the presence of TRF2$^{\Delta B\Delta M}$ could be due to generalized loss of the telomeric DNA, telomere length was compared between wt IMR90 cells and IMR90 cells expressing TRF2$^{\Delta B\Delta M}$ (Figure 1-6). The analysis revealed no differences in telomere length between these cells (but see below for the description of telomere length in HTC75 T4 cells). Furthermore, when peptide nucleic acid (PNA) telomeric probe was employed to perform fluorescent in-situ hybridization (FISH) on the metaphases harboring fusions, telomeric signal was always found at the sites of fusion (Figure 1-7). The signal often appeared to be much brighter at the site of fusion than on the adjacent sister chromatids, consistent with preservation of both telomeric repeat arrays at the fusion site.

As opposed to IMR90 cells in which Southern blot with a telomeric probe revealed no changes in hybridization pattern when TRF2$^{\Delta B\Delta M}$ was expressed, the HTC75 T cell lines revealed a new class of DNA that was hybridizing with a telomeric probe. This new class of TTAGGG positive DNA first appeared faintly on the 4th day of induction

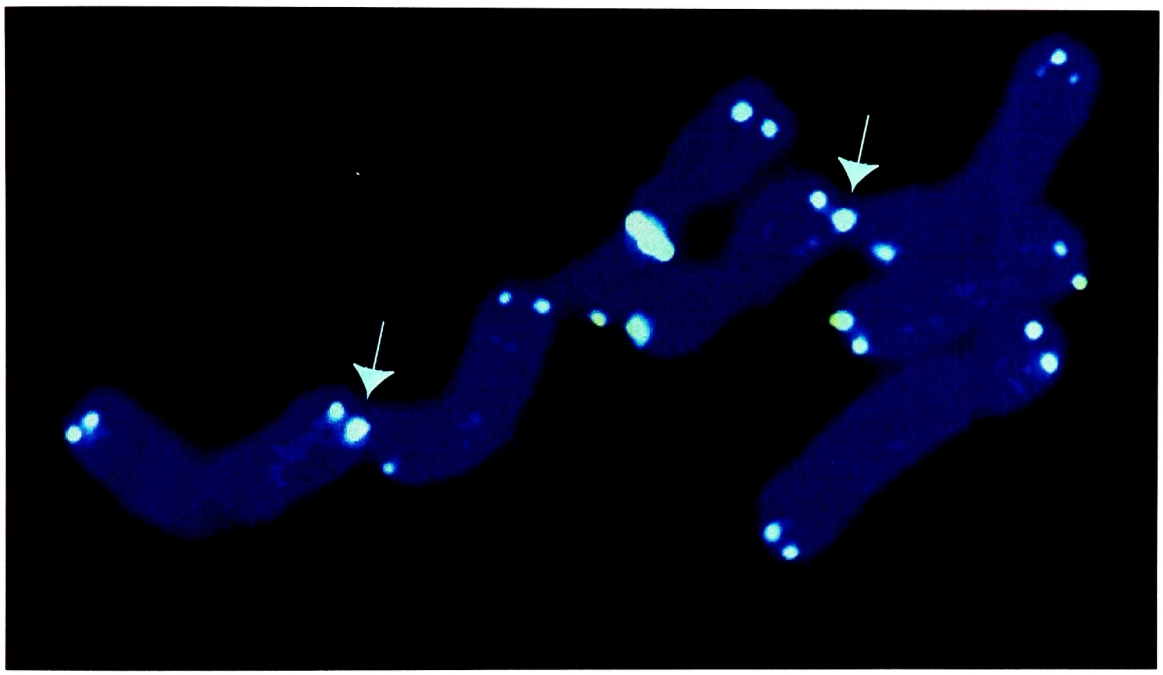

Figure 1-7. **TTAGGG repeats at the sites of fusions in a metaphase of TRF2$^{\Delta B \Delta M}$-expressing HTC75 cells.** Peptide neucleic acid (PNA) fluorescence in-situ hybridization with a telomeric probe on chromosomes of HTC75-T4 cells induced to express TRF2$^{\Delta B \Delta M}$ for 6 days. Telomeric DNA was visualized using a fluorescently labled PNA $(CCCTAAA)_3$ probe. DNA was counterstained with DAPI. Arrows point to sites of fusion.

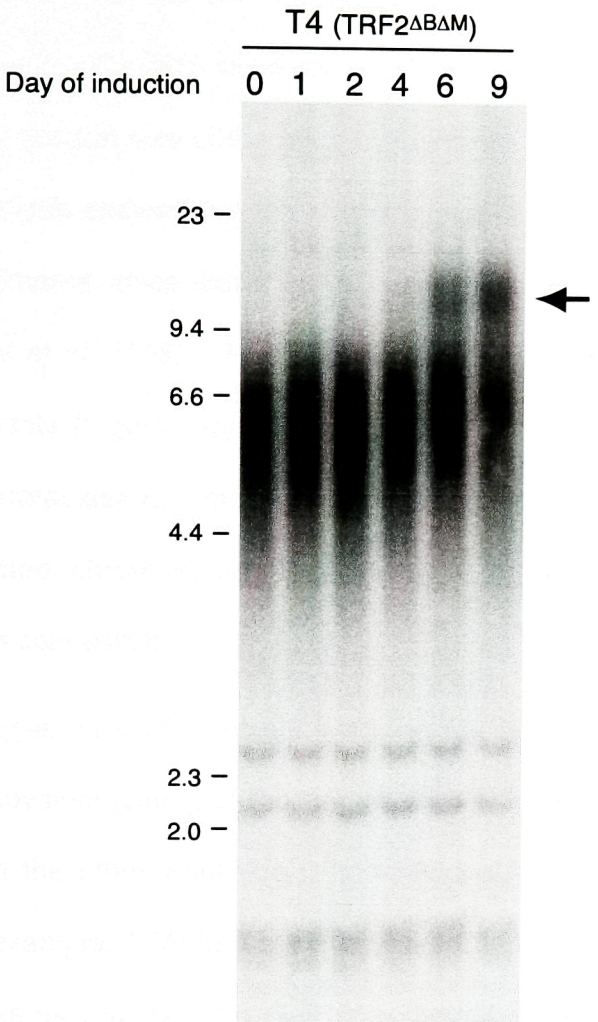

Figure 1-8. **Time course of changes in telomere structure with expression of TRF2$^{\Delta B\Delta M}$ in HTC75 T4 cell line.** Southern blot of telomeric restriction fragments from HTC75 T4 cells induced to express TRF2$^{\Delta B\Delta M}$. Genomic DNA was isolated from cells on the indicated days after induction, digested with HinfI and RsaI, and hybridized with a TTAGGG repeat probe after fractionation on a native 0.7% agarose gel. The molecular weights of marker DNAs are indicated in kb. The arrow points to a new high molecular weight DNA that appears after induction of TRF2$^{\Delta B\Delta M}$ but not in control cell line (not shown). The mean length of the new species is around 10 kb and mean length of the telomeres before induction is about 5 kb.

This experiment was performed by Bas van Steensel (van Steensel, Smogorzewska, and de Lange, 1998).

of TRF2$^{\Delta B\Delta M}$ (Figure 1-8 and van Steensel et al. 1998). The strength of hybridization to this new class of telomeric DNA increased with time. However, the median size of this new class of telomeric DNA remained stable with time and in all cell lines examined it was twice the median size of the original telomeres (van Steensel et al. 1998). Further molecular analysis showed that the higher molecular weight telomeric DNA represented the fused telomeres, since that DNA was resistant to an exonucleolytic activity of Bal31 (van Steensel et al. 1998). The Southern blot visualizing the new class of TTAGGG repeat fragments (Figure 1-8) was performed on the DNA that has been extensively treated with proteinase K, hence, it was concluded that the fusions arose from joining of the deprotected chromosome ends at the DNA level and are not formed by a proteinaceous connection.

Two types of joining events involving telomeric DNA might be imagined. One would be a covalent joining of the deprotected ends where the DNA would be ligated together, and the other would be a non-covalent, but very stable interactions at the termini. For example, TTAGGG repeats present in the single-stranded G-overhangs of human telomeres readily form G-G base-paired structures *in vitro* (for review see Henderson 1995) and this type of interaction could be responsible for the end-to-end fusions. To address whether the telomere fusions induced by TRF2 removal were covalent, the fusions were analyzed under denaturing alkaline conditions.

DNA was isolated from HTC75 T4, T19, and T22 cell lines with or without induction of TRF2$^{\Delta B\Delta M}$ (Figure 1-9). Protein free genomic DNA was isolated, digested with HinfI and RsaI, and size-fractionated on native (Figure 1-9, A) or alkaline (Fig. 1-9, B and C) agarose gels. Comparison of the pattern of TTAGGG repeat containing restriction fragments in cells grown with or without the induction of TRF2$^{\Delta B\Delta M}$, as

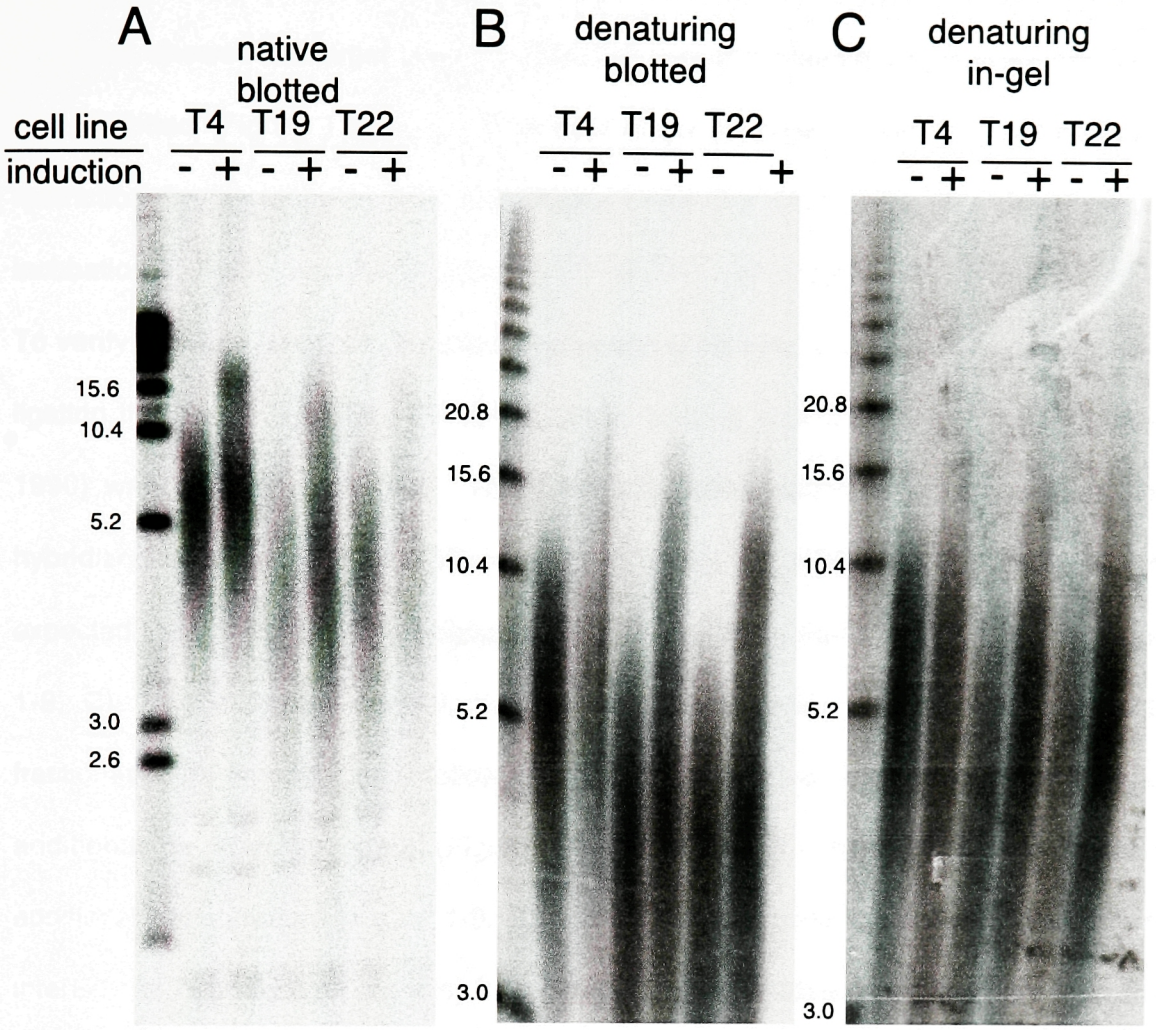

Figure 1-9. **Visualization of fusions in HTC75 cells expressing TRF2$^{\Delta B \Delta M}$ under native and denaturing conditions.** Southern blot of telomeric restriction fragments from HTC75 T4, T19, and T22 cell lines resolved under native (A) and denaturing (B and C) conditions. Three independent cell lines (T4, T19, and T22) were grown under conditions resulting in repression (-) or induction (+) of the dominant negative allele of TRF2, TRF2$^{\Delta B \Delta M}$. Protein-free genomic DNA was isolated, digested with HinfI and RsaI and fractionated on a native 0.7% agarose gel (A), or treated with 0.05 N NaOH and fractionated on an alkaline 0.5% agarose gel (B and C). The native gel (A) and one half of the denaturing gel (B) were blotted onto a nylon membrane and hybridized with the TTAGGG repeat probe. The other half of the denaturing gel (C) was hybridized in-situ without blotting onto a membrane. The molecular weights marker were prepared by digesting a TTAGGG repeat bearing 2.6 kb pTH5 plasmid with HindIII and self religation of the cut plasmid. Markers are in the first lane in each gel and their size is indicated in kb.

expected, showed the larger class of TTAGGG repeat containing fragments when TRF2 was inhibited (Figure 1-9, left). This new class of larger TTAGGG repeat-bearing restriction fragments was also detectable when the DNA was fully denatured by incubation in NaOH and fractionated on an alkaline gel (compare Figure 1-9 A and B). To verify that this treatment denatured telomeric DNA fully, a DNA ladder generated by ligating the HindIII linearized TTAGGG repeat bearing plasmid (pTH5; de Lange et al. 1990) was used as a marker. This DNA was fractionated on an alkaline gel and hybridized *in situ* to a TTAGGG repeat probe without additional denaturation. As expected this control DNA hybridized to the probe showing that it was denatured (Figure 1-9, C). As a further control, the genomic DNAs were analyzed in parallel by fractionation on an alkaline gel followed by either blotting onto a membrane (involving an additional denaturation step) (Figure 1-9, B) or in-gel hybridization (not involving additional denaturation) (Figure 1-9, C). Since both protocols gave similar pattern and intensity of hybridization signals, it is likely that the alkaline gel procedure had fully denatured the genomic DNA.

These experiments demonstrated that the telomeric fusions induced by the removal of TRF2 are formed by a covalent linkage of chromosome ends. Given the presence of long G-overhangs at the end of all chromosomes (Makarov et al. 1997) such ligation is unexpected. To assess the state of G-overhangs in cells expressing $TRF2^{\Delta B \Delta M}$ allele, a G-overhang assay (Makarov et al. 1997) was performed. HTC75 T4 cells were induced and the DNA was isolated at different days of induction. After digestion with RsaI and HinfI, equal amounts of DNA were hybridized in solution with a radiolabled $(CCCTAA)_4$ probe under non denaturing conditions (50°C). The reactions were fractionated under native conditions (Figure 1-10) and the resulting signal from the

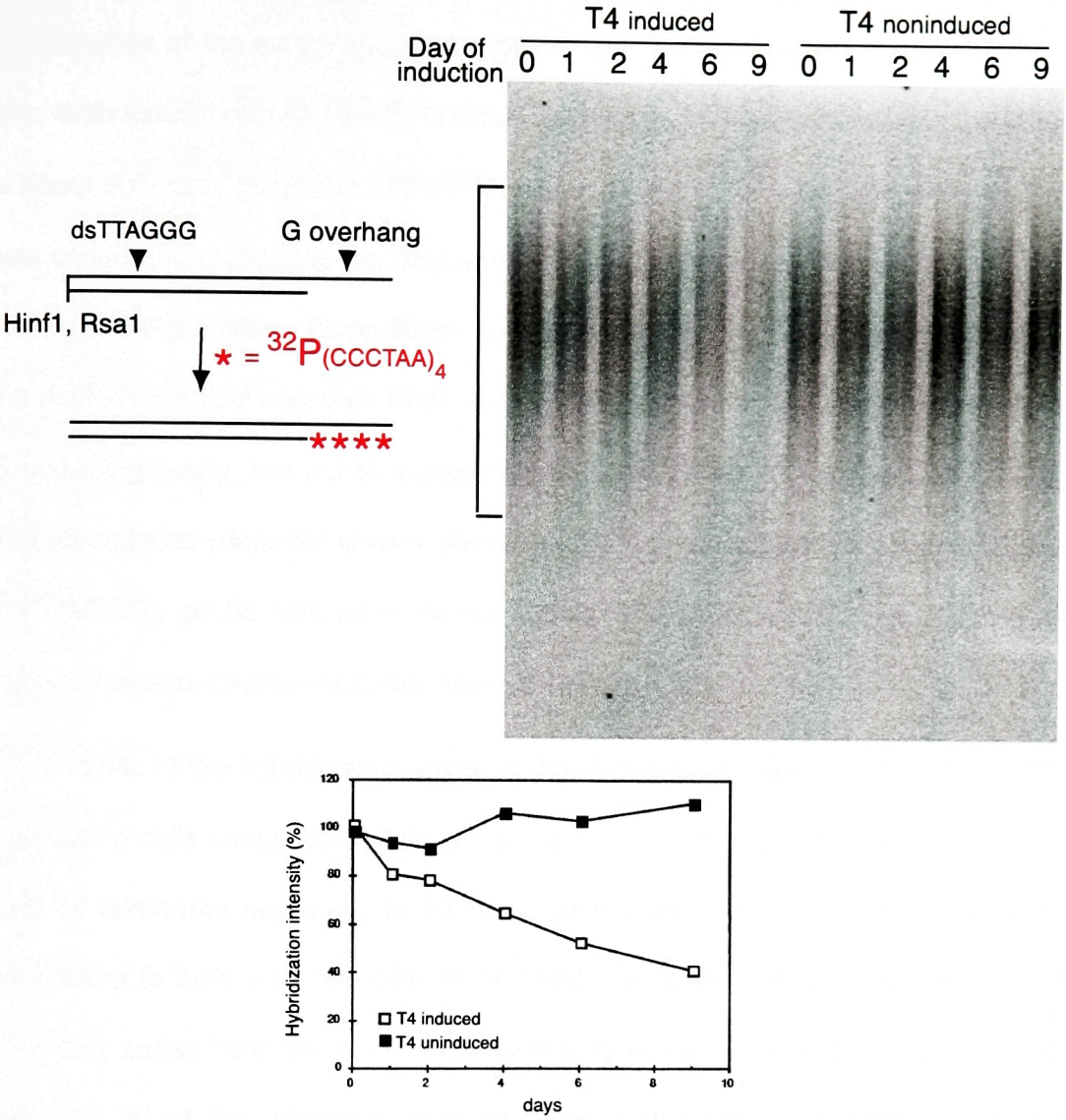

Figure 1-10. **Time course of disappearance of G-strand overhang signal in cell expressing TRF2$^{\Delta B\Delta M}$.** G-strand overhang assay (Makarov et al., 1997) performed on genomic DNA isolated from HTC75 T4 cells. HTC75 T4 cells were grown under conditions resulting in repression or induction of the dominant negative allele of TRF2, TRF2$^{\Delta B\Delta M}$. DNA was isolated from cells on the indicated days after induction, digested with HinfI and RsaI, and hybridized without denaturing with a radiolabled $(CCCTAA)_4$ visualizing only the single-stranded telomeric DNA (Top). Loss of G-strand overhangs was quantified after induction of TRF2$^{\Delta B\Delta M}$ in two independent experiments performed with the T4 clone (bottom). The data were derived from two experiments similar to those shown and the average value was plotted.

This experiment was performed by Bas van Steensel (van Steensel, Smogorzewska, and de Lange, 1998).

hybridization of the single-stranded probe to the G-overhang was quantified (Figure 1-10). With induction of TRF2$^{\Delta B \Delta M}$, G-overhang signal diminished to reach a minimum level of about 50% of the signal in TRF2$^{\Delta B \Delta M}$ non-expressing cells. The specificity of the signal was confirmed by treating the DNA with Mung Bean nuclease prior to hybridization with the $(CCCTAA)_4$ probe. Mung Bean nuclease removes the overhang without degrading the double-stranded telomeric DNA, which resulted in a loss of hybridization signal in the G-overhang assay, but not in a Southern blot performed on the Mung Bean nuclease-treated samples (data not shown, performed by Bas van Steensel). Furthermore, when a $(TTAGGG)_4$ probe was used for the hybridization, G-overhangs were not visualized (data not shown, performed by Bas van Steensel).

Loss of the hybridization signal in the G-overhang assay on DNA from TRF2$^{\Delta B \Delta M}$-expressing cells could not be fully accounted for by formation of fusions, since only 10-20% of telomeres appeared to be fused at the time when the overhang signal was diminished to 50% (van Steensel et al. 1998). It is impossible to discern from the G-overhang assay how much of the G-overhang is lost at an individual telomere. For instance, all of the telomeres may have lost half of the G-overhang or half of the telomeres lost the entire overhang. However, the detection of covalent fusions suggests that at least some of the chromosomes lost all of the G-overhangs preceding their fusion.

Under normal growth conditions the G-overhangs are thought to invade the double-stranded telomeric repeats, forming t-loops. Disappearance of the G-overhang upon induction of TRF2$^{\Delta B \Delta M}$ suggested that t-loop formation may be diminished when TRF2 is absent from telomeres. This would parallel the *in vitro* findings, in which TRF2 was shown to aid in formation and/or stabilization of t-loops (Griffith et al. 1999; Stansel

et al. 2001). To test the hypothesis that removal of TRF2 from telomeres would lead to dissolution of t-loops, electron microscopic analysis was performed on DNA from cells expressing no exogenous protein, FLTRF2 and TRF2$^{\Delta B\Delta M}$ (Figure 1-11, table 1-3). For these experiments IMR90 cells were first infected with SV40 Tag to allow continuous division while expressing TRF2$^{\Delta B\Delta M}$ (see Chapter 2). Subsequently, a second infection was performed with a control vector (pLPC) or with TRF2 alleles (pLPC TRF2 and pLPC TRF2$^{\Delta B\Delta M}$). Nuclei were prepared from about 2x10^8 cells per cell type and the DNA was cross-linked by exposing the nuclei to 365 nm UV light in the presence of 4'-aminomethyltrioxsalen (AMT). Further analysis was done by Jack Griffith using a modification of a procedure previously used to discover t-loops at the ends of chromosomes (Griffith et al. 1999). An example of a t-loop from IMR90 cells infected with a vector control is shown in Figure 1-11. Preliminary analysis showed that a number of t-loops visible in samples obtained from TRF2$^{\Delta B\Delta M}$-expressing cells was diminished when compared to control or FLTRF2-expressing cells and dropped to 40% of the control levels. In this experiment only 65% of cells used for the analysis expressed TRF2$^{\Delta B\Delta M}$ as assessed by immunofluorescence staining. This means that the TRF2$^{\Delta B\Delta M}$-expressing sample contained a substantial fraction of cells that no longer expressed the dominant negative allele of TRF2, resulting in an underestimate of the effect of TRF2$^{\Delta B\Delta M}$ on the t-loop frequency

The above experiments suggest that removal of TRF2 from telomeres results in the loss of at least some of the t-loops, loss of the G-overhang and a covalent fusion of deprotected telomeres. To ask whether the non-homologous-end-joining (NHEJ) pathways are responsible for formation of end-to-end fusions after inhibition of TRF2, mouse embryonic fibroblasts (MEFs) lacking Ligase IV (Lig4) (Frank et al. 2000) were

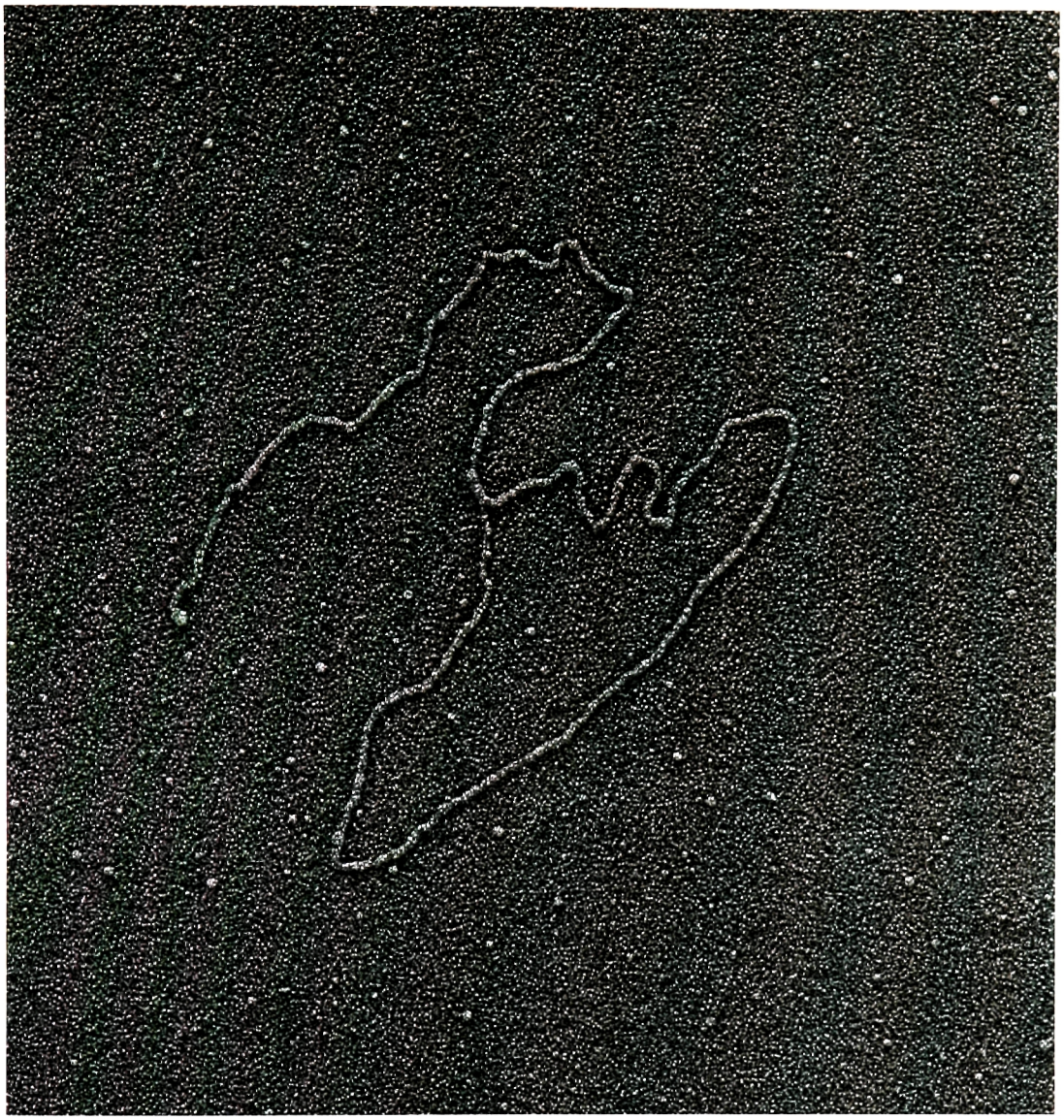

Figure 1-11 **A t-loop from IMR90 cells expressing SV40 large T antigen but no exogenous TRF2 allele.** An electron micrograph of a telomeric DNA fragment isolated from IMR90 cells expressing SV40 large T antigen. Nuclei of logarithmically growing cells were prepared and their DNA was crosslinked using 4'-aminomethyltrioxsalen (AMT). DNA was digested with MboI and AluI and after fractionation over a Biogel A5M column, fractions containing telomeric DNA were spread for EM analysis as described in materials and methods.

Collection of cells was done with the help of Jan Karlseder. All preparation and analysis following crosslinking including the EM analysis was performed by Jack Griffith, University of North Carolina, Chapel Hill.

Table 1-3. T-loop frequency in IMR90 primary fibroblasts expressing SV40 Large T antigen infected with control vector, full length TRF2, and TRF2$^{\Delta B \Delta M}$ On average 2x10^8 cells per experiment were harvested and their DNA was crosslinked using 4'-aminomethyltrioxsalen (AMT). DNA was digested with MboI and AluI and after fractionation over a Biogel A5M column, fractions containing telomeric DNA were spread for EM analysis (as descried in materials and methods).

EM analysis was performend by Jack Griffith, University of North Carolina, Chapel Hill.

Viral vector	% cells expressing TRF2$^{\Delta B \Delta M}$	Molecules scored	t-loops found	# t-loops/ 1000 molecules	Relative t-loop frequency per experiment
pLPC (exp1)	n.a	621	33	53	100
pLPC TRF2 (exp1)	n.a	689	36	52	98
pLPCTRF2$^{\Delta B \Delta M}$(exp1)	65%	717	15	21	40
pLPC (exp2)	n.a	n.d.	n.d.	n.d.	n.d.
pLPCTRF2$^{\Delta B \Delta M}$(exp2)	50%	n.d.	n.d.	n.d.	n.d.
pLPC(exp3)	n.a	n.d.	n.d.	n.d.	n.d.
pLPCTRF2$^{\Delta B \Delta M}$(exp3)	50%	n.d.	n.d.	n.d.	n.d.

n.a- not applicable
n.d- not determined

used to investigate fusion formation after expression of TRF2$^{\Delta B\Delta M}$. Lig4 has been shown to be necessary for the NHEJ in human cells (Grawunder et al. 1998). Mice that are devoid of Lig4 or that lack a Lig4 accessory factor (XRCC4) die during embryonic development and cells recovered from the embryos are unable to perform NHEJ resulting in their sensitivity to irradiation ((Barnes et al. 1998; Frank et al. 1998; Gao et al. 1998; Frank et al. 2000), reviewed in Sekiguchi et al. 1999). Because MEFs lacking Lig4 grow extremely poorly, Lig4 MEFs that also lacked p53 were used for the analysis (Frank et al. 2000). Lack of p53 rescues the organismal lethality of the Lig4 KO as well as allows for faster and continuous growth of the population, while not influencing the primary NHEJ defect of these MEFs in non-homologous end joining pathway (Ferguson et al. 2000; Frank et al. 2000). For the analysis of fusions, Lig4+/+p53-/- and Lig4-/-p53-/- MEFs obtained from the same litter were infected with the pLPC control or the TRF2$^{\Delta B\Delta M}$-expressing virus. Chromosomal abnormalities in 30 metaphase spreads of each type were assessed on coded samples. To aid in distinguishing between end-to-end fusions that are formed due to TRF2$^{\Delta B\Delta M}$ expression and fusions that form between broken chromosomes that are expected to be present in Lig4 null cells, PNA FISH was performed to visualize telomeric DNA. Metaphases from Lig4+/+p53-/- cells infected with a control vector (Table 1-4) showed presence of some breaks and fragments and low level of chromosome fusions without the telomeric DNA, but no chromosome fusions with telomeric signal. Expression of TRF2$^{\Delta B\Delta M}$ led to appearance of the expected telomere fusions (Figure 1-12). Such fusions were never seen when TRF2$^{\Delta B\Delta M}$ was expressed in MEFs that were devoid of Lig4, despite the fact that these cells showed a general increase in chromosomal abnormalities. Abnormalities in Lig4-/-p53-/- cells included breaks, fragments, and chromosome fusions without telomeric signal (Figure 1-12 and Table 1-4) and they were all independent of TRF2$^{\Delta B\Delta M}$ expression. The only

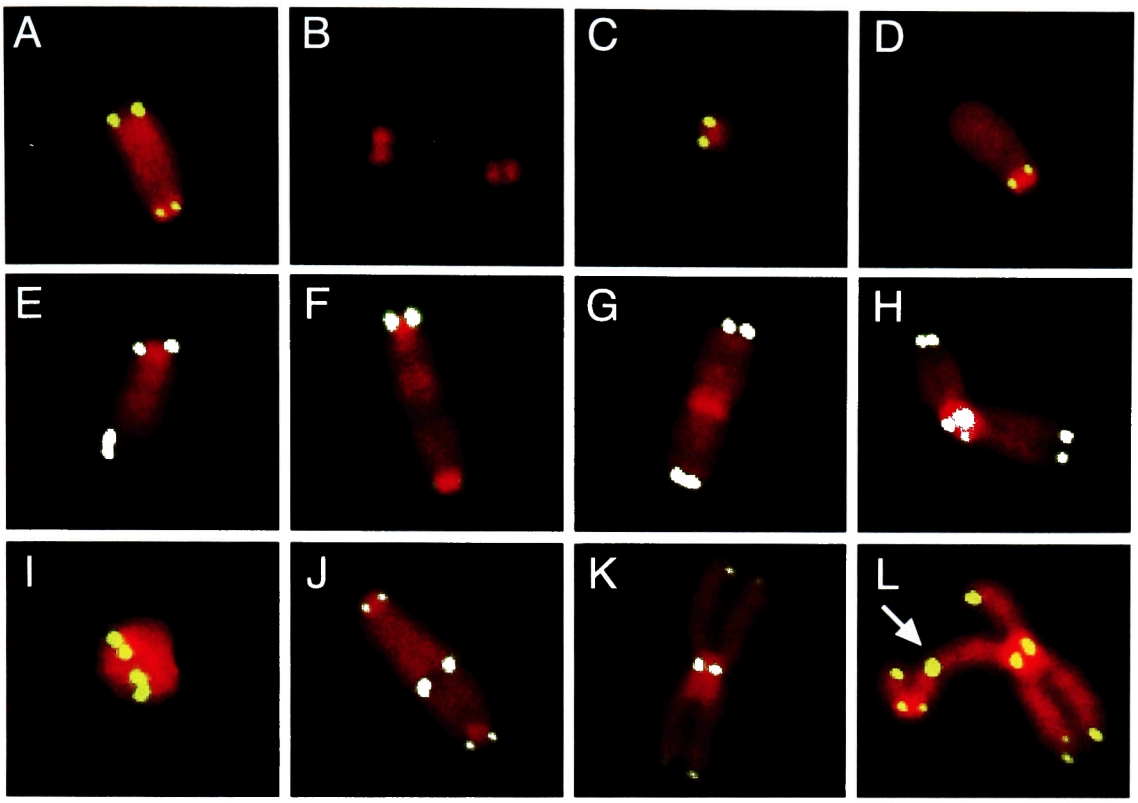

Figure 1-12. **Chromosomal abnormalities observed in mouse embryonic fibroblasts expressing TRF2$^{\Delta B \Delta M}$.** Peptide nucleic acid (PNA) fluorescence in-situ hybridization with a telomeric probe on chromosomes from mouse cells infected with TRF2$^{\Delta B \Delta M}$. Metaphase spreads of LIg4+/+ p53-/- and Lig4-/- p53 -/- cells expressing TRF2$^{\Delta B \Delta M}$ were prepared on the third day of selection. DNA was counterstained with DAPI and chromosomes were false-colored in red. LIg4+/+ p53-/- MEFs expressing TRF2$^{\Delta B \Delta M}$ showed all abnormalities documented in **B** to **L**. Lig4-/- p53 -/- expressing TRF2$^{\Delta B \Delta M}$ cells showed no abnormalities of the type illustrated in **I** to **L**, and short arm chromatid fusion shown in **H** was seen independent of presence or absence of TRF2$^{\Delta B \Delta M}$ (also see Table 1-2). **(A)** Normal chromosome **(B)** Fragments without telomeric signal **(C)** Fragment with telomeric signals **(D)** Chromosome with telomeric signal missing from the long arms **(E)** Break **(F)** Long arm chromosome fusion without telomeric signal **(G)** Short arm chromosome fusion without telomeric signal **(H)** Short arm chromatid fusion with telomeric signal **(I)** Two-chromosome ring chromosome with telomeric signal at the fusion sites **(J)** Long arm chromosome fusion with telomeric signal **(K)** Short arm chromosome fusion with telomeric signal **(L)** Long arm chromatid fusion with telomeric signal (arrow) and short arm chromosome fusion with telomeric signal (as in panel **K**).

Table 1-4. Chromosomal abnormalities in 30 metaphase spreads of primary Lig4+/+p53-/- and Lig4-/-p53-/- mouse embryonic fibroblasts infected with control vector (pLPCpuro) or pLPCTRF2$^{\Delta B\Delta M}$ Peptide nucleic acid fluorescence in-situ hybridization was performed on metaphase spreads from cells on the 3rd day of selection. Abnormalities were scored on coded samples. The data reflect two separate experiments.

Genotype + Expressed allele	Breaks and fragments*	Chromatid fusions without telomeric signal	Chromatid fusions with telomeric signal	Chromosome fusions without telomeric signal	Chromosome fusions with telomeric signal	Chromosome fusions with telomeric signal per cell §
Lig4+/+p53-/- vector	17	1	3	2	0	0
Lig4+/+p53-/- TRF2$^{\Delta B\Delta M}$	28	1	6	4	45	1.5
Lig4-/-p53-/- vector	59	2	2†	17	0	0
Lig4-/-p53-/- TRF2$^{\Delta B\Delta M}$	60	3	2†	3	0	0

* Including fragments with and without telomeric signal, as well as chromosomes with missing telomeric signal at two chromatids (see examples Figure 1-11, panels B-E)

† All were short arm chromatid fusions (see example Figure 1-11 2H)

§ Average number of chromosomes per cell: 64 (Lig4+/+p53-/-, vector), 64(Lig4+/+p53-/-, TRF2$^{\Delta B\Delta M}$), 71 (Lig4-/-p53-/-, vector), and 74 (Lig4-/-p53-/-, TRF2$^{\Delta B\Delta M}$)

fusion with a telomeric signal at the site of fusion in Lig4-/-p53-/- MEFs was of the chromatid type (Figure 12-H) and only at the short arm of the mouse chromosome. Formation of this type of fusion was also independent of TRF2$^{\Delta B \Delta M}$ expression, because examples of such fusions were seen in all cells examined, even when they were infected with a vector control (Table 1-4). Taken together, the main conclusion of this experiment is that ligase 4 and hence non-homologus end joining, is necessary for the fusion formation after inhibition of TRF2.

As shown above, end-to-end fusions formed after expression of the dominant negative TRF2 allele can be visualized as anaphase bridges, representing dicentric chromosomes being pulled apart to opposite spindle poles. Resolution of such bridges may give rise to broken chromosomes, giving rise to chromosome translocations. To ask whether lack of TRF2 presence on telomeres can cause genomic instability, multiplex fluorescence in situ hybridization (M-FISH) was employed in collaboration with Dr. Anna Jauch at Institute für Humangenetik in Heidelberg (Speicher et al. 1996; Eils et al. 1998). This technique relies on hybridization of metaphase spreads with a set of fluorescent probes representing individual chromosomes. Each chromosome is recognized by computer-assisted decoding of its unique hybridization color, enabling detection of translocated chromosome segments. M-FISH analysis performed on 35 metaphase spreads of normal human primary fibroblasts revealed two breaks in the centromere region of chromosome 10 and 2 [del(10p) and del(2p), see Table 1-5] but no translocations. In contrast, cells expressing TRF2$^{\Delta B \Delta M}$ showed a high number of chromosome translocations (Table 1-5). Many of them were end-to-end chromosome fusions (also known as telomere associations) (Figure 1-13, C, indicated by the asterisk). However, other translocations that involved terminal fragments and not

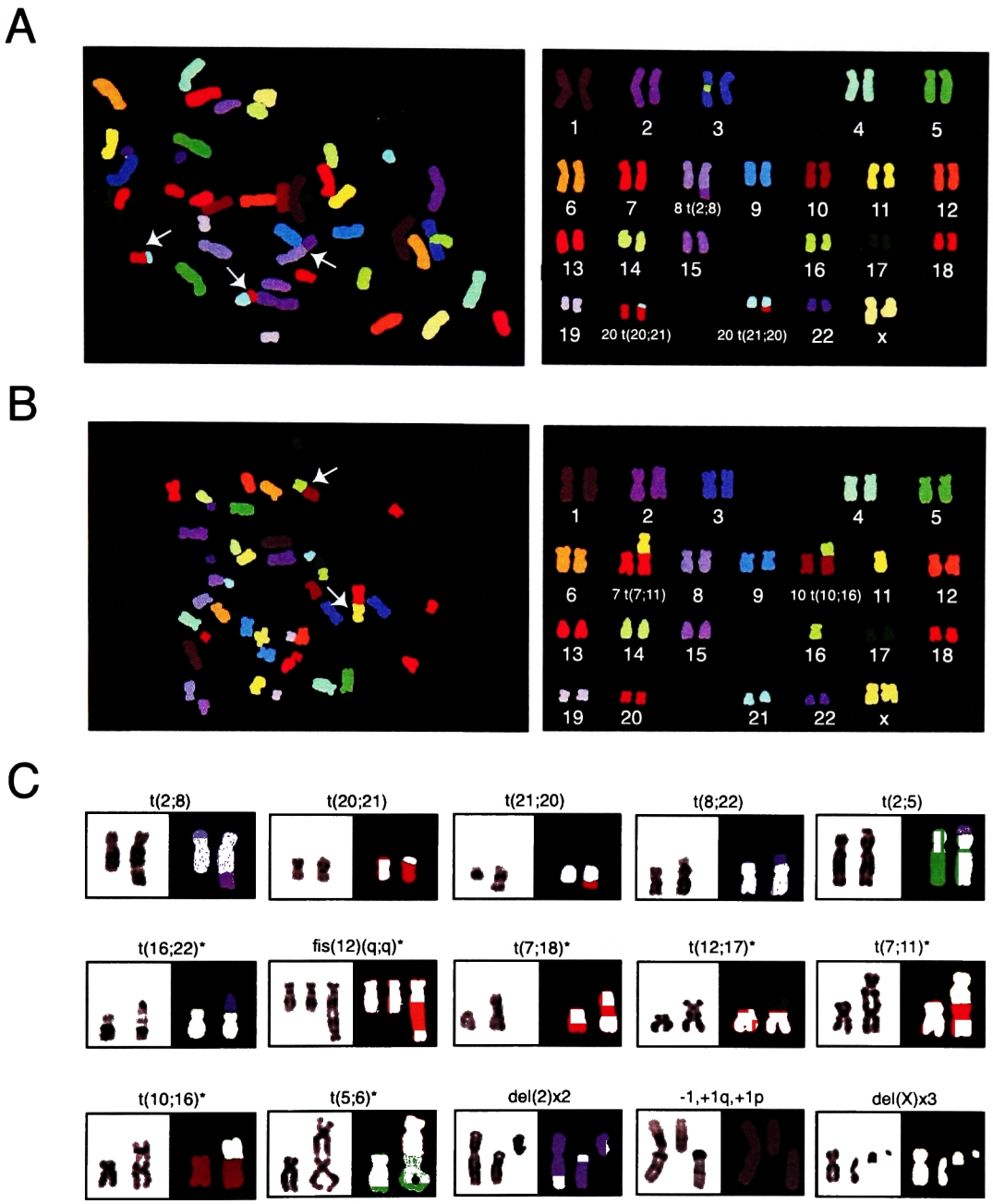

Figure 1-13. **Chromosomal abnormalities in metaphase spreads of IMR90 fibroblasts expressing TRF2$^{\Delta B \Delta M}$.** Multiplex fluorescence in situ hybridization (M-FISH) on metaphase spreads of cells expressing TRF2$^{\Delta B \Delta M}$. Spreads were prepared on day 6 of selection, after 12-hour colcemid treatment. **A.** and **B.** Examples of full metaphase spreads. **C.** Examples of translocation (top row), likely telomere associations (indicated by *), and other chromosomal abnormalities

(Experiments done in collaboration with Heidi Holtgreve-Grez and Anna Jauch (Institute für Humangenetik, Heidelberg, Germany)

Table 1-5. Chromosomal abnormalities in metaphase spreads of IMR90 fibroblasts infected with control vector (pLPC puro), full length TRF2 (FL TRF2) or the dominant negative allele of TRF2 (pLPCTRF2$^{\Delta B \Delta M}$), as assessed by M-FISH. Metaphase spreads were prepared on day 6 of selection after a 12 hour colcemid treatment. Chromatid fusions are not scored by this method. All alleles were untagged.

(Experiments done in collaboration with Heidi Holtgreve-Grez, Anna Jauch (Institute für Humangenetik, Heidelberg, Germany)

Viral vector	Number of Metaphases scored	Cumulative abnormalities*
pLPC puro	35	del(10p), del(2p)
PLPC TRF2	10	t(2;7)
pLPCTRF2$^{\Delta B \Delta M}$	44	<u>translocations</u> t(2;5), t(8;22), t(2;8), t(20;21), t(20;21), <u>telomere associations</u>† t(16;22), t(7;18), t(12;12), t(7;11), t(10;16), t(5;6), t(12;17) <u>deletions and fragments</u> del(2)x2, +1q, +1p, del(X)x3, del(5p), del (5q), del(11p), del(11q), fra(1p) <u>other abnormalities</u> dup12, chrg(12)§

* excluding numerical changes, which was seen in all samples, most likely due to imperfect spreading
†likely an end-to end fusion-cytogenetically referred to as telomeric association (tas)
§chrg= chromosome gap

complete chromosomes were also seen (Figure 1-12, A, B, and C, top row). The existence of such translocations suggest that removal of TRF2 can lead to genomic instability even in the otherwise normal human fibroblasts. Chromosomal abnormalities are generally underdetected by M-FISH, since chromatid fusions are not scored (unless they give rise to true translocations) and terminal deletions that should be formed during translocations involving telomeric DNA are not well visualized, given that they result in loss and not gain of the chromosome DNA.

Discussion

This chapter provided evidence that the maintenance of protection at human telomeres is highly dependent on TRF2, one of the two TTAGGG binding factors present in all mammalian cells tested to date. Removal of TRF2 from telomeres by overexpression of the dominant negative ($TRF2^{\Delta B \Delta M}$) allele leads to telomere deprotection which can be deduced from the presence of end-to-end fusions in metaphase and in anaphase cells.

The striking finding that telomeric DNA is present at sites of fusions when TRF2 is removed, shows that the telomeric DNA itself is insufficient to provide protection to chromosome ends and that it must act in concert with TRF2 and possibly other proteins to confer protection. A strong requirement for the TTAGGG repeats has been noted during the de novo telomere formation in human cells (Hanish et al. 1994). In other experiments, addition of non-TTAGGG repeats by a mutant telomerase resulted in telomere dysfunction leading to the formation of end-to-end fusions (Guiducci et al. 2001) and the decline in growth potential of cells harboring mutated telomeric sequence (Guiducci et al. 2001; Kim et al. 2001). Based on the results presented in this chapter, it is likely that the acquisition of TRF2 by the transfected telomere seed allows for the

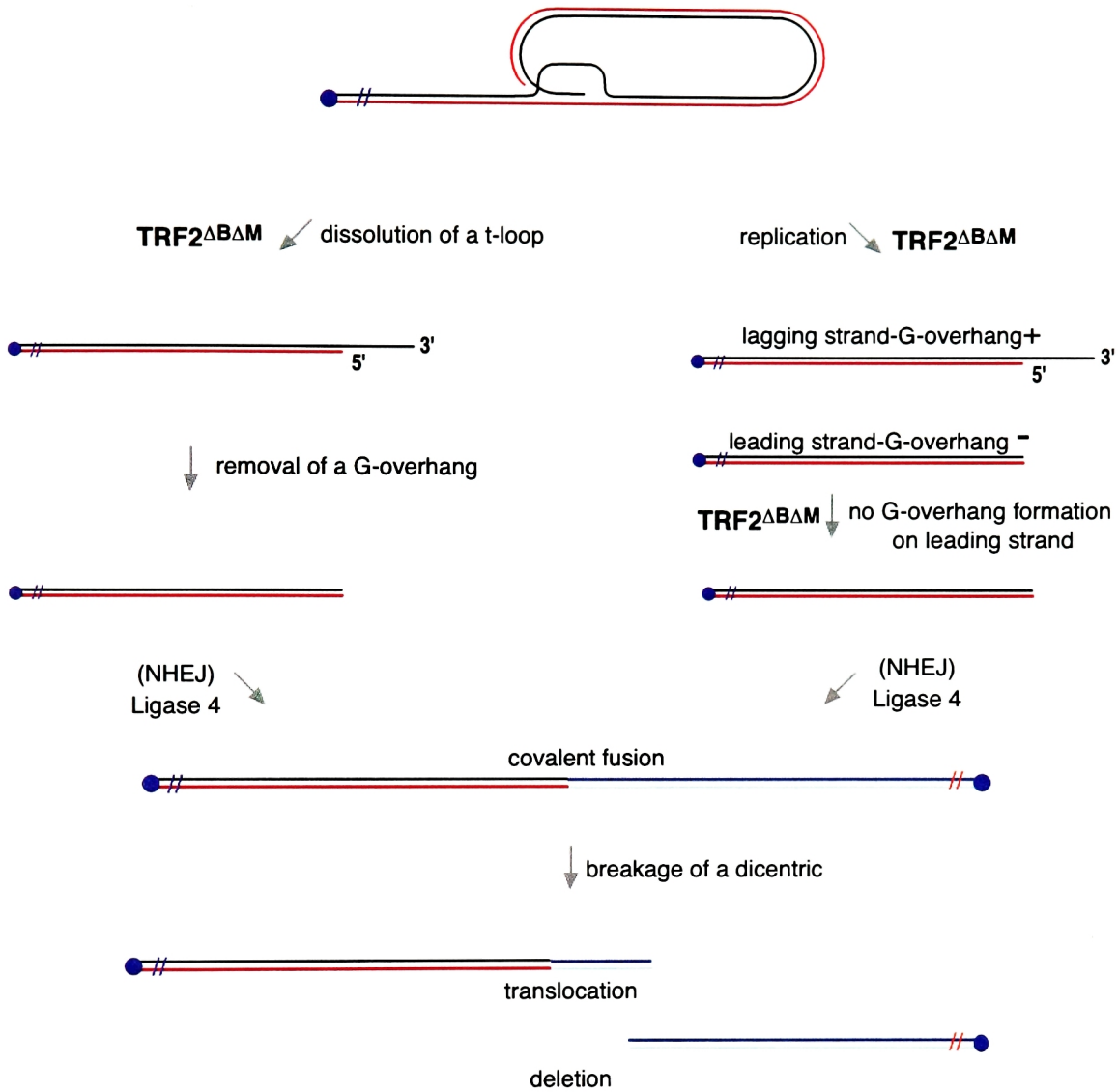

Figure 1-14. **Model of chromosomal events following inhibition of TRF2.** Two alternative pathways from t-looped state to deprotected and fusogenic state are shown. (Left) Expression of TRF2$^{\Delta B\Delta M}$ leads to dissolution of t-loops. G-overhangs become deprotected and degraded. (RIght) Expression of TRF2$^{\Delta B\Delta M}$ leads to lack of re-establishment of t-loops on chromosome ends that were replicated by leading strand synthesis. For example, TRF2 could be necessary for the formation of G-overhangs. Both pathways converge when the telomeres lacking the G-overhang are repaired by the non homologous end joining (NHEJ) pathway employing ligase 4 in the covalent ligation of DNA strands. Breakage of a dicentric chromosome formed by the end-to-end fusion leads to formation of a translocation and a deletion.

development of the fully functional new telomere. Conversely, inability of the non-TTAGGG repeats synthesized by the mutated telomerase to recruit TRF2, can be now proposed to lead to telomere deprotection seen in these cells.

The mechanism of how TRF2 and telomeric DNA collaborate to ensure the protected state has been proposed to involve formation of the t-loop (Griffith et al. 1999). In preliminary experiments described here, t-loop formation was significantly reduced in cells that express TRF2$^{\Delta B \Delta M}$, but normal when cells expressed a full length TRF2 (FLTRF2). In light of this finding, two different scenarios for telomere fusions can be envisioned (Figure 1-14). In one scenario, expression of TRF2$^{\Delta B \Delta M}$ could lead to the dissolution of t-loops. T-loop opening would then make the G-overhang susceptible to degradation (Figure 1-14, left) resulting in the formation of a suitable substrate for ligation by the NHEJ pathway. Alternatively, cells expressing TRF2$^{\Delta B \Delta M}$ could be unable to re-establish t-loops on chromosome ends after replication. For example, TRF2 could be necessary for the formation of G-overhangs after replication by leading strand synthesis. Such a role for TRF2 would not be unexpected since it interacts with the Mre11 complex, which has been proposed to act in the formation of the overhang (de Lange and Petrini 2001). As in the first scenario, a telomere remaining devoid of an overhang would then be a substrate for the NHEJ.

The above proposals are not mutually exclusive; however, a recent study by Bailey and colleagues (Bailey et al. 2001) substantiates parts of the second proposal. In these studies end-to-end fusions in HTC75 cells expressing TRF2$^{\Delta B \Delta M}$ were analyzed using chromosome orientation-FISH (CO-FISH), a technique to differentiate between chromatids formed by leading and lagging DNA synthesis. The conclusion reached from these studies was that all of the chromatid fusions seen in the HTC75 T lines were due

to fusion of two chromatids synthesized using leading strand synthesis ("leading to leading" chromatid fusions).

Based on these studies, one might assume that TRF2 is responsible for protection of only half of the chromatids- those that are formed by the leading strand synthesis. Such interpretation would not be prudent at this point since there are many caveats to these experiments. The dominant negative effect of the TRF2$^{\Delta B \Delta M}$ construct might never be complete in these experiments. The fact that the dominant negative effect is often not complete is stressed by the fact that many of the metaphases of the TRF2$^{\Delta B \Delta M}$-expressing cells did not show any abnormalities, while others showed as many as 30 aberrations (van Steensel et al. 1998). There might be also variability of the dominant negative effect within each cell so that some telomeric TRF2 might be resistant to stripping by the dominant negative allele. In this case only the most vulnerable sites might reveal themselves in forms of fusions. Chromatids that were replicated by the leading strand synthesis might represent such vulnerable sites. Finally, one example (Figure 1-5 top panel, three-chromosome fusion on the right of the picture) possibly demonstrates that a leading to lagging chromosome fusion could occur. The caveat here is that without the CO-FISH on this very spread one will never know if one of these fusions represent a true lagging-to leading chromatid fusion.

In general, further studies of how t-loops are resolved and re-established during the cell cycle, and how and when the G-overhang is formed on the chromatids replicated by the leading strand synthesis, will aid in an understanding of the details of telomere protection by TRF2. Study of the cells that lack any TRF2 will also be needed to confirm and further develop the details presented in this chapter. The dominant negative approach of TRF2 inhibition has added to the knowledge about the mechanism of

Table 1-5. Chromosomal abnormalities in metaphase spreads of IMR90 fibroblasts infected with control vector (pLPC puro), full length TRF2 (FL TRF2) or the dominant negative allele of TRF2 (pLPCTRF2$^{\Delta B \Delta M}$), as assessed by M-FISH. Metaphase spreads were prepared on day 6 of selection after a 12 hour colcemid treatment. Chromatid fusions are not scored by this method. All alleles were untagged.

(Experiments done in collaboration with Heidi Holtgreve-Grez, Anna Jauch (Institute für Humangenetik, Heidelberg, Germany)

Viral vector	Number of Metaphases scored	Cumulative abnormalities*
pLPC puro	35	del(10p), del(2p)
PLPC TRF2	10	t(2;7)
pLPCTRF2$^{\Delta B \Delta M}$	44	<u>translocations</u> t(2;5), t(8;22), t(2;8), t(20;21), t(20;21), <u>telomere associations</u>† t(16;22), t(7;18), t(12;12), t(7;11), t(10;16), t(5;6), t(12;17) <u>deletions and fragments</u> del(2)x2, +1q, +1p, del(X)x3, del(5p), del (5q), del(11p), del(11q), fra(1p) <u>other abnormalities</u> dup12, chrg(12)§

* excluding numerical changes, which was seen in all samples, most likely due to imperfect spreading
†likely an end-to end fusion-cytogenetically referred to as telomeric association (tas)
§chrg= chromosome gap

complete chromosomes were also seen (Figure 1-12, A, B, and C, top row). The existence of such translocations suggest that removal of TRF2 can lead to genomic instability even in the otherwise normal human fibroblasts. Chromosomal abnormalities are generally underdetected by M-FISH, since chromatid fusions are not scored (unless they give rise to true translocations) and terminal deletions that should be formed during translocations involving telomeric DNA are not well visualized, given that they result in loss and not gain of the chromosome DNA.

Discussion

This chapter provided evidence that the maintenance of protection at human telomeres is highly dependent on TRF2, one of the two TTAGGG binding factors present in all mammalian cells tested to date. Removal of TRF2 from telomeres by overexpression of the dominant negative ($TRF2^{\Delta B \Delta M}$) allele leads to telomere deprotection which can be deduced from the presence of end-to-end fusions in metaphase and in anaphase cells.

The striking finding that telomeric DNA is present at sites of fusions when TRF2 is removed, shows that the telomeric DNA itself is insufficient to provide protection to chromosome ends and that it must act in concert with TRF2 and possibly other proteins to confer protection. A strong requirement for the TTAGGG repeats has been noted during the de novo telomere formation in human cells (Hanish et al. 1994). In other experiments, addition of non-TTAGGG repeats by a mutant telomerase resulted in telomere dysfunction leading to the formation of end-to-end fusions (Guiducci et al. 2001) and the decline in growth potential of cells harboring mutated telomeric sequence (Guiducci et al. 2001; Kim et al. 2001). Based on the results presented in this chapter, it is likely that the acquisition of TRF2 by the transfected telomere seed allows for the

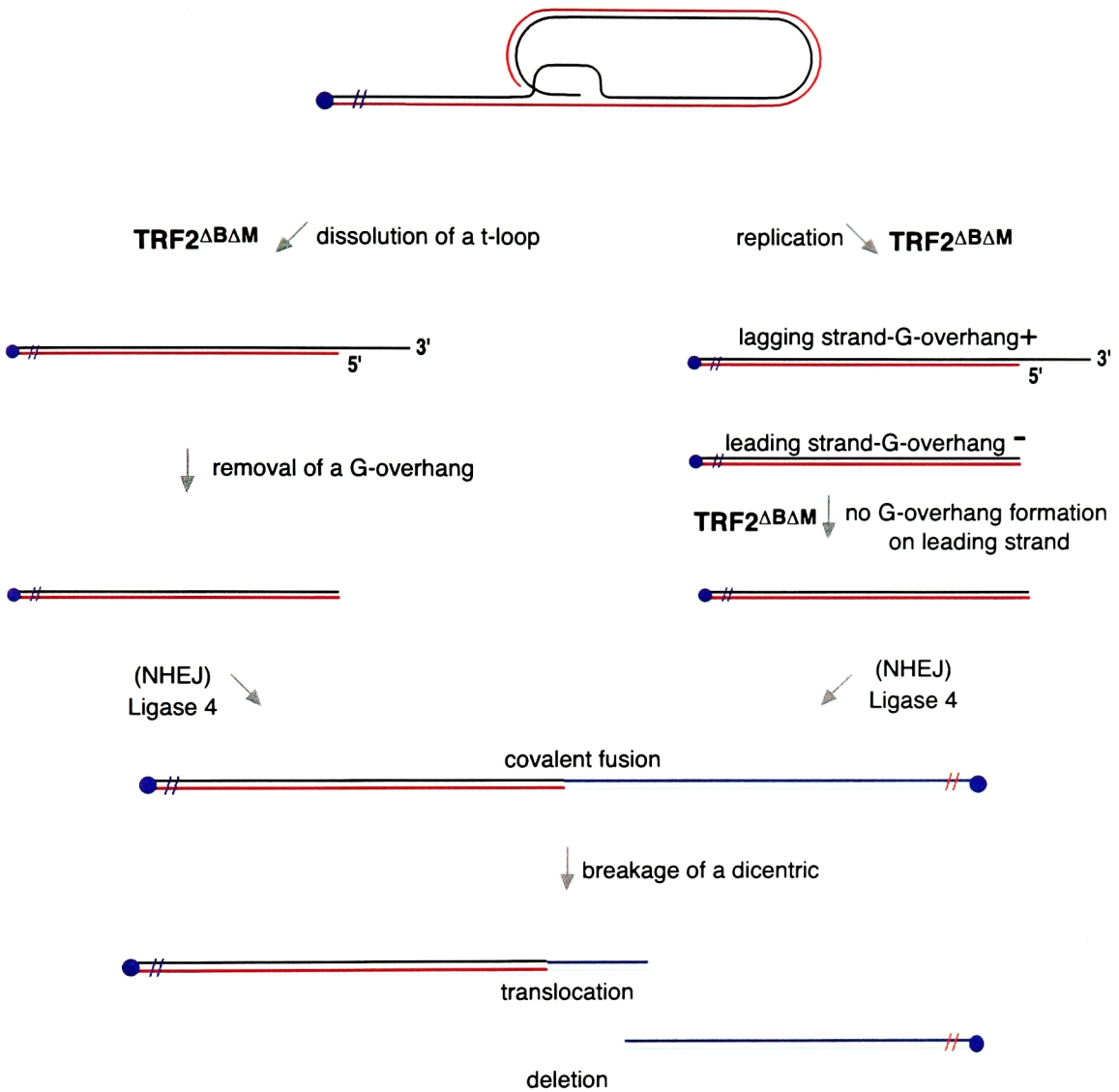

Figure 1-14. **Model of chromosomal events following inhibition of TRF2.** Two alternative pathways from t-looped state to deprotected and fusogenic state are shown. (Left) Expression of TRF2$^{\Delta B\Delta M}$ leads to dissolution of t-loops. G-overhangs become deprotected and degraded. (RIght) Expression of TRF2$^{\Delta B\Delta M}$ leads to lack of re-establishment of t-loops on chromosome ends that were replicated by leading strand synthesis. For example, TRF2 could be necessary for the formation of G-overhangs. Both pathways converge when the telomeres lacking the G-overhang are repaired by the non homologous end joining (NHEJ) pathway employing ligase 4 in the covalent ligation of DNA strands. Breakage of a dicentric chromosome formed by the end-to-end fusion leads to formation of a translocation and a deletion.

development of the fully functional new telomere. Conversely, inability of the non-TTAGGG repeats synthesized by the mutated telomerase to recruit TRF2, can be now proposed to lead to telomere deprotection seen in these cells.

The mechanism of how TRF2 and telomeric DNA collaborate to ensure the protected state has been proposed to involve formation of the t-loop (Griffith et al. 1999). In preliminary experiments described here, t-loop formation was significantly reduced in cells that express $TRF2^{\Delta B\Delta M}$, but normal when cells expressed a full length TRF2 (FLTRF2). In light of this finding, two different scenarios for telomere fusions can be envisioned (Figure 1-14). In one scenario, expression of $TRF2^{\Delta B\Delta M}$ could lead to the dissolution of t-loops. T-loop opening would then make the G-overhang susceptible to degradation (Figure 1-14, left) resulting in the formation of a suitable substrate for ligation by the NHEJ pathway. Alternatively, cells expressing $TRF2^{\Delta B\Delta M}$ could be unable to re-establish t-loops on chromosome ends after replication. For example, TRF2 could be necessary for the formation of G-overhangs after replication by leading strand synthesis. Such a role for TRF2 would not be unexpected since it interacts with the Mre11 complex, which has been proposed to act in the formation of the overhang (de Lange and Petrini 2001). As in the first scenario, a telomere remaining devoid of an overhang would then be a substrate for the NHEJ.

The above proposals are not mutually exclusive; however, a recent study by Bailey and colleagues (Bailey et al. 2001) substantiates parts of the second proposal. In these studies end-to-end fusions in HTC75 cells expressing $TRF2^{\Delta B\Delta M}$ were analyzed using chromosome orientation-FISH (CO-FISH), a technique to differentiate between chromatids formed by leading and lagging DNA synthesis. The conclusion reached from these studies was that all of the chromatid fusions seen in the HTC75 T lines were due

to fusion of two chromatids synthesized using leading strand synthesis ("leading to leading" chromatid fusions).

Based on these studies, one might assume that TRF2 is responsible for protection of only half of the chromatids- those that are formed by the leading strand synthesis. Such interpretation would not be prudent at this point since there are many caveats to these experiments. The dominant negative effect of the TRF2$^{\Delta B\Delta M}$ construct might never be complete in these experiments. The fact that the dominant negative effect is often not complete is stressed by the fact that many of the metaphases of the TRF2$^{\Delta B\Delta M}$-expressing cells did not show any abnormalities, while others showed as many as 30 aberrations (van Steensel et al. 1998). There might be also variability of the dominant negative effect within each cell so that some telomeric TRF2 might be resistant to stripping by the dominant negative allele. In this case only the most vulnerable sites might reveal themselves in forms of fusions. Chromatids that were replicated by the leading strand synthesis might represent such vulnerable sites. Finally, one example (Figure 1-5 top panel, three-chromosome fusion on the right of the picture) possibly demonstrates that a leading to lagging chromosome fusion could occur. The caveat here is that without the CO-FISH on this very spread one will never know if one of these fusions represent a true lagging-to leading chromatid fusion.

In general, further studies of how t-loops are resolved and re-established during the cell cycle, and how and when the G-overhang is formed on the chromatids replicated by the leading strand synthesis, will aid in an understanding of the details of telomere protection by TRF2. Study of the cells that lack any TRF2 will also be needed to confirm and further develop the details presented in this chapter. The dominant negative approach of TRF2 inhibition has added to the knowledge about the mechanism of

telomere protection; however, this approach depended on the overexpression of $TRF2^{\Delta B \Delta M}$. It is formally possible that the phenotype is caused by the dominant negative allele not only removing TRF2 from telomeres but also non-specifically titrating other proteins. To control for effect of overexpression, a FLTRF2 was overexpressed and the overexpressing cells were noted not to have phenotypes associated with deprotection; however, FLTRF2 when overexpressed might suppress some of the phenotypes by increased telomeric localization. Two approaches might be useful in addressing this problem. First of all, using the information from the crystal structure of the TRFH domain, a dominant negative allele containing a much smaller portion of the molecule might be created, decreasing its ability to titrate other proteins. Secondly, a mouse KO of TRF2 will be very informative. Based on the phenotypes observed after expression of the dominant negative allele of TRF2, it is likely that the mouse deficient in TRF2 would not be able to develop, thus the KO needs to be of the conditional type.

Another point that needs to be addressed is the discrepancy in fusion types visualized in studies in HTC75 T cell lines (Bailey et al. 2001) and studies presented in this chapter. Chromosome fusions (those in which two sister chromatids of one chromosome are joined with two sister chromatids of a second chromosomes, (see Figure 1-15) were often observed and are shown in Figures 1-5, 1-12, and 1-13. Even in the HTC75 T lines, such fusions were clearly visualized (van Steensel et al. 1998). However, Bailey et al. (Bailey et al. 2001) have noted that they only observed chromatid fusions (Figure 1-15), but never chromosome fusions. Chromosome fusions can form in two ways; both arms can fuse in S or G2 stage of the cell cycle, or a single chromatid fusion, which was not broken during metaphase to anaphase transition can be

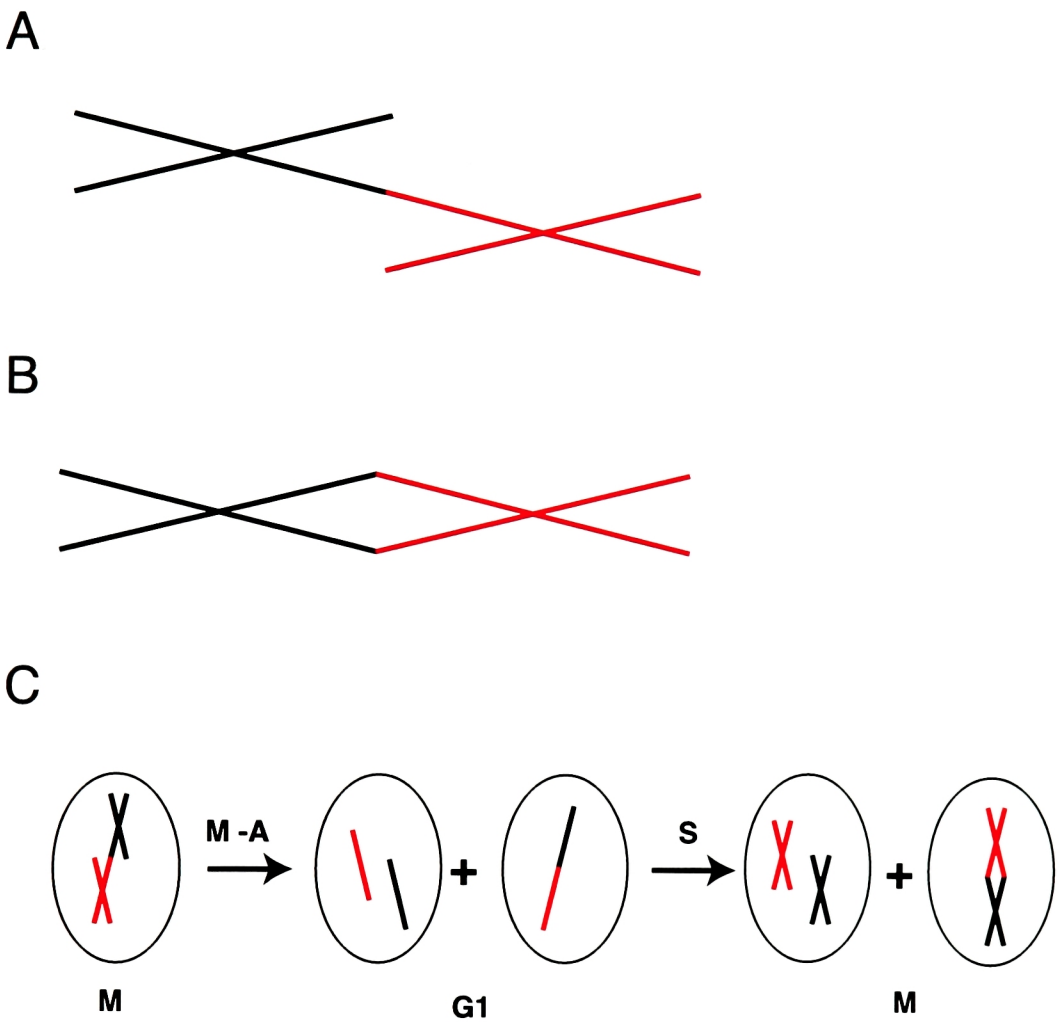

Figure 1-15. **Types of fusions following inhibition of TRF2** A. Chromatid fusion, B. Chromosome fusion, C. Schematic of events leading to formation of a chromosome fusion through a replication of a chromatid fusion, which was not severed during the metaphase to anaphase transition (M-A).

duplicated in a subsequent S phase (Figure 1-15). Chromosome fusions formed through the second process should have been visualized in the studies of Bailey et al. The reason why they were not observed probably stems from the fact that the experiments in that study were done soon after expression of the TRF2$^{\Delta B\Delta M}$ (day 5). Also, the procedure used in that study, included contact inhibition of the cells during the first days of expression and release from this inhibition followed by collection of cells after 24 hours of growth (personal communication). Therefore, only fusion events in the first cell cycle after inhibition of TRF2 were being studied. Inhibition of TRF2 leads to covalent joining of telomeric DNA, since, as shown, the fused DNA is resistant to alkaline conditions. The lack of telomeric fusions in TRF2$^{\Delta B\Delta M}$-expressing MEFs lacking NHEJ activity revealed a requirement for this pathway in the end-to-end fusion formation. Ligase IV, in particular, was required for formation of fusions after inhibition of TRF2. The requirement for DNA-PK was not assessed since the results would be confounded by the fact that all three components of DNA-PK themselves play some, although small, role in telomere protection (Bailey et al. 1999; Samper et al. 2000; Goytisolo et al. 2001). Participation of the NHEJ pathway in the repair of deprotected chromosomes validates a long-standing presumption that unprotected telomeres can behave like double stranded breaks. Such a conclusion has also been reached in *S. pombe* (Godhino Ferreira and Promisel Cooper 2001). Nitrogen starvation of cells lacking Taz1, or a combination of taz1- and rad22- leads to telomere deprotection in this yeast. Telomeres can be shown to fuse to each other and fusion is dependent on the NHEJ since it does not occur when Ku70 or Lig4 are mutated (Godhino Ferreira and Promisel Cooper 2001).

This repair of telomeres through NHEJ pathway is not a desired event. M-FISH analysis of metaphase spreads from cells expressing TRF2$^{\Delta B\Delta M}$, not only confirmed

presence of chromosome end-to-end fusions, but also showed that abnormalities resulting from such fusions may persist as translocations. Translocations, as demonstrated in these experiments can even occur in a setting of wild type primary human fibroblasts, which generally are very sensitive to damage (Di Leonardo et al. 1994), Chapter 2. This experiment shows that telomere deprotection can induce genomic instability in human cells.

The findings presented in this chapter might also shed light on what defines a critically short telomere, a telomere that is too short to function. Critically short telomeres are usually described in the setting of somatic cells at the end of their replicative life-span, or tumor cells that have not (yet) reactivated telomerase. Cells that have critically short telomeres harbor dicentric chromosomes (reviewed in de Lange 1995). Hence, some of the telomeres in the population had reached a length that could no longer support proper protection. Since the protected state is proposed to be a t-looped state and TRF2 is thought to aid in formation and/or stabilization of t-loops, the critical length would be the length of the DNA that can no longer recruit sufficient TRF2 to form a proper t-loop. Several experiments could be performed to check the validity of this hypothesis. First of all, senescent human primary fibroblasts should have a decreased frequency of t-loops. Similarly, tumors with critically short telomeres and frequent telomere fusions may also be expected to have fewer t-loops, but tumors that have reactivated telomerase and show no sign of deprotection should have normal levels of t-loops, even if such tumors still harbor very short telomeres. Finally, adding TRF2 to cells with critically short telomeres might aid in their protection by facilitating t-loops formation even on very short telomeres.

Other proteins, besides TRF2 might also participate in telomere protection in human cells. One candidate is Pot1, a single-strand TTAGGG DNA binding protein recently identified in the human database (Baumann and Cech 2001). Lack of Pot1 in *S. pombe* leads to rapid degradation of both strands of telomeric DNA. It will be very interesting to compare results after removal of human Pot1 from telomeres with the outcome of removal of telomeric TRF2 described in this chapter.

Chapter 2

$TRF2^{\Delta B \Delta M}$ induces senescence through the p53 and the Rb pathways

Introduction

The first description of the limited replicative capacity of human fibroblasts has been reported 40 years ago by Hayflick and Moorhead (Hayflick and Moorhead 1961), and the point at which human fibroblasts cease to divide when cultured *in vitro* is referred to as the Hayflick limit or senescence (from Latin senescere- to grow old). The limited life-span of human fibroblasts is a consequence of the accumulated number of cell divisions and not the calendar time spent in culture (Dell'Orco et al. 1973; Goldstein and Singal 1974), suggesting that the counting of cell divisions by a mitotic clock is responsible for the scheduling of senescence entry.

It has been proposed that *in vivo*, senescent cells might be contributing to a number of age-related diseases (Stanulis-Praeger 1987; Dimri et al. 1995) however, the best evolutionary reason for the existence of a limit to the number of divisions of human cells is its tumor suppressive potential (reviewed in de Lange 1998). Most of the known tumor cells are immortal, suggesting that senescence represents one of the obstacles that need to be overcome during tumorigenesis.

The indication that telomeres might determine the timing of entry into senescence came from the findings that telomeres shorten in most human somatic cells (Harley et al. 1990; Hastie et al. 1990). It has been proposed that lack of telomere maintenance stems from the deficiency in telomerase activity in cells (Cooke and Smith 1986). Indeed, telomerase activity is repressed in most normal human tissues (Kim et al. 1994). Activity can be found only in ovaries and testis (Wright et al. 1996), where it assures immortality of the germline, and highly proliferative tissues including hematopoietic cells (Broccoli et al. 1995; Counter et al. 1995).

However, the formal proof that telomere shortening leads to senescence was provided by experiments in which the catalytic subunit of telomerase was expressed in telomerase-negative primary human cells (Bodnar et al. 1998; Vaziri and Benchimol 1998). Telomerase-expressing cells exhibited elongated telomeres and divided well beyond the scheduled senescence timepoint. Importantly, although not surprisingly, ectopic expression of telomerase did not change the karyotype, the growth requirements, or the cell cycle checkpoint responses of the cells (Morales et al. 1999).

The above experiments have established the causal relationship between telomere shortening and senescence. However, it is not understood, what exactly is the trigger for senescence. Lack of telomere maintenance leads to attrition of telomeres, until they reach a certain length setting, commonly referred to as the "critical telomere length". At that stage, telomeres lose their ability to protect the chromosome ends and become fusogenic, resulting in the formation of dicentric chromosomes as observed in senescent cells (Thompson and Holliday 1975; Benn 1976). It is unclear what is the length of the "critically short" telomeres. It is difficult to imagine how loss of just a few kbp from a telomere of 10 kbp could lead to such a critical difference in telomere function. The high median telomere length in senescent cells might suggest that it is not the telomere length alone that determines the senescence entry. Alternatively, it is possible that some of the telomeres in each senescent cell are much shorter than the median size, and that those telomeres are responsible for the signaling into senescence.

The main effectors of the senescence entry seem to be the p53 and Rb pathways (reviewed in (Shay et al. 1991) and (Sedivy 1998)). Expression of SV40 Tag, which neutralizes the activity of p53 and Rb (reviewed in Pipas and Levine 2001) or simultaneous expression of HPV16 E6 and E7 (Shay et al. 1991) suppresses

senescence and allows for additional divisions (see Figure 2-1 for a schematic). However, the cells do not become automatically immortal since they have not stabilized their telomeres. After about 20 to 30 divisions (Ide et al. 1984; Neufeld et al. 1987; Shay and Wright 1989) they enter a state of crisis, in which there is no net gain in cell growth resulting from equal rates of cell division and cell death.

Viral oncogenes, although useful in the initial dissection of the requirements for the induction of senescence are not perfect for such studies since they have pleiotropic effects. Mouse cells are also not ideal to study senescence since their replicative life-span in culture is not determined by telomere length (reviewed in Sherr and DePinho 2000). A knockout approach in human cells has been used to assess the role of p21, an inhibitor of cyclin-dependent kinases (Brown et al. 1997), resulting in the proposal that p21 is one of the main effectors of the senescence program. However, it is not excluded that other genes were also altered during the long culture period required for this experiment. A more defined system is needed to study the pathways that lead to senescence induction in human primary fibroblasts.

Inhibition of TRF2, one of the two proteins able to directly bind to human telomeres, leads to dissolution of t-loops, loss of the G-overhangs and eventually repair of the deprotected ends resulting in formation of end-to-end fusions (See Chapter 1). In many cells, inhibition of TRF2 leads to induction of apoptosis (Karlseder et al. 1999). Cells can undergo apoptosis even before they enter the first S phase after TRF2$^{\Delta B \Delta M}$ is expressed. This points out that the signal resulting in cell apoptosis appears to come from the deprotected telomeres and not from the secondary damage that ensues after the inhibition (e.g. dicentrics ruptured in mitosis). Apoptosis is mediated by

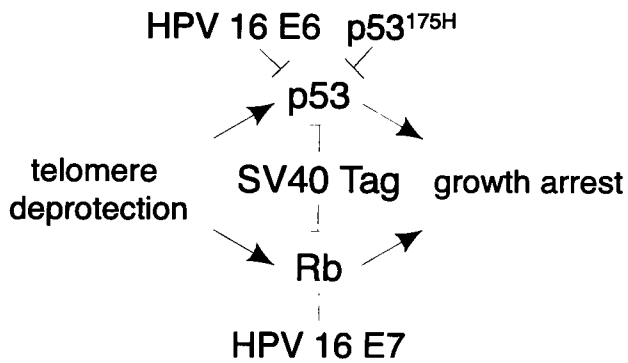

Figure 2-1. **Schematic of experimental strategies to inhibit p53 and Rb pathways.** p53 and Rb can be simultaneously inactivated using SV40 Tag antigen (reviewed in [Pipas and Levine,2001]) or they can be individually inactivated by HPV16 E6 and E7 proteins (reviewed in [zur Hausen, 2000]). p53 can also be inhibited by overexpression of a dominant negative allele of p53 (Serrano et al., 1997).

the ATM kinase and p53 since cells that are deficient in either of these proteins fail to undergo programmed cell death.

Human primary fibroblasts are another exception to the apoptotic response. To further study the cellular outcomes of inhibition of TRF2 in primary human fibroblasts that naturally undergo a telomere-directed senescence, retroviral infection was used to deliver $TRF2^{\Delta B \Delta M}$, the dominant negative allele of TRF2. Removal of TRF2 from telomeres in primary human fibroblasts resulted in rapid induction of a permanent growth arrest with characteristics of senescence. Strikingly, simultaneous elimination of the p53 and Rb pathways by expression of SV40 Tag bypassed the arrest. These findings suggest that critically short telomeres existing in pre-senescent human primary cells are unable to recruit sufficient TRF2 to achieve proper protection, which results in signaling into arrest through the DNA damage checkpoint pathways.

Results

As shown in the previous chapter, removal of TRF2 from telomeres by overexpression of a dominant negative TRF2 allele ($TRF2^{\Delta B \Delta M}$) leads to telomere deprotection. To study the influence of inhibition of TRF2 on the growth of human primary fibroblasts, IMR90 cells were infected with a $TRF2^{\Delta B \Delta M}$ retrovirus, a control virus carrying no exogenous protein, or a FLTRF2 virus. All experiments followed the timeline presented in Figure 1-2 (Chapter 1) and all the TRF2 alleles were untagged. In growth studies, in which the cells were plated at the same density on day 4 of selection and counted on day 5 and every-other day until day 15 of selection, $TRF2^{\Delta B \Delta M}$-expressing cells always fared much worse than the control counterparts (Figure 2-2, A).

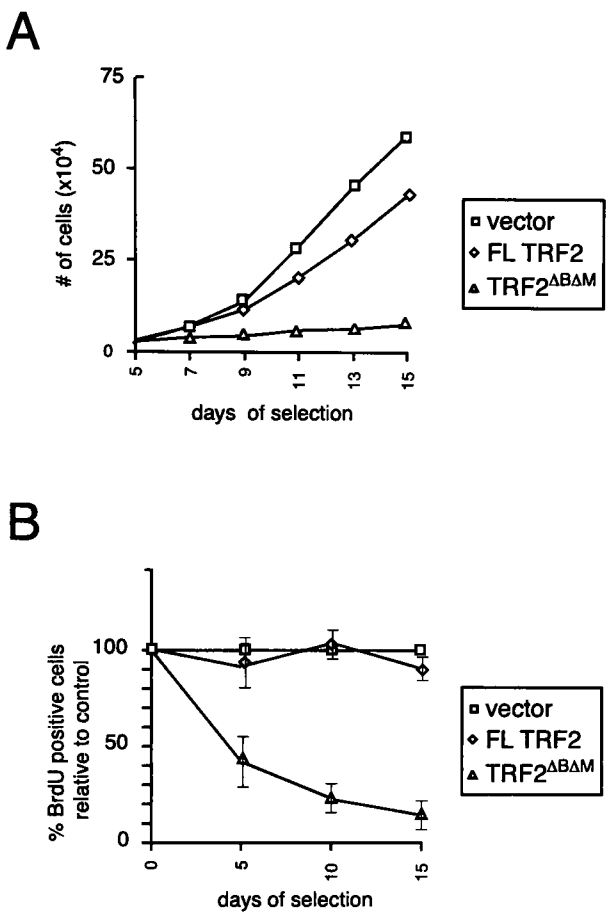

Figure 2-2. **Effects of expression of TRF2 and TRF2$^{\Delta B\Delta M}$ on growth of human primary fibroblasts. A**. Representative growth curve of cells expressing no exogenous protein (vector), FLTRF2 (FLTRF2) or TRF2$^{\Delta B\Delta M}$ (TRF2$^{\Delta B\Delta M}$). At later time points, TRF2 expressing cells grow as fast as vector control cells. On the 4th day of selection, cells were plated in duplicate at $3x10^4$ cells per well in a six-well plate. On the indicated days cells from 2 wells were washed, trypsinized and counted in duplicate using a Coulter counter. **B.** % of cells in S-phase as measured by 1 hour bromo-deoxyuridine (BrdU) incorporation on day 5, 10 and 15. All numbers are normalized to the level of BrdU incorporation in vector control cells using the formula: (fraction of BrdU-positive cells in TRF2$^{\Delta B\Delta M}$-expressing cells/ fraction of BrdU-positive cells in vector control cells) x100%. For example if 30% of cells infected with vector control were positive for BrdU and 15% of TRF2$^{\Delta B\Delta M}$-expressing cells were positive, the plotted number would be 50%. Average values and SDs derived from 5 experiments for vector and TRF2$^{\Delta B\Delta M}$, and 4 experiments for TRF2 are shown.

Within 10 days of the growth assays, the control cells gained 4.4 population doublings (PDs), FLTRF2-expressing cells gained 3.9 PDs, but TRF2$^{\Delta B\Delta M}$-expressing cells gained only 1.5 PDs. When the growth curve was continued for an extended time, the FLTRF2-expressing cells reached the growth rates of the control cells. However, TRF2$^{\Delta B\Delta M}$-expressing cells continued to be very sparse. Growth assays were also performed in HS68 and WI38 cells with similar results. Between day 5 and 11 of selection control HS 68 cells gained 3.4 PDs, FLTRF2-expressing HS68 cells, 3.7 PDs and TRF2$^{\Delta B\Delta M}$-expressing HS68 cells only 1.9 PDs. During the same period, control WI38 cells gained 1.8 PDs, FLTRF2-expressing WI38 cells, 2.1 PDs and TRF2$^{\Delta B\Delta M}$-expressing WI38 cells only 0.7 PDs.

Lack of gain in number of population doublings can be due to rapid division followed by death of the produced cells, or alternatively can be due to the cessation of cellular division. To differentiate between these two possibilities, a BrdU incorporation assay was performed to assess the number of actively cycling cells. Cells on day 4, 9, and 14 of selection were plated in equal numbers and incorporation of BrdU into the newly synthesized DNA was assessed during a 1-hour interval on the following day. A rapid decline in percentage of cells in S phase in the TRF2$^{\Delta B\Delta M}$ population was documented when compared to control or FLTRF2-expressing cells (Figure 2-2, B). In 5 experiments, the % of S phase cells among TRF2$^{\Delta B\Delta M}$-expressing cells on day 15 averaged only 17% (+/- 7%) of the control cells found in S phase. The declining numbers of cells in S phase specifically among TRF2$^{\Delta B\Delta M}$-expressing cells led to the conclusion that TRF2 inhibition causes cell cycle arrest. Similar results were obtained in other primary cell lines including WI38, and BJ hTERT fibroblasts (Table 2-1).

Table 2-1. Effects of expression of TRF2 and TRF2$^{\Delta B \Delta M}$ on growth of human primary fibroblasts. Relative % of cells in S-phase as measured by 1 hour bromo-deoxyuridine (BrdU) incorporation on day 5, 10 and 15. All numbers are normalized to the level of BrdU incorporation in vector control cells as explained in Figure 2-2.

		Relative % of cells in S-phase		
Celll line	TRF2 allele	Day 5*	Day10§	Day 15
Wi38	FL TRF2	104	104	117
	TRF2$^{\Delta B \Delta M}$	21	5	2
WI38 T ag	FL TRF2	120	124	105
	TRF2$^{\Delta B \Delta M}$	102	100	70
BJ hTERT	FL TRF2	93	97	n.d
	TRF2$^{\Delta B \Delta M}$	17	23	n.d

*BrdU in BJ hTERT cells was assessed on day 4
§ BrdU in BJ hTERT cells was assessed on day 9
n.d- not determined

The morphology of TRF2$^{\Delta B \Delta M}$-expressing cells was also suggestive of a growth arrest. With time, cells became enlarged and flat, and often harbored multilobed nuclei (Figure 2-3). These cells were strikingly similar to primary IMR90 fibroblasts at the end of their natural replicative life-span. Positive staining for β-galactosidase at pH6 (so called senescence associated β-galactosidase activity SA-β-gal) has been described to be one of the markers of senescent cells (Dimri et al. 1995). The SA-β-gal staining intensity of TRF2$^{\Delta B \Delta M}$-expressing cells was high, although not as intense as in senescent cells stained under the same conditions (Figure 2-3,). In contrast, FLTRF2-expressing cells or control cells did not exhibit staining for SA-β-gal. However, all cells were positive when control staining was performed at pH 4, which revealed the lysosomal activity of β-galactosidase.

To define the cell cycle phase of the arrest, a Fluorescence Activated Cell Sorting (FACS) analysis was performed on day 15 of the selection and revealed that cells were accumulating in broad 2n and 4n peaks when stained with propidium iodide (Figure 2-4). This pattern of growth arrest has also been seen in senescent cells.

Because of the striking similarities between the phenotype of senescent cells and cells expressing TRF2$^{\Delta B \Delta M}$, their protein expression profiles were compared. This analysis has also included IMR90 cells treated with γ-rays. It has been reported that primary human cells irradiated with γ rays, a treatment leading to formation of double stranded breaks (DSB), undergo a permanent growth arrest that resembles senescence (Di Leonardo et al. 1994). To directly compare results of irradiation and expression of TRF2$^{\Delta B \Delta M}$, the irradiated cells were maintained for 15 days after treatment. The three conditions, expression of TRF2$^{\Delta B \Delta M}$, senescence and irradiation, resulted in a very similar

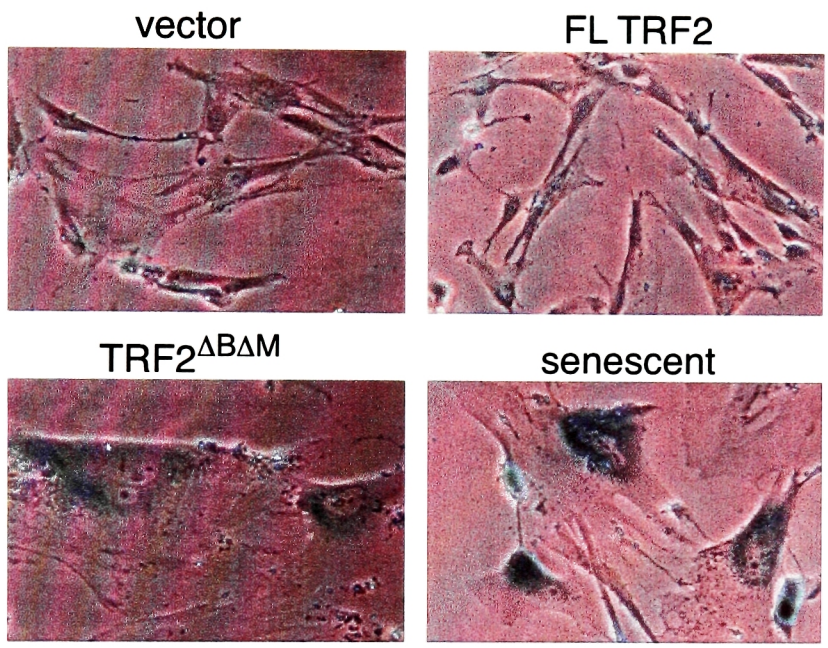

Figure 2-3. **Cell morphology and SA-β–activity in control, TRF2, TRF2$^{\Delta B\Delta M}$ infected IMR90 cells and IMR90 cells undergoing replicative senescence.** Cells infected with TRF2 alleles were plated at low density and stained for β-galactosidase activity on day 16 of selection. Note the differences in cell size and staining. At pH 4, which assesses the lysosomal activity, and acts as a control, all cells showed very intense level of staining.

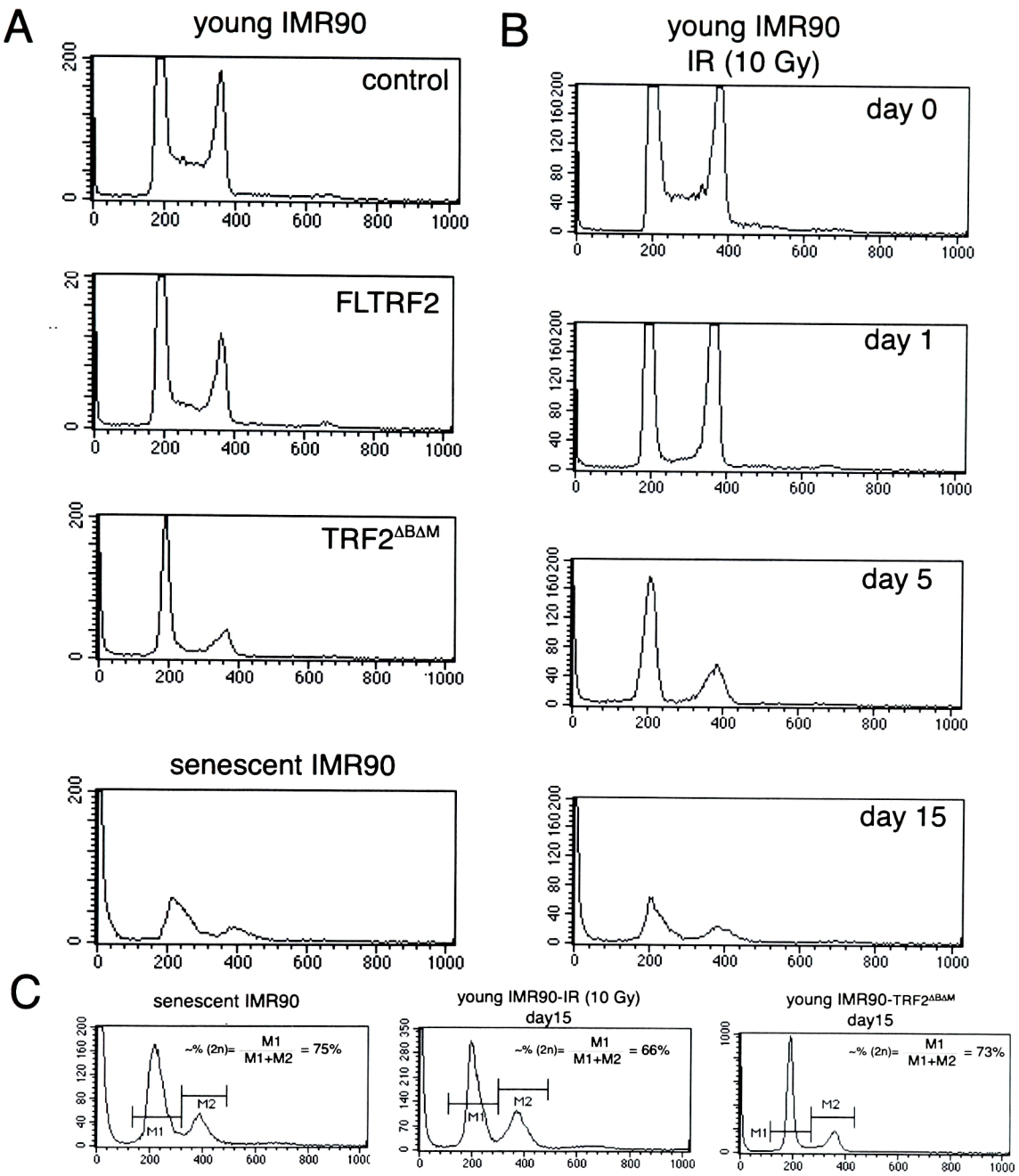

Figure 2-4. **Effects of expression of TRF2 and TRF2$^{\Delta B\Delta M}$ on cell cycle profile in human primary fibroblasts- comparison with senescent and irradiated cells.** FACS analysis of control, TRF2, TRF2$^{\Delta B\Delta M}$, senescent fibroblasts, and fibroblasts treated with 10 Gy IR. **A.** Control, TRF2, TRF2$^{\Delta B\Delta M}$ cells were analyzed on day 15 of selection, senescent cells were analysed when the cells completely ceased dividing **B.** The irradiated cells were maintained for 1,5, or 15 days with feeding before analysis. 50000 events were collected per sample and the data are presented without gating. **C**. Same cells as in A. and B. except 10000 events above "4n" were collected. Note different scales that were used to normalize for different cell numbers in M1 and M2 regions. An approximate % of 2n cells is given.

pattern of protein expression, including increased levels of p53 and its transcriptional target p21, accumulation of p16 and a switch from the hyper- to hypo-phosphorylated state of Rb (Figure 2-5). The Rb protein was almost not detectable in the senescent cells and after irradiation, and it was greatly reduced in $TRF2^{\Delta B\Delta M}$-expressing cells. Consistent with consequence of the cell cycle arrest, cyclin A (Figure 2-5) and cyclin B (Figure 4-8) levels were very low.

In order to test the role of the p53 and Rb pathways in the induction of senescence by $TRF2^{\Delta B\Delta M}$, viral oncoproteins were used (see Figure 2-1). Young fibroblasts were first infected with SV40 Tag or with pBabeNeo control virus and subsequently with control, TRF2, or $TRF2^{\Delta B\Delta M}$ carrying viruses. Comparison of BrdU labeling in these cells showed that the cell cycle arrest induced by $TRF2^{\Delta B\Delta M}$ was eliminated in IMR90 cells expressing SV40 Tag (IMR90-SV40Tag) (Figure 2-6, B). On day 15 of selection, the fraction of cells in S phase in $TRF2^{\Delta B\Delta M}$-expressing cells was close to that in control cells (88% [+/- 9]). However, the growth curves of these cells revealed that the population of $TRF2^{\Delta B\Delta M}$-expressing SV40 Tag cells did not grow as fast as the control populations also expressing the SV40 T antigen (Figure 2-6, C). At day 10 of the growth assay, the control cells gained 4.9 PDs, FLTRF2-expressing cells gained 5.1 PDs, and $TRF2^{\Delta B\Delta M}$-expressing cells gained 3.7 PDs. Since cells lacking the SV40 Tag but expressing $TRF2^{\Delta B\Delta M}$ only gained 1.5 PDs, SV40 Tag clearly has a strong suppressive effect on $TRF2^{\Delta B\Delta M}$-induced arrest.

The morphology of the $TRF2^{\Delta B\Delta M}$-expressing IMR90-SV40T cells was non-senescent (Figure 2-7), they did not stain for SA-β-galactosidase, and the only difference between these and control Tag cells was the presence of many refractile cells detached from the plate (Figure 2-7). Such cells are presumed to be unable to divide, explaining

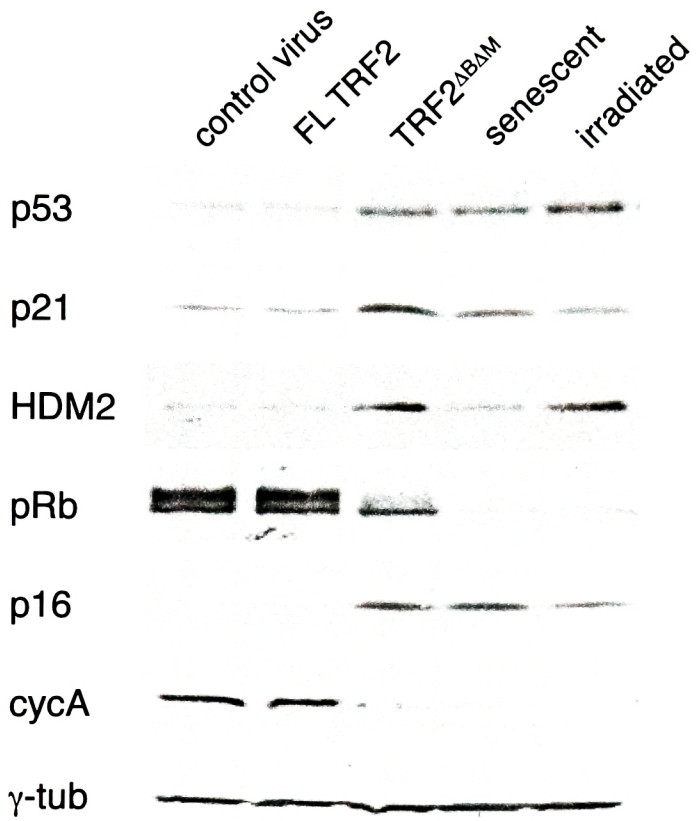

Figure 2-5. **Effects of expression of TRF2 and TRF2$^{\Delta B\Delta M}$ on protein profiles in human primary fibroblasts- comparison with senescent and irradiated cells.** Western blot analysis of cell cycle regulatory proteins in control, TRF2, TRF2$^{\Delta B\Delta M}$, senescent fibroblasts, and cells treated with 10 Gy IR from a ^{137}Cs source. Control, TRF2, TRF2$^{\Delta B\Delta M}$ cells were collected on day 15 of selection, senescent cells were collected when the cells completely ceased dividing and the irradiated cells were left in tissue culture for 15 days with feeding before preparation of a lysate. Lysates from the five cell types represented the same number of cells.

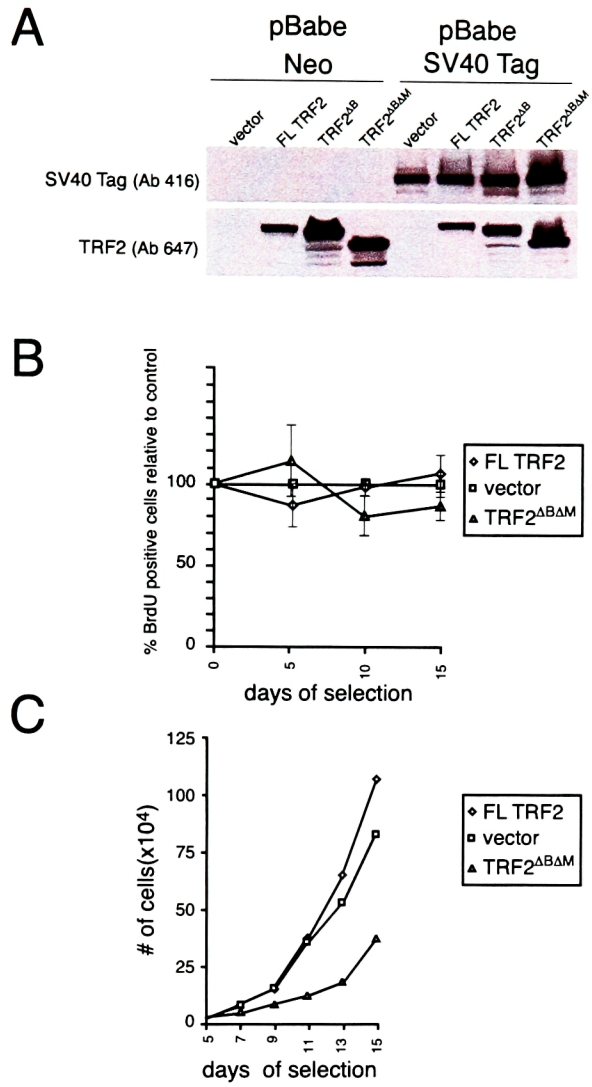

Figure 2-6. **Effects of expression of TRF2 and TRF2$^{\Delta B\Delta M}$ on growth of human primary fibroblasts that also express SV40 Tag. A.** Western blot showing expression of SV40 Tag and of TRF2 alleles in young IMR90 cells infected with pBabe SV40 Tag or a pBabe Neo control. Endogenous TRF2 is not detectable under these conditions. The IMR90 SV40 Tag cells were used for experiments shown in panels B and C. **B.** Relative % of cells in S-phase as measured by 1 hour BrdU incorporation on day 5, 10 and 15. All numbers are normalized to the level of BrdU incorporation in vector control cells as explained in Figure 2-2. Mean values and and SDs derived from 3 experiments are shown. **C.** Representative growth curve of cells expressing no exogenous protein (vector), FLTRF2 (FLTRF2) or TRF2$^{\Delta B\Delta M}$ (TRF2$^{\Delta B\Delta M}$). On the 4th day of selection, cells were plated in duplicate at 3x10^4 cells per well in a six-well plate. On the indicated days cells from 2 wells were washed, trypsinized and counted in duplicate using a Coulter counter.

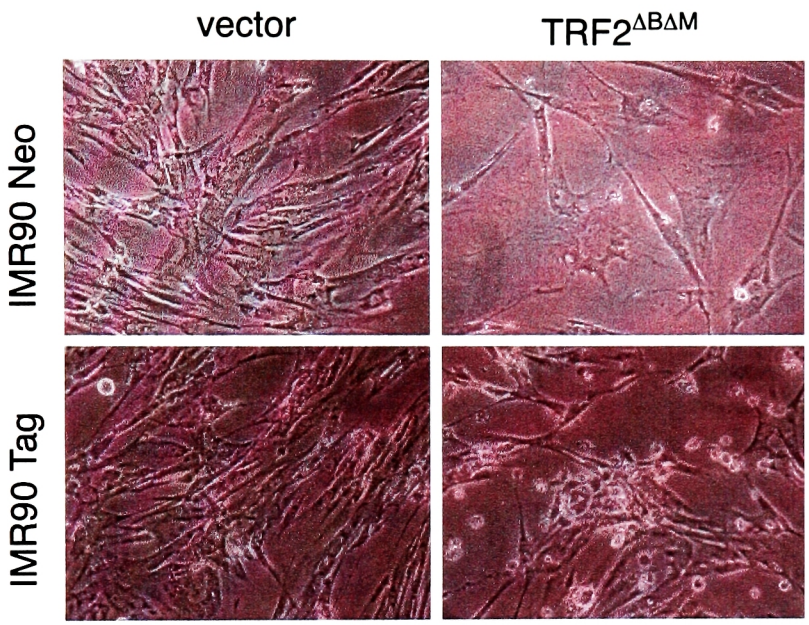

Figure 2-7. **Comparison of cellular morphology of cells with or without SV40 large T antigen, expressing no exogenous protein or TRF2$^{\Delta B\Delta M}$.** Micrographs showing cell morphology on day 13 of selection. Young IMR90 were first infected with SV40 Tag or a Neo marker alone and were confirmed to express the large T antigen by immunofluorescence and western blotting (see Figure 2-5). Subsequently these cells were infected with a vector control or a TRF2$^{\Delta B\Delta M}$ carrying virus. On the 4th day of selection, cells were plated at $3x10^4$ cells per well in a six-well plate for the growth curve shown in Figure 2-5. Photographs were taken on day 13 of selection. Note that in SV40 Tag cells expressing TRF2$^{\Delta B\Delta M}$, the cell density is similar to SV40 T antigen cells infected with a vector control but the latter culture has many floating cells that are round and refractile .

the discrepancy between the hindered population growth and the normal levels of the BrdU labeling in $TRF2^{\Delta B \Delta M}$-expressing cells.

To further analyze the requirements for p53 and Rb in the induction of senescence by $TRF2^{\Delta B \Delta M}$, these pathways were separately inhibited by expression of HPV16E6 or HPV16E7 respectively. The expression of E7 was verified by immunoblotting (Figure 2-8, A). Since the available antibodies against E6 do not seem to recognize the protein in western blots, loss of p53 protein acted as a surrogate marker for the presence of E6 (Figure 2-8, A). As expected from the results of the Tag experiments, simultaneous expression of E6 and E7 abrogated the arrest caused by the TRF2 inhibition in primary human cells (Figure 2-8, B), but separate repression of the p53 and the Rb pathways led only to a limited suppression of the growth arrest. Additionally, expression of $p53^{175H}$, a dominant negative allele of p53 (Serrano et al. 1997) could not overcome the arrest (Figure 2-8, B), even though it was expressed at very high levels. These experiments suggested that signaling through either one of the pathways is sufficient to induce and maintain the arrest after TRF2 inhibition.

Signaling from the unprotected telomere to growth arrest might be expected to involve the PI-3 kinases that have been implicated in DNA damage signaling. Based on the previous experiments, in which the induction of apoptosis by telomere deprotection depended on the ATM gene product (Karlseder et al. 1999), it was pertinent to test whether the arrest induced by $TRF2^{\Delta B \Delta M}$ expression also required the ATM kinase. Three different primary fibroblast lines from patients affected with Ataxia Telangiectasia and one control line from a heterozygous parent of one of the affected patients were analyzed for the ability to undergo growth arrest after inhibition of TRF2. The ATM status of the cell lines was confirmed by immunoblot analysis with an antibody directed

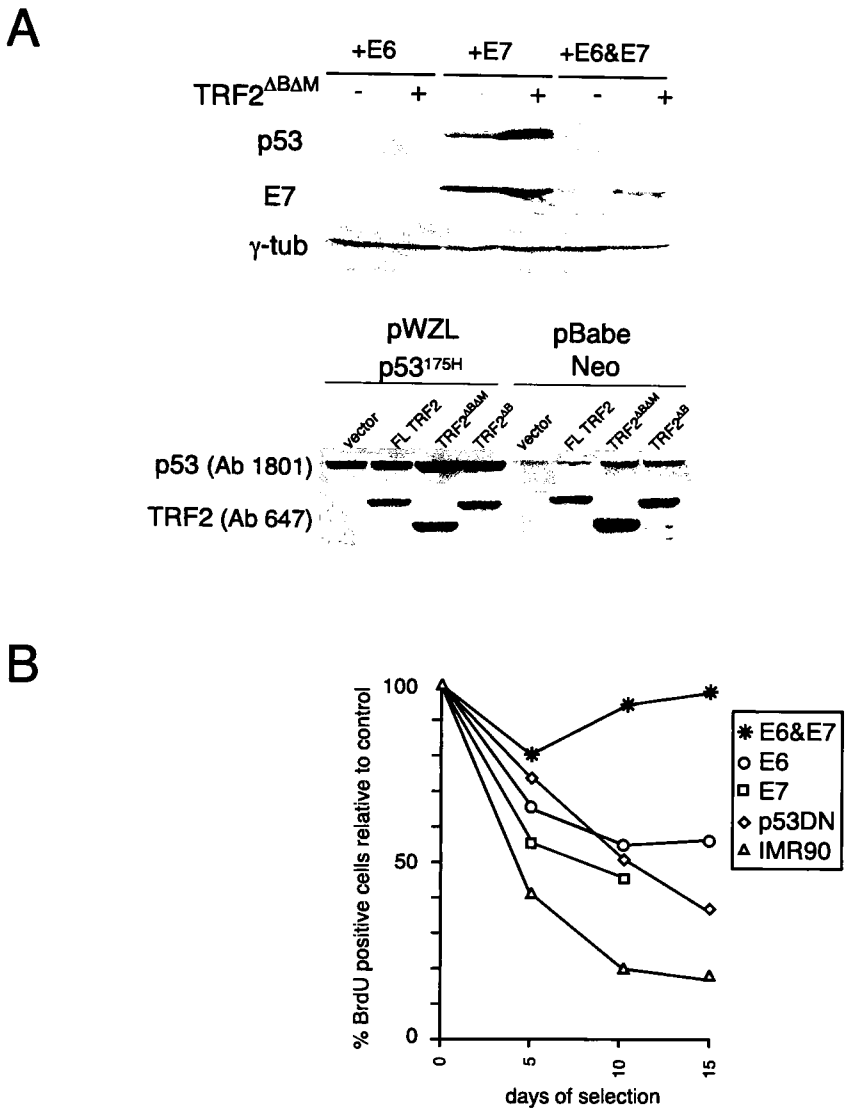

Figure 2-8. **Effects of expression of TRF2$^{\Delta B\Delta M}$ on growth of human primary fibroblasts that co-express HPV16 E6, HPV16 E7, HPV16 E6 and E7, p53^{175H}, or pBabe Neo. A.** Western blot confirming presence or absence of HPV16 E7 or p53 in cells that were infected with viruses carrying HPV16 E6, HPV16 E7, both HPV16 E6 and HPV16 E7, or p53DN (p53^{175H}). Lack of p53 acts as a surrogate marker of expression of HPV16 E6. **B.** Relative % of cells in S-phase as measured by 1 hour BrdU incorporation on day 5, 10 and 15 of selection after infection with TRF2$^{\Delta B\Delta M}$. All numbers are normalized to the level of BrdU incorporation in vector cells as explained in Figure 2-2.

against the ATM kinase (Figure 2-9, A). The AT status did not influence the percentage of cells that were in S phase (Figure 2-9, B) nor the morphology of the cells after expression of $TRF2^{\Delta B\Delta M}$, suggesting that the ATM kinase is dispensable for the induction of the arrest but not excluding the possibility that ATM, when present, can be involved in signaling from unprotected telomeres in primary fibroblasts.

One possibility is that ATM signals to p53 and that in its absence inhibition of TRF2 induces senescence via the Rb pathway. The prediction would be that p53 is not upregulated in AT cells expressing $TRF2^{\Delta B\Delta M}$. However, western blot analysis showed increased levels of p53 in $TRF2^{\Delta B\Delta M}$-expressing AT cells (Figure 2-9, C). This indicates that ATM is not solely responsible for p53 activation in this setting. Furthermore, suppression of Rb in AT cells by expression of HPV16E7 (Figure 2-10, A) led to only minimal suppression of the growth arrest caused by $TRF2^{\Delta B\Delta M}$ expression (Figure 2-10, B). However, parallel experiments in which HPV16E7 was expressed in cells that already expressed $p53^{175H}$ (dominant negative allele of p53 (Serrano et al. 1997)) also led to a minimal suppression of the growth arrest caused by $TRF2^{\Delta B\Delta M}$ expression. This might indicate that inhibition of the endogenous p53 with $p53^{175H}$ and HPV16E6 proteins are not equivalent, and makes the lack of full suppression of growth arrest caused by $TRF2^{\Delta B\Delta M}$ expression in AT cells expressing HPV16E7 hard to interpret.

Telomere directed senescence does not seem to occur in mouse cells (reviewed in Sherr and DePinho 2000); however, telomere dysfunction can have deleterious effects as shown by studies using the mTERC KO mice (Lee et al. 1998; Rudolph et al. 1999; Hemann et al. 2001) or inhibition of TRF2 in MEFs (Karlseder et al. 1999). In both settings, cells undergo apoptosis, appearance of which can be temporarily inhibited (Chin et al. 1999; Hemann et al. 2001), or completely suppressed (Karlseder et al. 1999)

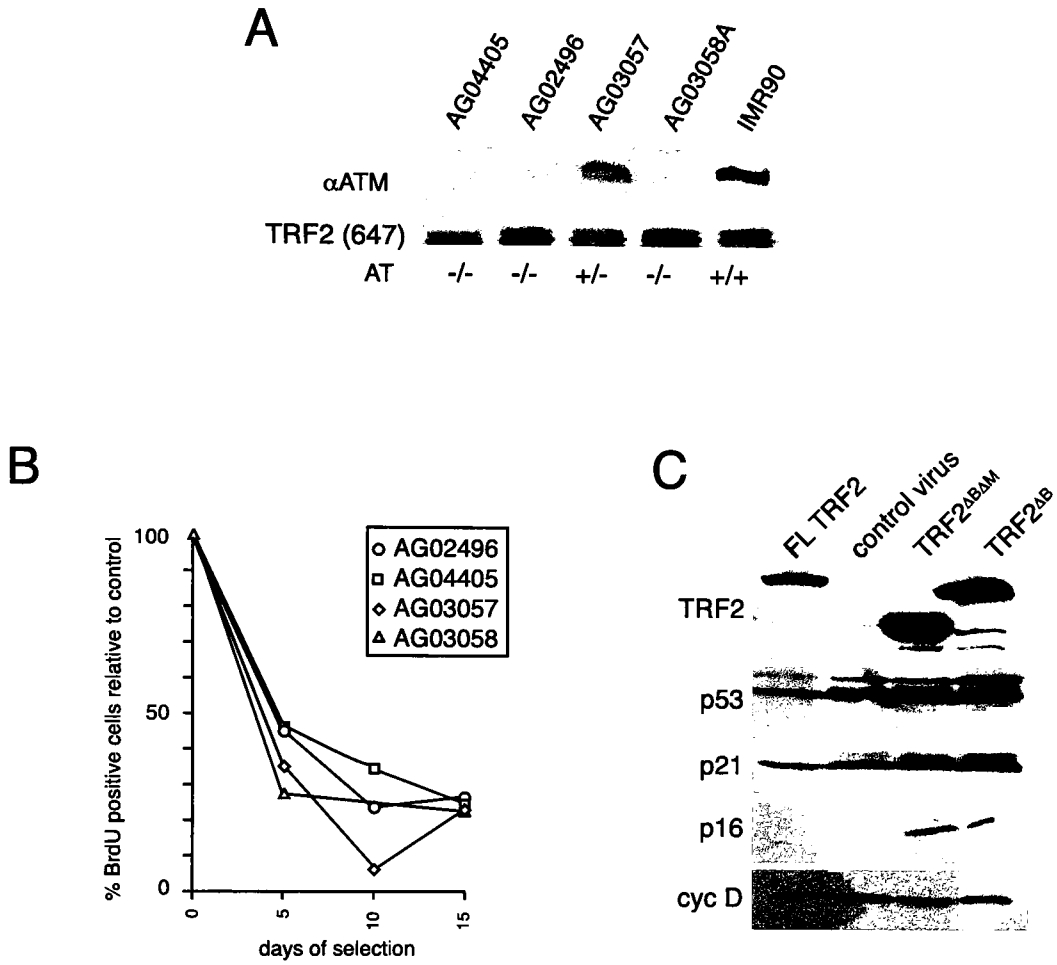

Figure 2-9. **Effects of expression of TRF2$^{\Delta B\Delta M}$ on growth of human primary fibroblasts that express or lack endogenous ATM protein.** **A.** Western blot confirming presence or absence of ATM in primary fibroblasts obtained from individuals affected with Ataxia Telengiectasia (AG04405, AG02496, AG03058A), fibroblasts from heterozygous mother of the individual who donated the AGO3058A cells (AG03057) or wt primary fibroblasts (IMR90). **B.** Relative % of cells in S-phase as measured by 5 hour BrdU incorporation on day 5, 10 and 15 of selection after infection with TRF2$^{\Delta B\Delta M}$. All numbers are normalized to the level of BrdU incorporation in vector cells as explained in Figure 2-2. **C.** Western blots in the AG02496 cells after expression of TRF2 alleles on day 15 of selection. Note that the loading is in different order than in previous westerns. Also, the loading is not equal (best visualized on cyclin D western). Lysates made from ~5700 FL TRF2-expressing cells, ~17500 control cells, ~ 10000 TRF2$^{\Delta B\Delta M}$-expressing cells, and ~10000 TRF2$^{\Delta B}$-expressing cells were loaded.

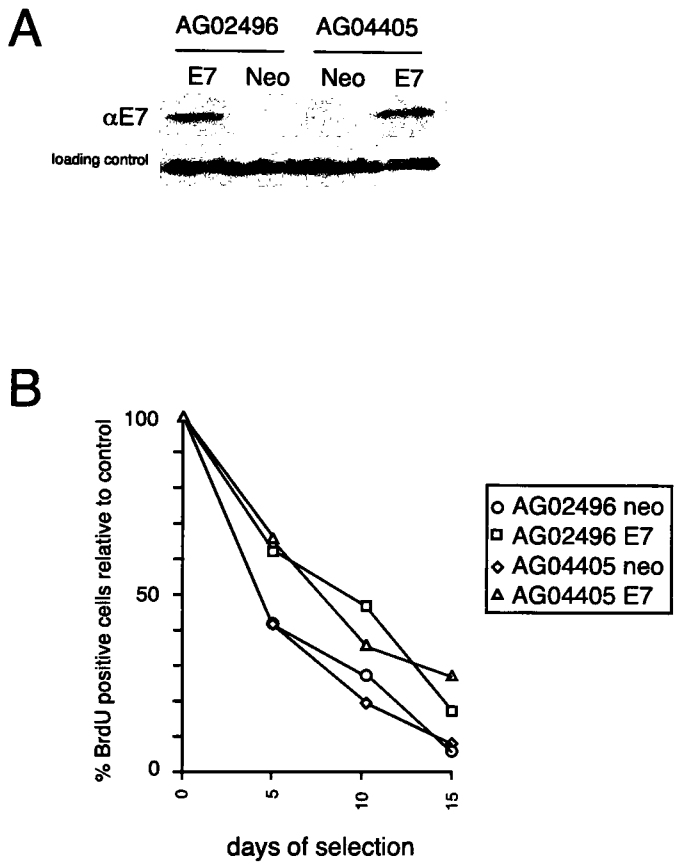

Figure 2-10 **Effects of expression of TRF2$^{\Delta B\Delta M}$ on growth of human primary fibroblasts that lack ATM and express HPV E7 or Neo control** **A.** Western blot confirming presence or absence of HPV16 E7 in two AT cell lines (AG02496 and AG04405). Loading control is a cross-reacting band observed with the antibody against E7 antibody. **B.** Relative % of cells in S-phase as measured by 5 hour BrdU incorporation on day 5, 10 and 15 of selection after infection with TRF2$^{\Delta B\Delta M}$. All numbers are normalized to the level of BrdU incorporation in vector cells as explained in Figure 2-2.

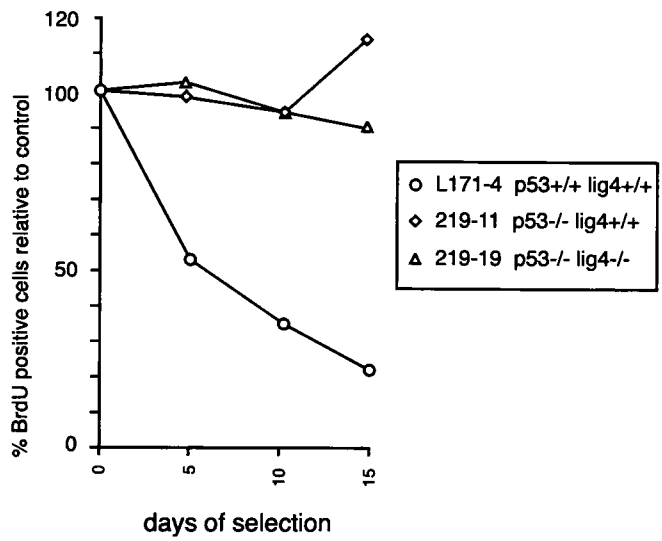

Figure 2-11. **Effects of expression of TRF2$^{\Delta B \Delta M}$ on growth of wt primary MEFs and MEFs deficient in p53 protein.** Relative % of cells in S-phase as measured by 1 hour BrdU incorporation on day 5, 10 and 15 of selection after infection with TRF2$^{\Delta B \Delta M}$. All numbers are normalized to the level of BrdU incorporation in vector cells as explained in Figure 2-2.

by the lack of p53 protein. To determine if primary MEFs, like human cells, undergo growth arrest after inhibition of TRF2, they were infected with a control virus or TRF2$^{\Delta B\Delta M}$ virus. Indeed, the primary MEFs arrested very efficiently after inhibition of TRF2 (Figure 2-11). The arrest was dependent on p53 protein because MEFs deficient in p53 did not undergo arrest (Figure 2-11) despite having clear markers of telomere dysfunction (see Figure 1-12). These data suggest that lack of TRF2 on telomeres is sensed by the DNA damage checkpoint, and that lack of p53 alone suppresses the TRF2$^{\Delta B\Delta M}$–induced arrest in mouse cells.

Discussion

The data presented in this chapter show that the presence of TRF2 on telomeres is required for continuous growth of human primary fibroblasts. This finding parallels the conclusion that inhibition of TRF2 is incompatible with cell survival and leads to apoptosis in certain cells (Karlseder et al. 1999). Senescence can be viewed as a different terminal phenotype assuring that cells with chromosomes that are not properly protected, no longer divide.

Telomeres devoid of TRF2 become deprotected and it was surmised that the state of being deprotected results from the inability of the telomere to fold into a t-loop (see Chapter 1). An unfolded telomere on a chromosomal level leads to telomere fusion through the NHEJ pathway, which suggests that it is recognized as a double stranded break (DSB). Here it is shown that chromosome ends that are without TRF2, and thought to be in a non t-looped state, can activate checkpoint pathways resulting in growth arrest. The striking similarity of the phenotypes and pathways required for the

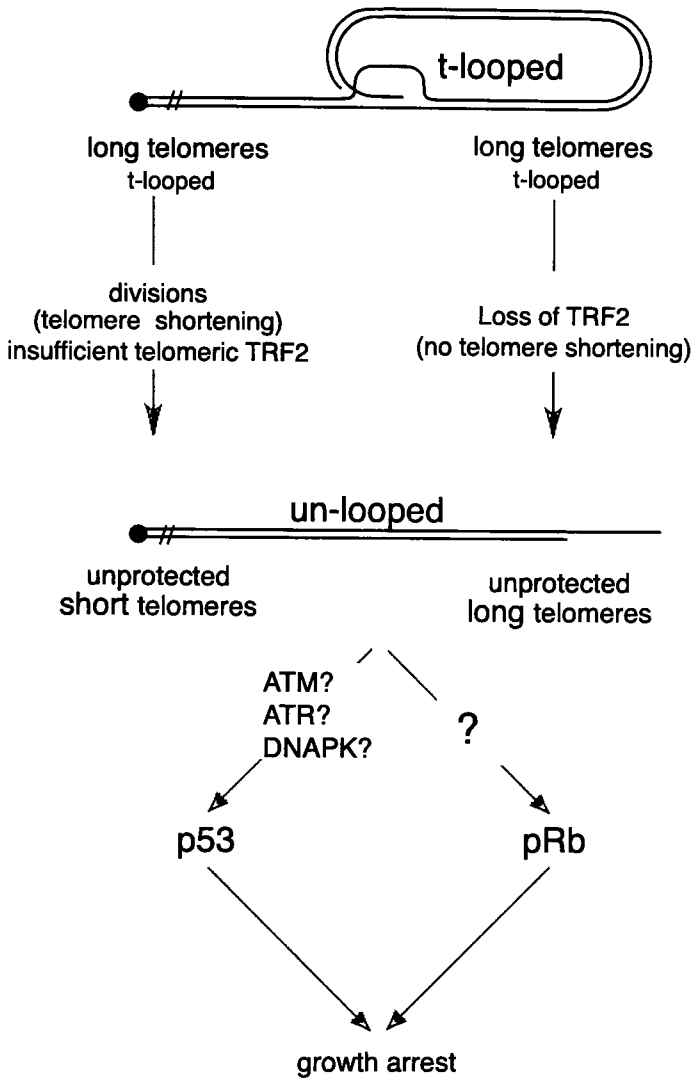

Figure 2-12. **A model of parallels between events leading to growth arrest in replicative senescence and after inhibition of TRF2 in human primary fibroblasts.** Inhibition of TRF2 (right) leads to t-loop opening and signaling to p53 and Rb pathways resulting in growth arrest. Telomere shortening due to the "end replication problem" (left) eventually is proposed to lead to loss of sufficient TRF2 from the telomere, resulting in opening of t-loops and downstream events that activate p53 and Rb pathways bringing about the arrest.

arrest induced by inhibition of TRF2 and naturally occurring senescence suggests the possibility that the inability of short telomeres in pre-senescent cells to fold into a t-loop leads to activation of the senescence program (Figure 2-12). If this hypothesis is correct, senescent cells should have greatly diminished levels of t-loops, a prediction that is currently being tested

The similarity of protein expression in cells at the end of their replicative life-span and cells expressing TRF2$^{\Delta B\Delta M}$ led to the conclusion that the same pathways are activated in both states. In testing the necessity for signaling through the p53 and Rb pathways, it was found that expression of TRF2$^{\Delta B\Delta M}$ in the presence of the SV40 Tag overcomes senescence but that the population seems to enter a state similar to crisis. An analogy can be drawn between inhibition of TRF2 in the presence of Tag and life-span extension of wt primary fibroblasts in which both p53 and Rb are inhibited by expression of Tag, or simultaneous expression of HPV16E6 and E7 proteins. In such cells, the signal to halt proliferation is presumably disregarded, resulting in suppression of senescence and continued growth despite considerable telomere dysfunction, evidenced by frequent dicentrics and other chromosomal abnormalities present in these cells (Ray et al. 1992). After 20-30 population doublings of additional growth, such cultures enter crisis, a state in which cell numbers do not increase because cell division is offset by cell death. The cause of crisis is unclear and may stem from loss of essential subtelomeric genes that are normally protected by telomeres. The crisis-like state induced by TRF2$^{\Delta B\Delta M}$ in SV40Tag expressing cells occurs without loss of telomeric DNA, making it unlikely that subtelomeric genes were lost. Perhaps, a more plausible explanation for crisis is the cumulative genome damage caused by cells that divide with unstable chromosomes.

There are many remaining questions about the induction of senescence. A very important question is what the upstream signals are that activate the p53 pathway. ATM, even though clearly involved in signaling from DSB (Rotman and Shiloh 1998), is not essential for the induction or the maintenance of the arrest after inhibition of TRF2. This is in agreement with findings that fibroblasts from patients afflicted with A-T undergo replicative senescence (Vaziri et al. 1997). p53 is also induced in senescent A-T cells, suggesting that other pathways are also responsible for signaling to p53. Similarly, in a mouse model of A-T, gamma irradiation leads to a partial G1 cell cycle arrest (Xu and Baltimore 1996), which is completely removed when p53 is also mutated (Xu et al. 1998).

Two other PI-3 kinases, ATR and DNA-PK are candidates for the signaling from damaged DNA, and thus potential candidates for the sensors of unprotected telomere. ATR is able to phosphorylate p53 *in vitro* and *in vivo* (Lakin et al. 1999; Tibbetts et al. 1999) and its inhibition leads to hypersensitivity to damaging agents (Cliby et al. 1998). DNA-PK also phosphorylates p53 *in vitro* (Lees-Miller et al. 1990; Shieh et al. 1997); however, recent analysis of DNA-PKcs deficient mice suggests that DNA-PK is not essential for signaling after general genome damage (Jhappan et al. 2000). It will be important to test the requirements for ATR and DNA-PK in induction of arrest after the inhibition of TRF2.

p53 can also be regulated by $p14^{ARF}$ (Kamijo et al. 1997; Stott et al. 1998). Semi quantitative RT-PCR has shown increased levels of $p14^{ARF}$ message in senescent cells, and overexpression of the protein can result in growth arrest of human primary fibroblasts (Dimri et al. 2000). It remains to be determined if TRF2 inhibition also can result in increased levels of $p14^{ARF}$.

Rb hypophosphorylation in replicative senescence and after inhibition of TRF2 seems to result from p16 upregulation. When present, p16 inhibits the Cdk4 and Cdk6-cyclin D complexes, leading to inhibition of Rb phosphorylation; however, events leading to increase in p16 expression are much less well defined than events leading to p53 stabilization. With ongoing divisions, p16 mRNA as well as p16 protein accumulate in human fibroblasts (Hara et al. 1996). This accumulation seems to be at least partially dependent on the increase in the transcriptional factor Ets1 (Ohtani et al. 2001), although other pathways of p16 regulation are also expected to operate in human cells, based on the finding that mouse cells deficient in Bmi-1, a transcriptional repressor belonging to the Polycomb group, p16 levels are increased (Jacobs et al. 1999).

Again, at this point it is not known how p16 is induced in cells in which TRF2 was inhibited. It might be informative to use some of the mouse KO and overexpression model systems to confirm the involvement of the discussed proteins in growth response to telomere deprotection.

It is also of interest to point out that growth arrest in human primary fibroblasts can be induced by DSBs resulting from irradiation ((Di Leonardo et al. 1994) and Figure 2-5), as well as by an inappropriate mitogenic stimulus originating from expression of oncogenic Ras (Serrano et al. 1997; Zhu et al. 1998). Under these conditions, the pattern of protein expression is very similar to the pattern of expression after inhibition of TRF2, suggesting a common pathway that is engaged in implementation and/or maintenance of the arrest.

One of the important questions in the senescence field pertains to the signal that induces the growth arrest when telomeres reach the critical length. Some suggest that progressive telomere shortening might change expression of genes that would

eventually lead to growth arrest (Baur et al. 2001); however, as of yet, no candidate genes were found to be localized in the subtelomeric regions of human cells. Others propose that there is a telomere specific checkpoint that examines the telomere status and dictates the arrest. Finally, the critically short telomere might signal as a double stranded break inducing common DNA damage response pathways. The data presented in this chapter support the last model of how senescence signals into arrest. Additionally, based on the data presented in Chapter 1, it can be further proposed, that the signal to these pathways is brought on by the unfolding of the t-loop as a consequence of insufficient TRF2 being recruited to the critically short telomere or telomeres.

Chapter 3

TRF2 and telomere length regulation

Introduction

Human cells that lack telomerase generally do not maintain telomere length. They can activate a poorly understood alternative lengthening pathway (ALT) (Bryan et al. 1995), which has been proposed to rely on homologous recombination (Dunham et al. 2000). However, activation of ALT is a very rare event even in tumor cells, and all human primary cells lacking telomerase do not maintain their telomeres, which results in loss of 50 to 200 bp of telomeric DNA from each telomere per division (Cooke and Smith 1986; Harley et al. 1990; Hastie et al. 1990). Shortening originates from the inability of the DNA polymerases to fully replicate some of the termini, but also from nucleolytic activities that may participate in the formation of the G-overhangs. Eventually, lack of telomere maintenance leads to deprotection of telomeres (discussed in Chapter 1) and senescence (discussed in Chapter 2).

Expression of hTERT, a catalytic subunit of telomerase restores telomerase activity as well as stabilizes telomere length in most primary cells tested to date (Bodnar et al. 1998; Vaziri and Benchimol 1998). This is in agreement with findings that telomerase activity in human cells is regulated at the level of expression of the catalytic subunit (hTERT) and hTERT expressing cells usually have detectable telomerase activity (Kilian et al. 1997; Meyerson et al. 1997; Nakamura et al. 1997). Tissues that express hTERT at a very low level but have no discernable telomerase activity in extracts have been proposed to produce a telomerase variant that is able to act as a dominant negative allele poisoning the wt activity (Colgin et al. 2000).

Although existence of the functional telomerase enzyme in the cell is often a requirement for telomere maintenance, its presence does not automatically lead to

telomere elongation. A number of findings suggest that telomere length is regulated in cis at each telomere. Despite high telomerase activity in the germline (Mantell and Greider 1994; Prowse and Greider 1995; Wright et al. 1996), telomere length is species specific (Kipling and Cooke 1990, Zhu et al. 1998). While expressing high telomerase activity, many tumor cell lines maintain their telomeres at a stable length (Counter et al. 1992; Counter et al. 1994; van Steensel and de Lange 1997). Finally, new telomeres that are synthesized after transfection of telomeric DNA (so called "telomeric seeds") into the cultured cells are elongated to match the length of the other telomeres in those cells (Barnett et al. 1993; Hanish et al. 1994; Sprung et al. 1999). To achieve such control, the length of each telomere has to be monitored and regulated separately.

Telomere length control studies in human cells have shown that the TTAGGG binding factor 1 (TRF1) is a negative regulator of telomerase-directed elongation (Karlseder and de Lange; van Steensel and de Lange 1997). Removal of TRF1 from telomeres by overexpression of a dominant negative allele of TRF1 in cells that also express telomerase leads to telomere elongation (van Steensel and de Lange 1997). Overexpression of TRF1 in the same cell line causes telomeres to shorten (van Steensel and de Lange 1997). Under conditions of inhibition or overexpression of TRF1, the telomere length stabilizes at a new length setting, which can be maintained for many population doublings (Smogorzewska et al. 2000). Based on these findings it was proposed that TRF1 acts in cis and regulates length of each individual telomere (van Steensel and de Lange 1997). According to the model, a large amount of TRF1 is recruited to long telomeres. This blocks telomerase from adding more repeats and telomeres gradually shorten. When they reach a length at which they no longer can

recruit enough TRF1 to cause inhibition, telomerase again is able to add more repeats. Through multiple cycles of such changes, telomeres achieve length equilibrium.

To establish that TRF1 affects telomere length through regulating the telomerase pathway, TRF1 or its dominant negative allele were introduced into primary human cells. Because these cells lack telomerase, their telomeres naturally shorten with cell divisions. This characteristic shortening rate did not change when any of the TRF1 alleles were added and confirmed that TRF1 acts through modulating the telomerase pathway (Karlseder and de Lange, unpublished).

TRF1 is regulated by one of its interacting proteins. Tankyrase1, a poly (ADP-ribose) polymerase (PARP), binds to an acidic N-terminus of TRF1 and modifies it using its catalytic activity (Smith et al. 1998). Upon this modification TRF1 loses its affinity for the telomeric DNA, which can be demonstrated both *in vitro* and *in vivo* (Smith et al. 1998; Smith and de Lange 2000). In agreement with its ability to inhibit TRF1, expression of tankyrase leads to telomere elongation (Smith and de Lange 2000), and the effect requires the PARP activity of tankyrase since an allele lacking the PARP domain does not affect telomere length. Taken together, these experiments suggest that tankyrase acts through TRF1 to modulate telomere length. However, the ultimate experiment showing that tankyrase acts only through regulating TRF1 by creation of a TRF1 allele that cannot be modified by tankyrase has not been done yet.

TRF1 has a second binding partner, TIN2 (Kim et al. 1999), which also participates in telomere length regulation (Kim et al. 1999). Expression of a number of truncation alleles of this protein leads to telomere elongation that is dependent on telomerase. Since TIN2 exists in a complex with TRF1 (Kim et al. 1999) and tankyrase (Ye and de Lange, unpublished), it is likely that the proteins act in the same pathway.

This chapter defines TRF2, the second TTAGGG repeat binding factor, as a regulator of telomere length. Overexpresion of TRF2 leads to telomere shortening in telomerase positive but also in telomerase negative cells showing that TRF2 can influence the shortening activities at the telomere. At this point, it is impossible to discern whether TRF2 can also influence the telomerase pathway, but the fact that it interacts with Rap1, which when overexpressed causes mild telomere elongation, suggests that TRF2 might endow the telomere with both the positive regulators of shortening and negative regulators of elongation.

Results

One of the indications that both TRF1 and TRF2 might influence telomere length comes from the observations that long telomeres seem to accumulate much more TRF1 and TRF2 than short telomeres. Immunofluorescent staining of telomeric proteins was performed in HeLaI.2.11, a HeLa subclone with very long telomeres (15-40kbp), and HelaII, a subclone with considerably shorter telomeres (3-6.5 kbp) (Saltman et al. 1993) (Figure 3-1). Telomere staining of TRF2 was generally less visible than staining of TRF1, and staining with αTRF2 antibodies always resulted in a higher nucleoplasmic signal than staining with αTRF1 antibodies. Although quantification of the signal was not feasible, the punctate pattern of staining against both proteins was reproducibly much more prominent in HeLaI.2.11 than HeLaII (Figure 3-1, B, pictures were taken at the same exposure time and are reproduced without any adjustments). Many cells in HeLaII population had almost no punctate staining visible above the overall nucleoplasmic staining. These results indicate that the length of the telomere tract influences accumulation of telomeric proteins at the chromosome termini. However, this apparent differential presence of TRF1 and TRF2 on short and long telomeres does not seem to

correlate with the expression levels of these proteins since TRF1 levels were comparable in Helal.2.11 and HeLaII cells, and levels of TRF2 in Helal.2.11 were slightly lower than in HeLaII (Figure 3-1, A). It needs to be noted that another study found a two fold difference in the TRF1 levels between HeLa cells with short and long telomeres, and much smaller difference for TRF2 (Okabe et al 2000). This group has also calculated that the number of molecules of TRF1 present in the cell per each kb of TTAGGG repeats is higher in cells with shorter telomeres than with longer telomeres. This inverse correlation was weaker for TRF2 (Okabe et al 2000).

To gain understanding of how TRF2 influences telomere length, a previously established Tetracyclin-inducible expression system was used ((van Steensel and de Lange 1997), and see Chapter 1 for a more detailed description). An untagged full length TRF2 was placed under the control of a Tetracyclin-controlled promoter and was stably transfected into the HTC75 cells, a derivative of HT1080 human fibrosarcoma cell line characterized by high telomerase activity and stable telomere length (van Steensel and de Lange 1997). A number of clonal lines were established by Bas van Steensel and were called P lines. In short term experiments induction of TRF2 had no effect on growth ((van Steensel et al. 1998), Chapters 1 and 2). To study the influence of TRF2 on telomere dynamics, cells induced and non-induced for expression of TRF2 were grown in parallel for 124 population doublings (PDs). Telomere length was assessed periodically by Southern blot hybridization with a telomeric probe. Out of the four clonal cell lines examined, one (P4) showed erratic changes in telomere length that did not correlate with presence or absence of TRF2. This cell line was not studied further. Three other cell lines (P7, P12, and P33), when grown without induction, maintained their telomeres at a stable length. TRF2 induction in these cells produced a complex

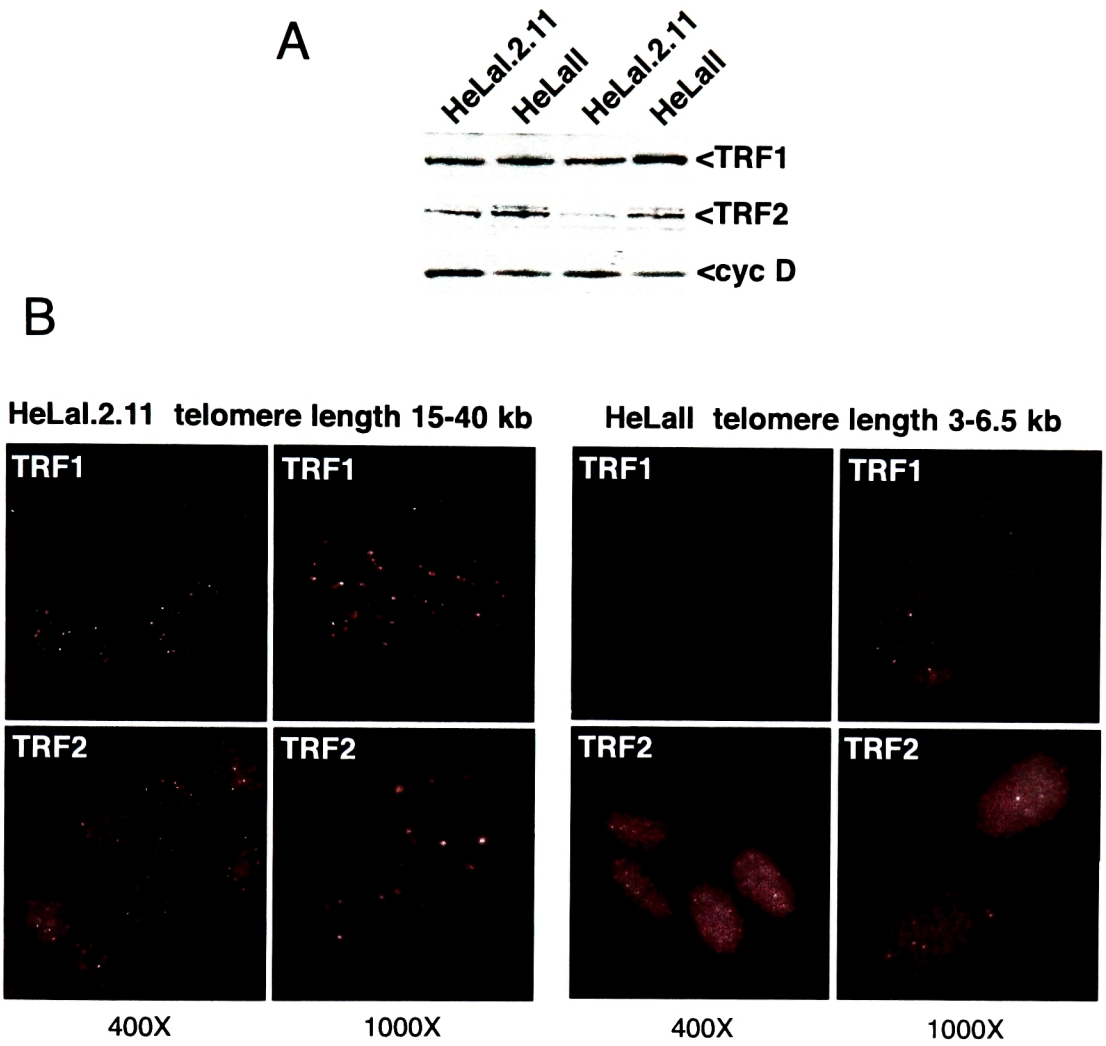

Figure 3-1. **Immunofluorescent analysis of TRF1 and TRF2 staining in cells with long and short telomeres**. **A.** Western blot showing expression of TRF1 and TRF2 in buffer C extracts from two HeLa cell lines with different telomere lengths. TRF1 was detected with antibody 371; TRF2 was detected with antibody 647. Cyclin D is used as a loading control. In the first two lanes, loading was based on cell numbers and the second two lanes were normalized based on protein amounts (30 μg). **B.** Indirect immunofluorescence staining for TRF1 and TRF2 in two HeLa cell lines with the indicated telomere lengths. All samples were processed identically and in parallel and images are presented without any adjustment. For each combination of cell line and antibody, nuclei are presented at two magnifications. DNA was stained with DAPI.

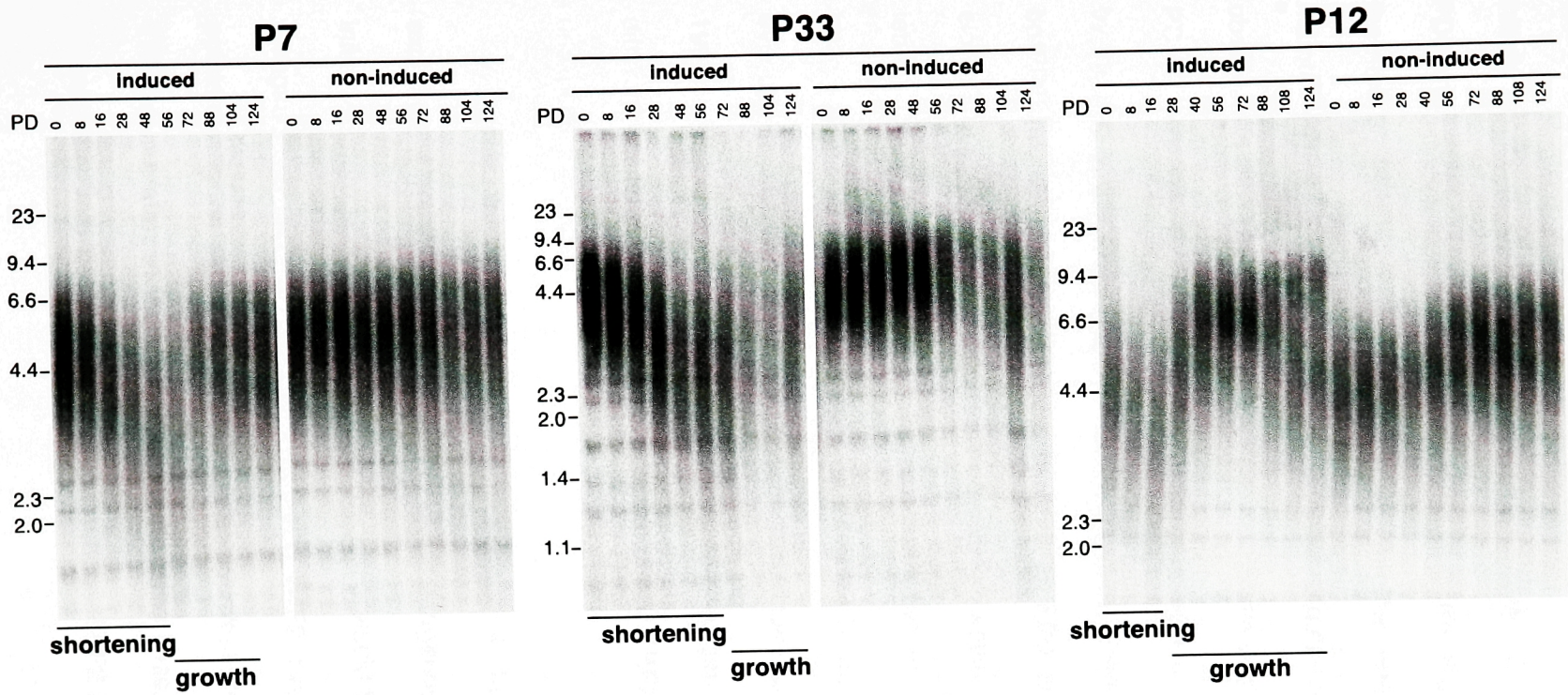

Figure 3-2. **Telomere length analysis in FL TRF2 expressing HTC75 cells.** Southern blot of telomeric restriction fragments from two independent FL TRF2 expressing HTC75 cell lines (P7 and P33) grown in the absence or presence of doxycyclin (resulting in induction and repression of TRF2, respectively) for 124 population doublings (PD). Genomic DNA was isolated from cells at the indicated PDs, digested with HinfI and RsaI, and hybridized with a TTAGGG probe. The molecular weights of marker DNAs are indicated in kb. Periods of telomere shortening and growth are highlighted below the lanes.

pattern of telomere length changes, which generally was comprised of an initial period of telomere shortening, followed by telomere re-growth (Figure 3-2). In the P7 cell line, initially telomeres shortened at 82 bp per PD (calculated from telomere lengths between PD0 and PD28). Unexpectedly, this trend of shortening halted around PD 48 and within the next 30 PDs telomeres regained their original length, which appeared to be stably maintained until the end of the experiment. Similar changes in telomere length were observed in P33 cell line, in which the initial shortening (47 bp/PD, calculated for PD0 to PD 40) was followed by elongation, which started around PD72 and was not completed by the end of the experiment. P12 cell line also showed initial telomere shortening (51 bp/PD, calculated from telomere lengths at PD0 and PD8), but telomeres started elongating soon after that and reached a length setting that was longer than the original length setting in this cell line. Such telomere behavior was very different from the one observed in TRF1 studies where TRF1 overexpression led to telomere shortening and eventual stabilization of telomere length at the lower setting (van Steensel and de Lange 1997). However, these complex telomere changes were consistently seen in three different cell lines, which led to a conclusion that TRF2 was the causative agent of such unexpected changes.

Changes in telomere dynamics seen in the above experiments could be explained if the initial high expression of the exogenous TRF2 subsided with time. The initial telomere shortening determined by TRF2 would then also stop, leading to telomere elongation. In order to test this hypothesis TRF2 levels were analyzed at different time points during the experiment (Figure 3-3). Western blots have shown very high levels of TRF2 at the start of the experiment in all three lines. With time, the levels decreased dramatically with no, or very little exogenous TRF2 being produced at the end of the

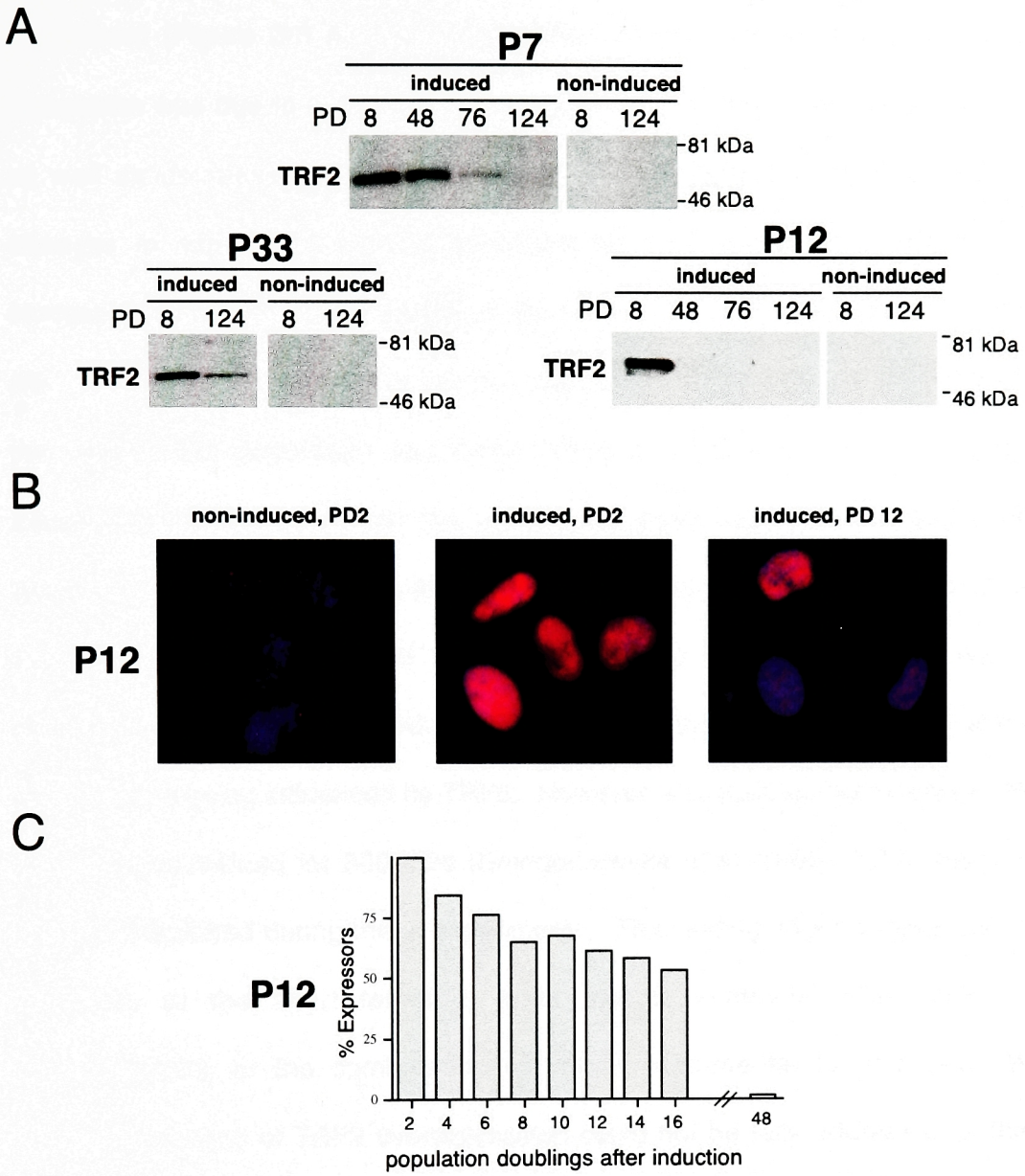

Figure 3-3. **TRF2 expression in P7, P12 and P33 HTC75 cells at various times during growth. A.** Immunoblot analysis of TRF2 levels in P7, P12 and P33 cells grown under induced and non-induced conditions. Buffer C extracts were prepared at indicated population doublings (PDs), and TRF2 was detected with antibody 508. Endogenous TRF2 is below detection limit under these conditions. **B.** Immunofluorescence with antibody 508 in non-induced and induced P12 cells at PD2, and induced P12 cells at PD12. Note that at PD 12 the level of expression is invisioble in two cells, very low in other two, and high in one. C. % expressing P12 cells at different PDs. All expressing cells were counted, so that 3 out of the 5 cells in right panel of B. would be counted as being positive for expression.

experiment (Figure 3-3 A). As documented by immunofluorescence, this decline in expression was due to a decrease in numbers of cells that expressed exogenous TRF2 as well as decrease in levels of TRF2 in the expressing cells (Figure 3-3 B). The changes in expression roughly coincided with the switch from the shortening to elongation states. P12 line exhibited this switch at a very early time point (before PD 28). Loss of expression in this cell line also occurred very early and by PD 48 none of the cells in the population expressed TRF2 as determined by IF (Figure 3-3, C). Exogenous TRF2 in the P7 cell line, on the other hand, expressed robustly at PD 48 and telomeres were still shortening at that time. However, at PD 76, only 20% of cells were expressing TRF2 in that cell line and telomeres in the population were already elongating. Overall, this correlation further stresses that telomere changes in the HTC75 cell line were being influenced by TRF2. However, it is curious that whereas TRF1 could be stably maintained for 300 PDs (Smogorzewska et al. 2000), TRF2 expression was being extinguished during these experiments. This finding might suggest that presence of TRF2, or the short telomere state that is achieved when TRF2 is being overexpressed, or the combination of both is detrimental for the cell. While the deleterious nature of TRF2 overexpression could not be fully addressed in this system because of the asynchrony of TRF2 loss, it has been noted that the morphology of cells in the population, which was about to lose TRF2 expression, differed from uninduced cells, and many cells appeared to have multilobulated nuclei (Figure 3-4).

To further understand the events that led to the initial telomere shortening in HTC75 cells, the ability of TRF2 to influence telomerase activity and expression of the telomerase subunits was examined. Telomeric repeat amplification protocol (TRAP) assay was performed on extracts from HTC75 cells induced or not induced to express a

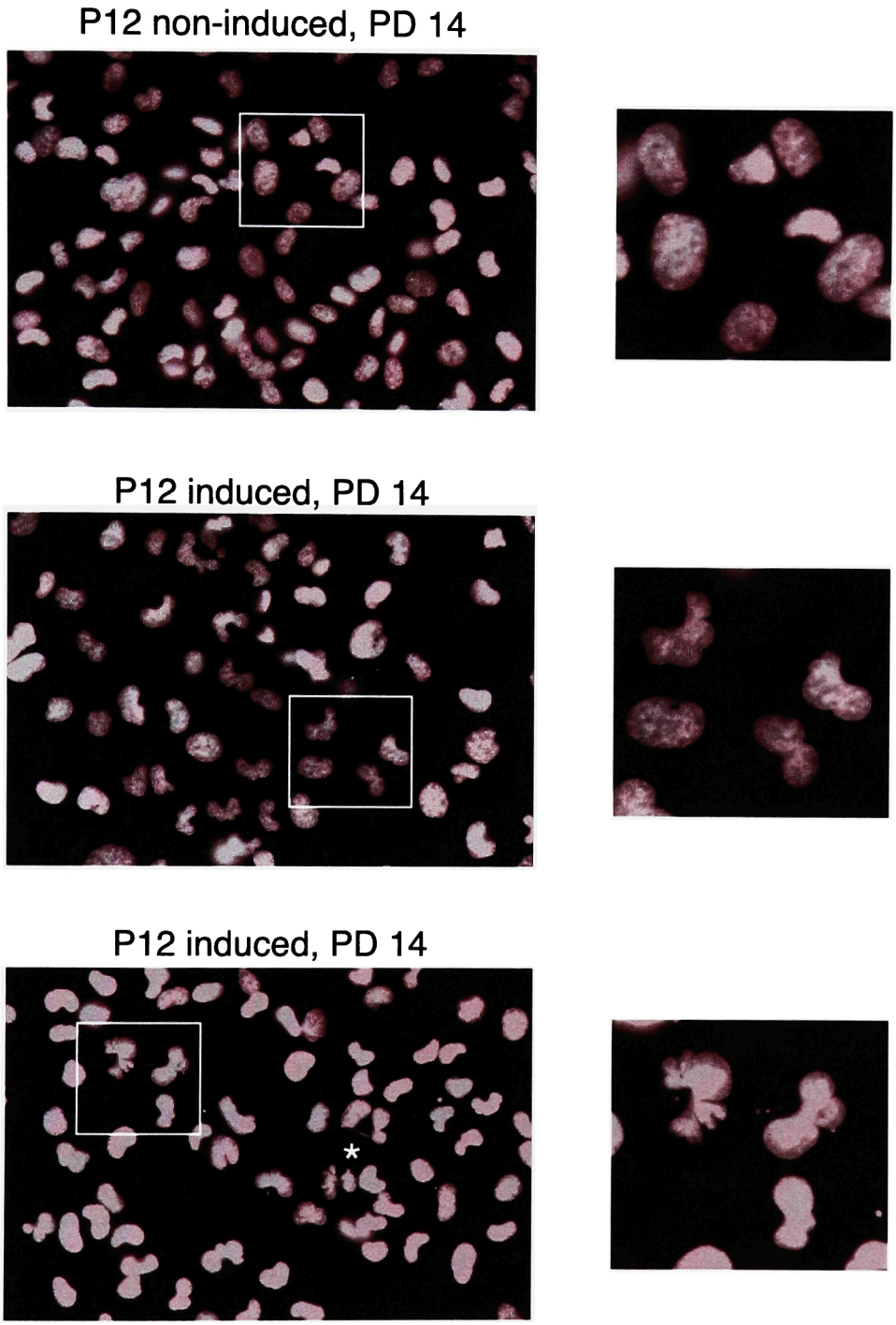

Figure 3-4. **Cell morphology of P12 HTC75 cells at PD 14.** DAPI staining of P12 HTC75 cells uninduced or induced to express TRF2. Note the presence of multilobulated nuclei and DAPI positive material joining two interphase cells (indicated as * in the lower panel) in cells expressing TRF2.

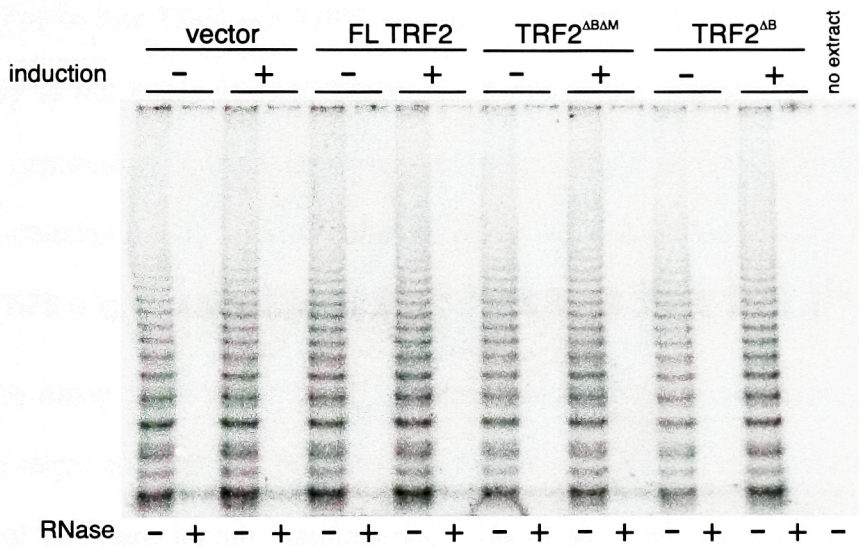

Figure 3-5. **Effects of expression of TRF2, TRF2$^{\Delta B\Delta M}$ and TRF2$^{\Delta B}$ on telomerase activity.** Telomeric repeat amplification protocol (TRAP) assay in HTC75 grown in the presence or absence of doxycyclin (- and + induction respectively). 0.5 μg total protein of buffer C extract as assayed by Bradford assay (BioRad) was used per reaction. RNase digestions were done in parallel to the untreated reactions by addition of 0.2 μg DNase-free RNAse. Buffer C was used instead of extract in the "no extract" control (last lane on the right).

full length TRF2 and the two truncation alleles ($TRF2^{\Delta B\Delta M}$ and $TRF2^{\Delta B}$). To assure that only telomerase activity was being assayed, RNAse was included in parallel reactions. Additionally, one reaction was performed without any extract to control for any contamination during the polymerase chain reaction. Telomerase activity appeared to be comparable in all cells examined (Figure 3-5). This parallels findings that TRF1 or any of the truncation alleles of TRF1 also did not change the *in vitro* telomerase activity, showing that neither TRF1 nor TRF2 modulate the global activity of telomerase, but are more likely to act in cis at each telomere. Furthermore, expression of TRF2 did not influence expression of the telomerase subunits, hTERT or hTR, as shown using the RNAse protection assay on total RNA from HTC75 P lines induced or not induced to express TRF2 (Figure 3-6).

The many parallels between telomere behavior upon overexpression of TRF1 and TRF2 might suggest that the two proteins act in concert to modulate the telomerase pathway of telomere length maintenance. However, there remains a possibility that TRF2, unlike TRF1, influences the shortening activities at the telomere. In an attempt to address this issue, TRF2 was induced in the HTC75 cell lines previously infected with a dominant negative allele of hTERT ($hTERT^{D710A}$) (Hahn et al. 1999). Expression of $hTERT^{D710A}$ in three HTC75 cell lines examined (P7, P12, P33) inhibited, although not fully abolished the endogenous telomerase activity (Figure 3-7). Nevertheless, telomere shortening expected after inhibition of telomerase was seen in all three cell lines (Figure 3-8, A, indicated as "- induction" in the blots, black squares in the graphs). Parallel induction of TRF2 in these cells led to an increased rate of telomere shortening (Figure 3-8, A, indicated as "+ induction" in the blots, red diamonds in the graphs). One interpretation of this finding would be that TRF2 is capable of influencing the shortening

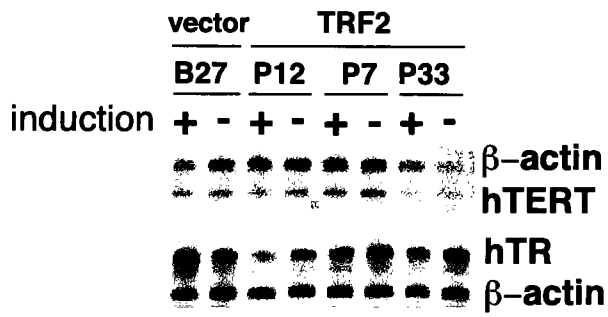

Figure 3-6. **Effects of induction of TRF2 on expression levels of hTERT and hTR RNA.** RNase protection assay on total RNA in B27, P12, P7, P33 HTC75 cells grown in the presence or absence of doxycyclin (- and + induction respectively) for 9 days. β-actin served as a control.

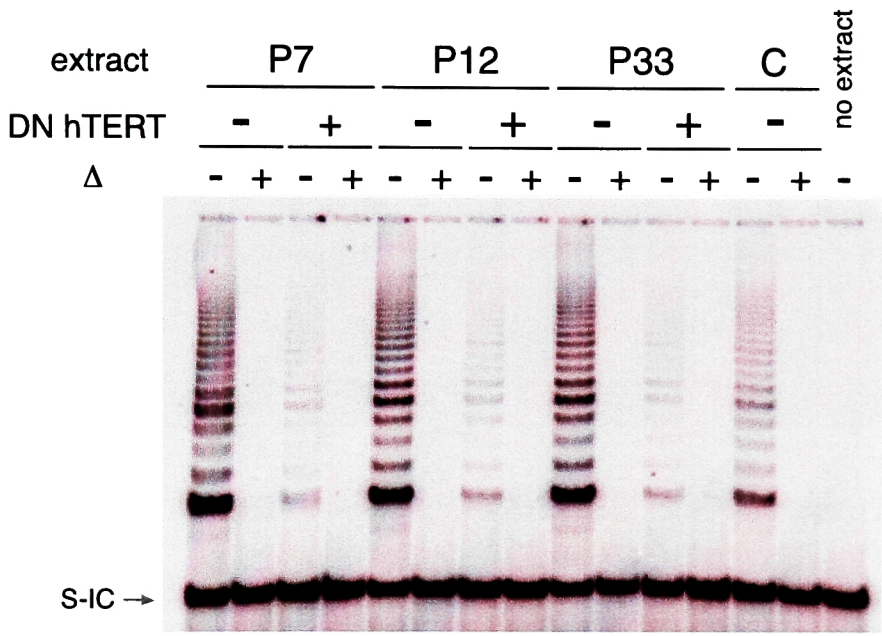

Figure 3-7. **Effects of expression of the dominant negative hTERT in P7, P12, P33 HTC75 cells on telomerase activity.** Telomeric repeat amplification protocol (TRAP) assay in non-induced P7, P12, and P33 HTC75 expressing the dominant negative hTERT allele ($hTERT^{D710A)}$ (Hahn et al., 1999). The TRAPeze telomerase detection kit (Intergen) was used for this assay. Activity was in a linear range. Δ signifies heat treatment which was done in parallel to the untreated reactions by incubation of the extract at 85°C for 10 minutes prior to telomerase extension. C is a positive control, and the "no extract" lane contains product of reaction performed with lysis buffer supplied with the kit instead of the extract. S-IC is an internal control during a PCR step

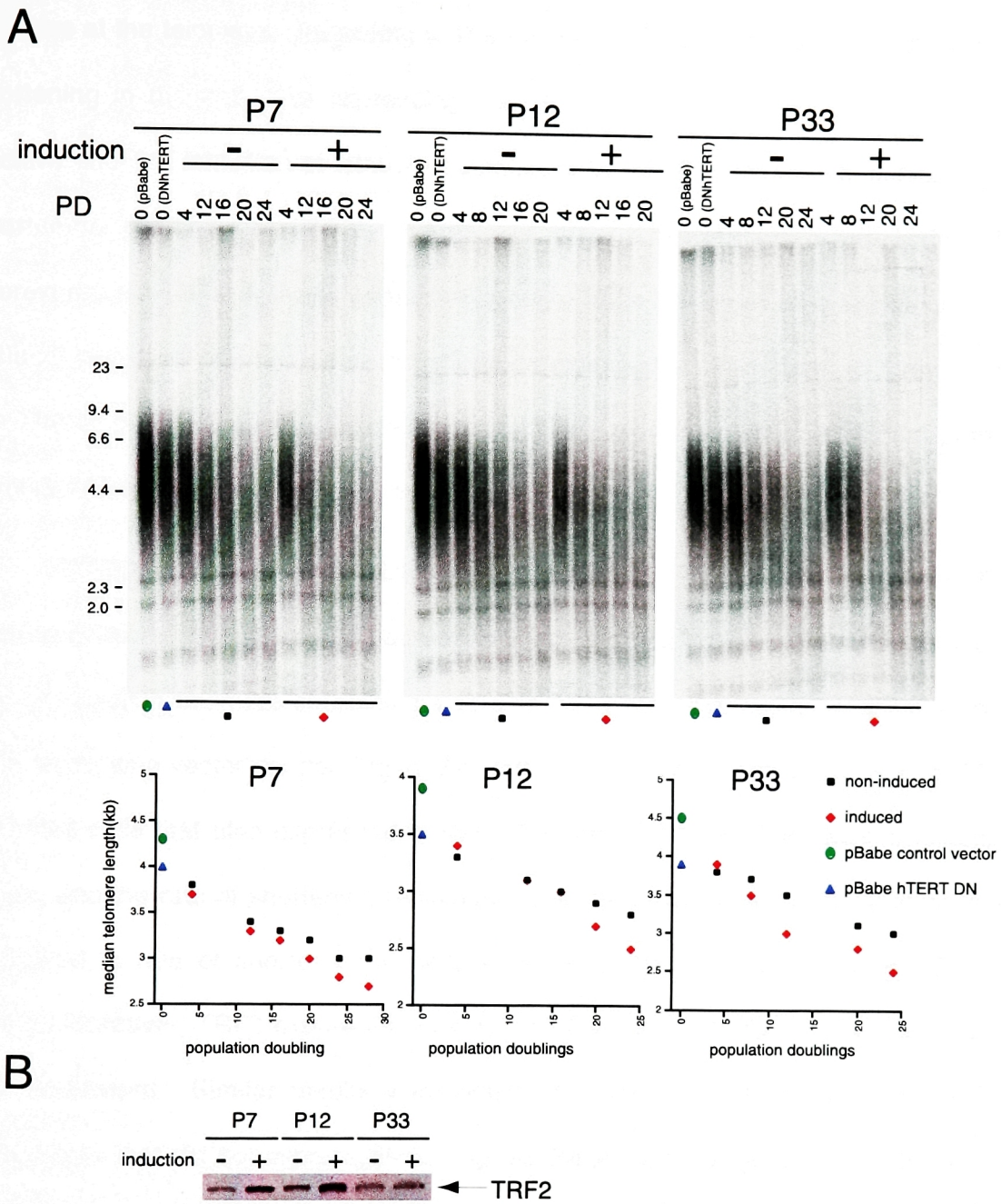

Figure 3-8. **Telomere dynamics analysis in HTC75 cells co-expressing the dominant negative hTERT(DNhTERT) and TRF2.** **A.** Southern blot of telomeric restriction fragments from P7, P12, and P33 HTC75 cells carrying DNhTERT ($hTERT^{D710A}$) grown in the presence or absence of doxycyclin, resulting in repression (-) or induction (+) of TRF2. The molecular weights of marker DNAs are indicated in kb. Length changes were quantified and plotted as median telomere length (Y axis) against population doublings (PDs) (X axis). **B.** Immunoblot analysis of TRF2 levels in P7, P12, and P33 HTC75 cells carrying DN hTERT grown under induced and non-induced conditions. TRF2 was detected with antibody 647.

activities at the telomere. According to this interpretation, an increased rate of telomere shortening in the cell lines expressing both hTERT^{D710A} and TRF2 results from the additive effect of inhibition of telomerase pathway by hTERT^{D710A} and stimulation of the shortening pathway by TRF2. Although this interpretation is attractive, the overexpressed TRF2 in these experiments might have still been able to modulate the residual activity of telomerase at the shortening telomeres. Therefore, to further study the effects of TRF2 on the shortening rate, TRF2 was expressed in human primary fibroblasts, which naturally lack any telomerase activity.

IMR90, primary lung fibroblasts were infected with an untagged full length TRF2 allele and telomere length was observed in short term experiments. Already by the 5th day of selection telomere shortening was evident in cells expressing TRF2 but not in cells expressing vector control (Figure 3-9, left panel). A long-term expression of TRF2 in IMR90 cells that also expressed a SV40 Tag led to a steady decrease in telomere length, and the rate of shortening remained increased throughout the experiment when compared to rate of shortening in cells expressing vector control (Figure 3-9, right panel). Moreover, TRF2 expression was not lost from the FLTRF2 infected cells during this experiment. Similar results were obtained in long-term expression of TRF2 in IMR90 cells that did not express SV40 Tag (Karlseder and de Lange, unpublished). In those studies, quantification of telomere shortening revealed that telomeres shortened at a rate of 110 bp/PD in cells infected with a control vector or any of the TRF1 alleles, but at a rate of 165-180 bp/PD in cells expressing TRF2 (Karlseder and de Lange). These results unequivocally demonstrate that although TRF2 is a negative regulator of telomere length maintenance, it does so primarily through positively regulating telomere shortening.

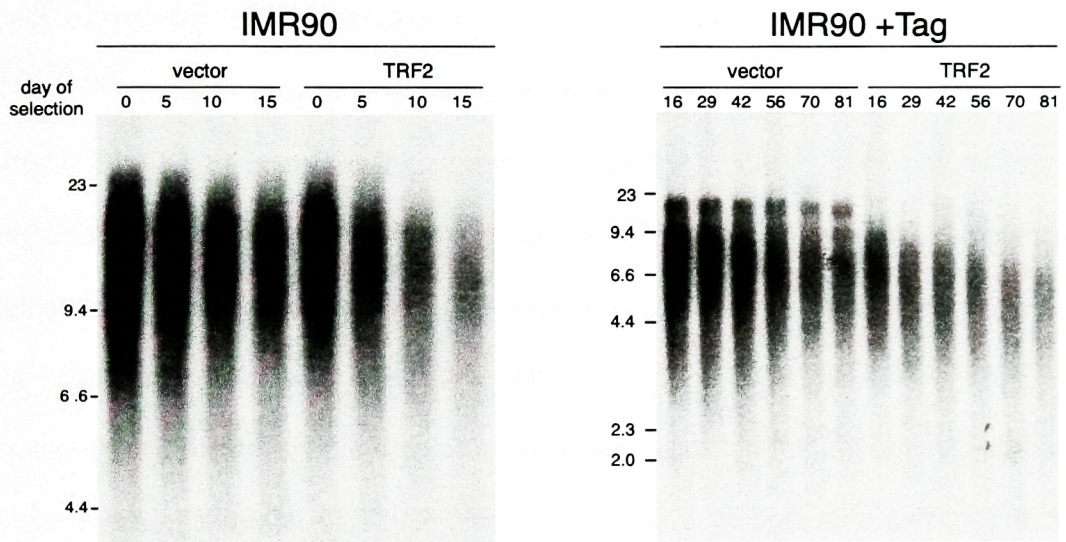

Figure 3-9. **Telomere length analysis in IMR90 primary fibroblasts infected with control virus or with FLTRF2.** Southern blot of telomeric restriction fragments from cells carrying no exogenous TRF2 (vector) or TRF2 (TRF2). On the left, a short term experiment is shown in wt IMR90 cells. On the right, a longer term experiment is shown in IMR90 expressing Tag. Similar results are obtained in long term experiments when T ag is absent (Jan Karlseder and Titia de Lange, unpublished). Genomic DNA was isolated from cells on the indicated days of selection, digested with HinfI and RsaI, and hybridized with a TTAGGG repeat probe. The molecular weights of marker DNAs are indicated in kb.

However, these findings do not exclude the possibility that besides being a positive regulator of telomere shortening, TRF2 might also influence the telomerase pathway. Addressing this question is difficult given current experimental methods. In an attempt to show that the telomerase pathway of telomere length regulation can be affected by TRF2, $TRF2^{\Delta B \Delta M}$, the dominant negative allele of TRF2, was expressed in the BJ primary cells expressing hTERT (Bodnar et al. 1998). As shown in Chapter 2, expression of $TRF2^{\Delta B \Delta M}$ leads to growth arrest even in telomerase positive lines. To circumvent the arrest, SV40 Tag was also expressed in hTERT BJ cells. The expectation was that removal of TRF2 from the telomeres under conditions permitting cell growth would allow telomerase to elongate the exposed telomere ends. Indeed, the telomeres appeared to be slightly longer in cells expressing $TRF2^{\Delta B \Delta M}$ (Figure3-10, top panel lane 6 and 7). However, the pattern of this elongation was reminiscent of the appearance of end-to-end fusions after inhibition of TRF2 (see Chapter 1). To test if this apparent telomere elongation in $TRF2^{\Delta B \Delta M}$-expressing cells is due to fusion formation, the genomic DNA extracted from these cells was fractionated on an agarose gel and without denaturation hybridized in situ to a $(CCCTAA)_4$ probe. Under these conditions only the telomeres with G-overhangs are detected and DNA of fused telomeres should not be revealed. As shown in Figure 3-10, lower left panel, telomeres from vector control cells and cells expressing $TRF2^{\Delta B \Delta M}$ appeared to be of similar length when hybridization was performed under native conditions. When the same gel was denatured, the higher molecular weight telomeric DNA reappeared in $TRF2^{\Delta B \Delta M}$-expressing cells. These results showed that the apparent increase in telomere length in $TRF2^{\Delta B \Delta M}$-expressing cells seen in Figure 3-10 was due to fusion formation and not true telomerase-mediated elongation.

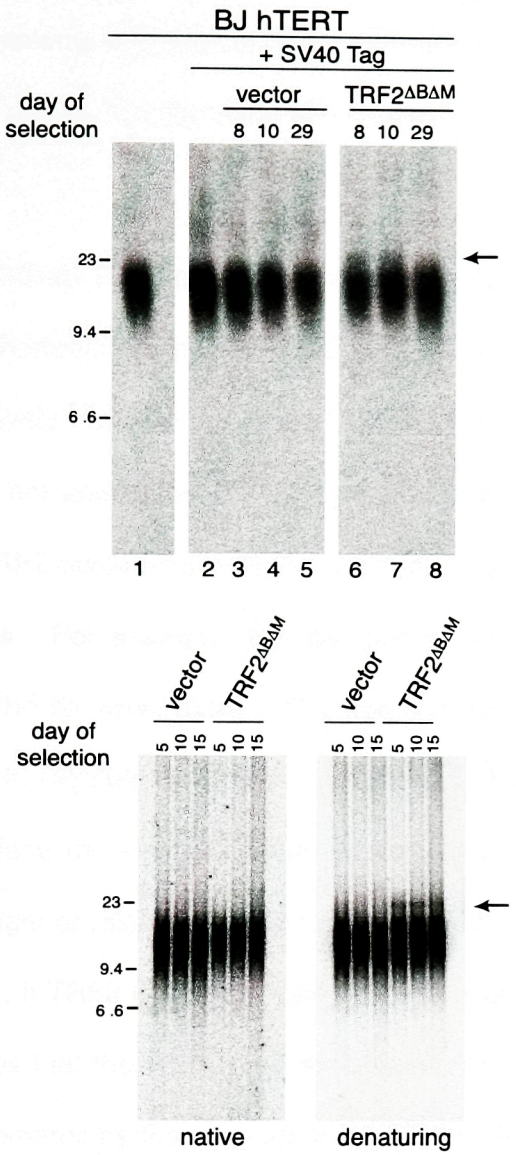

Figure 3-10. **Telomere length analysis in BJhTERT fibroblasts infected with control virus or TRF2$^{\Delta B\Delta M}$.** **A.** Southern blot of telomeric restriction fragments from cells carrying no exogenous TRF2 (vector) or TRF2$^{\Delta B\Delta M}$ (TRF2$^{\Delta B\Delta M}$). Genomic DNA was isolated from cells on the indicated days of selection, digested with HinfI and RsaI, and hybridized with a TTAGGG repeat probe. The molecular weights of marker DNAs are indicated in kb. The arrow points to a higher molecular weight telomeric DNA present only in lanes 6 and 7. **B.** In gel hybridization of telomeric restriction fragments with an end-labeled telomeric probe under non-denaturing conditions (left) and denaturing conditions (right). Under the non-denaturing conditions only the DNA which has G overhangs is revealed, and under denaturing conditions, all telomeric DNA is visualized. Arrow points to a higher molecular weight telomeric DNA visualized only under denaturing conditions.

This suggests that a telomere devoid of TRF2 cannot be elongated by telomerase but it still does not exclude that TRF2 affects the telomerase-pathway.

Discussion

This chapter has identified TRF2 as a regulator of telomere length. The ability of TRF2 to cause telomere shortening in human cells lacking telomerase led to the conclusion that TRF2 can positively regulate the rate of telomere shortening. The mechanism of such regulation was not addressed in these experiments and a number of possibilities can be proposed. TRF2 could influence the shortening rate by affecting the replication through the terminus. For example, the last primer on the lagging strand could be placed farther from the tip when more TRF2 was present on the telomere. Secondly, TRF2 might be able to regulate nucleases involved in telomere shortening. Expressing more TRF2 might place more of the nuclease activity on telomeres leading to faster shortening. TRF2 might physically be able to interact with a nuclease or might positively regulate it. However, if TRF2 were to physically be in a complex with such a nuclease, this proposal assumes that there would be an excess of nucleases in the cell that could be brought to the telomeres by the overexpressed TRF2. Another possibility pertinent to regulation of the putative telomeric nuclease is to propose that TRF2 interacts with an inhibitor of shortening and that expression of TRF2 in the nucleoplasm titrates away this activity from telomeres, leading to the decreased presence of this inhibitor on the telomeres, increased nuclease activity and telomere shortening. These proposals are testable especially in light of a putative nuclease, the Mre11 complex localizing to telomeres (Zhu et al. 2000, Lombard and Guarente 2000).

TRF2 expression in primary human cells led to persistent and continuous telomere shortening. Eventually cells senesced (Karlseder and de Lange, unpublished)

and although the dynamics of senescence with overexpressed TRF2 will not be discussed here, these findings shed light on the reasons why telomerase positive HTC75 cells induced to express TRF2 might have lost expression of the allele (Figure 3-2 and Figure 3-3). It seems that the telomerase activity present in the HTC75 cells was unable to compensate for the loss of telomeres caused by the shortening activities stimulated by the overexpression of TRF2. Evidently, the shortening activities are dominant in this setting. With time, telomeres become critically short and probably become non functional. Although presence of fusions was not noted in the P lines when the telomeres were short, such an event could have been missed because of the asynchrony of the telomere shortening and emergence of cells that have lost expression. However, the HTC75 P cell lines were noted to have an altered morphology at the time when cells had short telomeres. The multilobulated nuclei of cells could have represented events of cells trying to undergo anaphase with a large number of fusions, aborting such event and returning to a G1 like state resulting in a dumbbell shaped cell or a phenotype that has been described as a "cut" phenotype in yeast. If the HTC75 cells were unable to select for the non-expressing cells when their telomeres were very short, the population probably would have ceased to grow.

The findings presented here stress the differences in how TRF1 and TRF2 regulate telomere length. Although the two proteins are paralogs and are able to interact with the same DNA sequence, they act in two different pathways to regulate telomere length. This ability of TRF1 and TRF2 to impinge on different pathways must stem from their capacity to interact with different partners. As pointed out earlier, two of the TRF1 binding proteins- tankyrase1 and TIN2 are also involved in telomere length regulation. It

will be interesting to see what are the other functions of TRF1, since studies to date suggest that the complex is devoted exclusively to telomere length regulation.

So far, TRF2 has not been shown to have the ability to regulate telomere elongation. It would be surprising if TRF2 did not have such capacity since Rap1, which seems to exists in a 1:1 complex with TRF2 (Zhu et al. 2000) behaves as a negative regulator of telomere elongation (Li et al. 2000). A protein that anchors a regulator of telomere elongation should be itself functioning as such. However, if TRF2 can influence the telomerase pathway it would do so in cis at each telomere. Overexpression of any of the alleles had no influence on the telomerase activity as assayed by TRAP assay. Expression of a full length TRF2 also did not affect the presence of hTERT or hTR RNA messages.

Although expression of the dominant negative allele of TRF2 in telomerase positive cells failed to show that TRF2 acts as a regulator of telomere elongation, it did suggest that a telomere devoid of TRF2 is inert with regards to its interaction with telomerase. Without TRF2, the chromosome end might no longer be seen as a telomere. Such an end does not get degraded and it does not seem to get elongated. It now behaves like a break (see Chapter 1) and as such it might be initially protected and then repaired by the NHEJ pathway. This also suggests that the presence of TRF2 is necessary for the proper elongation of the telomere.

Parenthetically, it is useful to note that IMR90 Tag control infected cells show a prominent band that is likely to represent telomere fusions (Figure 3-9, right panel, vector). This band is not observed in cells that also express TRF2, consistent with the ability of TRF2 to protect telomeres from the NHEJ pathway (Chapter 1).

Chapter 4

Chromosome and telomere breakage in cells expressing $TRF2^{\Delta B}$

Introduction

Besides being present at the telomeres, TTAGGG repeats are found at interstitial sites in many species (Meyne et al. 1990). In human cells, there are a number of interstitial sites containing telomeric repeats (Ijdo et al. 1991; Azzalin et al. 1997). The origin of all of them is not yet known; however, at least one of them, consisting of a long stretch of degenerate TTAGGG repeats in head to head orientation, most likely arose from fusion of ancestral ape chromosomes (Ijdo et al. 1991). It has been proposed that the interstitial sites can be the sites of recombination, breakage, and fragility (Hastie and Allshire 1989). Supporting such a proposal, a number of studies in hamster cells have correlated the presence of interstitial sites with instability (Slijepcevic et al. 1997; Day et al. 1998). In human cells, interstitial repeats participate in rearrangements including jumping translocations, (Park et al. 1992; Jewett et al. 1998) and might represent fragile sites (Boutouil et al. 1996), although it is not understood what the requirements are for an interstitial site to become recombinogenic.

A recent study focused on a more defined interstitial site engineered in a way that allows for efficient scoring of rearrangements at that site (Kilburn et al. 2001). A stretch of 800 bp TTAGGG repeats were placed within an intron of the adenosine phosphoribosyltransferase gene (APRT). Interstitial placement of the TTAGGG repeats did not influence homologous recombination at this site; however, local rearrangements involving the interstitial telomeric sequence increased 30 fold. The rearrangements included deletions, insertions and translocations (Kilburn et al. 2001).

The study described above has defined the interstitial 800 bp of telomeric DNA as destabilizing element in human chromosomes. However, it did not give insight in to

the mechanism underlying the destabilizing behavior. One possibility is that TTAGGG repeat DNA is able to form structures that somehow are destabilizing when present at interstitial sites. A second possibility can now be proposed based on the finding that both TTAGGG binding proteins, TRF1 and TRF2, are found to bind interstitial $(TTAGGG)_n$ sites (Smogorzewska et al. 2000). BHK-21, a Syrian hamster cell line and CHO-K1, a Chineses hamster cell line, but not AHL-1, an Armenian hamster cell line, contain very large blocks of pericentromeric satellite sequences that contain TTAGGG and related repeats (Meyne et al. 1990; Ashley and Ward 1993). Indirect immunofluorescence against the basic domain of human TRF2 showed that the endogenous hamster TRF2 was binding at the interstitial sites (Smogorzewska et al. 2000). TRF1 is much less conserved between the species (Broccoli et al. 1997; Smith and de Lange 1997), and antibodies against human or mouse TRF1 do not cross-react with the hamster TRF1; however, a transfected human TRF1 was also able to bind to the Syrian and Chinese hamster interstitial sites (Smogorzewska et al. 2000, Krutilina et al. 2001). It is possible that an interstitial site bound by a telomeric protein might be inappropriately processed to give a break. This proposal can now be directly tested by examining the frequency of rearrangements in cells expressing different alleles of TRF1 and TRF2 (also see discussion).

One of the striking differences between TRF1 and TRF2 are their N terminal domains. The acidic domain in TRF1 is functionally important, as suggested by its interaction with tankyrase. So far no protein has been found to interact with the basic domain of TRF2. The only known direct interaction of TRF2 is with Rap1 and it maps to the TRF homology domain of TRF2. It is not yet known if the Mre11 complex interacts directly with TRF2 or whether the interaction occurs via Rap1. This chapter explores the

function of the basic domain of TRF2 by studying the truncation allele of TRF2, TRF2$^{\Delta B}$. It is shown that TRF2$^{\Delta B}$ localizes to telomeres very efficiently where it replaces the endogenous TRF2 but not TRF1 from the telomeres. Expression of TRF2$^{\Delta B}$ leads to rapid telomere loss that is distinct from the telomere shortening in the presence of increased levels of TRF2 (see Chapter 3). Large portions of telomeric DNA seem to be lost from single chromatids. The loss of telomeric DNA is also visible on telomere blots and seems to be caused by loss of the duplex DNA and not a specific strand of the telomeric DNA. Besides the telomere length phenotype, cells expressing TRF2$^{\Delta B}$ are found to have chromatid gaps and breaks, which leads to the appearance of chromosome pieces in anaphase cells and micronuclei in interphase cells. Primary human cells undergo a senescent-like growth arrest when they express TRF2$^{\Delta B}$. This growth arrest is very similar to the arrest seen with TRF2$^{\Delta B\Delta M}$-expressing cells although the kinetics of the arrest are somewhat slower. TRF2$^{\Delta B}$-induced arrest, just like the arrest following expression of TRF2$^{\Delta B\Delta M}$ or replicative senescence can be abrogated by expression of the SV40 Tag. It is not clear at this point what the primary source of the arrest is, although the prevalence of telomeres lacking any telomeric signal suggests that chromosomes become deprotected. Additionally, the presence of breaks might also lead to signaling into growth arrest.

Results

The function of the basic domain of TRF2 was indirectly studied by expression of an allele lacking this domain (TRF2$^{\Delta B}$) in a number of different cell lines. The effect of TRF2$^{\Delta B}$ on the endogenous TRF1 and TRF2 was shown by expression of the tagged TRF2$^{\Delta B}$ allele in HeLaI.2.11, a subclone of HeLa cells that is characterized by very long telomeres. Immunofluorescent staining against the tagged protein revealed that when

overexpressed, TRF2$^{\Delta B}$ gives high nucleoplasmic signal with overlaid punctate staining (Figure 4-1 A and B). The punctate pattern of TRF2$^{\Delta B}$ staining colocalized with that of TRF1 (Figure 4-1 B) showing that, like *in vitro* (Broccoli et al. 1997, van Breugel M. and de Lange T., unpublished, Stansel R, Griffith J. D., unpublished), TRF2$^{\Delta B}$ was able to bind to telomeric DNA *in vivo*. TRF2$^{\Delta B}$ expression did not seem to affect the presence of TRF1 on telomeres. However, fluorescent staining against the basic domain of the endogenous protein with antibody 508 in cells expressing TRF2$^{\Delta B}$, showed no punctate pattern, suggesting that the endogenous TRF2 was being replaced at the telomeres by the overexpressed TRF2$^{\Delta B}$ allele. Similar finding of a decreased amount of the endogenous TRF2 on telomeres were obtained in chromatin immunoprecipitation experiments performed on cells expressing TRF2$^{\Delta B}$ (Loayza D. and de Lange T, unpublished results).

In an attempt to characterize the phenotype of cells expressing the TRF2$^{\Delta B}$ allele, fluorescent in situ hybridization (FISH) with a peptide nucleic acid (PNA) telomeric probe was performed on cells infected with a vector control or the non-tagged TRF2$^{\Delta B}$ allele. BJ human primary fibroblasts expressing hTERT were particularly suitable for these studies, since their telomeres are very long (median around 15 kbp) and rather homogenous in length. These cells were also expressing SV40 Tag; however, its expression did not influence any of the phenotypes presented here. Telomere signals visualized by PNA FISH on metaphase spreads of cells infected with a vector control on day 6 after selection were usually very high, and as expected, telomeric staining on sister chromatids was typically equal in intensity (Figure 4-2, top). Parallel experiments performed with cells expressing TRF2$^{\Delta B}$ revealed an overall less bright telomere staining

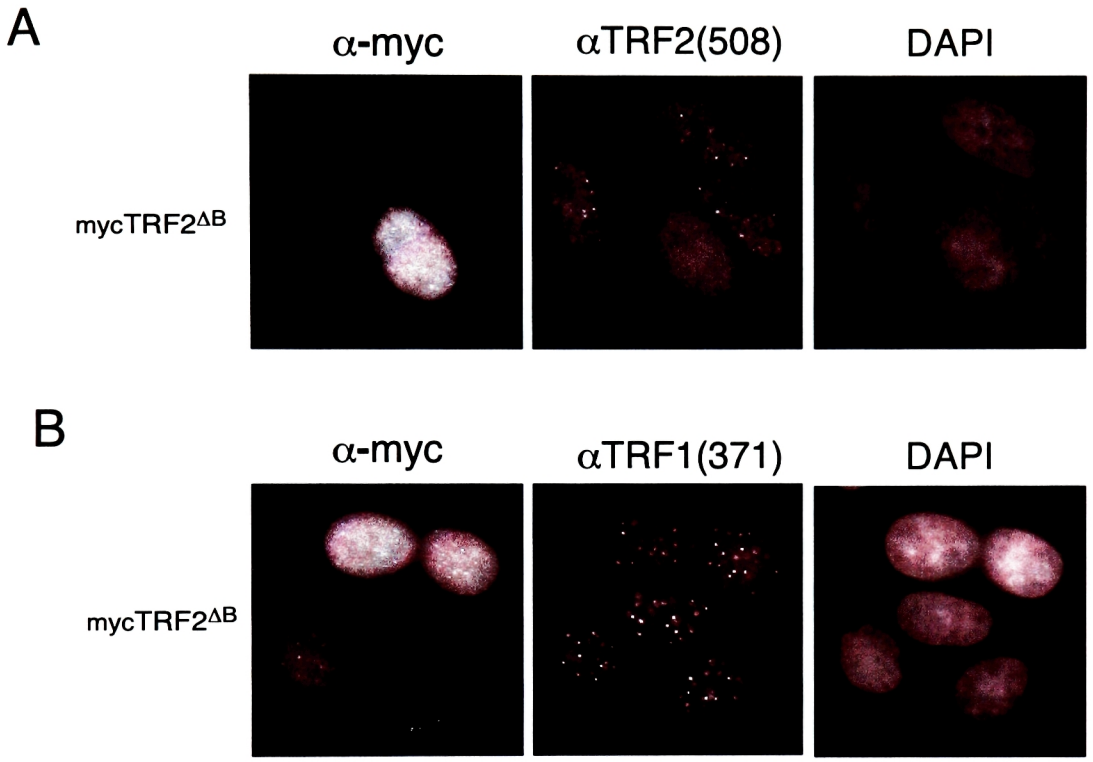

Figure 4-1. **Effects of expression of myc tagged TRF2$^{\Delta B}$ on endogenous TRF1 and 2 protein localization to telomeres**. Indirect immunofluorescence of HeLa 1.2.11 cells infected with myc tagged TRF2$^{\Delta B}$. Analysis was performed one day after infection on non-selected cells. Staining with an antibody against a myc tag (9E10) reveals infected cells. TRF2 is visualized with antibody 508 **(A)**, and TRF1 with antibody 371 **(B)**. Antibody 508 was raised against a peptide (GRRASRSSGRARRGRHEPGLGGPAEAG) present in the basic domain of TRF2 and it recognizes FLTRF2 but does not recognize TRF2$^{\Delta B}$. DNA was counterstained with DAPI.

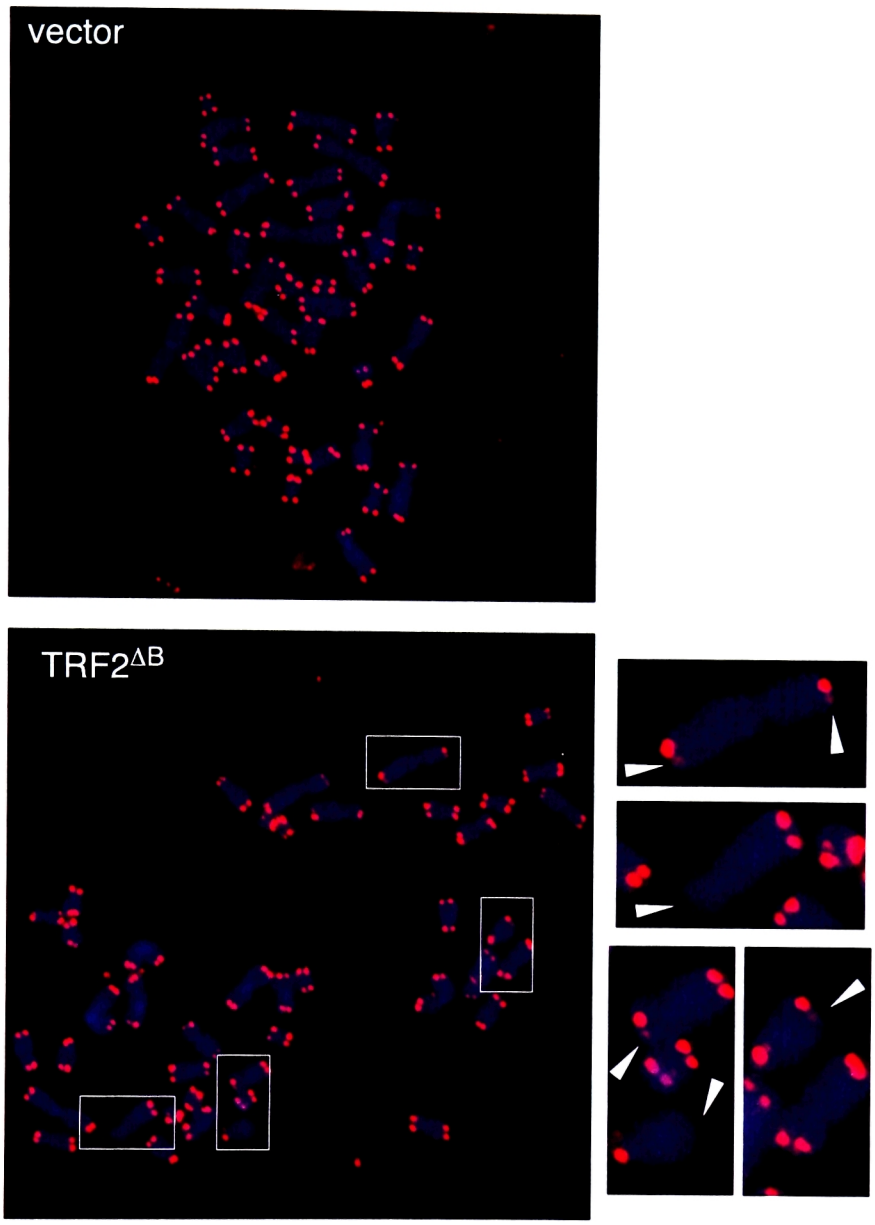

Figure 4-2 **Telomeric staining in BJ hTERT SV40 T ag cells expressing TRF2$^{\Delta B}$.** Peptide nucleic acid (PNA) fluorescence in-situ hybridization with a telomeric probe on spreads of BJ hTERT Tag cells infected with vector control (vector) or with TRF2$^{\Delta B}$ (TRF2$^{\Delta B}$). Spreads were prepared on the 6th day of selection. DNA was counterstained with DAPI. Overall the telomeric signal in TRF2$^{\Delta B}$ expressing cells was weaker (not shown here due to enhancement of the signal for the reproduction purposes). As shown at the lower right (arrows), many chromatids in the TRF2$^{\Delta B}$ expressing cells had very low or had no telomeric signal. Scoring 20 metaphases of vector cells revealed 9 single chromatids with no telomeric signal. In 21 spreads of cells expressing TRF2$^{\Delta B}$, 102 chromatids had no telomeric signal.

(data not shown, but see telomere blots below). Furthermore, many chromatids lacked any telomeric signal (Figure 4-2, bottom). In 21 spreads of cells expressing TRF2$^{\Delta B}$, 102 chromatids had no telomeric signal which corresponds to an 11 fold increase of such events over control cells in which 20 metaphases revealed only 9 single chromatids with no telomeric signal. Further analysis revealed that telomere signals on many chromatids of TRF2$^{\Delta B}$-expressing cells were substantially lower from the signals on the surrounding chromosomes. Curiously, often only one of the sister chromatids showed no signal. When two chromatids had very low signal, they frequently were on the opposite arms (Figure 4-2, top chromosome on the right). It is not clear yet if the distribution of lost signals represents a stochastic event or whether telomeres of specific chromatids are being lost (see discussion). Results of overall diminution of telomere signal and loss of some of the chromatid signals were first observed when TRF2$^{\Delta B}$ was expressed in mouse cells (Wang R. and de Lange T., unpublished).

Non-chromosomal telomeric signals were not seen on the spreads that revealed chromosomes without the telomeric signal, suggesting that the events of telomere DNA diminution were most likely not due to sudden separation of the telomere from the chromosome but rather a degradative process. However, telomere length changes after induction of TRF2$^{\Delta B}$ were very different from the gradual telomere shortening that was observed in cells expressing FLTRF2. Southern blot telomere length analysis of the cells used in the experiments described above revealed that as opposed to slow and constant telomere shortening seen in FLTRF2-expressing cells (Figure 4-3, also see Chapter 3), TRF2$^{\Delta B}$-expressing cells showed overall loss of the signal intensity. The telomeric hybridization signal also became more heterogenous with appearance of some signal in the lower molecular weight range. Loss of hybridization did not depend on the

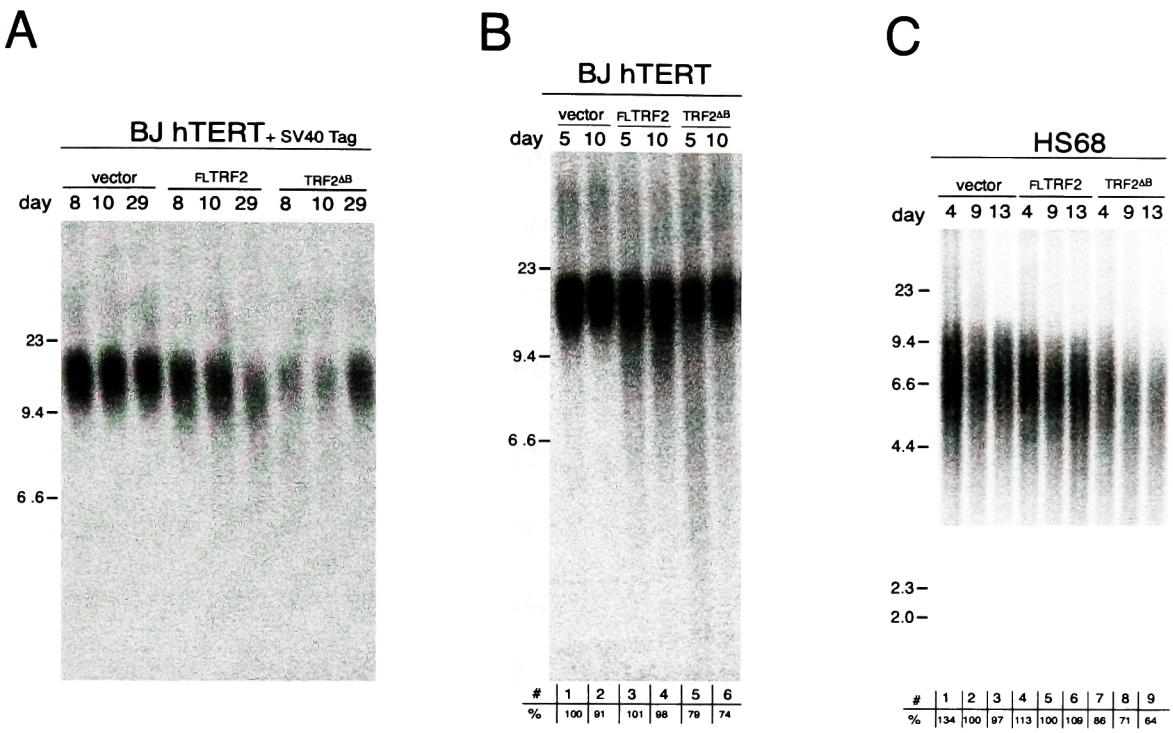

Figure 4-3. **Telomere length analysis in BJhTERT SV40 Tag, BJhTERT, and HS68 fibroblasts infected with control virus, FLTRF2, and TRF2$^{\Delta B}$.** Southern blot of telomeric restriction fragments from cells carrying no exogenous TRF2 (vector), FLTRF2 (FLTRF2), and TRF2$^{\Delta B}$ (TRF2$^{\Delta B}$). Genomic DNA was isolated from cells on the indicated days of selection, digested with HinfI and RsaI, fractionated on a 0.7% agarose gel, and hybridized with a TTAGGG repeat probe. Lane #1 of the gel shown in C. was overloded, the rest of lanes had equal loading as confirmed by ethidium bromide staining. The molecular weights of marker DNAs are indicated in kb. **A.** Telomere length analysis of BJhTERT SV40 Tag cells. Note the loss of the signal intensity and the increase in the heterogeneity of telomeric signal in TRF2$^{\Delta B}$ expressing cells at day 8 and 10. By day 29, most of the population of TRF2$^{\Delta B}$ cells have lost expression of the allele. The signal loss was not quantified in this experiment. Loss of intensity did not depend on presence of hTERT similar results were obtained with wt primary BJ cells (see fig 4-4). **B.** Telomere length analysis of BJhTERT cells. The signal in each lane was integrated, normalized to signal in lane #1 and is presented below each lane. The number was calculated as (signal in lane x/signal in lane 1)x100%. **C.** Telomere length analysis in HS68 cells. Because the first lane was overloaded, lane #2 was used to normalize the signal in all other lanes.

presence of hTERT or SV40 Tag because similar results were obtained with wt primary BJ cells (see Figure 4-4) as well as with BJhTERT cells not expressing SV40 Tag. The effect of telomere signal loss was also noted in HS68 primary human fibroblasts (Figure 4-3, C), although the effect was much harder to visualize on the blots of these cells since their starting telomere length was considerably shorter and appeared more heterogenous on standard telomere blots. TRF2$^{\Delta B}$-expressing HS68 cells on day 13 of the selection have lost about 35 % of the telomeric signal (Figure 4-3, C)

Findings of decreased hybridization intensity in cells expressing TRF2$^{\Delta B}$ corroborate that chromosomes lose telomeric signal when TRF2$^{\Delta B}$ is overexpressed. Interestingly, this loss appears to occur very fast, possibly within the first few divisions after TRF2$^{\Delta B}$ expression. When PNA FISH was performed on the metaphase spreads of the non-selected population of BJ hTERT cells on the third day of TRF2$^{\Delta B}$ expression, many cells showed decreased telomere staining and some chromatids already showed no telomeric signals. Also, Southern blots with DNA from cells on day 4 of selection already showed the decreased hybridization and increased heterogeneity of the telomere signal (Figure 4-3, C). It is possible that any additional decrease in telomere length might have been due to replication of the already shortened telomeres. Overexpression of TRF2$^{\Delta B}$ was deleterious to the cells because by day 29 most BJhTERT SV40 Tag cells lost expression of the allele (see Figure 4-8 for the description of the growth phenotype). After TRF2$^{\Delta B}$ expression was lost, telomere length of the population returned to normal length (Figure 4-3, day 29).

To ask if one of the telomeric strands was preferentially degraded in TRF2$^{\Delta B}$-expressing cells, an in-gel G-overhang assay was performed on DNA collected from primary BJ cells (this time not expressing SV40Tag or hTERT) expressing control vector,

FLTRF2, TRF2$^{\Delta B}$ and TRF2$^{\Delta B\Delta M}$. To visualize only G –overhang containing telomeres, the gel was hybridized under non-denaturating condition with a $(CCCTAA)_4$ probe (Figure 4-4, native). Subsequently, the gel was denatured and hybridized with the same probe to visualize all telomeric DNA (Figure 4-4, denatured). Although the TRF2$^{\Delta B}$-expressing cells showed the expected loss and smearing down of the telomeric signal, the ratio of the G-overhang signal to total telomere signal did not appear to change, suggesting that the G-overhangs in TRF2$^{\Delta B}$-expressing cells were unaltered. Similar experiments using a $(TTAGGG)_4$ probe, which recognizes the C strand telomeric DNA led to a conclusion that no single-stranded C strand telomeric DNA was produced during the degradation process induced by the TRF2$^{\Delta B}$ expression (Figure 4-5). These findings were further corroborated by experiments in which telomeric DNA from the same lines was run under alkaline conditions to separate the two strands of telomeric DNA. Hybridization with the $(CCCTAA)_4$ or the $(TTAGGG)_4$ probe resulted in the same pattern of hybridization, indicating that both of the telomeric strands were being degraded to a similar extent (Figure 4-6).

Telomere length data obtained from FISH analysis and from telomere blots have suggested that some of the chromosome ends might have completely lost their telomeric DNA. This conclusion cannot be made with full confidence since due to limits of detection, lack of FISH signal might not represent complete telomere loss. However, chromosomes that lack telomeres should become fusogenic. Examination of anaphase cells of IMR90 cells induced to express TRF2$^{\Delta B}$ indeed showed an increased level of fusion formation (Figure 4-7, top, Table 4-1). On the seventh day of the selection there were 0.6 fusions per anaphase in TRF2$^{\Delta B}$-expressing cells compared to 0.2 fusions per anaphase in control, and 0.3 fusions per anaphase in FLTRF2-expressing cells. As

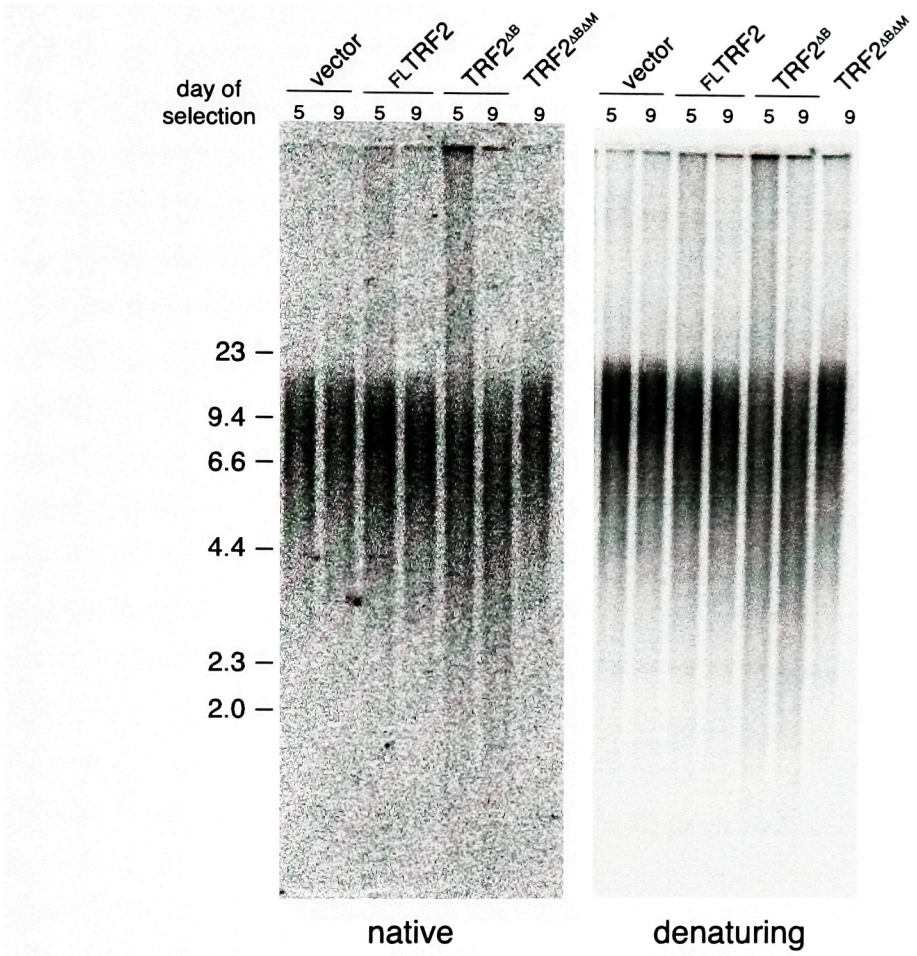

Figure 4-4. **Telomere length analysis in primary BJ fibroblasts infected with control virus, FLTRF2, TRF2$^{\Delta B}$, and TRF2$^{\Delta B\Delta M}$.** In gel hybridization of telomeric restriction fragments with an end-labeled $(CCCTAA)_4$ telomeric probe under non-denaturing conditions (left) and denaturing conditions (right). Genomic DNA was isolated from cells carrying no exogenous TRF2 (vector), FLTRF2 (FLTRF2), TRF2$^{\Delta B}$ (TRF2$^{\Delta B}$), and TRF2$^{\Delta B\Delta M}$ (TRF2$^{\Delta B\Delta M}$) on the indicated days of selection, digested with MboI and AluI and fractionated on a 0.7% agarose gel. Equal loading was confirmed by ethidium bromide staining. The gel was first hybridized under non-denaturing conditions (native). Subsequently, the same gel was denatured and hybridized with the same probe (denaturing). The molecular weights of marker DNAs are indicated in kb.

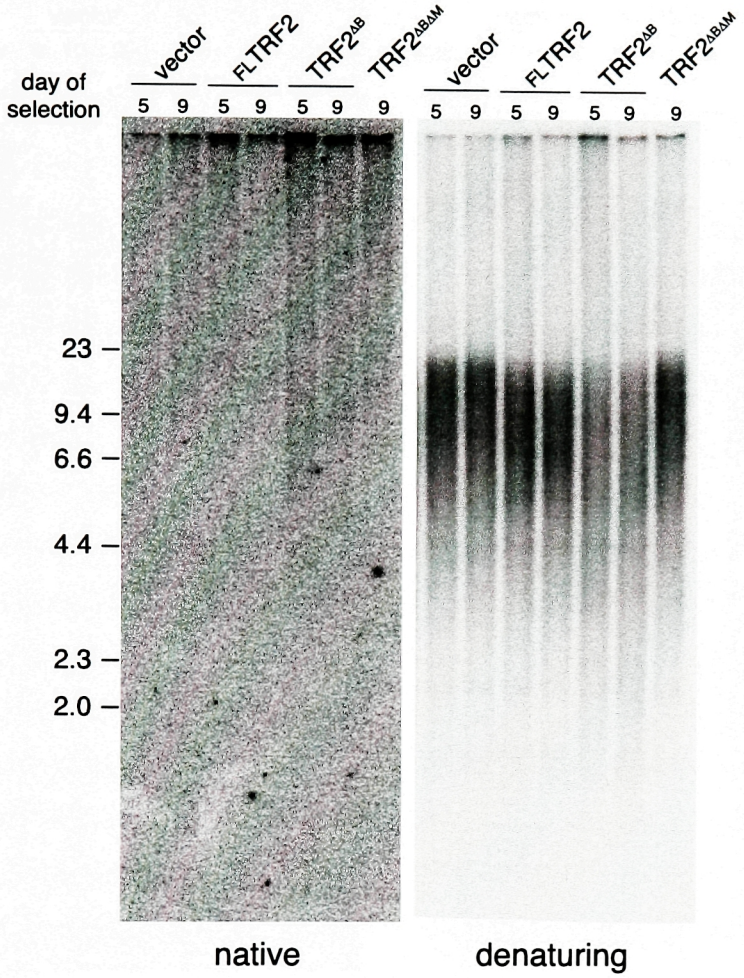

Figure 4-5. **Telomere length analysis in primary BJ fibroblasts infected with control virus, FLTRF2, TRF2$^{\Delta B}$, and TRF2$^{\Delta B\Delta M}$.** In gel hybridization of telomeric restriction fragments with an end-labeled $(TTAGGG)_4$ telomeric probe under non-denaturing conditions (left) and denaturing conditions (right). Genomic DNA was isolated from cells carrying no exogenous TRF2 (vector), FLTRF2 (FLTRF2), TRF2$^{\Delta B}$ (TRF2$^{\Delta B}$), and TRF2$^{\Delta B\Delta M}$ (TRF2$^{\Delta B\Delta M}$) on the indicated days of selection, digested with MboI and AluI and fractionated on a 0.7% agarose gel. Equal loading was confirmed by ethidium bromide staining. The gel was first hybridized under non-denaturing conditions (native). Subsequently, the same gel was denatured and hybridized with the same probe (denaturing). The molecular weights of marker DNAs are indicated in kb.

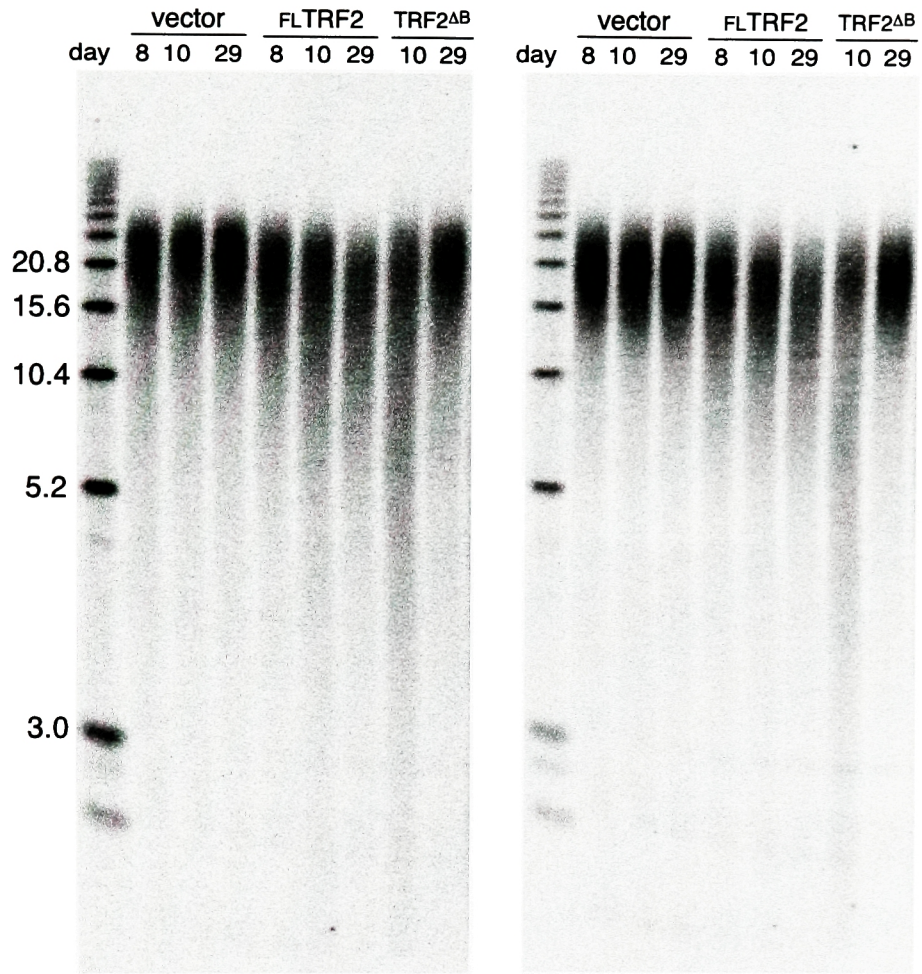

Figure 4-6. **Comparison between the C and the G strand length in BJhTERT SV40 Tag fibroblasts infected with control virus, FLTRF2, and TRF2$^{\Delta B}$.** Southern blot of telomeric restriction fragments fractionated under denaturing conditions. Genomic DNA was isolated from cells on the indicated days of selection, digested with MboI and AluI, fractionated on a 0.7% alkaline agarose gel, blotted onto a nylon membrane and hybridized first with a $(CCCTAA)_4$ probe and subsequently with a $(TTAGGG)_4$ probe. Equal loading was not confirmed due to the alkaline conditions of the electrophoresis. The molecular weights marker were prepared by digesting a TTAGGG repeat bearing 2.6 kb pTH5 plasmid with HindIII and self religation of the cut plasmid. Their size is indicated in kb .

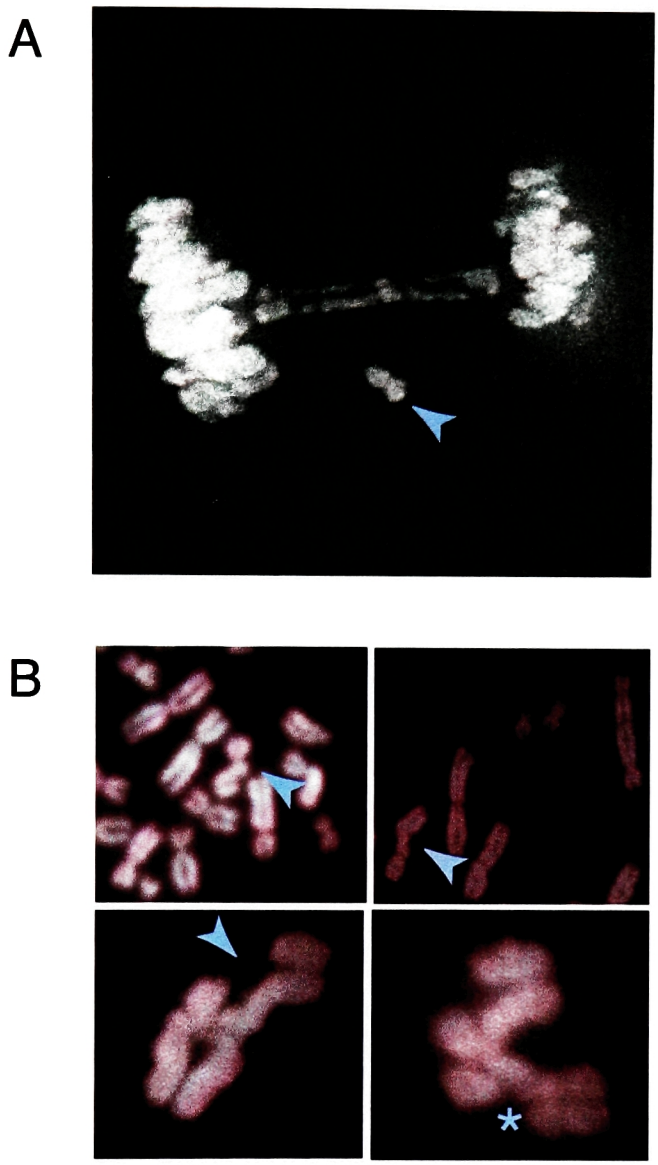

Figure 4-7. **Chromosomal abnormalities in TRF2$^{\Delta B}$ expressing cells. A.** Anaphase of IMR90 cells infected with TRF2$^{\Delta B}$, stained with DAPI on day 7 of selection. Arrow points to two pieces of DAPI positive material between the two future daughter cells. Two anaphase bridges are also visible. **B.** Partial metaphase spreads (top) and single chromosomes (bottom) of IMR90 cells expressing TRF2$^{\Delta B}$ showing chromatid breaks and gaps (arrow heads) and a possible fusion most likely formed after a chromatid break (asterisk). Chromosomes were stained with DAPI.

Table 4-1. No induction of fusions in metaphase and anaphase HTC75 cells expressing TRF2$^{\Delta B}$. HTC75 S13 cells were grown under conditions resulting in repression or induction of the N-terminal truncation of TRF2, TRF2$^{\Delta B}$ HTC75 B27 cell line, which does not express any exogenous protein, was used as a control. Metaphase spreads were prepared on day 4 of induction and number of fusions was assessed in 50 metaphase spreads.

			Fusions	
Cell line	TRF2 allele	Induction	per anaphase	per metaphase
HTC75 **B27**	none	-		0.2
HTC75 **S13**	TRF2$^{\Delta B}$	-	<0.1	0.1
HTC75 **S13**	TRF2$^{\Delta B}$	+	<0.1	0.2

described in Chapter 1, 1.5 fusions per anaphase were seen in TRF2$^{\Delta B\Delta M}$-expressing cells. There were also more fusions visible on metaphase spreads of TRF2$^{\Delta B}$-expressing cells than in control, or FLTRF2-expressing cells; however, FLTRF2 also had considerably higher numbers of fusions than control cells (Table4-2, see discussion). Contrary to finding of fusions in primary cells, examination of anaphase HTC75 cells induced to express TRF2$^{\Delta B}$ did not show increased fusion formation on the 4th day of induction ((van Steensel et al. 1998), Table 4-2). However, the 4th day might be too early to see fusions (also see discussion).

Another abnormality was noted in anaphases of TRF2$^{\Delta B}$-expressing cells. Besides the fusions discussed above, small DAPI-positive pieces were seen between the cells. This has been seen in the HTC75 TRF2$^{\Delta B}$-expressing cells (van Steensel et al. 1998), as well as in primary cells infected with TRF2$^{\Delta B}$ (Figure 4-7,A). 20 small chromosome pieces were seen when 100 anaphases of TRF2$^{\Delta B}$-expressing IMR90 cells were scored (Table 4-1). 2 pieces per 100 anaphases were seen in cells infected with all other TRF2 alleles examined. The presence of pieces in anaphase cells correlated with their presence in metaphase spreads (Table 4-2). Additionally, metaphases revealed the presence of chromosome breaks (Figure 4-7, B and Table 4-1). Breaks were of the chromatid type and they would be able to give rise to fusions. One such fusion has been observed in cells expressing TRF2$^{\Delta B}$ (Figure 4-7 B, bottom right panel)

A different way of assessing chromosome breakage is to look for its products. Pieces seen in the anaphase cells might represent broken fragments that contained no centromere and were left behind by the spindle when the cell was dividing. In telophase such fragments may get incorporated into one of the newly formed nuclei. Alternatively, they may reform their own nuclear envelope and persist next to a main nucleus as a

Table 4-2. Induction of abnormalities in metaphase and anaphase IMR90 cells expressing no exogenous protein, FLTRF2, TRF2$^{\Delta B}$, TRF2$^{\Delta B\Delta M}$. IMR90 cells infected with a vector control (pLPC), FLTRF2 (pLPCTRF2), TRF2$^{\Delta B}$ (pLPCTRF2$^{\Delta B}$), or TRF2$^{\Delta B\Delta M}$ (pLPCTRF2$^{\Delta B\Delta M}$) on day 7 of selection were scored on coded samples for the presence of abnormalities in metaphase and anaphase cells. All alleles were myc-tagged. Numbers in parentheses specify the fraction of metaphases or anaphases that had the indicated abnormality.

	Abnormalities per 100 metaphases[§]			Abnormalities per 50 anaphases	
Cell line	Fusions	Breaks	Pieces	Fusions*	Pieces
pLPC	6 (6%)	6 (6%)	0	9 (8%)	1 (2%)
pLPCTRF2	18 (17%)	28 (16%)	6 (6%)	14 (20%)	1 (2%)
pLPCTRF2$^{\Delta B}$	38 (28%)	41 (26%)	14 (11%)	33 (50%)	10 (18%)
pLPCTRF2$^{\Delta B\Delta M}$	219 (55%)	18 (15%)	4 (2%)	75 (78%)	1 (2%)

[§] 108 metaphases were scored for pLPC control, 115 for pLPCTRF2, 113 for pLPCTRF2$^{\Delta B}$, 57 for pLPCTRF2$^{\Delta B\Delta M}$.

* including bridges and lagging chromosomes

micronucleus. Primary BJ cells have very low level of micronuclei. Only 3% of control cells had a micronucleus (Table 4-3). This number stayed low when FLTRF2 was expressed (2%) but increased to 33% when $TRF2^{\Delta B}$ was expressed. Micronuclei were also frequent in $TRF2^{\Delta B\Delta M}$-expressing cells although not as prominent as in cells expressing $TRF2^{\Delta B}$. Micronuclei formed in $TRF2^{\Delta B\Delta M}$ might be due to the breakage of the anaphase bridges that are formed frequently in these cells.

Experiments described above indicate that $TRF2^{\Delta B}$ expression led to dramatic changes in the genome. Telomere degradation and chromosome breakage were observed when $TRF2^{\Delta B}$ was expressed in a variety of cells. Therefore it is not surprising that primary cells expressing $TRF2^{\Delta B}$ grow poorly. IMR90 cells expressing $TRF2^{\Delta B}$ behaved similarly to $TRF2^{\Delta B\Delta M}$-expressing cells in all growth assays (discussed in Chapter 2); however, the growth arrest was never complete in the population. $TRF2^{\Delta B}$ expressing cells grew very slowly, although slightly better than $TRF2^{\Delta B\Delta M}$-expressing cells (Figure 4-8, A). BrdU incorporation on day 15 in cells expressing $TRF2^{\Delta B}$ was only 40% of incorporation in control cells. This number was again significantly higher than in $TRF2^{\Delta B\Delta M}$-expressing cells. The morphology of the arresting cells in the $TRF2^{\Delta B}$-expressing population at day 15 was very similar to $TRF2^{\Delta B\Delta M}$-expressing cells, with cells becoming large and flat and becoming positive for the senescence-associated β-galactosidase activity (SA β-gal). However, the degree of the morphological change, as well as the intensity of the SA β-gal staining was again decreased when compared to $TRF2^{\Delta B\Delta M}$-expressing cells. The protein expression profile on day 15 has confirmed the above findings. Although p53 and p16 were induced to the same level as in $TRF2^{\Delta B\Delta M}$-expressing cells, $TRF2^{\Delta B}$-expressing cells showed some Rb hyperphosphorylation, as well as some cyclin A expression, suggesting that some of the cells in the population

Table 4-3. Micronuclei in primary BJ cells expressing no exogenous protein, FLTRF2, TRF2$^{\Delta B}$, TRF2$^{\Delta B\Delta M}$ Primary BJ1 cells were infected with a vector control (pLPC), FLTRF2 (pLPCTRF2), TRF2$^{\Delta B}$ (pLPCTRF2$^{\Delta B}$), or TRF2$^{\Delta B\Delta M}$ (pLPCTRF2$^{\Delta B\Delta M}$). On day 6 of selection, DAPI stained anaphase nuclei were scored. Most of the events comprised of a single micronucleus abutting the interphase nucleus.

Cell line	% cells with micronuclei
pLPC	3%
pLPC TRF2	2%
pLPCTRF2$^{\Delta B}$	33%
pLPCTRF2$^{\Delta B\Delta M}$	17%

*300 interphase cells were scored for pLPC, pLPCTRF2, and pLPCTRF2$^{\Delta B\Delta M}$, 602 interphase cells were scored for pLPCTRF2$^{\Delta B}$.

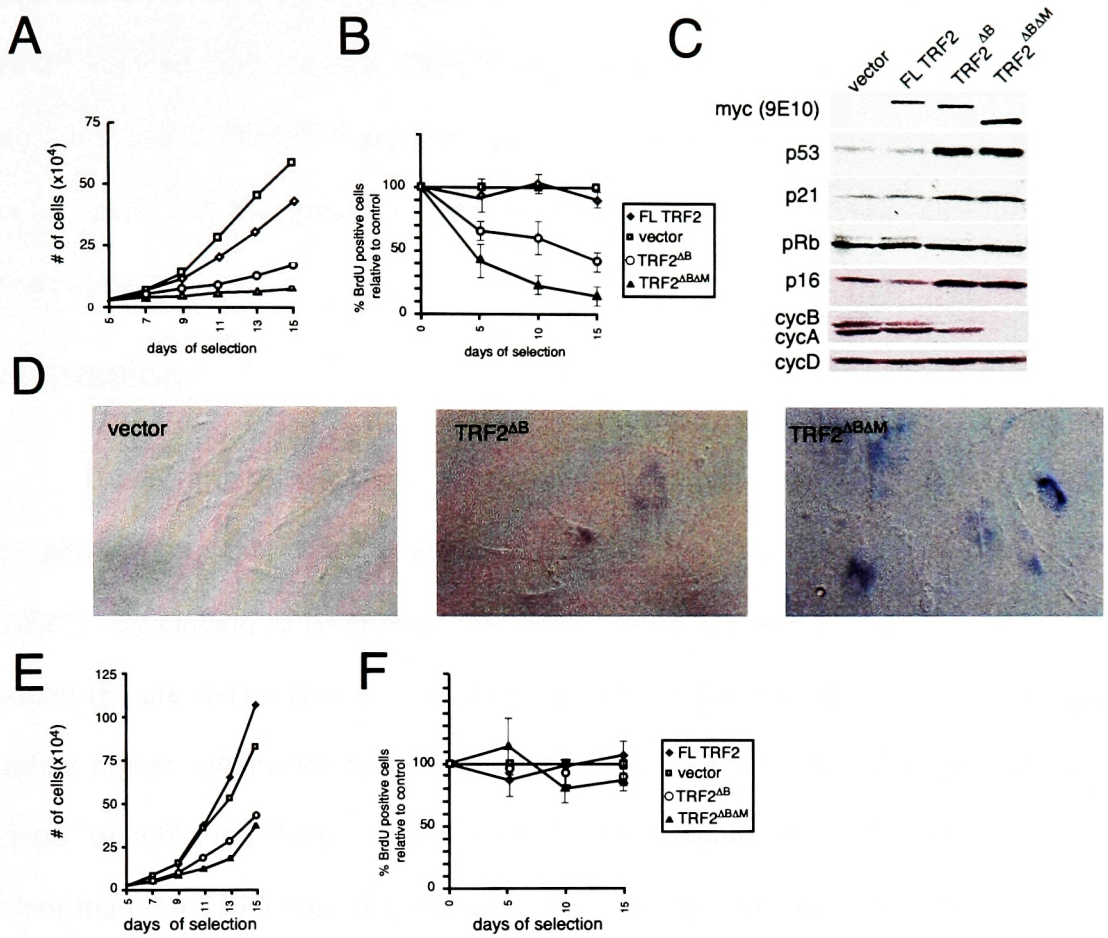

Figure 4-8. **Effects of expression of TRF2$^{\Delta B}$ on growth characteristics, protein expression profile and SA β-gal staining of young IMR90 cells- comparison with cells expressing TRF2$^{\Delta B\Delta M}$ (also see chapter 2).** **A.** Representative growth curve of vector control, TRF2, TRF2$^{\Delta B}$ or TRF2$^{\Delta B\Delta M}$ expressing IMR90 cells. On the 4th day of selection, cells were plated in duplicate at 3x10^4 cells per well in a six-well plate. On the indicated days cells from 2 wells were washed, trypsinized and counted in duplicate using a Coulter counter. **B.** % of cells in S-phase as measured by 1 hour bromo-deoxyuridine (BrdU) incorporation on day 5, 10 and 15. All numbers are normalized to the level of BrdU incorporation in vector control cells as explained in Figure 2-2. **C.** Western blot analysis of cell cycle regulatory proteins in control, TRF2, TRF2$^{\Delta B}$, and TRF2$^{\Delta B\Delta M}$ expressing cells. Cells were collected on day 14 of selection. **D.** Senescence associated β-galactosidase activity. Cells infected with TRF2 alleles were plated at low density and stained for β-galactosidase activity at pH 6 on day 14 of selection. **E.** Representative growth curve of IMR90 cells expressing SV40 large T antigen and vector control, TRF2, TRF2$^{\Delta B}$, or TRF2$^{\Delta B\Delta M}$ **F.** % of IMR90 cells expressing SV40 large T antigen and TRF2 alleles in S-phase as measured by 1 hour BrdU incorporation on day 5, 10 and 15.

were actively cycling. To determine if the SV40 Tag is able to rescue cells from the TRF2$^{\Delta B}$-induced growth arrest, TRF2$^{\Delta B}$ was expressed in cells already expressing SV40 Tag. Just like in TRF2$^{\Delta B\Delta M}$-expressing cells, the BrdU levels were restored to levels of control cells, but the growth curves showed that the TRF2$^{\Delta B}$-expressing populations grew poorly.

Discussion

This chapter has explored the function of the basic domain of TRF2 by studying the phenotypes associated with expression of the N-terminal truncation of TRF2, TRF2$^{\Delta B}$. By binding to telomeres, the TRF2$^{\Delta B}$ allele appears to displace the full-length protein (Figure 4-1). This is in agreement with the finding that *in vitro* TRF2$^{\Delta B}$ has a slightly higher affinity for telomeric repeats than FLTRF2 (van Breugel and Titia de Lange, unpublished data). *In vitro* TRF2$^{\Delta B}$ forms higher-order oligomers to a greater extent than the TRF2 (van Breugel and Titia de Lange, unpublished data), which might increase the affinity for DNA by bringing more myb domains in the vicinity of multiple binding sites on the telomeric DNA.

One of the phenotypes observed after expression of TRF2$^{\Delta B}$ is loss, or a significant reduction of telomere signal from many chromosome ends. Often only one of the sister chromatids on a mitotic chromosome had a decreased signal. Such a finding suggests that many of the events leading to appearance of shorter telomeres had to occur in S or G2 phase immediately preceding mitosis. One of the many possible scenarios of how TRF2$^{\Delta B}$ expression could lead to telomere loss on one chromatid is shown in Figure 4-9 (left column). It is proposed here that the presence of TRF2$^{\Delta B}$ creates a nick in one strand of the DNA. The site of the nick suggested in the model is not important for this discussion and could occur on any of the two strands, and at any

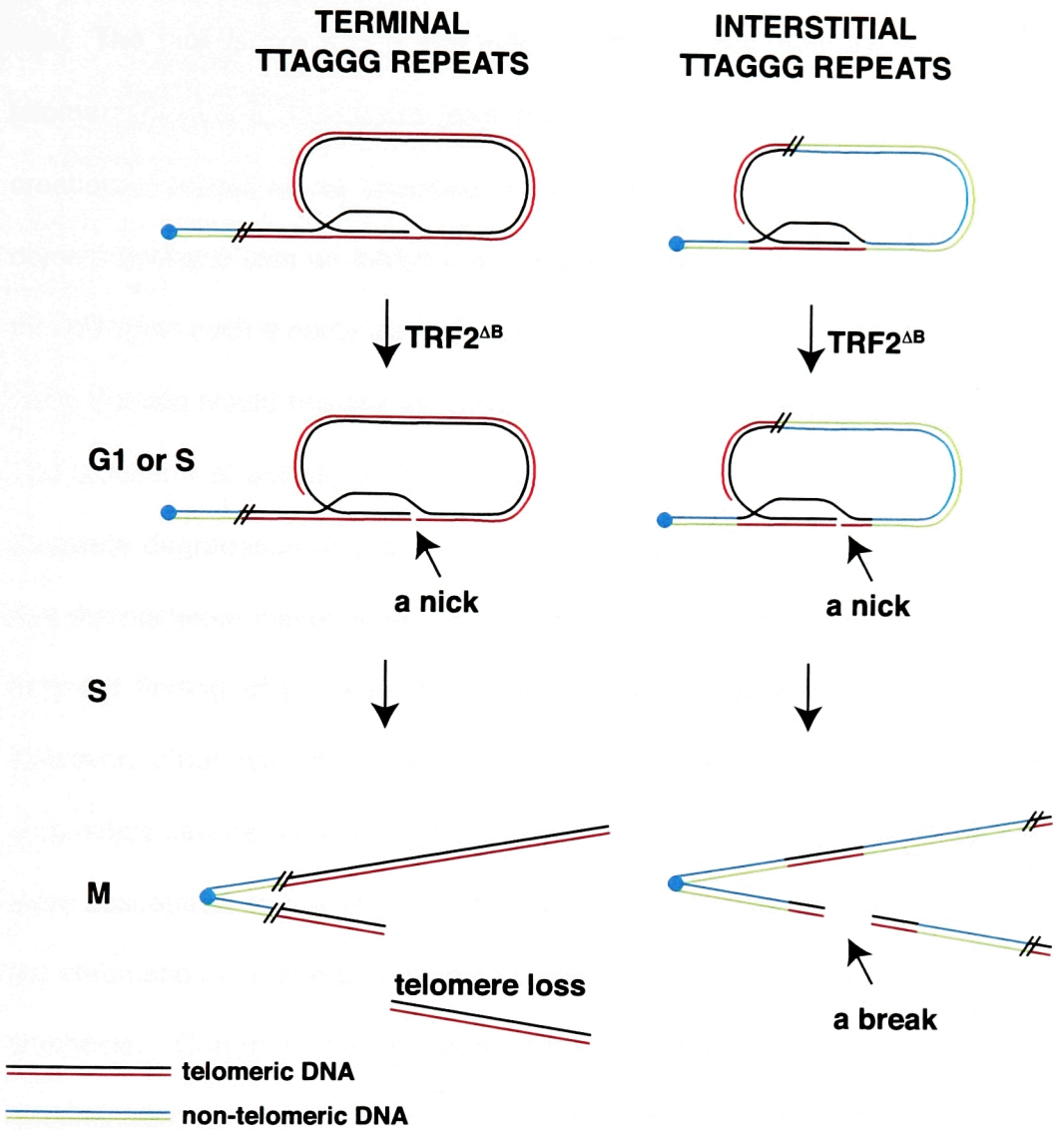

Figure 4-9 **Model of telomere loss and break formation upon induction of TRF2$^{\Delta B}$.** Presence of TFRF2$^{\Delta B}$ creates a nick (at any place in the loop not necessarily where indicated in the schematic). The nick is processed during the S phase and creates a shortened telomere on one chromatid and a normal telomere on the opposite chromatid. The telomeric DNA that has been severed gets degraded. Similarly, if a t-loop is made by an invasion of the overhang into the interstitial site, a break forms on one chromatid, but not on the other. Formation of t-loops involving the interstitial TTAGGG sites are not necessary for this model. TFRF2$^{\Delta B}$ through binding at the interstitial sites might bring the necessary factors for the fragmentation to occur. Also, multiple nicks might be formed due to TFRF2$^{\Delta B}$ expression, leading to a faster degradation of the telomere.

site. The nick is processed into a break during DNA replication and eventually the telomere piece that has been formed is degraded. How TRF2$^{\Delta B}$ would lead to the creation of a nick is not specified in the model, but one possibility is that the basic domain interacts with an inhibitor of a nuclease present at telomeres. At some point in the cell cycle such a nuclease might be needed for the resolution of the t-loop. Lack of a basic domain would repress the inhibition leading to increased activity of the nuclease. The biochemical activity of the nuclease would specify whether a nick, a break, or a complete degradation of one or both strands would be expected. It is proposed here that the nuclease makes a nick, since such a proposal would be in agreement with the frequent finding of decreased telomeric DNA only at one of the sister chromatids. However, other reasons for the presence of decreased signals on only one of the chromatids can be proposed. It is possible, for example, that one of the chromatids is more susceptible to the TRF2$^{\Delta B}$-induced loss. This might not be unlikely, since one of the chromatids is made by a leading strand synthesis, and the other by lagging strand synthesis. Chromosome orientation-FISH (CO-FISH) experiments, which allow for discrimination between the two types of chromatid, will be informative in this regard. The experiment needs to be performed at a very early timepoint after infection with TRF2$^{\Delta B}$ to aid in visualization of the events occurring in the first cell cycle after expression of TRF2$^{\Delta B}$. Disappearance of the signal from both of the sister chromatids, an event that was often seen in TRF2$^{\Delta B}$-expressing cells, could have been due to simultaneous loss of a substantial length of telomeric DNA from both chromatids, or replication of a chromosome that has lost the telomeric DNA in a previous division.

Loss of telomeric DNA was also documented on Southern blots visualizing telomeric DNA from cells expressing TRF2$^{\Delta B}$ (Figure 4-3 and 4-4). However, the signal

never fully disappeared in any of the experiments performed. This could be due to the growth arrest that ensues after TRF2$^{\Delta B}$ is expressed. Telomeres of non-cycling cells might not participate in the degradation events. Nonetheless, even when cells expressing the SV40 T antigen were used for the study, (Figure 4-3) the telomeres never completely disappeared. Instead telomere length returned to normal. This was most likely due to constant cell death (compare growth curve in Figure 4-8 E to BrdU labeling in Figure 4-8 F), and due to selection against the TRF2$^{\Delta B}$ allele. Another possibility comes from the proposal that telomeres can be lost from only one chromatid. If this is the case, it would take a very long time of constant division without the loss of TRF2$^{\Delta B}$ expression, to homogenize telomeres to the low length. In combination with obvious deleterious effects of TRF2$^{\Delta B}$ the expression, reaching such state would be impossible.

A related question pertains to the behavior of the HTC75 S cell lines that express TRF2$^{\Delta B}$. Expression of TRF2$^{\Delta B}$ led to appearance of breaks in these cells (see below); however, loss of telomeric DNA was not prominent (van Steensel et al. 1998). The telomere blots revealed a mere hint of loss of hybridization intensity, and the loss was much less pronounced than in any other cell line studied. It is possible that the combination of the already short telomeres present in these clones and the rapid induction of the growth arrest after TRF2$^{\Delta B}$ expression, precluded identification of telomere signal changes. Increased heterogeneity of the signal might also be missed because telomeres in the HTC75 cells already were represented by a heterogenous smear under electrophoresis conditions used in the experiments.

Besides the loss of telomeric DNA, metaphase spreads of cells expressing TRF2$^{\Delta B}$ also revealed the presence of chromatid breaks. Although the origin of such breaks is unknown at this point, a model that parallels the telomere loss model after

TRF2$^{\Delta B}$ expression is presented in Figure 4-9 (right hand side). It is proposed that TRF2$^{\Delta B}$ localizes to the interstitial TTAGGG sites and that a t-loop is made by invasion of the G-overhang into the interstitial TTAGGG repeats. Subsequent events, identical to the ones presented for the telomere loss would lead to a formation of a chromatid break.

This is also an attractive model for how interstitial $(TTAGGG)_n$ sites might be able to induce chromosomal breakage, visualized in many studies presented in the introduction. TRF2 is proposed to bind to the interstitial telomeric DNA repeats and an inappropriate formation of the t-loops and subsequent processing is proposed to lead to break formation. Binding of endogenous TRF2 to interstitial sites has been noted in a number of hamster cell lines, which are characterized by presence of blocks of telomeric DNA sequences at internal sites (Smogorzewska et al. 2000). The influence of telomeric proteins on break induction at interstitial sites can now be tested using the system described in the introduction, where a block of 800 bp of telomeric DNA has been inserted into the APRT locus in the hamster. Based on the proposal presented here expression of TRF2 should result in increased rates of rearrangements involving the engineered interstitial sites. Expression of the TRF2$^{\Delta B}$, due to its increased affinity for the telomeric DNA should result in even better binding to the interstitial sites giving rise to a greater number of rearrangements.

The chromatid breaks seen in the cells expressing TRF2$^{\Delta B}$, when repaired, should lead to formation of fusions. As seen in Figure 4-7, one of such events has been observed. In this case, a broken end seemed to fuse with another broken end or possibly a chromosome end, presumably after that end lost telomeric DNA. However, not enough fusions of this type were seen on metaphase spreads to explain the levels of anaphase bridges noted in cells expressing TRF2$^{\Delta B}$. Fusions might have also been

formed between chromosomes that lost their telomeres. Fusions resulting from joining of broken ends or chromosomes devoid of telomeres should not have telomeric DNA at the site of fusion. Whether fusions induced by $TRF2^{\Delta B}$ do, or do not have telomeric DNA remains to be determined.

In some of the experiments presented in this chapter, cell overexpressing FLTRF2 behaved in a similar way to $TRF2^{\Delta B}$-expressing cells. For example, formation of breaks and fusions was significantly higher in FLTRF2-expressing cells than in control cells (Table 4-1), although not as high as in $TRF2^{\Delta B}$-expressing cells. This behavior of cells infected with FLTRF2 could be explained in many ways. First, the alleles in this experiment were tagged at their N termini. For a full-length protein a tag would occur next to the basic domain. If the tag interfered with the correct functioning of the full length protein, a $TRF2^{\Delta B}$-like phenotype would be expected. Secondly, some $TRF2^{\Delta B}$ and possibly $TRF2^{\Delta B \Delta M}$ protein degradation products might be present in cells expressing FLTRF2. Presence of degradation products of FLTRF2 was observed on western blots of short-term experiments. Since $TRF2^{\Delta B}$ has a higher affinity for DNA, even if it is not present at very high level, it might be able to compete out the overexpressed TRF2. It is possible that with time the cells that had substantial levels of $TRF2^{\Delta B}$ were lost. The finding that the growth of TRF2 expressing cells is a little slower at the beginning of the experiments substantiates this interpretation (Figure 4-8, A). With time, the FLTRF2-expressing cells grew at the same rates as control cells. Finally, FLTRF2 might have been titrating away the protein that normally binds to the telomeric TRF2, and in particular to the basic domain of TRF2. As a result, there would be less of that protein present to telomeres leading to the partial telomere dysfunction.

The growth arrest of human primary cells expressing TRF2$^{\Delta B}$ is very reminiscent of the growth arrest induced by the dominant negative TRF2 (TRF2$^{\Delta B \Delta M}$). Based on the protein expression profile and the ability of the SV40 Tag to abrogate the arrest, it seems that the signaling through the same pathways caused the arrest. It is interesting to speculate about the cause of the arrest. Telomere loss is so pronounced in the cells expressing TRF2$^{\Delta B}$, that many, if not all cells in the population might have lost a few of their telomeres. Such event would lead to activation of the pathways that are naturally activated during senescence, leading to the permanent growth arrest. It is also possible that induction of breaks might lead to the growth arrest. This interpretation is supported by the findings that the HTC75 expressing TRF2$^{\Delta B}$, arrest and exhibit chromosome breakage but do not exhibit substantial telomere loss. However, as discussed above, the inability to visualize telomere shortening in these cells, does not preclude that some telomeres did get very short, leading to growth arrest

Based on the experiments presented here, the basic domain appears to be a vital regulatory domain of TRF2. It will be important to identify proteins interacting with the basic domain. Such proteins are predicted to be negative regulators of degradation. Further studies of such proteins have a potential of elucidating the degradative processes at the telomere.

Chapter 5

Centrosomal localization of TRF2 and centrosome/genome reduplication in cells expressing $TRF2^{\Delta B\Delta M}$ or $TRF2^{\Delta B}$

Introduction

A complicated network of proteins acting in concert to activate the cdk2 complexes regulates entry into S phase of the cell cycle (reviewed in Bartek and Lukas 2001). The CyclinE-Cdk2 complex integrates signals emanating from Rb-E2F and the Myc pathways, and is the main effector of these pathways leading to stimulation of DNA synthesis. To avoid DNA synthesis when DNA is damaged, multiple pathways are employed to keep Cdk2 in a non-active state. These pathways include the degradation of cyclin D1 releasing p21 to inhibit Cdk2 (Agami and Bernards 2000), degradation of Cdc25A phosphatase leading to persistence of inhibitory phosphates on Cdk2 (Mailand et al. 2000), and activation of p53 (reviewed in Vogelstein et al. 2000) leading to transcriptional activation of p21 resulting in a more permanent inhibition of S phase entry.

Centrosomes are the microtubule organizing centers of animal cells and they, like DNA, replicate once and only once per cell cycle. The cycle of centrosomal duplication is in fact coordinated with DNA replication, and the centrosomal duplication is also driven by the Cdk2 complexes (reviewed in Winey 1999), although controversy exists whether Cyclin A or E is the necessary cyclin partner of Cdk2. Other kinases, including the Polo-like, Aurora-related, and NIMA-related kinases, are important for proper duplication and/or function of the centrosomes (reviewed in Mayor et al. 1999).

An inability to control centrosome numbers has been found to be a characteristic of many tumor cells (reviewed in Duensing and Munger 2001). It appears that centrosomal reduplication is associated with inappropriate function of many proteins including p53 (Fukasawa et al. 1996), BRCA1 (Xu et al. 1999), STK15 (Zhou et al.

1998), and Skp2 (Nakayama et al. 2000). Based on the very high number of different proteins that are found at the centrosome (see Table 1, (Duensing and Munger 2001)), the centrosome appears to be a site where many signals could be integrated during cell growth.

A recent study has localized one of the telomeric proteins tankyrase, a TRF1 interacting factor, to mitotic centrosomes of human cells (Smith and de Lange 1999). Tankyrase co-localizes with NuMA (nuclear/mitotic apparatus protein), which resides at the periphery of mitotic centrosomes. The function of tankyrase at human centrosomes is unknown; however, based on its poly(ADP-ribose) polymerase activity, it has been proposed that tankyrase might regulate other centrosomal proteins.

This chapter presents two unexpected observations of genome and centrosome reduplication occurring after expression of TRF2$^{\Delta B\Delta M}$ or TRF2$^{\Delta B}$, and of centrosomal localization of TRF2.

Results

While examining metaphase spreads of primary human fibroblasts expressing TRF2$^{\Delta B\Delta M}$ and TRF2$^{\Delta B}$ (See Chapter 1 and 4), it was noted that some metaphases harbored an increased number of chromosomes. Although it was often impossible to determine the exact number of chromosomes on most metaphases, if it appeared that there were more than 70 chromosomes on a spread, it was considered to represent genome reduplication. According to this criterion ~37% of metaphases of cells expressing TRF2$^{\Delta B\Delta M}$ and ~23% of metaphases of cells expressing TRF2$^{\Delta B}$ showed genome reduplication (Table 5-1). In contrast, only ~3% of control cells expressing no exogenous protein showed reduplication of the genome. FLTRF2-expressing cells

Table 5-1 Genomic reduplication in young cells expressing no exogenous protein, FLTRF2, TRF2$^{\Delta B}$, TRF2$^{\Delta B\Delta M}$. Primary IMR90 cells were infected with a vector control (pLPC), FLTRF2 (pLPCTRF2), TRF2$^{\Delta B}$ (pLPCTRF2$^{\Delta B}$), or TRF2$^{\Delta B\Delta M}$ (pLPCTRF2$^{\Delta B\Delta M}$). All alleles were myc-tagged. On the day 7 of selection, metaphases were prepared after 90 min colcemid treatment and those that had more than 80 chromosomes were scored as reduplicated.

Cell line	% of metaphase spreads with reduplication*
pLPC	3%
PLPC TRF2	16%
pLPCTRF2$^{\Delta B}$	23%
pLPCTRF2$^{\Delta B\Delta M}$	37%

* 98 metaphases were scored for pLPC control, 115 for pLPCTRF2, 113 for pLPCTRF2$^{\Delta B}$, 57 for pLPCTRF2$^{\Delta B\Delta M}$.

showed an intermediate level of reduplication (~16%); however, this allele of TRF2 was N-terminally tagged, which could have created a partial $TRF2^{\Delta B}$ allele (for a more thorough discussion of why FLTRF2 might show some $TRF2^{\Delta B}$ phenotypes, please see the discussion to Chapter 4). The striking finding was that the reduplicated chromosomes most often occurred in pairs, an arrangement also known in cytogenetic literature as a diplochromosome (Figure 5-1). To assure that they were true diplochromosomes and not prematurely separated sister chromatids, chromosomes were observed under high magnification. Many spreads showed diplochromosomes with clearly delineated four chromatids. Some, but not all metaphases that revealed diplochromosomes also exhibited end-to-end fusions (Figure 5-1).

In one experiment, metaphases of $TRF2^{\Delta B\Delta M}$ and $TRF2^{\Delta B}$-expressing cells showed premature chromosome division (PCD) (Figure 5-2), which is characterized by dissolution of cohesion between sister chromatids not only along the arms but also at the centromere while cells are still in metaphase. Normally, the separation of sister chromatids occurs at the metaphase to anaphase transition, thus visualization of this event in metaphase spreads is abnormal. Among 44 metaphases of $TRF2^{\Delta B\Delta M}$-expressing cells, 87 chromosomes displayed PCDs, and among 10 metaphases of $TRF2^{\Delta B}$-expressing cells, 14 chromosomes displayed PCDs. Premature chromosome division was so far only visualized in one experiment in which metaphases were arrested for 12 hours by colcemid treatment. No premature chromosome division was visualized in control cells (35 metaphases examined) or FLTRF2-expressing cells (10 metaphases examined) prepared under identical conditions. In other experiments in which metaphases were examined, no attention was being paid to the occurrence of PCDs.

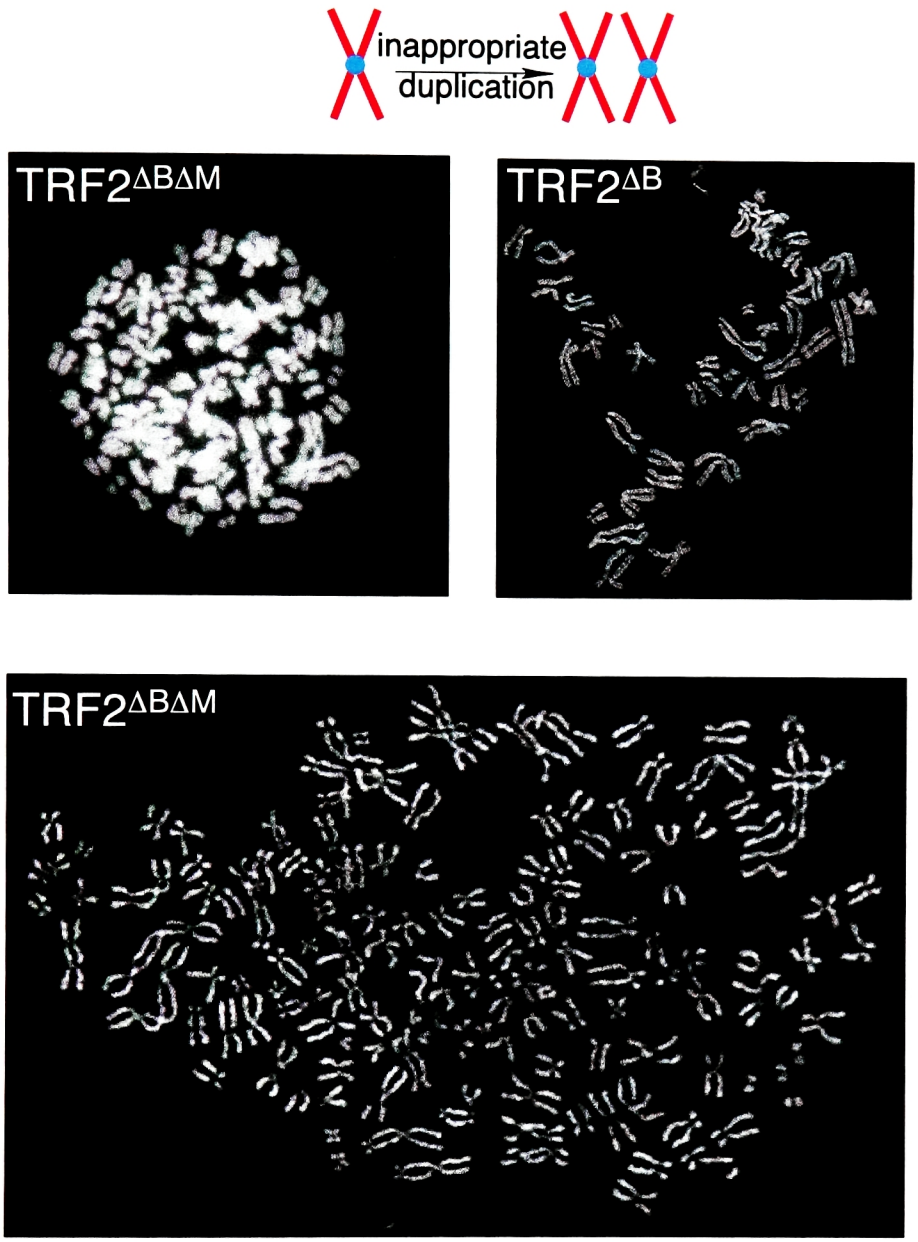

Figure 5-1. **Genome reduplication visualized on metaphases of TRF2$^{\Delta B\Delta M}$ and TRF2$^{\Delta B}$ expressing IMR90 human primary fibroblasts.** Metaphase spreads of IMR90 cells expressing TRF2$^{\Delta B\Delta M}$ and TRF2$^{\Delta B}$ were prepared on day 7 of selection. Chromosomes were stained with DAPI. The two top metaphase spreads show a reduplication which occurred in the division proceeding the metaphase shown. Reduplication shown in the bottom spread might have occurred in the preceding or an earlier division since many of the duplicated chromosomes do not show the diplochromosome arrangement. Please note that many end-to-end fusions are visible in the spreads (also see Figure 1-12 C).

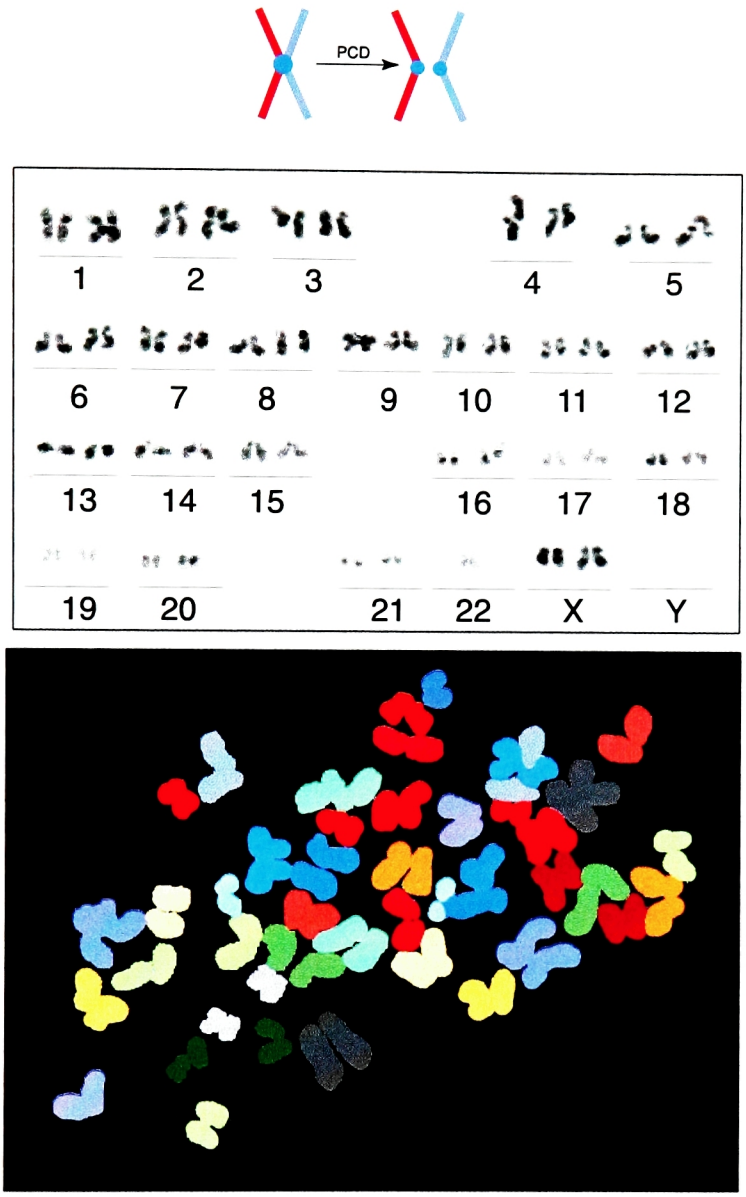

Figure 5-2. **Premature chromosome division (PCD) in metaphase spreads of IMR90 fibroblasts expressing TRF2$^{\Delta B \Delta M}$.** Multiplex fluorescence in situ hybridization (M-FISH) on metaphase spreads of cells expressing TRF2$^{\Delta B \Delta M}$. Spreads were prepared on day 6 of selection, after 12-hour colcemid treatment. Chromosomes 1, 2, 3, 4, 5, 6, 8, 9, 10, 11, 12, 13, 14, 16, 17, 21, and X show premature chromosome division

(Experiments done in collaboration with Heidi Holtgreve-Grez and Anna Jauch (Institute für Humangenetik, Heidelberg, Germany)

DNA replication and duplication of the centrosomes are highly synchronized and occur in S phase of cell cycle. The presence of metaphase spreads with twice the genetic information should be mirrored by the presence of interphase cells with more than two centrosomes, unless DNA replication and the centrosomal cycle were uncoupled. Indeed, many TRF2$^{\Delta B\Delta M}$-expressing interphase cells, when stained with an antibody directed against γ-tubulin, a protein only found in the pericentriolar region of the centrosomes, showed three or more centrosomes (Figure 5-3). They were often found in clusters of four, suggesting two rounds of duplication, although some cells carried more than 6 centrosomes. Quantification of centrosome numbers in interphase cells showed that expression of TRF2$^{\Delta B\Delta M}$ allele led to 3 to 5 fold increase in anaphase cells with 2 or more centrosomes (Table 5-2). TRF2$^{\Delta B}$ allele expression in IMR90 primary fibroblasts had less influence on centrosome numbers at an early timepoint after infection (day 5 of selection), but showed a fourfold increase in % of anaphase cells with 2 or more centrosomes at day 14 of selection (Table 5-2). In WI38 cells, the background of interphase cells with 2 or more centrosomes was higher than in IMR90 cells, reaching 9% of all interphase cells. This number was possibly higher than in the IMR90 cells because WI38 cells were cultured for a longer time before the infections thus they were closer to entry into senescence (see below). Nevertheless, there was an almost 3 fold increase in the % of cells with more than 3 centrosomes when TRF2$^{\Delta B\Delta M}$ was expressed.

Expression of TRF2$^{\Delta B\Delta M}$ and TRF2$^{\Delta B}$ was shown to lead to growth arrest with characteristics of senescence (Chapter 2 and 4). Population very close to a senescent state have been previously observed to have polyploid cells (Saksela and Moorhead 1963; Thompson and Holliday 1975). To examine the number of centrosomes in

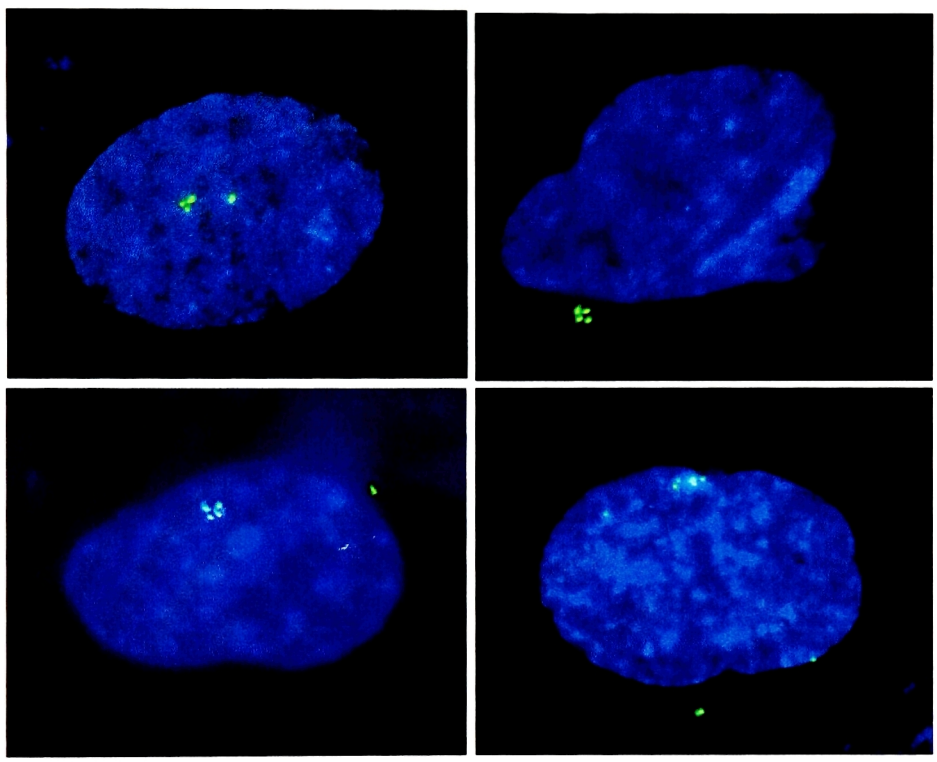

Figure 5-3. **Centrosomal reduplication in IMR90 human primary fibroblasts expressing TRF2$^{\Delta B \Delta M}$.** Indirect immunofluorescence against γ-tubulin (shown in green) in primary human cells infected with TRF2$^{\Delta B \Delta M}$. DNA was counterstained with DAPI.

Table 5-2 Centrosomal reduplication in young cells expressing no exogenous protein, FLTRF2, TRF2$^{\Delta B}$, TRF2$^{\Delta B\Delta M}$, and in senescent cells. Primary IMR90, WI38, and HS68 cells were infected with myc-tagged vector control (pLPC), FLTRF2 (pLPCTRF2), TRF2$^{\Delta B}$ (pLPCTRF2$^{\Delta B}$), or TRF2$^{\Delta B\Delta M}$ (pLPCTRF2$^{\Delta B\Delta M}$). On the indicated days of selection, cells were methanol fixed, indirect immunofluorescence against γ-tubulin was performed, and number of centrosomes was counted.

Cells	allele	Day of selection	% of cells with more than two centrosomes *
Young IMR90	pLPC	7	3 (310)
	PLPC TRF2	7	4 (335)
	pLPCTRF2$^{\Delta B}$	7	8 (303)
	pLPCTRF2$^{\Delta B\Delta M}$	7	15 (303)
	pLPC	14	5 (100)
	PLPC TRF2	14	5 (100)
	pLPCTRF2$^{\Delta B}$	14	23 (100)
	pLPCTRF2$^{\Delta B\Delta M}$	14	16 (100)
Senescent IMR90(~p43)	none		27 (100)
HS68	pLPC	5	3 (200)
	PLPC TRF2	5	4 (201)
	pLPCTRF2$^{\Delta B}$	5	5 (200)
	pLPCTRF2$^{\Delta B\Delta M}$	5	14 (203)
WI38	pLPC	5	9 (201)
	PLPC TRF2	5	12 (201)
	pLPCTRF2$^{\Delta B}$	5	16 (203)
	pLPCTRF2$^{\Delta B\Delta M}$	5	25 (200)

*In paranthesis number of cells scored is indicated

passage 43 (p43) IMR90 cells, which reached senescence a week or two earlier, centrosomes were visualized using anti γ-tubulin. 27% of cells had three or more centrosomes suggesting that centrosomal reduplication is one more characteristic of senescent cells.

In the experiments were numbers of centrosomes in each cell were quantified, TRF2 was often used to co-stain the nuclei that were being stained with γ-tubulin to check for the expression of the TRF2 alleles. It was surprising to find that endogenous TRF2 in the control cells besides forming a familiar punctate pattern in the nucleus, localized to centrosomes. Two separate antibodies raised against TRF2, rabbit antibody 647 and a goat antibody to TRF2 (Imgenex), recognized centrosomes both in mitosis as well as in interphase cells (Figure 5-4). Staining of centrosomal TRF2 was much dimmer in interphase cells, although it was still above background staining. Dimmer staining in anaphase cells was noted for other centrosomal components.

TRF2 staining in immunofluorescent studies surrounded centrin, which gave the expected double-dot staining of two centrioles per centrosome (Figure 5-4, top panel). Staining of γ-tubulin and TRF2 generally overlapped; however, staining of γ-tubulin in mitotic cells was often broader and seemed to extend onto the microtubules emanating from the centrosomes. Overall, the most overlap was found between TRF2 and pericentrin, a known component of a centrosome (Figure 5-4, third row).

Previous studies have localized tankyrase at centrosomes of metaphase and early anaphase cells, but not in late anaphase, telophase or interphase cells. To compare localization of TRF2 and tankyrase, HeLaI.2.11 were stained with antibodies recognizing the two proteins. Generally, tankyrase appeared to surround TRF2 in metaphase, leading to clear delineation of different compartments. Such exclusion was

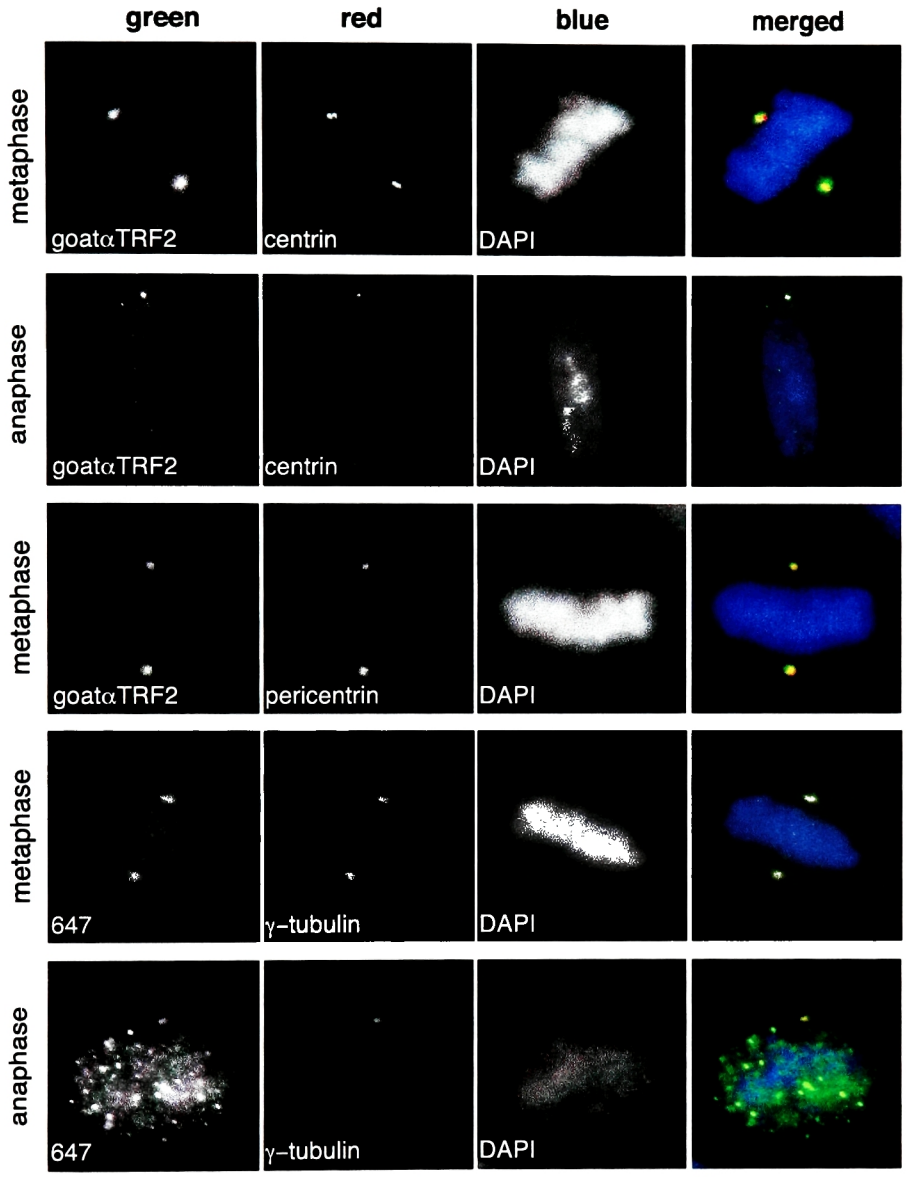

Figure 5-4. **Localization of TRF2 to centrosomes in HeLaI.2.11 cells.** Indirect immuofluorescence with antibodies raised against TRF2 (goat α TRF2 and rabbit α TRF2 #647), and with mouse α centrin, mouse α pericentrin , or mouse α γ-tubulin. HeLaI.2.11 were fixed in methanol and costained with the indicated antibodies. FITC-conjugated α rabbit or FITC-conjugated α goat and TRITC α mouse secondary antibodies were used to visualize the primary antibodies. DNA was counterstained ith DAPI. Cells in metaphase and interphase are shown as indicated on the left.

especially visible in early anaphase cells (Figure 5-5). Consistent with previous results, tankyrase staining was not present in some anaphase cells (Figure 5-5) or interphase cells.

Often in colocalization studies a concern arises that the proteins appear to colocalize because the signal of one of the proteins is so strong that it is seen in adjacent channels (often called bleed-through). The finding that the TRF2 signal did not colocalize with the tankyrase signal suggests that the signals were specific for each protein. However, to formally prove that there was no bleed-through, a control experiment was performed. Cells were stained separately with antibodies recognizing TRF2, tankyrase, γ-tubulin, and centrin. Subsequently, pictures were taken in all channels. The control channels that should have exhibited no staining stayed blank as expected (Figure 5-6), which led to the conclusion that the signal of TRF2 on centrosomes was specific.

Discussion

Reduplication of the genome is a prevented event when all checkpoints are active in the cell. It is surprising that expression of $TRF2^{\Delta B\Delta M}$ and $TRF2^{\Delta B}$ in human primary fibroblasts led to a frequent occurrence of apparent reduplication that was visualized on metaphase spreads and deduced from the presence of increased numbers of centrosomes in interphase cells. As shown in Chapter 2 and 4, expression of $TRF2^{\Delta B\Delta M}$ and $TRF2^{\Delta B}$ alleles leads to growth arrest, a result of activation of p53 and Rb pathways. Results described here, suggest that the growth arrest is preceded or accompanied by deregulation of the cell cycle.

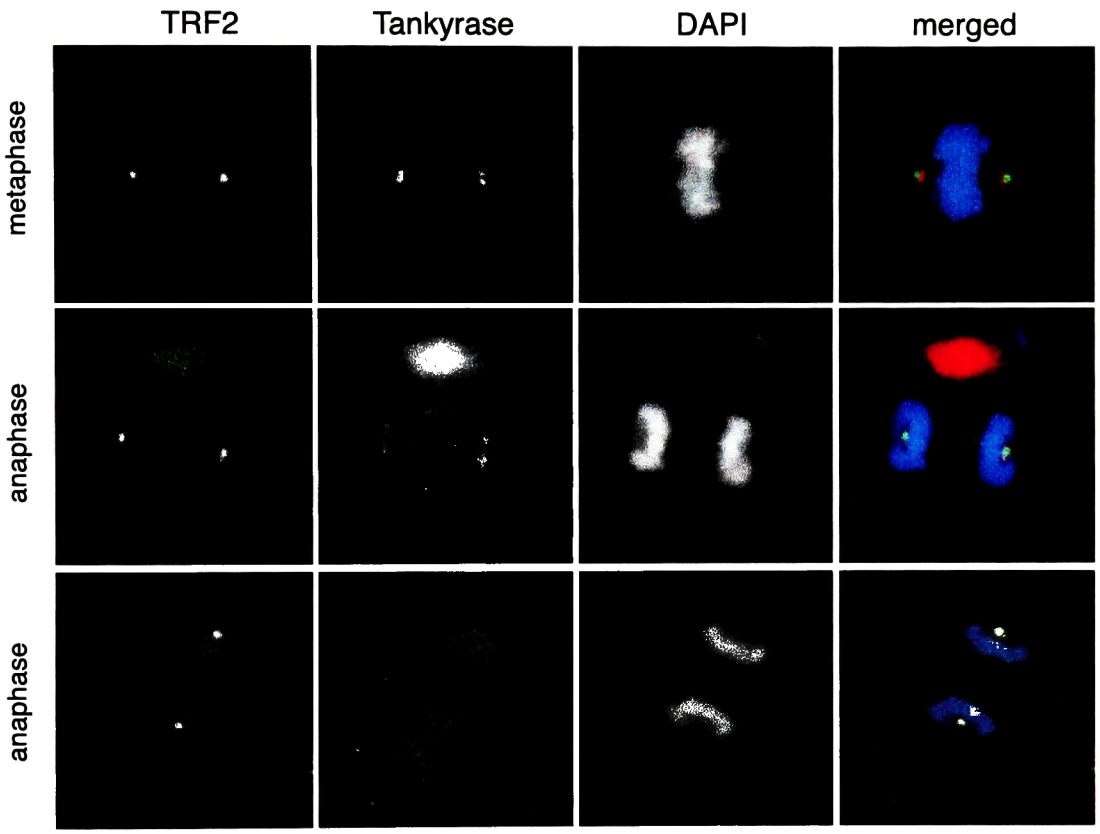

Figure 5-5. **Localization of TRF2 and tankyrase to centrosomes in HeLaI.2.11 cells.** Indirect immuofluorescence with rabbit α TRF2 (#647) and mouse α tankyrase. HeLaI.2.11 were fixed in methanol and costained with the indicated. FITC-conjugated α rabbit and TRITC α mouse secondary antibodies were used to visualize the primary antibodies. DNA was counterstained ith DAPI. Cells at different stages of mitosis are shown as indicated on the left.

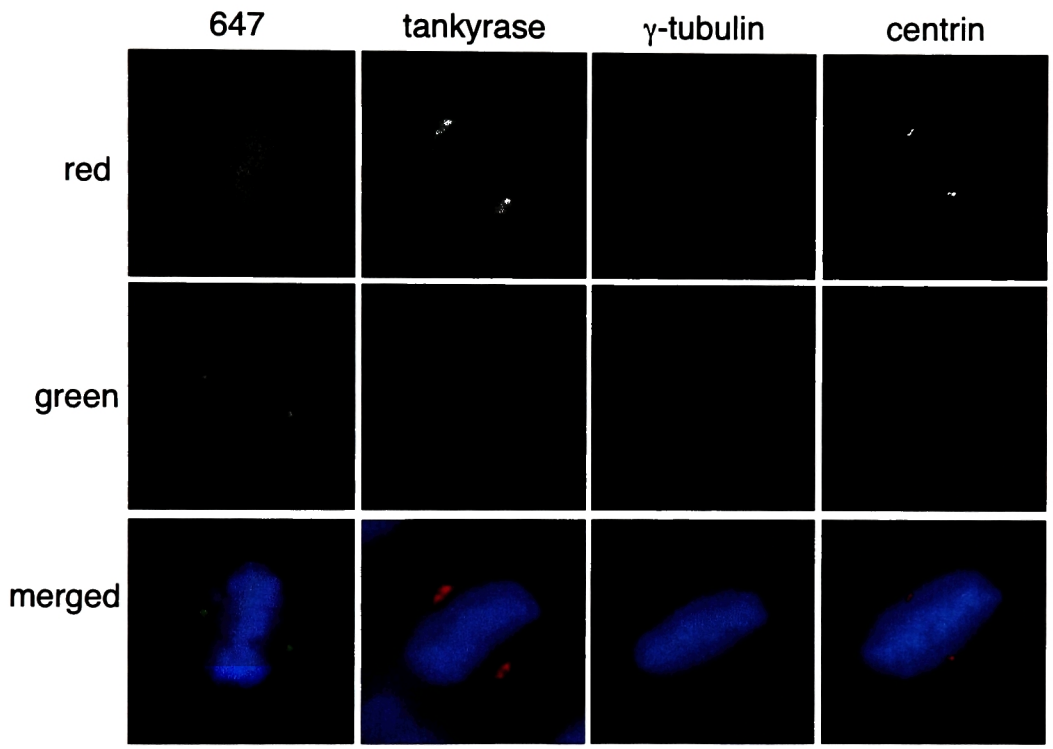

Figure 5-6. **Staining of centrosomes with 647, tankyrase, γ-tubulin, and centrin in HeLaI.2.11 cells.** Indirect immuofluorescence with rabbit α TRF2 (647), mouse α tankyrase, mouse α γ-tubulin, and mouse α centrin. HeLaI.2.11 were fixed in methanol and stained separately with the indicated antibody. FITC-conjugated α rabbit and TRITC α mouse secondary antibodies were used to visualize the primary antibodies. Green and red channels were both exposed for 0.2 s with 100% gain as a control for the bleed-through of the signal into the other channel.

Frequent arrangement of duplicated chromosomes in diplochromosomes implies that the events leading to the reduplication occurred in the same cell cycle (Figure 5-7). The reasons for reduplication of the genome are unclear at this point. As described in the introduction, expression of p53 should preclude any DNA or centrosomal reduplication. However, presence of an increased numbers of centrosomes in senescent cells might indicate that telomere dysfunction somehow triggers the reduplication in spite of high p53 expression. Expression of $TRF2^{\Delta B\Delta M}$ and $TRF2^{\Delta B}$ also gives rise to telomere dysfunction and because the events are fairly synchronized, the reduplication can be visualized to occur within one cell cycle. It remains to be explored if cells that are undergoing reduplication, and presumably characterized by high CyclinE-Cdk2 activity, also have high p53 levels.

The events leading to reduplication might be suggested by a finding of premature chromosome division on metaphases of $TRF2^{\Delta B\Delta M}$ and $TRF2^{\Delta B}$-expressing cells observed in one experiment (Figure 5-2). Normally, cohesion between sister chromatids is established during S phase of the cell cycle and persists until prophase of the M phase along the chromosomal arms, or until the metaphase to anaphase transition in the centromeric region. Observation of premature separation of centromere regions suggests that the cohesion has prematurely failed. These results were obtained by observing metaphase spreads that were prepared by arresting cells for 12 hours in colcemid. It could be argued that the centromere separation was an artifact of this prolonged colcemid treatment; however, the control and FLTRF2-expressing cells did not show this phenotype. This argues that presence of $TRF2^{\Delta B\Delta M}$ and $TRF2^{\Delta B}$, although not necessarily directly, might predispose cells to premature centromere division. If such a cell were to return to a G1 like state without undergoing anaphase and were allowed to

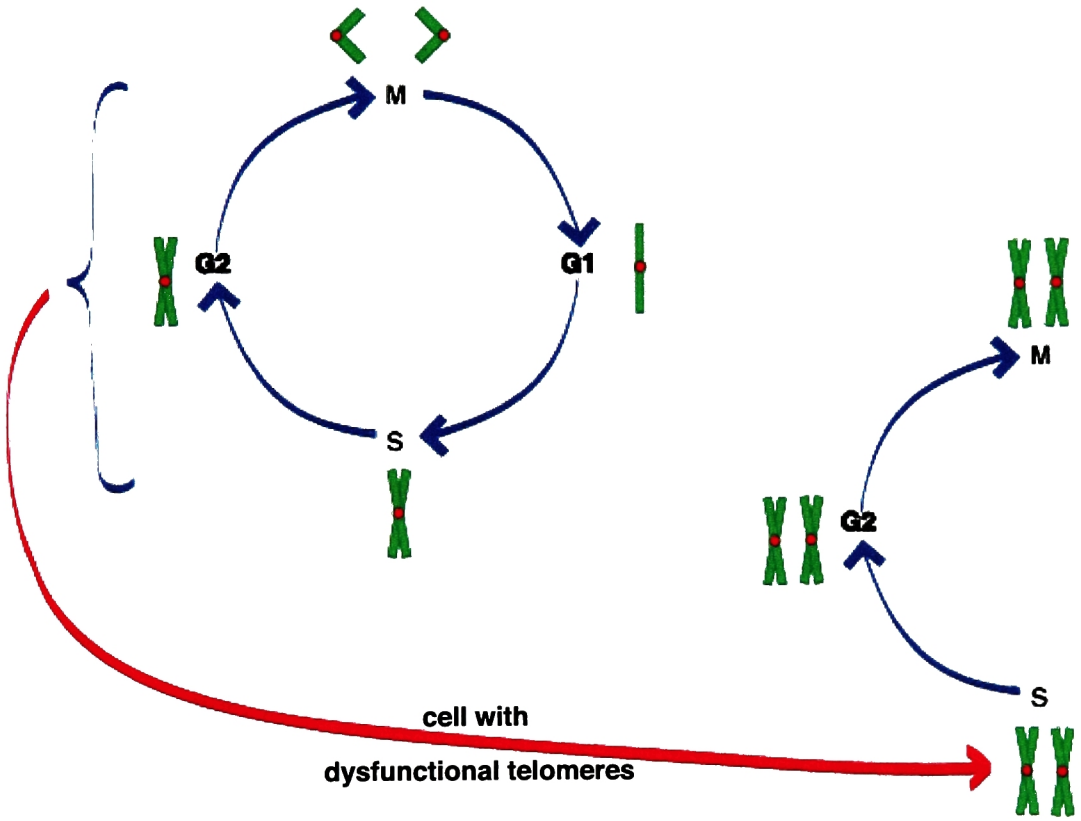

Figure 5-7. **Model of reduplication of the genome following telomere dysfunction** (see text for details).

undergo another round of DNA synthesis, the next metaphase would show diplochromosomes.

Presence of PCDs and diplochromosomes in metaphase cells might not be causally linked; however, they both suggest failure of the cohesion apparatus at some point in the cell cycle. Recent evidence suggests that a successful anaphase and cytokinesis require a proper dissolution of cohesion (Stratmann and Lehner 1996; Hauf et al. 2001). Expression of the non-cleavable SCC1, a component of the cohesion complex, which is cleaved at the onset of anaphase to relieve sister chromatid cohesion, results in inappropriate dissociation between progression of cytokinesis and progression of cyclin-driven cell cycle. This is documented by observation that cells expressing the non-cleavable SCC1 frequently exit mitosis and enter interphase without undergoing anaphase. These events result in formation of polyploid cells, some of them characterized by the presence of diplochromosomes (Hauf et al. 2001). It is interesting to speculate that the diplochromosome formation in cells that failed cohesion and cells expressing mutant forms of TRF2 might be related. It is possible that without proper telomere function, cohesion cannot be properly regulated. Further study of influence of telomere status on establishment and dissolution of cohesion will be necessary to understand the connection if there is any.

Another question is whether the reduplicated centrosomes are functional in making multiple spindles during subsequent anaphase. Anaphases with tri-polar spindles were not observed in the populations expressing $TRF2^{\Delta B\Delta M}$ and $TRF2^{\Delta B}$, which suggests that cells with reduplicated centrosomes were already arrested, or that centrosomes once reduplicated stayed together allowing for normal spindle formation. It is known that even cells without functional p53, which have multiple centrosomes, are

able to form normal bipolar spindles most of the time (Ring et al. 1982; Fukasawa et al. 1996).

The observation of the presence of TRF2 on centrosomes is also unexpected. It must be stressed that although reduplication of the genome and centrosomal localization of TRF2 are discussed in the same chapter, the two occurrences are not yet shown to be related in any way.

Currently, it is not clear what function telomeric proteins could have at centrosomes. Another telomeric protein, tankyrase, also localizes to centrosomes and its function is also unknown. The most pressing question about the presence of TRF2 at centrosomes is whether $TRF2^{\Delta B \Delta M}$ and $TRF2^{\Delta B}$ localize to centrosomes. It would be surprising if the Myb domain was necessary for the localization, since after a long debate it is currently clear that there is no nucleic acid at the centrosome (Marshall and Rosenbaum 2000). It is at this point also unknown, if $TRF2^{\Delta B \Delta M}$ removes the endogenous TRF2 from centrosomes. It is very hard to observe overexpressed TRF2 on centrosomes using immunofluorescence staining. A better approach will be to look if Rap1, a TRF2 binding partner, is present at centrosomes when different alleles are expressed. To avoid a titration effect; however, TRF2 will have to be engineered to be deficient for the Rap1 interaction domain. Also, the presence of all other telomeric proteins on centrosomes needs to be explored. With the finding of TRF2 and Tankyrase at centrosomes it is possible that the whole telomeric complex is also present there.

The presence of TRF2 on centrosomes might be important for meiosis. In many species telomeres form the so-called bouquet by juxtaposing their telomeres against the meiotic centrosome (reviewed in Scherthan 2001). There is some evidence that such an arrangement aids in the alignment of homologous chromosomes prior to recombination.

In *S.pombe*, Taz1, an ortholog of TRF proteins in mammalian cells, is responsible for the association of telomeres with a spindle pole body (SPB), a yeast equivalent of the centrosome. Lack of Taz1 leads to dissolution of the association between the SPB and the telomere, leading to failed alignment and unsuccessful meiosis (Nimmo et al. 1998). It will be interesting to learn how Taz1 is anchored to the SPB. Such knowledge might shed light on how TRF2 localizes to centrosomes.

Concluding Remarks

This thesis has concentrated on exploring the function of TRF2 in human cells. TRF2 was cloned by Dominique Broccoli and myself based on homology to the Myb domain of TRF1, the first human telomeric protein. Functional analysis has pointed out that despite high homology in the Myb domain as well as in the TRFH domain, TRF1 and TRF2 have completely divergent roles at telomeres.

As described in detail in the introduction, the main function of the telomere in all species is to protect the chromosome end from being recognized as a double-stranded break. Although the mechanisms might not be fully understood yet, it is now clear that TRF2 is able to supply this protective function to human telomeres. Deprotection after removal of TRF2 was observed in multiple human and mouse cell lines including a tumor cell line (HTC75), human primary fibroblasts (IMR90, BJ), and MEFs. Inhibition of TRF2 function led to appearance of end-to-end fusions visible in anaphase and metaphase cells. It was deduced that prior to fusion, the deprotected chromosome lost a single-stranded G-overhang, but not the double-stranded TTAGGG repeat array and the fusions were formed through a covalent ligation of the DNA strands. DNA ligase IV was responsible for the ligation since MEFs deficient in this ligase were also deficient in fusion formation. Division with deprotected telomeres led to induction of genomic instability visualized mainly as translocations.

TRF2 most likely protects telomeres by stimulating formation or stabilization of t-loops at chromosome ends. T-loops, in turn, are thought to conceal the very end of the telomere. The protective function of TRF2 has been uncovered using a dominant negative allele TRF2$^{\Delta B \Delta M}$. Expression of TRF2$^{\Delta B \Delta M}$ efficiently removes endogenous TRF2 from telomeres as evidenced by using immunofluorescent staining; however, it is impossible to say how complete this dominant negative effect is and some telomeres

may contain residual TRF2. Therefore, cells null for the protein might exhibit an even more dramatic telomere deprotection phenotype. Based on the phenotype of the $TRF2^{\Delta B\Delta M}$-expressing cells, it is very likely that a mouse deficient in TRF2 might not be able to develop properly. Thus, a conditional KO system needs to be employed to examine the null phenotype of TRF2 in a true *in vivo* mouse system or in mouse embryonic stem (ES) cells.

The deprotection phenotype observed in cells expressing $TRF2^{\Delta B\Delta M}$ was characterized by persistence of the double-stranded telomeric DNA. It is interesting to compare this phenotype to deprotection phenotypes seen in other organisms. Lack of Cdc13p leads to rapid degradation of the C-strand of the telomere in *S. cerevisiae*, whether as deficiency of Pot1 in *S.pombe* results in rapid degradation of both the C and the G strands of the telomere. Why is it that a telomere devoid of TRF2 seems to be inert towards the degradation processes? One possibility is that TRF2 is needed to anchor the degradative machinery to the telomere. Thus, without TRF2 being present at the telomere when $TRF2^{\Delta B\Delta M}$ is expressed, the proteins responsible for the degradation cannot be recruited there either. This results in maintenance of the double-stranded telomeric DNA.

Although TRF2 is shown to be a crucial protective agent at the telomere, its activity does not exclude other protective factors acting in concert or in parallel pathways to protect the end. An excellent candidate for such an activity is the newly-discovered hPot1, an ortholog of *S. pombe* Pot1, lack of which leads to clear telomere deprotection in fission yeast (Baumann and Cech 2001). Since the human protein has biochemical activities of a single-stranded binding protein with specificity for the TTAGGG repeats, it might protect the G-overhang at specific times in the cell cycle when the t-loop needs to

be dissolved, for example during the replication process. Alternatively, hPot1 could bind to the single-stranded DNA in the D-loop, which has been shown to be present at the base of the t-loop (Griffith et al. 1999). The distinction between the two possibilities might be made using electron microscopy, as well as the immunofluorescent approach. It will be also essential to know if the presence of Pot1 on telomeres depends on the TRF2. This might be done by inspection of telomeric localization of Pot1 in the cell lines expressing $TRF2^{\Delta B\Delta M}$ or $TRF2^{\Delta B}$. Based on the finding that the deficiency of Pot1 in *S. pombe* leads to the degradation of the double stranded telomeric DNA, one could speculate that the removal of human Pot1 would also result in such event. However, it is also possible that the lack of Pot1 will result in phenotypes that resemble the phenotypes of $TRF2^{\Delta B\Delta M}$ or $TRF2^{\Delta B}$–expressing cells. Overall, the chromosomal events leading to the deprotection after Pot1 removal might be more easily studied in human cells than in the yeast cells.

More biochemical analysis of TRF2 will be necessary to fully understand how the presence of this protein leads to formation or stabilization of the t-loops. Although current knowledge suggests that TRF2 forms homo-oligomers and not dimers like TRF1, it is not clear at this point how such oligomers might form. The crystal structure of the whole protein might aid in answering this question. Moreover, study of the binding partners of TRF2 and their participation in t-loop formation and resolution will be also necessary to fully understand how the protected state is achieved and maintained at the telomere throughout the cell cycle.

The dynamics of the t-loop formation and dissolution throughout the cell cycle need to be studied in detail. One of the times that t-loops need to be dissolved is in S phase. TRF2 does not seem to be differentially regulated at any stage of the cell cycle

(Karlseder, J. and de Lange, T., unpublished); however, one of the components of the TRF2 complex, NBS is differentially regulated. Arrival of NBS at telomeres coincides with S phase (Zhu et al. 2000), and it is possible that this changes the activity of the Mre11 complex and subsequently results in opening of the t-loop.

Deprotection of telomeres by expression of $TRF2^{\Delta B \Delta M}$ allele led to inhibition of growth in human primary fibroblasts. Induction of growth arrest was dependent on the activities of the p53 and the Rb pathways, but it did not depend on the activity of the ATM kinase. The genetic requirements for the arrest are thus unlike the ones observed for the induction of apoptosis after TRF2 inhibition. Entry into apoptosis requires function of the ATM kinase and the p53 protein and does not involve the Rb pathway (Karlseder et al. 1999).

It is clear that some cells are predisposed to react to damage by apoptosis and some by growth arrest (Di Leonardo et al. 1994; Yeargin and Haas 1995); however, such discrepancy in the signaling pathways into arrest or apoptosis is curious. It is possible that apoptosis response requires a very strong activation of the checkpoint and that ATM pathway is necessary for the achievement of the necessary strength. When it is absent, other proteins are able to substitute some of the activity; however, they might be unable to reach a level of function normally supplied by the ATM kinase. This results in lack of apoptosis and presumed growth arrest. In cells that normally do not undergo apoptosis (for example human fibroblasts) signaling through the substitute kinases is enough for induction of the arrest.

Another possibility is that the kinetic requirements of activation of apoptosis and arrest are different. Induction of apoptosis is usually a fast event. This event depends on p53 and most likely the downstream effectors like Bax (Miyashita et al. 1994). The

p16 induction, which seems to play a role in the growth arrest, is induced more slowly (Robles and Adami 1998). The proposal is that once the Rb pathway is induced, apoptosis is averted and the growth arrest ensues. This hypothesis can be restated to suggest that the growth arrest is a dominant response. However, because it is induced slowly, it might be defeated by the apoptotic response, which would remove the cells before they could arrest. One prediction of this hypothesis would be that the simultaneous and fast induction of the Rb pathway together with the generation of damage that normally would lead to apoptosis would result in inhibition of the apoptotic response and lead to growth arrest.

High similarity of $TRF2^{\Delta B\Delta M}$-induced growth arrest and growth arrest naturally occurring at the end of the replicative life-span of human primary fibroblasts has led to a proposal that critically short telomeres existing in pre-senescent human primary cells might be unable to recruit sufficient TRF2, resulting in signaling into arrest. As discussed in Chapter 2, the pathways leading to senescence are not very well defined at this point and further studies delineating the requirements for the growth arrest after $TRF2^{\Delta B\Delta M}$ expression might be useful in understanding telomere directed senescence.

Besides protecting the telomere and guarding against premature senescence of human primary cells, TRF2 is also clearly involved in telomere length regulation. Expression of TRF2 leads to telomere shortening and telomere length changes do not depend on the presence of telomerase. Thus TRF2 appears to control the shortening activities at the telomere. There are a number of ways TRF2 might be able to influence the telomere shortening. TRF2 might be able to regulate nucleases involved in telomere shortening or it could influence the shortening rate by affecting the replication through the terminus. The first proposal is highly testable once the putative nucleases are

known. Based on the telomere loss phenotype after expression of the TRF2$^{\Delta B}$, it was proposed that a factor interacting with the basic domain could be involved in the regulation of the putative nuclease. Discovery of this putative factor should lead to elucidation of the mechanism of how TRF2 affects the shortening rate of the telomeres.

The ability of TRF2 to influence telomere shortening does not exclude the possibility that this molecule is also responsible for recruitment of the regulators of telomere elongation. Based on the current data, it is actually very likely that TRF2, through its interacting partner Rap1, is able to influence telomere elongation. Direct studies of Rap1, will clarify the role of the TRF2 complex in regulation of telomere lengthening activities.

The basic domain was shown to be important for the proper function of TRF2 at telomeres. It has been proposed that this domain functions through interacting with yet unknown factors. Knowledge of these proteins will be important to fully understand the phenotypes of rapid telomere deletion and chromosome breakage in cells expressing TRF2$^{\Delta B}$. Studies of such a factor will be also necessary to show whether TRF2$^{\Delta B}$ is a hypomorphic or a gain of function allele of TRF2. The two phenotypes observed in TRF2$^{\Delta B}$-expressing cells are proposed to be created through the same mechanism, in which a nick followed by replication results in telomere deletion or internal breakage. However, through further studies it may be revealed that the two phenotypes occur through different mechanisms. Finally, it is interesting to point out that the TRF2$^{\Delta B}$-expressing cells have some characteristics of harboring deprotected telomeres and it remains to be seen it this deprotection is caused by loss of telomeric DNA.

The intriguing possibility that telomere dysfunction can lead to deregulation of the cell cycle even in otherwise wild type cells was suggested by genome wide reduplication

observed in cells expressing TRF2$^{\Delta B\Delta M}$ and TRF2$^{\Delta B}$ and in cells with critically shortened telomeres. The reasons for a connection between telomere status and entry into S phase are not obvious. These phenotypes as well as the centrosomal localization of TRF2 suggest that the telomeric complex may have an unanticipated role in regulating the centrosomal cycle.

Overall, studies of the human telomeric protein TRF2 have increased our understanding of the telomere function. Studies in human cells with their beautiful, condensed chromosomes have resulted in the detailed examination of the outcomes of telomere dysfunction. Ability to observe chromosomes and telomeres directly gave an opportunity to find telomeric DNA at the sites of end-to-end fusions after inhibition of TRF2 and allowed for observation of single chromatid deletions after expression of TRF2$^{\Delta B}$. Such ability, in combination with molecular techniques currently available, including the retroviral delivery of genes and the KO model systems, make mammals a very powerful addition to the traditional organisms of *Tetrahymena* or yeasts utilized to study telomeric complexes.

Materials and Methods

Cell culture:

Primary cells. Human primary fibroblasts IMR90, WI38, HS68, and packaging cells (PhoenixEco and Ampho) were obtained from the ATCC. They were grown in Dulbecco Modified Eagle medium (DMEM) supplemented with 100 units of penicillin per ml, 0.1 mg streptomycin per ml, L-glutamine (2 mM), non-essential amino acids (0.1 mM), and 15% (v/v) FBS (Hyclone) for primary cells or 10% (v/v) FBS for packaging cells. Fibroblasts from Ataxia Telangiectasia (A-T) patients (AG02496, AG04405, AG03058) and controls (AG03057) were obtained from Coriell Cell Repositories and cultivated as above, except that the media contained 20% (v/v) of FBS.

Cells were passaged by treatment with trypsin and seeding at $1x10^6$ cells per 10 cm dish. Cell numbers were determined by counting a 1:20 dilution of the cell suspension using a Coulter Counter. Population doublings were determined by a formula: $PD=PD_{\text{at plating}}+[\ln(\#\text{ of harvested cells}/\#\text{ of plated cells})/\ln(2)]$. For freezing, logarithmically growing cells were collected from a 15 cm plate (around $7x10^6$ cells) were resuspended in 1 ml of 2xA freezing media (2xA is made by combining 40 ml FBS [Hyclone], 0.4 ml gentamycin stock solution [stock solution is 50 mg/ ml gentamycin, Sigma], 4 ml HEPES stock solution [stock solution is 1M HEPES, {pH 7.6}], and 156 ml L15 media [Sigma], and sterilization through a 0.2 μm filter). Subsequently 1 ml of 2xD freezing media were added (2xD is made by combining 40 ml PVP stock solution [stock solution is 100 mg PVP [Sigma #P2307] per ml of HEPES buffered saline],.30 ml DMSO [Sigma], 4 ml HEPES stock solution [stock solution is 1M HEPES, {pH 7.6}], and 126 ml L15 media [Sigma], and sterilization through a 0.2 μm filter) and the cell suspension was aliquoted into 2 cryogenic vials. The vials were placed in a Styrofoam box at –80°C.

After at least one day, but no more than 3 months, the cells were moved to liquid nitrogen.

HTC75 and its derivatives. HTC75 is a hygromycin-resistant HT1080-derived clonal cell line that stably expresses the tetracyclin-controlled transfected activator (tTA) (Gossen and Bujard 1992; van Steensel and de Lange 1997). Cells were grown in DMEM supplemented with 10% (v/v) bovine calf serum free of Tetracyclin or its derivatives (HyClone), penicillin-streptomycin, L-glutamine, non-essential amino acids and either Hygromycin (90 μg/ml) or G418 (150 μg/ml). Drugs were alternated every other week. Cells were passaged at 1:16 when they reached 80% confluence. Non-induced and induced cells were grown in parallel with or without doxycycline (Sigma, 100 ng/ml). After induction, P12, P33, P4, and P7 cell lines expressed untagged full-length TRF2; T4, T19, and T22 cell lines expressed myc-tagged $TRF2^{\Delta B\Delta M}$; S13 and S19 cell lines expressed flag-tagged $TRF2^{\Delta B}$, and B27 did not express any exogenous proteins and served as control.

Mouse cells. Primary Lig4+/+p53-/- and Lig4-/- p53-/- MEFs were obtained from the Alt laboratory (Frank et al. 2000). They were grown in DMEM supplemented with 10% (v/v) fetal calf serum, non-essential amino acids, glutamine, and antibiotics. Early passage (p3 for experiment #1 and p5 for experiment #2) cells were used for infections.

Other cells. Hela I.2.11 and HeLa 2 were grown in DMEM supplemented with penicillin-streptomycin, L-glutamine, non-essential amino acids, and 10% (v/v) bovine calf serum (HyClone).

Plasmids and retroviral vectors

Standard techniques were used for cloning. TRF2 constructs were generated by PCR from a full-length cDNA clone (clone 16-1, (Broccoli et al. 1997)). The pUHD 10-3 Tet-vector was used to clone TRF2 alleles for transfection into HTC75 cells. pBabepuro, pLPCpuro, and pWZLhygro (gifts from Scott Lowe, CSHL) were used to clone N-terminally myc tagged and untagged alleles of TRF2. The untagged versions were used in most of the experiments and there were no expression level or phenotypic differences between infections with the three different vectors. pBabeTag was a gift from Greg Hannon and did not express SV40 small T antigen. PLXSNeoHPV16E6, pLXSNeoHPV16E7, and pLXSNeoHPV16E6E7 (Halbert et al. 1991),(Kiyono et al. 1998) were gifts from Denise Galloway, and pWZLp53^{175H} mutant (p53DN) from Scott Lowe (Serrano et al. 1997).

Stable transfections of HTC75 cells (performed by Bas van Steensel)

The empty vector pUHD10-3 and the pUHD10-3-derived constructs for expression of the TRF2 alleles were each cotransfected with neomycin resistance plasmid pNY-HI (H. Tommerup and T. d. L., unpublished data) into cell line HTC75 using the calcium phosphate coprecipitation. Transfected cells were grown in the presence of doxycyclin (100 ng/ml) and G418 (600μg/ml). For each construct, approximately 25 G418-resistant cell lines were isolated by ring cloning and tested for expression of TRF2 polypeptides after 24 hr of induction by omission of doxycyclin from the media (doxycyclin acts as a repressor of gene expression in this system). Expression of TRF2$^{\Delta B\Delta M}$ and TRF2$^{\Delta B}$ was determined by immunofluorescence microscopy and western blotting using anti-FLAG antibody M2 (Eastman Kodak or Sigma); expression of wild-type TRF2 was determined

by gelshift assays using a TTAGGG-repeat probe and by western blotting using antibody 508 or 647.

Retroviral infections

Procedures were as described (Serrano et al. 1997). Phoenix cells were plated at $5x10^6$ cells per 10 cm plate and transfected on the following day using calcium phosphate precipitation in the presence of 100 μM chloroquine per ml. For the transfection, 20 μg of DNA prepared by the CsCl method were combined with 62.5 μl of 2 M $CaCl_2$ and sterile water to 500μl and added dropwise into 500μl of 2xHBS (50 mM HEPES [pH 7.05], 10 mM KCl, 12 mM Dextrose, 280 mM NaCl, 1.5 mM Na_2HPO_4) while making bubbles. This solution was added directly to plates already containing 8 ml of media with chloroquine. The media were replaced with fresh 8 ml of media without chloroquine after 5 hours and replaced with 6 ml of media approximately 12 hours later. Media containing retroviral particles were collected for two days (30 ml total- first collection 6 ml, subsequent collections, 4 ml each) starting 24 hours after transfection and kept on ice in the cold room. The supernatant was not spinned prior to filtering into a new tube through a 0.45 μm filter. To avoid contamination with the packaging cells, a fresh cap was used to close the conical tube with the filtered supernatant. The supernatant was supplemented with 3 ml of FBS and 4 μg polybrene per ml and used for three infections (every 5 hours) of a 15 cm plate of fibroblasts plated the day before at $2.5x10^6$ cells per plate. The following evening cells were placed under selection with 2 μg of puromycin per ml, 90 μg of hygromycin per ml, or 600 μg of G418 per ml, depending on the vector used. Selection was completed after 3 days for puromycin, 5

days for hygromycin, and 2 weeks for G418 treatment. Expression of proteins after selection was confirmed by immunofluorescence or western blotting.

Transient transfection by electroporation

$8x10^6$ logarithmically growing cells were resuspended in 800 µl of transfection buffer (21 mM Hepes [pH 7.05], 137 mM NaCl, 0.7 mM Na_2HPO_4, 5 mM KCl, 6 mM glucose) and mixed with 15 µg of plasmid in an electroporation cuvette. Cells were electroporated at 300 mV with 960 µF capacitance. The time constant was between 10 and 13 miliseconds. The debris was removed with a pipette tip and one-third of the remaining cells were added to a 10 cm dish with media overlaying autoclaved coverslips for immunofluorescence. For protein extractions two-thirds of the cells were plated in a 10 cm dish with appropriate media. All transient transfections were analyzed after 24 hours.

Growth curves and BrdU labeling

On the 4th day of puromycin selection following retroviral infection, for each day of the growth curve, cells were plated in duplicate at $3x10^4$ cells per well in a six-well plate. On the subsequent days, the cells were washed, trypsinized and counted using a Coulter counter. For BrdU labeling, the method was adapted from the in situ cell proliferation kit (Roche), (Gratzner 1982). One day prior to labeling (day 4, 9, and 14), cells were plated on autoclaved coverslips at $1x10^5$ cells per well of a six-well plate in total of 3 ml of media. 24 hours later BrdU (Roche) was added to a final concentration of 10 µM (from a 100 µM stock made in media) without replacing the original media. After

an 1 hour incubation (or a 5 hour incubation for the A-T cells), the coverslips were washed once with PBS, fixed in 70% (v/v) ethanol in 50 mM glycine buffer (pH 2.0) for 45 minutes at room temperature, washed twice in PBS, denatured for 10 min in cold (4°C) 4 N HCl, washed 3 times in PBS 5 min each, and blocked in PBG (0.2% [w/v] Cold Water Fish Gelatin [Sigma], 0.5% [w/v] BSA [Sigma] in PBS). This was followed by a 2 hour incubation with affinity purified antibody 647 against TRF2 (Zhu et al. 2000) diluted 1:1000-1:2000 in PBG, three 5 minute washes each in PBG and a 45 minute incubation with a TRITC-conjugated donkey anti-rabbit secondary antibody (Jackson) at 1:100 dilution in PBG and FITC anti-BrdU antibody (Becton Dickinson) at 1:4 dilution in PBG. Following a 5 minute wash in PBG, 5 minute wash in PBG supplemented with 0.2 μg of DAPI per ml, another 5 minute wash with PBG, and a rinse with PBS, coverslips were embedded in 90% (v/v) glycerol/10% (v/v) PBS containing 1 mg p-phenylene diamine (Sigma) per ml and sealed with nail polish. Such dual labeling allowed scoring for BrdU positive cells that were also expressing TRF2 alleles of interest. The numbers were normalized using the formula: (% of BrdU positive cells in TRF2 or $TRF2^{\Delta B \Delta M}$-expressing cells/ % of BrdU positive cells in control vector cells) x100%.

Fluorescence activated cell sorting (FACS) analysis

Cells were collected from a 10 cm plate by trypsinization, spun down at 1000 rpm, washed in 5 ml PBS, spun down again and resuspended in 100 μl of phosphate buffered saline (PBS). While vortexing, 2 ml of ice cold 70% (v/v) ethanol were added dropwise and the suspension was stored at 4°C at least overnight. 30 min before FACS, the cells were spun down and resuspended in propidium iodine (PI) mix (500 μl PBS, 10 μl RNase [of stock solution of 10 mg/ml], 25 μl PI [of stock solution of 1 mg/ml]), and

incubated for 30 min at 37°C before analyzing on a Becton Dickinson FACS-SCAN II. Analysis was done without gating.

β-gal assay

The procedure used was adapted from (Dimri et al. 1995). Cells were plated in 2 well chamber glass slides (Lab-Tek. #177380) at a density of 1-3X10^4 cells per chamber. On the second or third day after plating, the cells were washed in phosphate-buffered saline (PBS) (pH 7.2), fixed for 5 min in 2% (v/v) formaldehyde/0.2% (v/v) glutaraldehyde solution in PBS , washed again in PBS, and stained with 1 mg X-gal per ml of 150 mM NaCl, 2 mM $MgCl_2$, 5 mM $K_3Fe(CN)_6$, 5 mM $K_4Fe(CN)_6$, and 40 mM NaPi (pH 6.0, pH 4.0 or pH 7.0) for 6–12 hr at 37°C.

Immunofluorescence and microscopy

Cells were plated at a density of 1x10^6 in a 10 cm plate on autoclaved coverslips. In preparation for immunofluorescence they were rinsed with phosphate-buffered-saline (PBS) and fixed in 2% (w/v) formaldehyde in PBS for 10 minutes at room temperature, or in ice-cold methanol for 10 minutes at -20°C. If the cells were fixed with formaldehyde, they were washed once with PBS, permeabilized in 0.5% (v/v) NP40 in PBS for 10 minutes, washed again in PBS, and incubated with PBG (0.2% [w/v] cold fish gelatin, 0.5% [w/v] BSA in PBS) for 20 minutes to block non-specific binding. If cells were fixed in methanol, no permeabilization was necessary, and cells were washed 3 times for 5 minutes each in PBS and incubated with PBG for 20 minutes. Coverslips were then incubated for 2 hours at room temperature in a humidified chamber with a

primary antibody appropriately diluted in PBG (dilutions were highly dependent on the antibody but typically they were around 1-500 to 1:2000 for polyclonal anti TRF1 and 2 antibodies, and 1:20 for monoclonal anti p53 and Tag antibodies). Subsequently, coverslips were washed 3 times 5 minutes each with PBG, and incubated with FITC or TRITC conjugated sheep-anti-mouse or donkey-anti-rabbit antibodies (Jackson) diluted 1:100 in PBG. Following a 5 minute wash in PBG, 5 minute wash in PBG supplemented with 0.2 μg of DAPI per ml, another 5 minute wash with PBG, and a rinse with PBS, coverslips were embedded in 90% (v/v) glycerol/10% (v/v) PBS containing 1 mg p-phenylene diamine (Sigma) per ml and sealed with nail polish. Pictures were taken on an Axioplan Zeiss microscope with a Photometrics digital camera or on an Axioplan2 Zeiss microscope with a Hamamatsu digital camera supported by OpenLab software.

Methanol: glacial acidic acid metaphase spreads

Cells grown to ~50-70% confluence in a 15 cm dish were incubated in 0.1 μg of demecolcin per ml of medium for 90 min to 4 hr depending on the experiment. Cells were harvested by trypsinization, and spun down at 1000 rpm for 5 minutes. Sometimes, in order to enrich for mitotic cells, just after addition of trypsin plates were hit hard on the side and the detached cells were collected and spun down as above. The supernatant was completely removed and cells were gently resuspended in 5 ml of 0.075 M KCl. After 7 minutes of incubation at 37°C, the cells were again spun down at 1000 rpm for 5 minutes and the supernatant was decanted. The cells were gently resuspended in the remaining fluid by tapping. 1 ml of freshly prepared fixative (3:1 [vol/vol] methanol: glacial acidic acid) was added dropwise to the cells while the tube was being tapped. The tube was filled up with fixative and stored overnight or longer

before dropping cells onto slides. When ready to prepare spreads, the cells were spun down at 1000 rpm for 5 minutes and the supernatant was replaced with approximately 500 µl of fresh fixative (this volume was adjusted to achieve a slightly cloudy suspension). The cells were dropped on the (room-temperature) water-wetted slide, air dried for a couple of seconds, washed with fresh fixative, and placed for about a minute on water-soaked paper towels positioned on a heat block warmed to 70-80°C. If spreads were to be used for fluorescence in-situ hybridization (FISH) they were left overnight in a chemical hood to age and used at that point or stored at 4° for later use. For staining of chromosomes with 4',6'-diamidino-2-phenylindole (DAPI), without FISH, cells were used immediately without aging. Slides were incubate for 5 minutes in 0.2 µg of DAPI per ml of phosphate-buffered saline (PBS), washed in PBS, and embedded in 90% (v/v) glycerol/10% (v/v) PBS containing 1 mg p-phenylene diamine (Sigma) per ml.

Formaldehyde metaphase spreads

The procedure was essentially as described in (Compton et al. 1991). Cells grown to ~50-70% confluence in a 15 cm dish were incubated in 0.1 µg of demecolcin per ml of medium for 90 min to 4 hr depending on the experiment. Cells were harvested by trypsinization, and spun down at 1000 rpm for 5 minutes. The supernatant was completely removed and cells were gently resuspended in 300 µl of RSB buffer (10 mM Tris-HCl, [pH 7.4], 10 mM NaCl, 5 mM $MgCl_2$) and incubated at 37°C for 10 minutes. 50 µl of this cell suspension was gently pipetted onto a 22 mm square coverslip at the bottom of a bucket of a RT6000 Sorvall tabletop centrifuge. The centrifuge was allowed to reach 3000 rpm and was immediately stopped. The coverslip was removed and cells spread on it were fixed with 2% (w/v) formaldehyde in PBS for 10 minutes, washed once

with PBS, permeabilized in 0.5% (v/v) NP40 in PBS for 10 minutes, washed again in PBS and used with a standard immunofluorescence protocol as described above.

Peptide nucleic acid (PNA) fluorescence in-situ hybridization (FISH) on metaphase spreads

The method was adapted from (Lansdorp et al. 1996). The slide with methanol:glacial acidic acid metaphase spreads (prepared as above) were rehydrated for 5 minutes in phosphate-buffered saline (PBS) (pH 7.4 throughout this procedure), fixed for 2 minutes in 4% (v/v) formaldehyde in PBS, washed 3 times for 5 minutes each in PBS, treated with 1 mg pepsin per ml of HCl acidified water (pH 2.0) for 10 minutes at 37°C, washed twice for 2 minutes each in PBS, fixed again in 4% (v/v) formaldehyde in PBS, washed 3 times for 5 minutes each in PBS, dehydrated in an alcohol series (5 minutes in 70% (v/v) ethanol, 5 minutes in 95% (v/v) ethanol, and 5 minutes in 100% (v/v) ethanol) and air-dried. A small amount (~50-100 µl) of a hybridization mix (10 mM Tris [pH 7.2], 70% (v/v) deionized formamide, 0.5% (w/v) blocking solution [Boehringer Mannheim], 0.5 µg Peptide-Nucleic Acid (PNA) probe per ml) was placed on the coverslip. The coverslip was then picked up by turning the slide upside down, touching the hybridization mix, and immediately turning the slide back up. This assured that there were no bubbles that would interfere with hybridization. The DNA was denatured by placing the slide at 80°C for 3 minutes, and the probe was allowed to hybridize for 2 hours in a humidified chamber at room temperature in the dark. Subsequently, the slide was washed 2 times, 15 minutes each in 10 mM Tris [pH 7.2], 70% (v/v) deionized formamide, 0.1% (w/v) BSA, washed 3 times 5 minutes each in 0.1 M Tris-HCl [pH 7.4], 0.15 M NaCl, 0.08% (v/v) Tween and dehydrated in an alcohol series as above. If the

PNA probe was FITC conjugated (FITC-CCCTAACCCTAACCCTAA, synthesized by Biotech GmbH) the DNA was counterstained with 4',6'-diamidino-2-phenylindole (DAPI) by adding 0.2 μg of DAPI per ml to a second 5 minute wash (see above), followed by washing for the third time, dehydration, air-drying and embedding in 90% (v/v) glycerol/10% (v/v) PBS containing 1 mg p-phenylene diamine (Sigma) per ml. If the PNA probe was biotynylated (bio-OO-CCCTAACCCTAACCCTAA, synthesized by PerSeptive Biosystems) the DNA was not counterstained at this point. After dehydration steps the slides were incubated with PBG (0.2% [w/v] cold fish gelatin, 0.5% [w/v] BSA in PBS) 2 times for 10 minutes each to block non-specific binding, and then incubated for 30 min at 37°C with fluorescein-conjugated avidin (AVIDIN DCS-FITC, Vectorlabs) diluted 1:400 in PBG. The slides were washed in PBG for 5 minutes, in PBG supplemented with 0.2 μg of DAPI per ml for 5 minutes, with PBG alone for 5 minutes, and with PBS for 5 minutes. Spreads were then embedded in 90% (v/v) glycerol/10% (v/v) PBS containing 1 mg p-phenylene diamine (Sigma) per ml and sealed with nail polish. Pictures were taken on Axioplan Zeiss microscope with a Photometrics digital camera or on Axioplan2 Zeiss microscope with a Hamamatsu digital camera supported by OpenLab software. Ambiguous abnormalities seen in the pictures were assessed directly under the microscope.

Multiplex fluorescence in situ hybridization (M-FISH) (performed by Anna Jauch in Heidelberg)

M-FISH was performed as described (Speicher et al. 1996; Eils et al. 1998) with minor modifications. Briefly, five pools of flow-sorted whole chromosome painting probes (kindly provided by Ferguson-Smith, Cambridge, UK) were amplified and labeled by

DOP-PCR using five different fluorochromes: FITC, Cy3, Cy3.5, Cy5, and Cy5.5, repectively. About 100 ng of each probe was precipitated in the presence of 30 μg Cot-1 DNA, dissolved in 10 μl hybridization mixture (15% (w/v) dextrane sulfate, 2xSSC) and hybridized for 48 hours. Microscopic evaluation was performed using a Leica DMRXA microscope (Leica, Wetzlar, Germany) equipped with a Sensys CCD camera (Photometrics, Tucson, AZ, USA) with a Kodak KAF 1400 chip. Images for each fluorochrome were acquired separately using highly specific filter sets (Chroma Technology Corp., Brattleboro, VT, USA) and processed using the Leica MCK software (Leica Microsystems Imaging Solutions Ltd., Cambridge, UK).

DNA extraction

The procedure was based on (de Lange 1992). Around $1x10^7$ cells were harvested by trypsinization on the indicated days, washed in cold PBS, collected by centrifugation, resuspended in 1 ml of TNE (10 mM Tris [pH 7.4], 100 mM NaCl, 10 mM EDTA) and squirted into 1 ml of TNES (10 mM Tris [pH 7.4], 10 mM EDTA, 100 mM NaCl, 1% (w/v) SDS) freshly supplemented with 100μg proteinase K per ml placed in a 15 ml phase lock heavy tube (Eppendorf) pre-spun as suggested by the manufacturer. After an overnight incubation at 37°C, the lysate was extracted with 2 ml of phenol: chloroform: isoamyl alcohol (25:24:1 [vol/vol/vol]), and the DNA in the aqueous fraction was precipitated by mixing the lysate with 2 ml iso-propanol and 0.22 ml 2 M NaAcetate (pH 5.2). The spooled DNA was added to 0.3 ml of TNE supplemented with 100 μg RNAse per ml, incubated for 30 min at 37°C, gently resuspended with a wide tip and incubated for 2 more hours at 37°C. 0.3 ml of TNES supplemented with 100 μg proteinase K per ml were added, and the incubation at 37°C was continued for another

hour. This DNA solution was extracted with 0.6 ml of phenol: chloroform: isoamyl alcohol (25:24:1 [vol/vol/vol]), and the DNA was precipitated by mixing the aqueous phase with 0.6 ml iso-propanol and 60 µl of 2 M NaAcetate (pH 5.2). The DNA was spooled and resuspended without shearing in 100 µl of TE (10 mM Tris HCl [pH 7.4], 0.1 mM EDTA). DNA was cleaved with a combination of HinfI and RsaI or MboI and AluI restriction enzymes as indicated in the text and quantified by fluorometry using Hoechst 33258.

DNA electrophoresis and Southern blots with a telomeric probe

The procedure was based on (de Lange et al. 1990). 1.5-3 µg of digested DNA was fractionated on a 0.7% (w/v) agarose gel in 0.5x Tris-borate- EDTA (TBE) in the presence of some ethidium bromide. During the run, the gel was photographed to check for equal loading of samples. After the run, the gel was photographed, soaked in 0.25 M HCl for 30 minutes, in denaturating solution (1.5 M NaCl, 0.5 M NaOH) twice for 30 minutes each, and in neutralizing solution (3 M NaCl, 0.5 M Tris-HCl, [pH 7.0]) twice for 30 minutes each, rinsed in 20x SSC (3 M NaCl, 0.3 M Sodium Citrate [pH 7.0] and blotted overnight in 20x SSC onto a nylon membrane (Hybond). Subsequently, the DNA was crosslinked to the membrane using UV, membrane was rinsed in water and was prehybridized in Church buffer (0.5 M $NaPO_4$, [pH 7.2], 1 mM EDTA [pH 8.0], 7% (w/v) SDS, 1% (w/v) BSA) for 45 min at 65ºC, hybridized overnight at 65°C with a telomeric probe prepared as described below, and washed 3 times 15 minutes each in Church wash (40 mM $NaPO_4$, [pH 7.2], 1 mM EDTA [pH 8.0], 1% (w/v) SDS). The membrane was exposed overnight on the phosphorimager. To make a telomeric probe, pSP73.Sty11 plasmid was digested with EcoRI, and the 800bp fragment corresponding

to the telomeric repeats was isolated using QIAEXII (Qiagen) and diluted to about 20 ng DNA per µl. To label the probe, 10µl of this insert were combined with 5 ng of $(CCCTAA)_3$ oligonucleotide in a total volume of 39 µl, boiled for 5 min, cooled down for one minute and mixed with 5 µl of 10xOLB (0.5 M Tris HCl [pH.6.8]. 0.1 M MgOAc, 1 mM DTT, 0.5 mg Bovine Serum Albumin per ml, 0.6 mM dATP, 0.6 mM dGTP, 0.6 mM dTTP), 5 µl of α-^{32}P -dCTP (3000 Ci/mmol), and 1 µl of Klenow polymerase. Labeling reaction was performed for 90 minutes at room temperature and was stopped by addition of 50 µl TES (10 mM Tris-HCl, 10 mM EDTA [pH 8.0], 0.1% (w/v) SDS), loaded onto a Sephasdex G-50 fine column made in a 3 ml syringe packed to the top with the resin, washed with 1000 µl of TES, eluted with 800 µl of TES, incubated at 100°C for 10 min, and added to 30 ml of Church buffer. The probe was filtered through a 0.2 µm syringe filter. Half of the probe was used for a 20 cm x 20 cm membrane.

In-gel G-overhang assay

The procedure was adapted from (Hemann and Greider 1999) with multiple changes. 5 µg of digested DNA was fractionated on a 0.7% (w/v) agarose gel in 0.5x Tris-borate-EDTA (TBE) in the presence of some ethidium bromide. During the run, the gel was photographed to check for equal loading of the samples. After the run, the gel was dried on two pieces of Whatman 3MM paper for 1 hour at 50°C with vacuum resulting in a paper-thin gel that could be treated like a membrane. The gel was removed from the paper by soaking it in water and without denaturing was prehybridized in Church buffer (0.5 M $NaPO_4$, [pH 7.2], 1 mM EDTA [pH 8.0], 7% (w/v) SDS, 1% (w/v) BSA) for 45 min at 55°C, hybridized overnight at 55°C with an oligonucleotide probe prepared as described below, and after hybridization washed 3 times 20 min each in 4x

SSC at room temperature. If there was a very high signal in the background, the gel was washed twice more, 20 minutes each in 4x SSC, and 0.1% (w/v) SDS at 57°C. The gel was exposed overnight in the phosphorimager cassette. Subsequently, the gel was denatured for 25 minutes in a denaturating solution (1.5 M NaCl, 0.5 M NaOH), neutralized for 25 min in a neutralizing solution (3 M NaCl, 0.5 M TrisHCl [pH 7.0]) and after rinsing with water and 45 min prehybridization at 55°C in Church buffer, hybridization was repeated using the same probe that was used for the hybridization with the native gel. The wash steps were identical to those given above for the native gel. To make a probe for the G-overhang, 50 ng of TELC oligonucleotide $(CCCTAA)_4$ or 50 ng of TELG oligonucleotide $(TTAGGG)_4$, which served as a strand-specificity control, were mixed with 1 µl of T4 polynucleotide kinase buffer (NEB), 2µl of water, 5 µl of ^{32}P-gamma-ATP (6000 Ci/mMol, 10 mCi/ml), and 1 µl of T4 polynucleotide kinase (NEB), and incubated at 37°C for 45 minutes. After adding 90 µl TES (10 mM Tris-HCl, 10 mM EDTA [pH 8.0], 0.1% (w/v) SDS), the reaction was loaded onto a Sephadex G-25 fine column made in a 3 ml syringe packed to the 3 ml mark with the resin. The column was washed with 700 µl of TES and the labeled oligonucleotide was eluted with 800 µl of TES and used after addition of 15 ml of Church buffer and filtering through a 0.2 µm filter. The same probe was used for hybridization with native and denaturing gels.

Alkaline gels

This procedure was based on (McDonell et al. 1977). 1.5-3µg of DNA were ethanol precipitated, and resuspended in 50 mN NaOH, 1 mM EDTA, mixed with 0.2 volumes of 6 x alkaline loading buffer (300 mM NaOH, 6 mM EDTA, 18% (v/v) Ficoll,

0.15% (w/v) bromocresol green, 0.25% (w/v) xylene cyanol FF) and run on a 0.5% (w/v) alkaline agarose gel in 50 mM NaOH and 1mM EDTA (pH 8.0) for 27 hr at 50 V at 4°C with two changes of running buffer. The gel was subsequently treated like described in section about Southern blotting or G-overhang assay. Markers were prepared by digesting a TTAGGG repeat bearing 2.6 kbp pTH5 plasmid (de Lange et al. 1990) with HindIII and self religation of the cut plasmid.

Estimation of telomere length

The median length of the telomeric restriction fragments was determined by using ImageQuant software after scanning with a PhosphorImager and was not corrected for dependence of signal intensity on telomere length.

Cell extracts

For buffer C-extracts, cells grown in 10 cm dishes were harvested by scraping in 5 ml cold phosphate-buffered saline (PBS) and centrifugation at 1000 rpm for 5 min. Cell pellets were resuspended in 4-6 volumes (50-200 µl) ice-cold buffer C (20 mM Hepes-KOH pH 7.9, 420 mM KCl, 25% (v/v) glycerol, 0.1 mM EDTA, 5 mM $MgCl_2$, 1 mM dithiothreitol (DTT), 0.5 mM phenylmethylsulfonyl fluoride (PMSF), 0.2% (v/v) Nonidet P-40, 1 µg of leupeptin, pepstatin, and aprotinin per ml, incubated for 30 min on ice and centrifuged 10 min at 14,000 g at 4°C. The supernatant was dialyzed for 2 hrs against buffer D (20 mM Hepes-KOH [pH 7.9], 100 mM KCl, 20% (v/v) glycerol, 0.2 mM EDTA, 0.2 mM EGTA, 0.5 mM DTT, and 0.5 mM PMSF) at 4°C, snap-frozen in liquid nitrogen

and stored at -80°C. Protein concentrations were determined using the Bradford assay (BioRad, Hercules, CA) using bovine serum albumin as a standard.

For whole cell lysates, cells were harvested by trypsinization, washed in cold PBS, counted, collected by centrifugation, and resuspended at $1x10^4$ cells per µl of Laemmli loading buffer (Laemmli loading buffer is made by combining 4 ml Buffer B [see below], 8 ml glycerol, 2 ml β-mercaptoethanol, 16 ml SDS stock solution [stock solution is 10% (w/v) SDS in water], 2 ml bromophenol blue stock solution [stock solution is 1% (w/v) bromophenol blue in water], and 8 ml H_20. Buffer B is made by combining 7.6 g Tris base, 5 ml SDS stock solution [stock solution is 10% (w/v) SDS in water], 5 ml concentrated HCl, and 30 ml of H_20, adjusting the pH to 6.8 and adjusting the total volume to 50 ml with H_20). The DNA was sheared by passing several times through a 25 G 5/8 needle.

For westerns visualizing ATM, the cells were harvested by trypsinization, washed in cold PBS, counted, collected by centrifugation and the extract was prepared by sonicating $5x10^6$ cells in a 250 µl cold buffer containing 50 mM Tris HCl, pH 7.5, 150 mM NaCl, 10% (v/v) glycerol, 1% (v/v) Tween 20, 50 mM Naβ-glycerophosphate, 1 mM NaF, 1 mM $NaVO_4$, 0.1 mM DTT, 0.5 mM PMSF, 0.5 µg/ml Leupeptin. The extract was centrifuged 10 min at 14,000 g at 4°C and the pellet was discarded.

Western blotting

For buffer C extracts, 30 µg were separated on a 9% (w/v) SDS-polyacrylamide gel (Sambrook et al. 1989) and transferred to nitrocellulose by electroblotting for 1 hour at 90 V at 4°C or overnight at 100 mA at room temperature. Membranes were stained

with Ponceau S (20 mg/ml in H_20) (Sambrook et al. 1989) for 2 min to verify that equal amounts of protein were fractionated in each lane. For whole cell extracts, 15 µl of the extract were fractionated on SDS-polyacrylamide gels and transferred onto nitrocellulose or PVDF (Millipore) (for anti E7 and anti ATM westerns) membranes. Blocking and incubation with primary and secondary antibodies was performed in 5% (w/v) milk and 0.1% (v/v) Tween in PBS. Antibodies were as follows: anti-TRF2- 647, 508 or mouse anti-TRF2 (Cat# 05-521, Upstate Biotechnology), anti p53-1801 (Levine lab), HDM2-3F3 (Levine lab), anti p21-F-5 (Santa Cruz Biotechnology), anti Rb (cat# 14001A, PharMingen), anti p16-NCLp16 (Novocastra laboratories), anti cyclin A- cat#sc-239 (Santa Cruz), anti γ-tubulin-clone GTU88 (Sigma), anti SV40 Tag-PAB416 (Levine lab), anti E7-Clone 8C9 (Zymed), ATM antibody 2C1 (GeneTex). After incubations with secondary antibodies (Amersham) all blots were developed using the ECL kit (Amersham)

RNA isolation

Total RNA was isolated as described (Auffray and Rougeon 1980). $1x10^7$ cells were washed in PBS, lysed in 3 M LiCl/6 M urea, sonicated, and incubated on ice for 6 hours. RNA was collected by centrifugation in a microcentrifuge at maximum speed for 20 min at 4°C, treated with proteinase K (50 mg/ml) in 200 µl 10 mM Tris-HCl (pH 7.5), 10 mM EDTA, 100 mM NaCl, 1% (w/v) SDS for 10 min at 37°C, extracted with phenol/chloroform/iso-amylalcohol (25:24:1), and precipitated with isopropanol in the presence of 0.2 M Na-acetate pH 5.5.

RNase protection

The hTERT sequence was subcloned from pCI Neo-hEST2-HA (a gift from R. A. Weinberg; (Meyerson et al. 1997)) into pcDNA3 (Invitrogen). A StyI fragment containing part of the hTERT sequence (nucleotide 3229-3452) and flanking vector sequences was purified and used in the MAXIscript *in vitro* transcription reaction (Ambion) using α-^{32}P-UTP (800 Ci/mmol, 10 mCi/ml). The template for the hTR RNase protection probe was similarly prepared by digesting pGRN78 (Kim et al. 1994) with XbaI, and the β-actin probe was obtained from Ambion. The β-actin probe was labeled to 200-fold lower specific activity than the hTERT and hTR probes by diluting out the radiolabelled UTP with cold UTP. RNase protection reactions were performed using solutions from the Direct Protect Lysate Ribonuclease Protection Assay Kit (Ambion) with 20 μg of total RNA (isolated as described above) instead of cell lysates.

TRAP assay

The assay was essentially performed as described (Broccoli et al. 1995). 0.5 μg protein of buffer C extract was mixed with 49 μl of premixed 5 μl of 10X buffer B (200 mM Tris HCl [pH 8.3], 15 mM MgCl2, 630 mM KCl, 0.05% (v/v) Tween 20, 10 mM EGTA, 1 mg BSA per ml), 2.5 mM dNTPs, 5 μl TS primer labeled as below, 0.05 μl T4 gene 32 protein, 2 units of Taq polymerase and water. The reaction was incubated at room temperature for 30 minutes to allow extension of the TS primer by telomerase. Subsequently, telomerase was inactivated by heating at 65°C for 3 minutes, and after addition of 1 μl of reverse primer CX, PCR was done for 27 cycles at 94°C for 30

seconds, at 50°C for 30 seconds, and at 72°C for 1 minute. RNase digestions were done in parallel to the untreated reaction by addition of 0.2 μg DNase-free RNAse A to the telomerase extension reaction. Each experiment also contained a negative control reaction where one μl of buffer C was used instead of the extract.

TS primer (0.1 μg) was radioactively labeled by mixing with 2 μl of T4 polynucleotide kinase buffer (NEB), 4 μl of water, 12 μl of γ-^{32}P-ATP (6000 Ci/mMol, 10 mCi/ml), and 1 μl of T4 polynucleotide kinase (NEB), and incubating at 37°C for 45 minutes. After adding 10 μg of unlabeled TS primer, and TES (10 mM Tris-HCl, 10 mM EDTA [pH 8.0], 0.1% (w/v) SDS) to 100 μl, the reaction was loaded onto a Sephadex G-25 fine column made in a 3 ml syringe packed to the top with the resin. The column was washed with 1000 μl of TES and the labeled oligonuclotide was eluted with 800 μl of TES and extracted with phenol:chloroform:isoamyl alcohol (25:24:1), ethanol precipitated and resuspended in 500 μl double-distilled water.

For some experiments (Figure 3-6) the Trapeze telomerase detection kit (Intergen) was used according to the manufacturer's instructions.

t-loop assay

$2x10^8$ cells were collected from about 50 15 cm plates by trypsinization, washed with PBS and carefully resuspended in 20 ml of homogenization buffer (10 mM Tris-HCl [pH 7.5], 15 mM NaCl, 60 mM KCl, 1 mM EDTA, 0.1 mM EGTA, 0.15 mM spermine, 0.5 mM spermidine, 0.2% (v/v) NP-40 (IPEGAL), 5% sucrose [w/v]). The cells were incubated on ice for 15 minutes, centrifuged at 1300 g (3800 rpm in the table-top centrifuge) in the cold for 15 min. The buffer was discarded and the nuclei were gently

resuspended in 16 ml of fresh homogenization buffer, spun down as above, and resuspended in 3 ml of homogenization buffer. 750 µl of 1 mg 4'-aminomethyltrioxsalen (AMT; SIGMA) per ml was added and the mixture was placed in a 10 cm dish on ice. The DNA was crosslinked by exposing the nuclei to 365 nm UV light for 30 minutes. The hand-held UV light was positioned 2 cm away from the sample which was being mixed with a tiny stirring bar. The crosslinked nuclei were collected, snap frozen in liquid nitrogen, and sent for analysis to Jack Griffith. Further processing and analysis were done as described (Griffith et al. 1999). Nuclear suspensions were treated with proteinase K in the presence of SDS, and DNA was isolated by phenol/chloroform extraction and ethanol precipitation. The deproteinized sample was suspended in 9 ml of 10 mM Tris (pH 7.5), 1 mM EDTA (TE) and cleaved with AluI and MboI for 12 hr at 37°C. During the final hour, RNase (Pharmacia) was added to 20 µg/ml. The sample was then extracted one time with phenol:chloroform:isoamyl alcohol, precipitated with ethanol, and suspended in 3 ml of TE. The sample was applied to a 2.5 x 100 cm Biogel A5M column (Biorad) and eluted at a flow rate of 0.2 ml/min. Fractions of 0.6 ml were taken and the OD_{260} of each determined. The droplet variation of the Kleinschmidt method (Kleinschmidt and Zahn 1959) was used for surface-spreading DNA. A 50 µl aliquot of DNA in TE was mixed with ammonium acetate (pH 7.9) to a final concentration of 0.25 M. Cytochrome C, Sigma Inc.) was added to 4 µg/ml and the drop placed on Parafilm Semifor 90 s. A parlodion-covered EM grid was touched to the drop and then dehydrated through two washes of 80% (v/v) ethanol followed by air drying and rotary shadowcast with platinum–paladium (80:20).

References

Agami, R. and R. Bernards (2000). "Distinct initiation and maintenance mechanisms cooperate to induce G1 cell cycle arrest in response to DNA damage." Cell **102**(1): 55-66.

Allshire, R. C., J. R. Gosden, S. H. Cross, G. Cranston, D. Rout, N. Sugawara, J. W. Szostak, P. A. Fantes and N. D. Hastie (1988). "Telomeric repeat from T. thermophila cross-hybridizes with human telomeres." Nature **332**: 656-659.

Artandi, S. E., S. Chang, S. L. Lee, S. Alson, G. J. Gottlieb, L. Chin and R. A. DePinho (2000). "Telomere dysfunction promotes non-reciprocal translocations and epithelial cancers in mice." Nature **406**(6796): 641-5.

Ashley, T. and D. C. Ward (1993). "A "hot spot" of recombination coincides with an interstitial telomeric sequence in the Armenian hamster." Cytogenet. Cell Genet. **62**: 169-171.

Auffray, C. and G. Rougeon (1980). "Purification of mouse immunoglobulin heavy-chain messenger RNAs from total myeloma tumor RNA." Eur. J. Biochem. **107**: 303-314.

Avilion, A. A., M. A. Piatyszek, J. Gupta, J. W. Shay, S. Bacchetti and C. W. Greider (1996). "Human telomerase activity in immortal cell lines and tumor tissues." Cancer Res. **50**: 645-650.

Azzalin, C. M., E. Mucciolo, L. Bertoni and E. Giulotto (1997). "Fluorescence in situ hybridization with a synthetic (T2AG3)n polynucleotide detects several intrachromosomal telomere-like repeats on human chromosomes." Cytogenet Cell Genet **78**(2): 112-5.

Bailey, S. M., C. M.N., A. Kurimasa, D. J. Chen and E. H. Goodwin (2001). "Strnd-specific Postreplicative Processing of Mammalian Telomeres." Science **in press**.

Bailey, S. M., J. Meyne, D. J. Chen, A. Kurimasa, G. C. Li, B. E. Lehnert and E. H. Goodwin (1999). "DNA double-strand break repair proteins are required to cap the ends of mammalian chromosomes." Proc Natl Acad Sci U S A **96**(26): 14899-904.

Barnes, D. E., G. Stamp, I. Rosewell, A. Denzel and T. Lindahl (1998). "Targeted disruption of the gene encoding DNA ligase IV leads to lethality in embryonic mice." Curr Biol **8**(25): 1395-8.

Barnett, M., V. Buckle, E. Evans, A. Porter, D. Rout, A. Smith and W. R. A. Brown (1993). "Telomere directed fragmentation of mammalian chromosomes." Nucl. Acids Res. **21**: 27-36.

Bartek, J. and J. Lukas (2001). "Pathways governing G1/S transition and their response to DNA damage." FEBS Lett **490**(3): 117-22.

Baumann, P. and T. R. Cech (2001). "Pot1, the putative telomere end-binding protein in fission yeast and humans." Science **292**(5519): 1171-5.

Baur, J. A., Y. Zou, J. W. Shay and W. E. Wright (2001). "Telomere position effect in human cells." Science **292**(5524): 2075-7.

Benn, P. A. (1976). "Specific chromosome aberrations in senescent fibroblast cell lines derived from human embryos." Am. J. Hum. Gen. **28**: 465-473.

Bianchi, A. (1999). Characterization of DNA binding activities at vertebrate telomeres, The Rockefeller University.

Bianchi, A. and T. de Lange (1999). "Ku binds telomeric DNA *in vitro*." J Biol Chem. **274**: 21223-21227.

Bianchi, A., S. Smith, L. Chong, P. Elias and T. de Lange (1997). "TRF1 is a dimer and bends telomeric DNA." EMBO J. **16**: 1785-1794.

Bianchi, A., R. M. Stansel, L. Fairall, J. D. Griffith, D. Rhodes and T. d. Lange (1999). "TRF1 binds a bipartite telomeric site with extreme spatial flexibility." EMBO Journal **18**: 5735-5744.

Bianchi, A., M. Van Breugel, R. Wang and T. de Lange "unpublished data."

Biessmann, H., J. M. Mason, K. Ferry, M. d'Hulst, K. Valgeirsdottir, K. L. Traverse and M.-L. Pardue (1990). "Addition of telomere-associated HeT DNA sequences "heals" broken chromosome ends in *Drosophila*." Cell **61**: 663-673.

Bilaud, T., C. Brun, K. Ancelin, C. E. Koering, T. Laroche and E. Gilson (1997). "Telomeric localization of TRF2, a novel human telobox protein." Nature Genetics **17**: 236-239.

Bilaud, T., C. E. Koering, E. Binet-Brasselet, K. Ancelin, A. Pollice, S. M. Gasser and E. Gilson (1996). "The telobox, a Myb-related telomeric DNA binding motif found in proteins from yeast, plants and human." Nucl. Acids Res. **24**: 1294-303.

Blackburn, E. and J. Gall (1978). "A tandemly repeated sequence at the termini of extachromosomal DNA coding for rRNA in Tetrahymena." J. Mol. Biology **120**: 33-53.

Blackburn, E. H. a. C., P.B. (1984). "Identification of a Telomeric DNA Sequence in *Trypanosoma brucei*." Cell **36**: 447-457.

Blasco, M. A., W. Funk, B. Villeponteau and C. W. Greider (1995). "Functional characterization and developmental regulation of mouse telomerase RNA." Science **269**: 1267-1270.

Blasco, M. A., H.-W. Lee, M. P. Hande, E. Samper, P. M. Lansdorp, R. A. DePinho and C. W. Greider (1997). "Telomere shortening and tumor formation by mouse cells lacking telomerase DNA." Cell **91**: 25-34.

Bodnar, A. G., M. Ouellette, M. Frolkis, S. E. Holt, C. P. Chiu, G. B. Morin, C. B. Harley, J. W. Shay, S. Lichtsteiner and W. E. Wright (1998). "Extension of life-span by introduction of telomerase into normal human cells." Science **279**: 349-52.

Bodnar, A. G., M. Ouellette, M. Frolkis, S. E. Holt, C. P. Chiu, G. B. Morin, C. B. Harley, J. W. Shay, S. Lichtsteiner and W. E. Wright (1998). "Extension of life-span by introduction of telomerase into normal human cells [see comments]." Science **279**: 349-52.

Boulton, S. J. and S. P. Jackson (1998). "Components of the Ku-dependent non-homologous end-joining pathway are involved in telomeric length maintenance and telomeric silencing." EMBO J. **17**: 1819-28.

Boutouil, M., R. Fetni, J. Qu, L. Dallaire, C. L. Richer and N. Lemieux (1996). "Fragile site and interstitial telomere repeat sequences at the fusion point of a de novo (Y;13) translocation." Hum Genet **98**(3): 323-7.

Broccoli, D., L. Chong, S. Oelmann, A. A. Fernald, N. Marziliano, B. van Steensel, D. Kipling, M. M. Le Beau and T. de Lange (1997). "Comparison of the human and mouse genes encoding the telomeric protein, TRF1: chromosomal localization, expression, and conserved protein domains." Hum. Mol. Genetics **6**: 69-76.

Broccoli, D., A. Smogorzewska, L. Chong and T. de Lange (1997). "Human telomeres contain two distinct Myb-related proteins, TRF1 and TRF2." Nature Gen. **17**: 231-235.

Broccoli, D., J. W. Young and T. de Lange (1995). "Telomerase activity in normal and malignant hematopoietic cells." Proc. Natl. Acad. Sci. USA **92**: 9082-9086.

Brown, J. P., W. Wei and J. M. Sedivy (1997). "Bypass of senescence after disruption of p21CIP1/WAF1 gene in normal diploid human fibroblasts." Science **277**: 831-4.

Bryan, T. M., A. Englezou, L. Dalla-Pozza, M. A. Dunham and R. R. Reddel (1997). "Evidence for an alternative mechanism for maintaining telomere length in human tumors and tumor-derived cell lines [see comments]." Nat. Med. **3**: 1271-4.

Bryan, T. M., A. Englezou, J. Gupta, S. Bacchetti and R. R. Reddel (1995). "Telomere elongation in immortal human cells without detectable telomerase activity." EMBO J. **14**: 4240-4248.

Cangiano, G., La Volpe, A. (1993). "Repetitive DNA sequences located in the terminal portion o the Canorhabditis elegans chromosomes." Nucleic Acid Research **21**: 1133-1139.

Carney, J. P., R. S. Maser, H. Olivares, E. M. Davis, M. Le Beau, J. R. Yates, 3rd, L. Hays, W. F. Morgan and J. H. Petrini (1998). "The hMre11/hRad50 protein complex and Nijmegen breakage syndrome: linkage of double-strand break repair to the cellular DNA damage response." Cell **93**(3): 477-86.

Cenci, G., R. B. Rawson, G. Belloni, D. H. Castrillon, M. Tudor, R. Petrucci, M. L. Goldberg, S. A. Wasserman and M. Gatti (1997). "UbcD1, a *Drosophila* ubiquitin-conjugating enzyme required for proper telomere behavior." Genes Dev. **11**: 863-875.

Chandra, A., T. R. Hughes, C. I. Nugent and V. Lundblad (2001). "Cdc13 both positively and negatively regulates telomere replication." Genes Dev **15**(4): 404-14.

Chen, J. L., M. A. Blasco and C. W. Greider (2000). "Secondary structure of vertebrate telomerase RNA." Cell **100**(5): 503-14.

Chin, L., S. E. Artandi, Q. Shen, A. Tam, S.L. Lee, G.J. Gottlieb, C. W. Greider, R. A DePinho (1999). "p53 deficiency rescues the adverse effects of telomere loss and cooperates with telomere dysfunction to accelerate carcinogenesis." Cell **97** (4): 527-38.

Chong, L., B. van Steensel, D. Broccoli, H. Erdjument-Bromage, J. Hanish, P. Tempst and T. de Lange (1995). "A human telomeric protein." Science **270**: 1663-1667.

Cliby, W. A., C. J. Roberts, K. A. Cimprich, C. M. Stringer, J. R. Lamb, S. L. Schreiber and S. H. Friend (1998). "Overexpression of a kinase-inactive ATR protein causes sensitivity to DNA-damaging agents and defects in cell cycle checkpoints." Embo J **17**(1): 159-69.

Cohen, H. and D. A. Sinclair (2001). "Recombination-mediated lengthening of terminal telomeric repeats requires the Sgs1 DNA helicase." Proc Natl Acad Sci U S A **98**(6): 3174-9.

Colgin, L. M., C. Wilkinson, A. Englezou, A. Kilian, M. O. Robinson and R. R. Reddel (2000). "The hTERTalpha splice variant is a dominant negative inhibitor of telomerase activity." Neoplasia **2**(5): 426-32.

Collins, K., R. Kobayashi and C. W. Greider (1995). "Purification of Tetrahymena telomerase and cloning of genes encoding the two protein components of the enzyme." Cell **81**: 677-686.

Compton, D. A., T. J. Yen and D. W. Cleveland (1991). "Identification of novel centromere/kinetochore-associated proteins using monoclonal antibodies generated against human mitotic chromosome scaffolds." J. Cell Biol. **112**: 1083-1097.

Conrad, M. N., J. H. Wright, A. J. Wolf and V. A. Zakian (1990). "RAP1 protein interacts with yeast telomeres *in vivo*

: Overproduction alters telomere structure and decreases chromosome stability." Cell **63**: 739-750.

Cooke, H. J. and B. A. Smith (1986). "Variability at the telomeres of the human X/Y pseudoautosomal region." Cold Spring Harbor Symp. Quant. Biol. **LI**: 213-219.

Cooper, J. P., E. R. Nimmo, R. C. Allshire and T. R. Cech (1997). "Regulation of telomere length and function by a Myb-domain protein in fission yeast." Nature **385**: 744-747.

Counter, C. M., A. A. Avilion, C. E. LeFeuvre, N. G. Stewart, C. W. Greider, C. B. Harley and S. Bacchetti (1992). "Telomere shortening associated with chromosome instability is arrested in immortal cells with express telomerase activity." EMBO J. **11**: 1921-1929.

Counter, C. M., J. Gupta, C. B. Harley, B. Lever and S. Bacchetti (1995). "Telomerase activity in normal leukocytes and in haematological malignancies." Blood **85**: 2315-2320.

Counter, C. M., H. W. Hirte, S. Bacchetti and C. Harley (1994). "Telomerase activity in human ovarian carcinoma." Proc. Natl. Acad. Sci. USA **91**: 2900-2904.

Critchlow, S. E. and S. P. Jackson (1998). "DNA end-joining: from yeast to man." Trends Biochem. Sci. **23**: 394-8.

d'Adda di Fagagna, F., M. P. Hande, T. W. M, D. Roth, P. M. Lansdorp, Z. Q. Wang and S. P. Jackson (2001). "Effects of DNA nonhomologous end-joining factors on telomere length and chromosomal stability in mammalian cells." Curr Biol **11**: 1192-1196.

d'Adda di Fagagna, F., M. P Hande, W. M. Tong, P. M. Lansdorp, Z. Q. Wang and S. P. Jackson (1999). "Functions of poly(ADP-ribose) polymerase in controlling telomere length and chromosomal stability." Nat Genet **23**(1): 76-80.

Day, J. P., C. L. Limoli and W. F. Morgan (1998). "Recombination involving interstitial telomere repeat-like sequences promotes chromosomal instability in Chinese hamster cells." Carcinogenesis **19**(2): 259-65.

de Lange, T. (1992). "Human telomeres are attached to the nuclear matrix." EMBO J. **11**: 717-724.

de Lange, T. (1995). Telomere dynamics and genome Instability in Human Cancer. Telomeres. C. W. Greider and E. H. Blackburn.

de Lange, T. (1998). "Telomeres and senescence: ending the debate." Science: in press.

de Lange, T. (2001). "Cell biology. Telomere capping--one strand fits all." Science **292**(5519): 1075-6.

de Lange, T. and J. Petrini (2001). "A new connection at human telomeres: association of the Mre11 complex with TRF2." Cold Spring Harb Symp Quant Biol **LXV**: 265-273.

de Lange, T., L. Shiue, R. M. Myers, D. R. Cox, S. L. Naylor, A. M. Killery and H. E. Varmus (1990). "Structure and variability of human chromosome ends." Mol. Cell. Biol **10**: 518-527.

Dell'Orco, R. T., J. G. Mertens and P. F. Kruse, Jr. (1973). "Doubling potential, calendar time, and senescence of human diploid cells in culture." Exp Cell Res **77**(1): 356-60.

DePinho, R. A. (2000). "The age of cancer." Nature **408**: 248-254.

Di Leonardo, A., S. P. Linke, K. Clarkin and G. M. Wahl (1994). "DNA damage triggers a prolonged p53-dependent G1 arrest and long-term induction of Cip1 in normal human fibroblasts." Genes Dev. **8**: 2540-51.

Dimri, G. P., K. Itahana, M. Acosta and J. Campisi (2000). "Regulation of a senescence checkpoint response by the E2F1 transcription factor and p14(ARF) tumor suppressor." Mol Cell Biol **20**(1): 273-85.

Dimri, G. P., X. Lee, G. Basile, M. Acosta, G. Scott, C. Roskelley, E. E. Medrano, M. Linskens, I. Rubelj, O. Pereira-Smith, M. Peacocke and J. Campisi (1995). "A biomarker that identifies senescent human cells in culture and in aging skin *in vivo*." Proc. Natl. Acad. Sci. USA **92**: 9363-9367.

Dionne, I. and R. J. Wellinger (1996). "Cell cycle-regulated generation of single-stranded G-rich DNA in the absence of telomerase." Proc. Natl. Acad. Sci. USA **93**: 13902-13907.

Duensing, S. and K. Munger (2001). "Centrosome abnormalities, genomic instability and carcinogenic progression." Biochim Biophys Acta **2**(8): M81-8.

Dunham, M. A., A. A. Neumann, C. L. Fasching and R. R. Reddel (2000). "Telomere maintenance by recombination in human cells." Nat Genet **26**: 447-450.

Eils, R., S. Uhrig, K. Saracoglu, K. Satzler, A. Bolzer, I. Petersen, J. Chassery, M. Ganser and M. R. Speicher (1998). "An optimized, fully automated system for fast and accurate identification of chromosomal rearrangements by multiplex-FISH (M-FISH)." Cytogenet Cell Genet **82**(3-4): 160-71.

Evans, S. K. and V. Lundblad (1999). "Est1 and Cdc13 as Comediators of Telomerase Access." Science **286**(5437): 117-120.

Evans, S. K. and V. Lundblad (2000). "Positive and negative regulation of telomerase access to the telomere." J Cell Sci **113 Pt 19**: 3357-64.

Fairall, L., L. Chapman, H. Moss, T. de Lange and D. Rhodes (2001). "Structure of the dimerization domain of the human Ttelomeric proteins TRF1 and TRF2." Molecular Cell **in press**.

Fan, X. and C. M. Price (1997). "Coordinate regulation of G- and C strand length during new telomere synthesis." Mol. Biol. Cell. **8**: 2145-55.

Fang, G. and T. R. Cech (1991). "Molecular cloning of telomere-binding protein genes from Stylonychia mytilis." Nucl. Acids Res. **19**: 5515-5518.

Fanti, L., G. Giovinazzo, M. Berloco and S. Pimpinelli (1998). "The heterochromatin protein 1 prevents telomere fusions in *Drosophila*." Molecular Cell **2**: 527-538.

Feng, J., W. D. Funk, S.-S. Wang, S. L. Weinrich, A. A. Avilion, C.-P. Chiu, R. R. Adams, E. Chang, R. C. Allsopp, J. Yu, S. Le, M. D. West, C. B. Harley, W. H. Andrews, C. W. Greider and B. Villeponteau (1995). "The RNA component of human telomerase." Science **269**: 1236-1241.

Ferguson, D. O., J. M. Sekiguchi, S. Chang, K. M. Frank, Y. Gao, R. A. DePinho and F. W. Alt (2000). "The nonhomologous end-joining pathway of DNA repair is required for genomic stability and the suppression of translocations." PNAS **97**(12): 6630-6633.

Fiset, S. and B. Chabot (2001). "hnRNP A1 may interact simultaneously with telomeric DNA and the human telomerase RNA *in vitro*." Nucleic Acids Res **29**(11): 2268-75.

Fitzgerald, M. S., K. Riha, F. Gao, S. Ren, T. D. McKnight and D. E. Shippen (1999). "Disruption of the telomerase catalytic subunit gene from *Arabidopsis* inactivates telomerase and leads to a slow loss of telomeric DNA." Proc Natl Acad Sci U S A **96**(26): 14813-8.

Ford, L. P., J. W. Shay and W. E. Wright (2001). "The La antigen associates with the human telomerase ribonucleoprotein and influences telomere length *in vivo*." Rna **7**(8): 1068-75.

Ford, L. P., J. M. Suh, W. E. Wright and J. W. Shay (2000). "Heterogeneous nuclear ribonucleoproteins C1 and C2 associate with the RNA component of human telomerase." Mol Cell Biol **20**(23): 9084-91.

Frank, K. M., J. M. Sekiguchi, K. J. Seidl, W. Swat, G. A. Rathbun, H. L. Cheng, L. Davidson, L. Kangaloo and F. W. Alt (1998). "Late embryonic lethality and impaired V(D)J recombination in mice lacking DNA ligase IV." Nature **396**(6707): 173-7.

Frank, K. M., N. E. Sharpless, Y. Gao, J. M. Sekiguchi, D. O. Ferguson, C. Zhu, J. P. Manis, J. Horner, R. A. DePinho and F. W. Alt (2000). "DNA ligase IV deficiency in mice leads to defective neurogenesis and embryonic lethality via the p53 pathway." Mol Cell **5**(6): 993-1002.

Fukasawa, K., T. Choi, R. Kuriyama, S. Rulong and G. F. Vande Woude (1996). "Abnormal centrosome amplification in the absence of p53." Science **271**(5256): 1744-7.

Gao, Y., D. O. Ferguson, W. Xie, J. P. Manis, J. Sekiguchi, K. M. Frank, J. Chaudhuri, J. Horner, R. A. DePinho and F. W. Alt (2000). "Interplay of p53 and DNA-repair protein XRCC4 in tumorigenesis, genomic stability and development." Nature **404**(6780): 897-900.

Gao, Y., Y. Sun, K. M. Frank, P. Dikkes, Y. Fujiwara, K. J. Seidl, J. M. Sekiguchi, G. A. Rathbun, W. Swat, J. Wang, R. T. Bronson, B. A. Malynn, M. Bryans, C. Zhu, J. Chaudhuri, L. Davidson, R. Ferrini, T. Stamato, S. H. Orkin, M. E. Greenberg and F. W. Alt (1998). "A critical role for DNA end-joining proteins in both lymphogenesis and neurogenesis." Cell **95**(7): 891-902.

Garvik, B., M. Carson and L. Hartwell (1995). "Single-stranded DNA arising at telomeres in cdc13 mutants may constitute a specific signal for the RAD9 checkpoint [published erratum appears in Mol Cell Biol 1996 Jan;16(1):457]." Mol. Cell. Biol. **15**: 6128-38.

Gatei, M., D. Young, K. M. Cerosaletti, A. Desai-Mehta, K. Spring, S. Kozlov, M. F. Lavin, R. A. Gatti, P. Concannon and K. Khanna (2000). "ATM-dependent phosphorylation of nibrin in response to radiation exposure." Nat Genet **25**(1): 115-9.

Godhino Ferreira, M. and J. Promisel Cooper (2001). "The fission yeast Taz1 protein protects chromosomes from Ku-dependent end-to-end fusions." Mol Cell **7**(1): 55-63.

Goldstein, S. and D. P. Singal (1974). "Senescence of cultured human fibroblasts: mitotic versus metabolic time." Exp Cell Res **88**(2): 359-64.

Gossen, M. and H. Bujard (1992). "Tight control of gene expression in mammalian cells by tetracyclin-responsive promoters." Proc. Natl. Acad. Sci. USA **89**: 5547-5551.

Gottschling, D. E. and V. A. Zakian (1986). "Telomere proteins: Specific recognition and protection of the natural termini of *Oxytricha* macronuclear DNA." Cell **47**: 195-205.

Goytisolo, F. A., E. Samper, S. Edmonson, G. E. Taccioli and M. A. Blasco (2001). "The absence of the dna-dependent protein kinase catalytic subunit in mice results in anaphase bridges and in increased telomeric fusions with normal telomere length and G-strand overhang." Mol Cell Biol **21**(11): 3642-51.

Grandin, N., C. Damon and M. Charbonneau (2001). "Ten1 functions in telomere end protection and length regulation in association with Stn1 and Cdc13." EMBO J. **20**(5): 1173-1183.

Grandin, N., S. I. Reed and M. Charbonneau (1997). "Stn1, a new *Saccharomyces cerevisiae* protein, is implicated in telomere size regulation in association with Cdc13." Genes Dev. **11**: 512-27.

Gratzner, H. G. (1982). "Monoclonal antibody to 5-bromo- and 5-iododeoxyuridine: A new reagent for detection of DNA replication." Science **218**(4571): 474-5.

Gravel, S., M. Larrivee, P. Labrecque and R. J. Wellinger (1998). "Yeast Ku as a Regulator of Chromosomal DNA End Structure." Science **280**: 741-4.

Grawunder, U., D. Zimmer, S. Fugmann, K. Schwarz and M. R. Lieber (1998). "DNA ligase IV is essential for V(D)J recombination and DNA double- strand break repair in human precursor lymphocytes." Mol Cell **2**(4): 477-84.

Greenberg, R. A., R. C. Allsopp, L. Chin, G. B. Morin and R. A. DePinho (1998). "Expression of mouse telomerase reverse transcriptase during development, differentiation and proliferation." Oncogene **16**(13): 1723-30.

Greenwell, P. W., S. L. Kronmal, S. E. Porter, J. Gassenhuber, B. Obermaier and T. D. Petes (1995). "TEL1, a gene involved in controlling telomere length in *S. cerevisiae*, is homologous to the human ataxia telangiectasia gene." Cell **82**: 823-829.

Greider, C. W. and E. H. Blackburn (1985). "Identification of a specific telomere terminal transferase activity in Tetrahymena extracts." Cell **43**: 405-413.

Greider, C. W. and E. H. Blackburn (1987). "The telomere terminal transferase of tetrahymena is a ribonucleoprotein enzyme with two kinds of primer specificity." Cell **51**: 887-898.

Griffith, J., A. Bianchi and T. de Lange (1998). "TRF1 promotes parallel pairing of telomeric tracts *in vitro*." J. Mol. Biol., **278**: 79-88.

Griffith, J. D., L. Comeau, S. Rosenfield, R. M. Stansel, A. Bianchi, H. Moss and T. d. Lange (1999). "Mammalian telomeres end in a large duplex loop." Cell **97**: 503-514.

Guiducci, C., M. A. Cerone, S. Bacchetti, (2001). "Expression of mutant telomerase in immortal telomerase-negative human cells results in cell cycle deregulation, nuclear and chromosomal abnormalities and rapid loss of viability." Oncogene, **20** (6) 714-725.

Haber, J. E. (1998). "The many inerfaces of Mre11." Cell **95**: 583-586.

Haber, J. E. (2000). "Partners and pathwaysrepairing a double-strand break." Trends Genet **16**(6): 259-64.

Hahn, W. C., S. A. Stewart, M. W. Brooks, S. G. York, E. Eaton, A. Kurachi, R. L. Beijersbergen, J. H. Knoll, M. Meyerson and R. A. Weinberg (1999). "Inhibition of telomerase limits the growth of human cancer cells." Nat Med **5**(10): 1164-70.

Halbert, C. L., G. W. Demers and D. A. Galloway (1991). "The E7 gene of human papillomavirus type 16 is sufficient for immortalization of human epithelial cells." J Virol **65**(1): 473-8.

Hande, M. P., A. S. Balajee, A. Tchirkov, A. Wynshaw-Boris and P. M. Lansdorp (2001). "Extra-chromosomal telomeric DNA in cells from Atm(-/-) mice and patients with ataxia-telangiectasia." Hum Mol Genet **10**(5): 519-28.

Hande, P., P. Slijepcevic, A. Silver, S. Bouffler, P. van Buul, P. Bryant and P. Lansdorp (1999). "Elongated telomeres in scid mice." Genomics **56**(2): 221-3.

Hanish, J. P., J. Yanowitz and T. de Lange (1994). "Stringent sequence requirements for telomere formation in human cells." Proc. Natl. Acad. Sci. USA **91**: 8861-8865.

Hara, E., R. Smith, D. Parry, H. Tahara, S. Stone and G. Peters (1996). "Regulation of p16CDKN2 expression and its implications for cell immortalization and senescence." Mol Cell Biol **16**(3): 859-67.

Harley, C. B., A. B. Futcher and C. W. Greider (1990). "Telomeres shorten during ageing of human fibroblasts." Nature **345**: 458-460.

Harrington, L., T. McPhail, V. Mar, W. Zhou, R. Oulton, M. B. Bass, I. Arruda and M. O. Robinson (1997). "A mammalian telomerase-associated protein." Science **275**: 973-977.

Harrington, L. A. and C. W. Greider (1991). "Telomerase primer specificity and chromosome healing." Nature **353**: 451-454.

Hastie, N. D. and R. C. Allshire (1989). "Human telomeres: fusion and interstitial sites." Trends Gen. **5**: 326-331.

Hastie, N. D., M. Dempster, M. G. Dunlop, A. M. Thompson, D. K. Green and R. C. Allshire (1990). "Telomere reduction in human colorectal carcinoma and with ageing." Nature **346**: 866-868.

Hauf, S., I. C. Waizenegger and J. M. Peters (2001). "Cohesin cleavage by separase required for anaphase and cytokinesis in human cells." Science **293**(5533): 1320-3.

Hayflick, L. and P. S. Moorhead (1961). "The serial cultivation of human diploid cell strains." Exp. Cell Res. **25**: 585-621.

Heiss, N. S., S. W. Knight, T. J. Vulliamy, S. M. Klauck, S. Wiemann, P. J. Mason, A. Poustka and I. Dokal (1998). "X-linked dyskeratosis congenita is caused by mutations in a highly conserved gene with putative nucleolar functions." Nat Genet **19**(1): 32-8.

Hemann, M. T. and C. W. Greider (1999). "G-strand overhangs on telomeres in telomerase-deficient mouse cells." Nucleic Acids Res **27**(20): 3964-9.

Hemann, M. T., K. L. Rudolph, M. A. Strong, R. A. DePinho, L. Chin and C. W. Greider (2001). "Telomere dysfunction triggers developmentally regulated germ cell apoptosis." Mol Biol Cell **12**(7): 2023-30.

Henderson, E. (1995). Telomere DNA structure. Telomeres. E. H. Blackburn and C. W. Greider. Cold Spring Harbor, Cold Spring Harbor Press: 11-35.

Henderson, E. R. and E. H. Blackburn (1989). "An overhanging 3' terminus is a conserved feature of telomeres." Mol. Cell. Biol. **9**: 345-348.

Herrera, E., E. Samper, J. Martin-Caballero, J. M. Flores, H. W. Lee and M. A. Blasco (1999). "Disease states associated with telomerase deficiency appear earlier in mice with short telomeres." Embo J **18**(11): 2950-60.

Hiraoka, Y., E. Henderson and E. H. Blackburn (1998). "Not so peculiar: fission yeast telomere repeats." Trends Biochem Sci **23**(4): 126.

Hoeijmakers, J. H. (2001). "Genome maintenance mechanisms for preventing cancer." Nature **411**(6835): 366-74.

Horvath, M. P., V. L. Schweiker, J. M. Bevilacqua, J. A. Ruggles and S. C. Schultz (1998). "Crystal Structure of the *Oxytricha nova* Telomere End Binding Protein Complexed with Single Strand DNA." Cell **95**: 963-974.

Hsu, H. L., D. Gilley, S. A. Galande, M. P. Hande, B. Allen, S. H. Kim, G. C. Li, J. Campisi, T. Kohwi-Shigematsu and D. J. Chen (2000). "Ku acts in a unique way at the mammalian telomere to prevent end joining." Genes Dev **14**(22): 2807-12.

Huang, P., F. E. Pryde, D. Lester, R. L. Maddison, R. H. Borts, I. D. Hickson and E. J. Louis (2001). "SGS1 is required for telomere elongation in the absence of telomerase." Curr Biol **11**(2): 125-9.

Hughes, T. R., S. K. Evans, R. G. Weilbaecher and V. Lundblad (2000). "The Est3 protein is a subunit of yeast telomerase." Curr Biol **10**(13): 809-12.

Ide, T., Y. Tsuji, T. Nakashima and S. Ishibashi (1984). "Progress of aging in human diploid cells transformed with a tsA mutant of simian virus 40." Exp Cell Res **150**(2): 321-8.

Ijdo, J. W., A. Baldini, D. C. Ward, S. T. Reeders and R. A. Wells (1991). "Origin of human chromosome 2: An ancestral telomere-telomere fusion." Proc. Natl. Acad. Sci. USA **88**: 9051-9055.

Ishikawa, F., M. J. Matunis, G. Dreyfuss and T. R. Cech (1993). "Nuclear proteins that bind the pre-mRNA 3' splice site sequence r(UUAG/G) and the human telomeric DNA sequence d(TTAGGG)$_n$." Mol. Cell. Biol. **13**: 4301-4310.

Jacob, N. K., R. Skopp and C. M. Price (2001). "G-overhang dynamics at Tetrahymena telomeres." Embo J **20**(15): 4299-308.

Jacobs, J. J., K. Kieboom, S. Marino, R. A. DePinho and M. van Lohuizen (1999). "The oncogene and Polycomb-group gene bmi-1 regulates cell proliferation and senescence through the ink4a locus." Nature **397**(6715): 164-8.

James, T. C., J. C. Eissenberg, C. Craig, V. Dietrich, A. Hobson and S. C. R. Elgin (1989). "Distribution patterns of HP1, a heterochromatin-associated nonhistone chromosomal protein of *Drosophila*." Eur J Cell Biol **50**: 170-180.

Jewett, T., D. Marnane, W. Stewart, R. Hayworth-Hodge, L. Finklea, K. Klinepeter, P. N. Rao and M. J. Pettenati (1998). "Jumping translocation with partial duplications and triplications of chromosomes 7 and 15." Clin Genet **53**(5): 415-20.

Jhappan, C., T. M. Yusufzai, S. Anderson, M. R. Anver and G. Merlino (2000). "The p53 response to DNA damage *in vivo* is independent of DNA-dependent protein kinase." Mol Cell Biol **20**(11): 4075-83.

Johnson, F. B., R. A. Marciniak, M. McVey, S. A. Stewart, W. C. Hahn and L. Guarente (2001). "The *Saccharomyces* cerevisiae WRN homolog Sgs1p participates in telomere maintenance in cells lacking telomerase." Embo J **20**(4): 905-13.

Kamijo, T., F. Zindy, M. F. Roussel, D. E. Quelle, J. R. Downing, R. A. Ashmun, G. Grosveld and C. J. Sherr (1997). "Tumor suppression at the mouse INK4a locus mediated by the alternative reading frame product p19ARF." Cell **91**(5): 649-59.

Kaminker, P. G., S. H. Kim, R. D. Taylor, Y. Zebarjadian, W. D. Funk, G. B. Morin, P. Yaswen and J. Campisi (2001). "TANK2, a new TRF1-associated PARP, causes rapid induction of cell death upon overexpression." J Biol Chem **13**: 13.

Karlseder, J., D. Broccoli, Y. Dai, S. Hardy and T. de Lange (1999). "p53- and ATM-dependent apoptosis induced by telomeres lacking TRF2." Science **283**: 1321-5.

Kilburn, A. E., M. J. Shea, R. G. Sargent and J. H. Wilson (2001). "Insertion of a telomere repeat sequence into a mammalian gene causes chromosome instability." Mol Cell Biol **21**(1): 126-35.

Kilian, A., D. D. Bowtell, H. E. Abud, G. R. Hime, D. J. Venter, P. K. Keese, E. L. Duncan, R. R. Reddel and R. A. Jefferson (1997). "Isolation of a candidate human telomerase catalytic subunit gene, which reveals complex splicing patterns in different cell types." Hum. Mol. Genet. **6**: 2011-9.

Killan, A., K. Heller and A. Kleinhofs (1998). "Development patterns of telomerase activity in barley and maize." Plant Mol Biol **37**(4): 621-8.

Kim, M. M., M.A. Rivera, I. L.Botchkina, R. Shalaby, A. D.Thor, E. Blackburn (2001). "A low threshold level of expression of mutant-template telomerase RNA inhibits human tumor cell proliferation." Proc Natl Acad Sci U S A. **98**(14): 7982-7.

Kim, N. W., M. A. Piatyszek, K. R. Prowse, C. B. Harley, M. D. West, P. L. C. Ho, G. M. Coviello, W. E. Wright, S. L. Weinrich and J. W. Shay (1994). "Specific association of human telomerase activity with immortal cells and cancer." Science **266**: 2011-2015.

Kim, S. H., P. Kaminker and J. Campisi (1999). "TIN2, a new regulator of telomere length in human cells." Nat Genet **23**(4): 405-12.

Kipling, D. and H. J. Cooke (1990). "Hypervariable ultra-long telomeres in mice." Nature **347**: 400-402.

Kirk, K. E., B. P. Harmon, I. K. Reichardt, J. W. Sedat and E. H. Blackburn (1997). "Block in anaphase chromosome separation caused by a telomerase template mutation." Science **275**: 1478-81.

Kironmai, K. M. and K. Muniyappa (1997). "Alteration of telomeric sequences and senescence caused by mutations in RAD50 of *Saccharomyces cerevisiae*." Genes Cells **2**(7): 443-55.

Kiyono, T., S. A. Foster, J. I. Koop, J. K. McDougall, D. A. Galloway and A. J. Klingelhutz (1998). "Both Rb/p16INK4a inactivation and telomerase activity are required to immortalize human epithelial cells." Nature **396**(6706): 84-8.

Kleinschmidt, A. K. and R. K. Zahn (1959). "Uber desoxyribonucleinsauremolekuln in protein mischfilmen." Z. Naturforsch. B 14: 770–779.

Klobutcher, L. A., M. T. Swanton, P. Donini and D. M. Prescott (1981). "All gene-sized DNA molecules in four species of hypotrichs have the same terminal sequence and an unusual 3' terminus." Proc. Natl. Acad. Sci. USA **78**: 3015-3019.

Konig, P., R. Giraldo, L. Chapman and D. Rhodes (1996). "The crystal structure of the DNA-binding domain of yeast RAP1 in complex with telomeric DNA." Cell **85**: 125-136.

Kota, R. S. and K. W. Runge (1998). "The yeast telomere length regulator TEL2 encodes a protein that binds to telomeric DNA." Nucleic Acids Res **26**(6): 1528-35.

Kota, R. S. and K. W. Runge (1999). "Tel2p, a regulator of yeast telomeric length *in vivo*, binds to single- stranded telomeric DNA *in vitro*." Chromosoma **108**(5): 278-90.

Krutilina, R. I., S. Oei, G. Buchlow, P. M. Yau, A. O. Zalensky, I. A. Zalenskaya, E. M. Bradbury, N. V. Tomilin (2001). "A negative regulator of telomere-length protein trf1 is associated with interstitial (TTAGGG)n blocks in immortal Chinese hamster ovary cells." Biochem Biophys Res Commun 280 (2): 471-5.

LaBranche, H., S. Dupuis, Y. Ben-David, M. R. Bani, R. J. Wellinger and B. Chabot (1998). "Telomere elongation by hnRNP A1 and a derivative that interacts with telomeric repeats and telomerase." Nat. Genet. **19**: 199-202.

Lakin, N. D., B. C. Hann and S. P. Jackson (1999). "The ataxia-telangiectasia related protein ATR mediates DNA-dependent phosphorylation of p53." Oncogene **18**(27): 3989-95.

Lamb, J., P. C. Harris, A. O. M. Wilkie, W. G. Wood, J. G. Dauwerse and D. R. Higgs (1993). "De novo truncation of chromosome 16p and healing with (TTAGGG)n in the a-thalassemia/mental retardation syndrome (ATR-16)." Am. J. Hum. Genet. **52**: 668-676.

Lansdorp, P. M., N. P. Verwoerd, F. M. van de Rijke, V. Dragowska, M.-T. Little, R. W. Dirks, A. K. Raap and H. J. Tanke (1996). "Heterogeneity in telomere length of human chromosomes." Hum. Mol. Gen. **5**: 685-691.

Le, S., J. K. Moore, J. E. Haber and C. W. Greider (1999). "RAD50 and RAD51 define two pathways that collaborate to maintain telomeres in the absence of telomerase [In Process Citation]." Genetics **152**: 143-52.

Le, S., R. Sternglanz and C. W. Greider (2000). "Identification of two RNA-binding proteins associated with human telomerase RNA." Mol Biol Cell **11**(3): 999-1010.

Lee, H. W., M. A. Blasco, G. J. Gottlieb, J. W. Horner, 2nd, C. W. Greider and R. A. DePinho (1998). "Essential role of mouse telomerase in highly proliferative organs." Nature **392**: 569-74.

Lees-Miller, S. P., Y. R. Chen and C. W. Anderson (1990). "Human cells contain a DNA-activated protein kinase that phosphorylates simian virus 40 T antigen, mouse p53, and the human Ku autoantigen." Mol. Cell. Biol. **10**: 6472-81.

Lendvay, T. S., D. K. Morris, J. Sah, B. Balasubramanian and V. Lundblad (1996). "Senescence mutants of *Saccharomyces cerevisiae* with a defect in telomere replication identify three additional EST genes." Genetics **144**: 1399-412.

Levis, R. W., R. Ganesan, K. Houtchens, L. A. Tolar and F.-M. Sheen (1993). "Transposons in place of telomeric repeats at a *Drosophila* telomere." Cell **75**: 1083-1093.

Li, B., S. Oestreich and T. de Lange (2000). "Identification of human Rap1: implications for telomere evolution." Cell **101**(5): 471-83.

Lieber, M. R. (1999). "The biochemistry and biological significance of nonhomologous DNA end joining: an essential repair process in multicellular eukaryotes." Genes Cells **4**(2): 77-85.

Lim, D. S., S. T. Kim, B. Xu, R. S. Maser, J. Lin, J. H. Petrini and M. B. Kastan (2000). "ATM phosphorylates p95/nbs1 in an S-phase checkpoint pathway." Nature **404**(6778): 613-7.

Lin, J.-J. and V. A. Zakian (1996). "The *Saccharomyces* CDC13 protein is a single-strand TG1-3 telomeric DNA binding protein *in vitro* that affects telomere behavior *in vivo*." Proc. Natl. Acad. Sci. USA **93**: 13760-13765.

Lingner, J. and T. R. Cech (1996). "Purification of telomerase from *Euplotes* aediculatus: requirement of a primer 3' overhang." Proc. Natl. Acad. Sci. USA **93**: 10712-10717.

Lingner, J., T. R. Cech, T. R. Hughes and V. Lundblad (1997). "Three Ever Shorter Telomere (EST) genes are dispensable for *in vitro* yeast telomerase activity." Proc. Natl. Acad. Sci. USA **94**: 11190-5.

Lingner, J., T. R. Hughes, A. Shevchenko, M. Mann, V. Lundblad and T. R. Cech (1997). "Reverse transcriptase motifs in the catalytic subunit of telomerase." Science **276**: 561-567.

Liu, Y., B. E. Snow, M. P. Hande, G. Baerlocher, V. A. Kickhoefer, D. Yeung, A. Wakeham, A. Itie, D. P. Siderovski, P. M. Lansdorp, M. O. Robinson and L. Harrington (2000). "Telomerase-associated protein TEP1 is not essential for telomerase activity or telomere length maintenance *in vivo*." Mol Cell Biol **20**(21): 8178-84.

Liu, Y., B. E. Snow, M. P. Hande, D. Yeung, N. J. Erdmann, A. Wakeham, A. Itie, D. P. Siderovski, P. M. Lansdorp, M. O. Robinson and L. Harrington (2000). "The telomerase reverse transcriptase is limiting and necessary for telomerase function *in vivo*." Curr Biol **10**(22): 1459-62.

Lombard, D. B., L. Guarente (2000). "Nijmegen breakage syndrome disease protein and

MRE11 at PML nuclear bodies and meiotic telomeres." Cancer Res **60** (9): 2331-4.

Lundblad, V. and E. H. Blackburn (1993). "An alternative pathway for yeast telomere maintenance rescues est1- senescence." Cell **73**: 347-360.

Lundblad, V. and J. W. Szostak (1989). "A mutant with a defect in telomere elongation leads to senescence in yeast." Cell **57**: 633-643.

Lustig, A. J., S. Kurtz and D. Shore (1990). "Involvement of the silencer and UAS binding protein RAP1 in regulation of telomere length." Science **250**: 549-553.

Lustig, A. J. and T. D. Petes (1986). "Identification of yeast mutants with altered telomere structure." Proc. Natl. Acad. Sci. USA **83**: 1398-1402.

Mailand, N., J. Falck, C. Lukas, R. G. Syljuasen, M. Welcker, J. Bartek and J. Lukas (2000). "Rapid destruction of human Cdc25A in response to DNA damage." Science **288**(5470): 1425-9.

Makarov, V., Y. Hirose and J. P. Langmore (1997). "Long G tails at both ends of human chromosomes suggest a C strand degradation mechanism for telomere shortening." Cell **88**: 657-666.

Mallory, J. C. and T. D. Petes (2000). "Protein kinase activity of Tel1p and Mec1p, two *Saccharomyces cerevisiae* proteins related to the human ATM protein kinase." Proc Natl Acad Sci U S A **97**(25): 13749-54.

Mantell, L. L. and C. W. Greider (1994). "Telomerase activity in germline and embryonic cells of Xenopus." EMBO J. **13**: 3211-7.

Marcand, S., E. Gilson and D. Shore (1997). "A protein-counting mechanism for telomere length regulation in yeast." Science **275**: 986-990.

Marciniak, R. A., D. B. Lombard, F. B. Johnson and L. Guarente (1998). "Nucleolar localization of the Werner syndrome protein in human cells." Proc Natl Acad Sci U S A **95**(12): 6887-92.

Marshall, W. F. and J. L. Rosenbaum (2000). "Are there nucleic acids in the centrosome?" Curr Top Dev Biol **49**: 187-205.

Martin-Rivera, L., E. Herrera, J. P. Albar and M. A. Blasco (1998). "Expression of mouse telomerase catalytic subunit in embryos and adult tissues." Proc Natl Acad Sci U S A **95**(18): 10471-6.

Mayor, T., P. Meraldi, Y. D. Stierhof, E. A. Nigg and A. M. Fry (1999). "Protein kinases in control of the centrosome cycle." FEBS Lett **452**(1-2): 92-5.

McClintock, B. (1938). The fusion of broken ends of sister half-chromatids following chromatid breakage at meiotic anaphase. The discovery and characterization of transposable elements. The collected papers of Barbara McClintock. New York and London, Garland Publishing, Inc.: 1-48.

McDonell, M. W., M. N. Simon and F. W. Studier (1977). "Analysis of restriction fragments of T7 DNA and determination of molecular weights by electrophoresis in neutral and alkaline gels." J Mol Biol **110**(1): 119-46.

McEachern, M. J. and E. H. Blackburn (1994). "A conserved sequence motif within the exceptionally diverse telomeric sequences of budding yeasts." Proc. Natl. Acad. Sci. USA **91**: 3453-3457.

McEachern, M. J. and E. H. Blackburn (1995). "Runaway telomere elongation caused by telomerase RNA gene mutations." Nature **376**: 403-409.

Melek, M. and D. E. Shippen (1996). "Chromosome healing: spontaneous and programmed de novo telomere formation by telomerase." Bioessay **18**(4): 301-308.

Metcalfe, J. A., J. Parkhill, L. Campbell, M. Stacey, P. Biggs, P. J. Byrd and A. M. Taylor (1996). "Accelerated telomere shortening in ataxia telangiectasia." Nat. Genet. **13**: 350-3.

Meyerson, M., C. M. Counter, E. N. Eaton, L. W. Ellisen, P. Steiner, S. D. Caddle, L. Ziaugra, R. L. Beijersbergen, M. J. Davidoff, Q. Liu, S. Bacchetti, D. A. Haber and R. A. Weinberg (1997). "hEST2, the putative human telomerase catalytic subunit gene, is up-regulated in tumor cells and during immortalization." Cell **90**: 785-795.

Meyne, J., R. J. Baker, H. H. Hobart, T. C. Hsu, O. A. Ryder, O. G. Ward, J. E. Wiley, D. H. Wurster-Hill, T. L. Yates and R. K. Moyzis (1990). "Distribution of non-

telomeric sites of the (TTAGGG)n telomeric sequence in vertebrate chromosomes." Chromosoma **99**: 3-10.

Miller, M. C. and K. Collins (2000). "The Tetrahymena p80/p95 complex is required for proper telomere length maintenance and micronuclear genome stability." Mol Cell **6**(4): 827-37.

Mitchell, J. R., J. Cheng and K. Collins (1999). "A box H/ACA small nucleolar RNA-like domain at the human telomerase RNA 3' end." Mol Cell Biol **19**(1): 567-76.

Mitchell, J. R., E. Wood and K. Collins (1999). "A telomerase component is defective in the human disease dyskeratosis congenita." Nature **402**(6761): 551-5.

Miyashita, T., S. Krajewski, M. Krajewska, H. G. Wang, H. K. Lin, D. A. Liebermann, B. Hoffman and J. C. Reed (1994). "Tumor suppressor p53 is a regulator of bcl-2 and bax gene expression *in vitro* and *in vivo*." Oncogene **9**(6): 1799-805.

Morales, C. P., S. E. Holt, M. Ouellette, K. J. Kaur, Y. Yan, K. S. Wilson, M. A. White, W. E. Wright and J. W. Shay (1999). "Absence of cancer–associated changes in human fibroblasts immortalized with telomerase." Nature Genetics **21**: 115-118.

Moretti, P., K. Freeman, L. Coodly and D. Shore (1994). "Evidence that a complex of SIR proteins interacts with the silencer and telomere-binding protein RAP1." Genes Dev. **8**: 2257-2269.

Morin, G. B. (1989). "The human telomere terminal transferase enzyme is a ribonucleoprotein that synthesizes TTAGGG repeats." Cell **59**: 521-529.

Morin, G. B. (1991). "Recognition of a chromosome truncation site associated with alpha-thalassaemia by human telomerase." Nature **353**: 454-456.

Moyzis, R. K., J. M. Buckingham, L. S. Cram, M. Dani, L. L. Deaven, M. D. Jones, J. Meyne, R. L. Ratliff and J.-R. Wu (1988). "A highly conserved repetitive DNA sequence, (TTAGGG)n, present at the telomeres of human chromosomes." Proc. Natl. Acad. Sci. USA **85**: 6622-6626.

Muller, H. J. (1938). "The remaking of chromosomes." The Collecting Net - Woods Hole **13**: 181-195.

Munoz-Jordan, J. L., G. A. Cross, T. de Lange and J. D. Griffith (2001). "t-loops at trypanosome telomeres." Embo J **20**(3): 579-88.

Murti, K. G. and D. M. Prescott (1999). "Telomeres of polytene chromosomes in ciliated protozoan terminate in duplex DNA loops." Proc Natl Acad Sci U S A **96**: 14436-14439.

Naito, T., A. Matsuura and F. Ishikawa (1998). "Circular chromosome formation in a fission yeast mutant defective in two ATM homologues." Nat. Genet. **20**: 203-6.

Nakamura, T. M. and T. R. Cech (1998). "Reversing time: origin of telomerase." Cell **92**: 587-90.

Nakamura, T. M., J. P. Cooper and T. R. Cech (1998). "Two modes of survival of fission yeast without telomerase." Science **282**: 493-6.

Nakamura, T. M., G. B. Morin, K. B. Chapman, S. L. Weinrich, W. H. Andrews, J. Lingner, C. B. Harley and T. R. Cech (1997). "Telomerase catalytic subunit homologs from fission yeast and human." Science **277**: 955-9.

Nakayama, J., M. Saito, H. Nakamura, A. Matsuura and F. Ishikawa (1997). "TLP1: A gene encoding a prein component of mammalian telomerase is a novel member of WD repeats family." Cell **88**: 875-884.

Nakayama, K., H. Nagahama, Y. A. Minamishima, M. Matsumoto, I. Nakamichi, K. Kitagawa, M. Shirane, R. Tsunematsu, T. Tsukiyama, N. Ishida, M. Kitagawa and S. Hatakeyama (2000). "Targeted disruption of Skp2 results in accumulation of cyclin E and p27(Kip1), polyploidy and centrosome overduplication." Embo J **19**(9): 2069-81.

Nelms, B. E., R. S. Maser, J. F. MacKay, M. G. Lagally and J. H. Petrini (1998). "In situ visualization of DNA double-strand break repair in human fibroblasts." Science **280**: 590-2.

Neufeld, D. S., S. Ripley, A. Henderson and H. L. Ozer (1987). "Immortalization of human fibroblasts transformed by origin-defective simian virus 40." Mol Cell Biol **7**(8): 2794-802.

Niida, H., T. Matsumoto, H. Satoh, M. Shiwa, Y. Tokutake, Y. Furuichi and Y. Shinkai (1998). "Severe growth defect in mouse cells lacking the telomerase RNA component." Nat Genet **19**: 203-206.

Niida, H., Y. Shinkai, M. P. Hande, T. Matsumoto, S. Takehara, M. Tachibana, M. Oshimura, P. M. Lansdorp and Y. Furuichi (2000). "Telomere maintenance in telomerase-deficient mouse embryonic stem cells: characterization of an amplified telomeric DNA." Mol Cell Biol **20**(11): 4115-27.

Nikaido, R., T. Haruyama, Y. Watanabe, H. Iwata, M. Iida, H. Sugimura, N. Yamada and F. Ishikawa (1999). "Presence of telomeric G-strand tails in the telomerase catalytic subunit TERT knockout mice." Genes Cells **4**(10): 563-72.

Nimmo, E. R., A. L. Pidoux, P. E. Perry and R. C. Allshire (1998). "Defective meiosis in telomere-silencing mutants of *Schizosaccharomyces pombe*." Nature **392**(6678): 825-8.

Nugent, C., G. Bosco, L. Ross, S. Evans, A. Salinger, J. Moore, J. Haber and V. Lundblad (1998). "Telomere maintenance is dependent on activities required for end repair of double-strand breaks." Curr Biol. **8**: 657-660.

Nugent, C. I., T. R. Hughes, N. F. Lue and V. Lundblad (1996). "Cdc13p: a single-strand telomeric DNA-binding protein with a dual role in yeast telomere maintenance." Science **274**: 249-252.

Ohtani, N., Z. Zebedee, T. J. Huot, J. A. Stinson, M. Sugimoto, Y. Ohashi, A. D. Sharrocks, G. Peters and E. Hara (2001). "Opposing effects of Ets and Id proteins on p16INK4a expression during cellular senescence." Nature **409**(6823): 1067-70.

Okabe, J., A. Eguchi, A. Masago, T. Hayakawa, M. Nakanishi (2000). "TRF1 is a critical trans-acting factor required for de novo telomere formation in human cells." Hum Mol Genet **9** (18) 2639-50.

Okazaki, S., K. Tsuchida, H. Maekawa, H. Ishikawa and H. Fujiwara (1993). "Identification of a pentanucleotide telomeric sequence $(TTAGG)_n$, in the silkworm Bombyx mori and in other insects." Mol. Cell. Biol. **13**: 1424-1432.

Olovnikov, A. M. (1973). "A theory of marginotomy." J. Theor. Biol. **41**: 181-190.

Park, V. M., K. M. Gustashaw and T. M. Wathen (1992). "The presence of interstitial telomeric sequences in constitutional chromosome abnormalities." Am J Hum Genet **50**(5): 914-23.

Pennock, E., K. Buckley and V. Lundblad (2001). "Cdc13 delivers separate complexes to the telomere for end protection and replication." Cell **104**(3): 387-96.

Petrini, J. H. (1999). "The mammalian Mre11-Rad50-nbs1 protein complex: integration of functions in the cellular DNA-damage response." Am J Hum Genet **64**(5): 1264-9.

Pipas, J. M. and A. J. Levine (2001). "Role of T antigen interactions with p53 in tumorigenesis." Semin Cancer Biol **11**(1): 23-30.

Pluta, A. F., B. P. Kaine and B. B. Spear (1982). "The terminal organization of macronuclear DNA in *Oxytricha fallax*." Nucl. Acids Res. **10**: 8145-8154.

Polotnianka, R., J. Li and A. Lustig (1998). "The yeast Ku heterodimer is essential for protection of the telomere against nucleolytic and recombinational activities." Curr Biol **8**: 831-834.

Porter, S. E., P. W. Greenwell, K. B. Ritchie and T. D. Petes (1996). "The DNA-binding protein Hdf1p (a putative Ku homologue) is required for maintaining normal telomere length in *Saccharomyces cerevisiae*." Nucl. Acids Res. **24**: 582-5.

Powers, J. A. and J. C. Eissenberg (1993). "Overlapping domains of the heterochromatin-associated protein HP1 mediate nuclear localization and heterochromatin binding." J Cell Biol **120**(2): 291-9.

Price, C. M. (1997). "Synthesis of the telomeric C-strand. A review." Biochemistry (Mosc) **62**: 1216-23.

Prowse, K., A. Avilion and C. Greider (1993). "Identification of a nonprocessive telomerase activity from mouse cells." Proc. Natl. Acad. Sci. USA **90**: 1493-1497.

Prowse, K. and C. W. Greider (1995). "Developmental and tissue specific regulation of mouse telomerase and telomere length." Proc. Natl. Acad. Sci. USA **92**: 4818-4822.

Runge, K. W. and V. A. Zakian (1996). "TEL2, an essential gene required for telomere length regulation and telomere position effect in *Saccharomyces cerevisiae*." Mol. Cell. Biol. **16**: 3094-105.

Saksela, E. and P. S. Moorhead (1963). "Aneuploidy in the Degenerative Phase of Serial Cultivation of Human Cell Strains." Proc Natl Acad Sci U S A **50**: 390-395.

Saltman, D., R. Morgan, M. L. Cleary and T. de Lange (1993). "Telomeric structure in cells with chromosome end associations." Chromosoma **102**: 121-128.

Sambrook, J., E. F. Fritsch and T. Maniatis (1989). Molecular Cloning. A Laboratory Manual.

Samper, E., F. A. Goytisolo, J. Menissier-de Murcia, E. Gonzalez-Suarez, J. C. Cigudosa, G. de Murcia and M. A. Blasco (2001). "Normal telomere length and chromosomal end capping in poly(ADP-ribose) polymerase-deficient mice and primary cells despite increased chromosomal instability." J Cell Biol **154**(1): 49-60.

Samper, E., F. A. Goytisolo, P. Slijepcevic, P. P. van Buul and M. A. Blasco (2000). "Mammalian Ku86 protein prevents telomeric fusions independently of the length of TTAGGG repeats and the G-strand overhang." EMBO Rep **1**(3): 244-52.

Scherthan, H. (2001). "A bouquet makes ends meet." Nat Rev Mol Cell Biol **2**(8): 621-7.

Schulz, V. P. and V. A. Zakian (1994). "The *Saccharomyces* PIF1 DNA helicase inhibits telomere elongation and de novo telomere formation." Cell **76**: 145-55.

Schulz, V. P., V. A. Zakian, C. E. Ogburn, J. McKay, A. A. Jarzebowicz, S. D. Edland and G. M. Martin (1996). "Accelerated loss of telomeric repeats may not explain accelerated replicative decline of Werner syndrome cells " Hum. Genet. **97**: 750-4.

Sedivy, J. M. (1998). "Can ends justify the means?: Telomeres and the mechanisms of replicative senescence and immortaiization in mammalian cells." PNAS **95**(16): 9078-9081.

Sekiguchi, J. M., Y. Gao, Y. Gu, K. Frank, Y. Sun, J. Chaudhuri, C. Zhu, H. L. Cheng, J. Manis, D. Ferguson, L. Davidson, M. E. Greenberg and F. W. Alt (1999). "Nonhomologous end-joining proteins are required for V(D)J recombination,

normal growth, and neurogenesis." Cold Spring Harb Symp Quant Biol **64**: 169-81.

Serrano, M., A. W. Lin, M. E. McCurrach, D. Beach and S. W. Lowe (1997). "Oncogenic ras provokes premature cell senescence associated with accumulation of p53 and p16INK4a." Cell **88**(5): 593-602.

Seto, A. G., A. J. Zaug, S. G. Sobel, S. L. Wolin and T. R. Cech (1999). "*Saccharomyces cerevisiae* telomerase is an Sm small nuclear ribonucleoprotein particle." Nature **401**(6749): 177-80.

Shampay, J. and E. H. Blackburn (1988). "Generation of telomere-length heterogeneity in *Saccharomyces cerevisiae*." Proc. Natl. Acad. Sci. USA **85**: 534-8.

Shampay, J. and E. H. Blackburn (1989). "Tetrahymena micronuclear sequences that function as telomeres in yeast." Nucl. Acids Res. **17**: 3247-3260.

Shampay, J., J. W. Szostak and E. H. Blackburn (1984). "DNA sequences of telomeres maintained in yeast." Nature **310**: 154-157.

Shay, J., W. E. Wright and H. Werbin (1991). "Defining the molecular mechanisms of human cell immortalization." Biochim. Biophys. ACTA **1072**: 1-7.

Shay, J. W. and S. Bacchetti (1997). "A survey of telomerase activity in human cancer." Eur. J. Cancer **33**: 787-91.

Shay, J. W., O. M. Pereira-Smith and W. E. Wright (1991). "A role for both RB and p53 in the regulation of human cellular senescence." Exp. Cell. Res. **196**: 33-9.

Shay, J. W. and W. E. Wright (1989). "Quantitation of the frequency of immortalization of normal human diploid fibroblasts by SV40 large T-antigen." Exp Cell Res **184**(1): 109-18.

Sheen, F. M. and R. W. Levis (1994). "Transposition of the LINE-like retrotransposon TART to *Drosophila* chromosome termini." Proc. Natl. Acad. Sci. USA **91**: 12510-4.

Sherr, C. J. and R. A. DePinho (2000). "Cellular senescence: mitotic clock or culture shock?" Cell **102**(4): 407-10.

Shieh, S. Y., M. Ikeda, Y. Taya and C. Prives (1997). "DNA damage-induced phosphorylation of p53 alleviates inhibition by MDM2." Cell **91**: 325-34.

Shippen-Lentz, D. and E. H. Blackburn (1990). "Functional evidence for an RNA template in telomerase." Science **247**: 546-552.

Singer, M. S. and D. E. Gottschling (1994). "TLC1: template RNA component of *Saccharomyces cerevisiae* telomerase." Science **266**: 404-9.

Singh, P. B., J. R. Miller, J. Pearce, R. Kothary, R. D. Burton, R. Paro, T. C. James and S. J. Gaunt (1991). "A sequence motif found in a *Drosophila* heterochromatin protein is conserved in animals and plants." Nucl. Acids Res. **19**: 789-94.

Slijepcevic, P., Y. Xiao, A. T. Natarajan and P. E. Bryant (1997). "Instability of CHO chromosomes containing interstitial telomeric sequences originating from Chinese hamster chromosome 10." Cytogenet Cell Genet **76**(1-2): 58-60.

Smith, S. and T. de Lange (1997). "TRF1, a mammalian telomeric protein." Trends Gen. **13**: 21-26.

Smith, S. and T. de Lange (1999). "Cell cycle dependent localization of the telomeric PARP, tankyrase, to nuclear pore complexes and centrosomes." J Cell Sci **112**(Pt 21): 3649-56.

Smith, S. and T. de Lange (2000). "Tankyrase promotes telomere elongation in human cells." Curr Biol **10**(20): 1299-302.

Smith, S., I. Giriat, A. Schmitt and T. de Lange (1998). "Tankyrase, a poly(ADP-ribose) polymerase at human telomeres [see comments]." Science **282**: 1484-7.

Smogorzewska, A., B. van Steensel, A. Bianchi, S. Oelmann, M. R. Schaefer, G. Schnapp and T. de Lange (2000). "Control of human telomere length by TRF1 and TRF2." Mol Cell Biol **20**(5): 1659-68.

Song, K., D. Jung, Y. Jung, S. G. Lee and I. Lee (2000). "Interaction of human Ku70 with TRF2." FEBS Lett **481**(1): 81-5.

Speicher, M. R., S. Gwyn Ballard and D. C. Ward (1996). "Karyotyping human chromosomes by combinatorial multi-fluor FISH." Nat Genet **12**(4): 368-75.

Sprung, C. N., T. M. Bryan, R. R. Reddel and J. P. Murnane (1997). "Normal telomere maintenance in immortal ataxia telangiectasia cell lines." Mutat Res **379**(2): 177-84.

Sprung, C. N., G. E. Reynolds, M. Jasin and J. P. Murnane (1999). "Chromosome healing in mouse embryonic stem cells." Proc Natl Acad Sci U S A **96**: 6781-6.

Stansel, R., T. de Lange and J. Griffith (2001). "T-loop assembly *in vitro* involves binding of TRF2 near the 3' telomeric overhang." EMBO J.: in press.

Stanulis-Praeger, B. M. (1987). "Cellular senescence revisited: a review." Mech Ageing Dev **38**(1): 1-48.

Stewart, G. S., R. S. Maser, T. Stankovic, D. A. Bressan, M. I. Kaplan, N. G. Jaspers, A. Raams, P. J. Byrd, J. H. Petrini and A. M. Taylor (1999). "The DNA double-strand break repair gene hMRE11 is mutated in individuals with an ataxia-telangiectasia-like disorder." Cell **99**(6): 577-87.

Stott, F. J., S. Bates, M. C. James, B. B. McConnell, M. Starborg, S. Brookes, I. Palmero, K. Ryan, E. Hara, K. H. Vousden and G. Peters (1998). "The alternative product from the human CDKN2A locus, p14(ARF), participates in a regulatory feedback loop with p53 and MDM2." Embo J **17**(17): 5001-14.

Stratmann, R. and C. F. Lehner (1996). "Separation of sister chromatids in mitosis requires the *Drosophila* pimples product, a protein degraded after the metaphase/anaphase transition." Cell **84**(1): 25-35.

Sugawara, N., Szostak, J.W. (1986). "Telomeres of *Schizosaccharomyces pombe*." Yeast (Suppl.) 1(S373).

Thompson, K. V. and R. Holliday (1975). "Chromosome changes during the *in vitro* ageing of MRC-5 human fibroblasts." Exp Cell Res **96**(1): 1-6.

Tibbetts, R. S., K. M. Brumbaugh, J. M. Williams, J. N. Sarkaria, W. A. Cliby, S. Y. Shieh, Y. Taya, C. Prives and R. T. Abraham (1999). "A role for ATR in the DNA damage-induced phosphorylation of p53." Genes Dev **13**(2): 152-7.

Usui, T., H. Ogawa and J. H. Petrini (2001). "A DNA damage response pathway controlled by Tel1 and the Mre11 complex." Mol Cell **7**(6): 1255-66.

Van der Ploeg, L. H., A. Y. Liu and P. Borst (1984). "Structure of the growing telomeres of Trypanosomes." Cell **36**: 459-68.

van Steensel, B. and T. de Lange (1997). "Control of telomere length by the human telomeric protein TRF1." Nature **385**: 740-743.

van Steensel, B., J. Delrow and S. Henikoff (2001). "Chromatin profiling using targeted DNA adenine methyltransferase." Nat Genet **27**(3): 304-8.

van Steensel, B., A. Smogorzewska and T. de Lange (1998). "TRF2 protects human telomeres from end-to-end fusions." Cell **92**: 401-413.

Varon, R., C. Vissinga, M. Platzer, K. M. Cerosaletti, K. H. Chrzanowska, K. Saar, G. Beckmann, E. Seemanova, P. R. Cooper, N. J. Nowak, M. Stumm, C. M. Weemaes, R. A. Gatti, R. K. Wilson, M. Digweed, A. Rosenthal, K. Sperling, P. Concannon and A. Reis (1998). "Nibrin, a novel DNA double-strand break repair protein, is mutated in Nijmegen breakage syndrome." Cell **93**(3): 467-76.

Vaziri, H. and S. Benchimol (1998). "Reconstitution of telomerase activity in normal human cells leads to elongation of telomeres and extended replicative life span." Curr. Biol. **8**: 279-82.

Vaziri, H., M. D. West, R. C. Allsopp, T. S. Davison, Y. S. Wu, C. H. Arrowsmith, G. G. Poirier and S. Benchimol (1997). "ATM-dependent telomere loss in aging human diploid fibroblasts and DNA damage lead to the post-translational activation of p53 protein involving poly(ADP-ribose) polymerase." EMBO J. **16**: 6018-33.

Vogelstein, B., D. Lane and A. J. Levine (2000). "Surfing the p53 network." Nature **408**(6810): 307-10.

Walker, J. R., R. A. Corpina and J. Goldberg (2001). "Structure of the Ku heterodimer bound to DNA and its implications for double-strand break repair." Nature **412**(6847): 607-14.

Watson, J. D. (1972). "Origin of concatemeric T7 DNA." Nature **239**: 197-201.

Watt, P. M., I. D. Hickson, R. H. Borts and E. J. Louis (1996). "SGS1, a homologue of the Bloom's and Werner's syndrome genes, is required for maintenance of genome stability in *Saccharomyces cerevisiae*." Genetics **144**(3): 935-45.

Wellinger, R. J., A. J. Wolf and V. A. Zakian (1993). "Origin activation and formation of single-strand TG_{1-3} tails occur sequentially in late S phase on a yeast linear plasmid." Mol. Cell. Biol. **13**: 4057-4065.

Wellinger, R. J., A. J. Wolf and V. A. Zakian (1993). "*Saccharomyces* telomeres acquire single-strand TG_{1-3} tails late in S phase." Cell **72**: 51-60.

Wilkie, A. O. M., J. Lamb, P. C. Harris, R. D. Finney and D. R. Higgs (1990). "A truncated human chromosome 16 associated with a thalassaemia is stabilized by addition of telomeric repeat (TTAGGG)n." Nature **346**: 868-871.

Winey, M. (1999). "Cell cycle: driving the centrosome cycle." Curr Biol **9**(12): R449-52.

Wolman, S. R., K. Hirschhorn , G.J.Todaro (1964). "Early Chromosomal Changes in SV40-Infected Human Fibroblast Culture." Cytogenetics **3**: 45-61.

Wotton, D. and D. Shore (1997). "A novel Rap1p-interacting factor, Rif2p, cooperates with Rif1p to regulate telomere length in *Saccharomyces cerevisiae*." Genes Dev **11**(6): 748-60.

Wright, W. E., M. A. Piatyszek, W. R. Rainey, W. Byrd and J. W. Shay (1996). "Telomerase activity in human germline and embryonic tissues and cells." Dev. Genetics **18**: 173-179.

Wu, X., V. Ranganathan, D. S. Weisman, W. F. Heine, D. N. Ciccone, T. B. O'Neill, K. E. Crick, K. A. Pierce, W. S. Lane, G. Rathbun, D. M. Livingston and D. T. Weaver (2000). "ATM phosphorylation of Nijmegen breakage syndrome protein is required in a DNA damage response." Nature **405**(6785): 477-82.

Xu, X., Z. Weaver, S. P. Linke, C. Li, J. Gotay, X. W. Wang, C. C. Harris, T. Ried and C. X. Deng (1999). "Centrosome amplification and a defective G2-M cell cycle checkpoint induce genetic instability in BRCA1 exon 11 isoform-deficient cells." Mol Cell **3**(3): 389-95.

Xu, Y. and D. Baltimore (1996). "Dual roles of ATM in the cellular response to radiation and in cell growth control." Genes Dev. **10**: 2401-10.

Xu, Y., E. M. Yang, J. Brugarolas, T. Jacks and D. Baltimore (1998). "Involvement of p53 and p21 in cellular defects and tumorigenesis in Atm- /- mice." Mol Cell Biol **18**(7): 4385-90.

Yankiwski, V., R. A. Marciniak, L. Guarente and N. F. Neff (2000). "Nuclear structure in normal and Bloom syndrome cells." Proc Natl Acad Sci U S A **97**(10): 5214-9.

Ye, J. and T. de Lange "unpublished data."

Yeargin, J. and M. Haas (1995). "Elevated levels of wild-type p53 induced b y raiolabeling of cells leads to apoptosis or sustained growth arrest." Current Biol. **5**: 423-431.

Yu, G.-L., J. D. Bradley, L. D. Attardi and E. H. Blackburn (1990). "*In vivo* alteration of telomere sequences and senescence caused by mutated Tetrahymena telomerase RNAs." Nature **344**: 126-132.

Zhang, X., V. Mar, W. Zhou, L. Harrington and M. O. Robinson (1999). "Telomere shortening and apoptosis in telomerase-inhibited human tumor cells." Genes Dev **13**(18): 2388-99.

Zhao, S., Y. C. Weng, S. S. Yuan, Y. T. Lin, H. C. Hsu, S. C. Lin, E. Gerbino, M. H. Song, M. Z. Zdzienicka, R. A. Gatti, J. W. Shay, Y. Ziv, Y. Shiloh and E. Y. Lee (2000). "Functional link between ataxia-telangiectasia and Nijmegen breakage syndrome gene products." Nature **405**(6785): 473-7.

Zhong, Z., L. Shiue, S. Kaplan and T. de Lange (1992). "A mammalian factor that binds telomeric TTAGGG repeats *in vitro*." Mol. Cell. Biol. **13**: 4834-4843.

Zhou, H., J. Kuang, L. Zhong, W. L. Kuo, J. W. Gray, A. Sahin, B. R. Brinkley and S. Sen (1998). "Tumour amplified kinase STK15/BTAK induces centrosome amplification, aneuploidy and transformation." Nat Genet **20**(2): 189-93.

Zhou, J., E. K. Monson, S. Teng, V. P. Schulz and V. A. Zakian (2000). "Pif1p helicase, a catalytic inhibitor of telomerase in yeast." Science **289**(5480): 771-4.

Zhu, J., D. Woods, M. McMahon and J. Bishop (1998). "Senescence of human fibroblasts induced by oncogenic Raf." Genes Development **12**: 2997-3007.

Zhu, L., K. S. Hathcock, P. Hande, P. M. Lansdorp, M. F. Seldin and R. J. Hodes (1998). "Telomere length regulation in mice is linked to a novel chromosome locus." Proc Natl Acad Sci U S A **95**: 8648-53.

Zhu, X. D., B. Kuster, M. Mann, J. H. Petrini and T. Lange (2000). "Cell-cycle-regulated association of RAD50/MRE11/NBS1 with TRF2 and human telomeres." Nat Genet **25**(3): 347-52.